

Progress Report

**REGENERATIVE LIFE SUPPORT SYSTEM  
RESEARCH AND CONCEPTS**

April 1988 - December 1988

NASA Grant NAG 9-253

Prepared by  
The Regenerative Concepts Team  
Texas A&M University

Submitted to:

NASA Johnson Space Center  
Houston, Texas 77058  
Through  
Texas A & M Research Foundation

## Table of Contents

1. Executive Summary.....	1
Introduction.....	1
Modeling .....	1
Laboratory Research.....	2
2. Team Interactions with Others.....	4
3. Computer Based Modeling Development.....	6
3.1 Intelligent Design Support Environment for Space Station System Engineering.....	6
3.2 Representation of Physical-Chemical-Biological Systems (PCBS).....	16
3.3 Analysis of Steady State Model.....	33
3.4 State Space Simulation.....	39
3.5 Biophysics of Plant Growth: Algae and Higher Plants.....	41
3.6 A Human Physiology Mode to be Interfaced with the Life Support System (LSS).....	55
4. Conceptual Modeling Studies for Waste Electrolyzer.....	61
4.1 Model Development.....	61
4.2 Calculational Procedure.....	83
4.3 Conclusions.....	84
5. Research Results.....	92
5.1 Electrochemistry.....	92
5.2 Water and Waste Management.....	118
5.3 Algae Property Measurements for Engineering Design.....	126
5.4 Plant Physiology Experiments.....	132
5.5 Artificial Chloroplast Membrane Stability Experiments.....	135
5.6 Lunar Soil Simulant Experiments.....	153
5.7 Plant Growth Control Experiments.....	158
6. Conceptual Design Studies.....	173
6.1 Air Revitalization.....	173
6.2 Water Recovery.....	178
6.3 Waste Management.....	190
6.4 Contaminant Management.....	195
6.5 Food Production.....	205
6.6 Food Preparation.....	210

# 1. EXECUTIVE SUMMARY

## Introduction

This report covers activities of the Texas A&M University Space Research Center Regenerative Concepts Team during the period April 1, 1988 through December 31, 1988. The team was organized in the Fall of 1985, and received its first grant award from NASA Johnson Space Center on May 15, 1986, for a study entitled "Conceptual Design for a Food Production, Water and Waste Processing, and Gas Regeneration Module". Since that time, the Regenerative Concepts Team, also known as the RECON team, has obtained additional funding from NASA, industry and university sources, and has continued to conduct research on methods of managing and recycling air, water, food, and waste in space.

During this report period, funding for team activities was provided by the Office of Aeronautics and Space Technology, Propulsion, Power and Energy Division, Ms. Peggy L. Evanich, through the Crew and Thermal Systems Division of the Johnson Space Center, Mr. Albert F. Behrend, Jr., Technical Monitor. From its inception, RECON team activities have provided an interdisciplinary focus for interaction of researchers interested in life support concepts, stimulating individual research tasks that have been funded on a discipline basis. To reflect the cohesive results of this larger, synergistic effort, several areas of research funded by other sources are discussed in addition to the team efforts directly funded by this grant. Most of these individual tasks evolved as a result of team interactions, and have continued to benefit from the feedback provided by the interdisciplinary team working toward a common goal.

On Earth, life is supported by physical, chemical and biological processes. From the beginning, the RECON team has always been composed of members covering essential disciplines from colleges of science, agriculture and engineering, who collectively have the necessary background to address physical, chemical, and biological matters. This integration of scientists and engineers has allowed a broad look to be taken at space life support systems, with the long term goal of closing the environmental life support processes. However, during this reporting period, over 90% of the funding was applied to physical and chemical processing of water and waste management, in accord with directions from the Grant Technical Monitor.

## Modeling

Life support systems that involve recycling of atmospheres, water, food and waste are so complex that models incorporating all the interactions and relationships are vital to design, development, simulations, and ultimately to control of space qualified systems. It has been a goal of the RECON team from its early organization to develop modeling tools capable of dealing with all aspects of regenerative life support systems.

Although many useful models have been evolved in the past through the efforts of John B. Hall of NASA Langley and others, expert systems or artificial intelligence techniques had not been applied. These powerful new capabilities offer great potential, assuming the necessary facts, relationships, and methodologies can be

integrated. This integration and development has been underway for some time at Texas A&M, and usable modeling tools are now available, although continuing refinement and expansion are required.

During early modeling studies, Fortran and Basic programs were used to obtain numerical comparisons of the performance of different regenerative concepts. Concurrently, LISP programs and KEE object-oriented methods were evolved to expand the capabilities for simulations and dynamic interactions. During recent months, modeling activities have been expanded to combine existing capabilities with expert systems to establish an Intelligent Design Support Environment for simplifying user interfaces and to address the need for the design and steady state analysis of various life support systems. This effort is primarily intended to serve the engineering aspects of model design, whereby tradeoffs can be readily made without reprogramming extensively as parametric inputs change.

Progress has also been made toward modeling and evaluating the operational aspects of closed loop life support systems using Time-step and Dynamic simulations over a period of time. Because of the subtle effects of recycling on the many chemical and biological relationships, the time dependent aspects are important and perhaps critical to effective regenerative systems. Both modeling efforts have common parametric and system input requirements, and both are being developed to serve the scientists and engineers who need to use them in a straightforward manner. Although advances will continue to be made, modeling results of value are already being obtained to guide research and design objectives.

Example models are presented in this report which will show the status and potential of developed modeling techniques. For instance, closed loop systems involving algae systems for atmosphere purification and food supply augmentation, plus models employing higher plants and solid waste electrolysis are described and results of initial evaluations presented. The utility of the modeling techniques is improving as members of the RECON team continue to upgrade the models and methodologies, while simultaneously obtaining comparative results for different concepts.

## Laboratory Research

As mentioned earlier, laboratory research during this reporting period was focused on water and waste processing, although some attention was given to air revitalization and food production and processing. Electrochemistry appears to offer attractive possibilities for waste processing, and results from experiments funded under separate grants were factored into RECON team modeling and design studies. Low temperature processing methods were used successfully to decompose synthesized fecal and urine waste materials and bioelectrochemical urine fuel cell experiments produced encouraging results.

Water and waste processing were studied in detail, based on a thorough literature review of research conducted during the past 20 years, and using experimental apparatus in the RECON lab that was obtained from GE and refurbished. Alternative technologies were studied, and the ground rules under which they were originally assessed were found to be important in considering their application to future space stations and bases. Venting of exhaust gases, available energy and heat rejection capabilities, applications for recycled

products, length of time between resupply, total time in space, and many mission design parameters affect trade studies and demand that earlier trade studies be reexamined carefully for applicability to projected missions. In many cases, trade studies done in the past were inconclusive because inadequate data required assumptions to allow comparisons. Current groundrules and more recent findings must be incorporated to increase the usefulness of early results.

An example of such a fresh look at earlier findings is presented for three water and waste processing concepts that achieved a fair degree of maturity about fifteen years ago. These involve dry incineration processing, wet oxidation processing, and incineration-distillation processing. Although earlier comparisons were not completely convincing, conclusions led to emphasis on wet oxidation as having promise, and much of the research emphasis on water and waste processing for the past few years concentrated in this area. Detailed examinations of earlier findings and current technologies suggest strongly that a combination of electrochemical and incineration processing may have merit over techniques considered in the past. Based on these conclusions, the RECON team has been giving attention to new concepts that may have near term application to Space Station as well as to future space bases.

Although much consideration has been given to the potential of algae as a food source, many questions raised by engineering considerations have never been answered. Research during this period addressed the basic liquid properties of algae solutions that would affect pump, pipe, and storage vessel designs for algae systems. Data were obtained that indicate suitable methods exist for handling algae solutions, and physical properties produced that will allow engineering design of reasonable algae systems.

Under separate grants, experiments were continued by RECON members on aspects of plant growth under various atmospheric conditions. New data on the effects of changes in atmospheric conditions were obtained, as well as information on the control capabilities inherent in plants as response mechanisms. These data are expected to be very useful in the design of plant facilities especially suited for space conditions.

Although it may be some time before a lunar base will require the use of lunar materials as soils for plant growth, modest efforts were expended toward development of lunar simulants to be used in laboratory developments. Studies of Arctic soils and laboratory synthesis of soils based on analysis of lunar materials and known soil requirements are described.

Results of several conceptual design studies for air revitalization, water recovery, waste management, contaminant management, food production and food preparation are reviewed. While some of these concepts were based on findings of other researchers, several are new ideas generated by RECON researchers as a result of synergistic involvement with related science and engineering activities. A number of suggestions are made for further study, and basic concepts are outlined for controlling odors, monitoring contaminants, for designing plant growth chambers and space-suitable means for food preparation.

## 2. TEAM INTERACTIONS WITH OTHERS

Because of the broad scope of Life Support System research, interactions with others who are interested and involved in related activities have always been encouraged. During the reporting period, many contacts were made with NASA, industry, and university counterparts. Some of the principal interactions are noted for the record and to acknowledge the significant inputs received.

In addition to attending meetings and conducting visits to other organizations, the RECON team was pleased to have many distinguished visitors who came to Texas A&M to discuss life support system research and to see laboratory facilities. Contacts were made with collaborators which are expected to develop into cooperative relationships over a long term. Industry interests are especially vital to the transfer of technologies and to the education of future scientists and engineers.

The following summary highlights contacts with NASA, industry, and university counterparts:

1. April 26, 1988: O. Nicks, F. Little and T. Rogers were at NASA/JSC where T. Rogers presented overview of team activities to Dr. Charles Bourland, Manned Systems Division (SN).
2. May 11-12, 1988: O. Nicks and F. Little attended the Skylab Reunion at MSFC. Discussions on RECON activities were held with NASA and Boeing representatives.
3. June 9, 1988: Bill Berry and Bob McElroy, NASA/Ames Research Center and Al Behrend, NASA/JSC Crew Systems Div. visited our campus and O. Nicks led discussions about the team activities followed by visits to several labs.
4. June 14, 1988: O. Nicks and J. Holste were at NASA Headquarters for a debriefing on our Space Engineering Research Center proposal. We are planning to resubmit when the next AO is released by NASA.
5. July 11-13, 1988: O. Nicks, F. Little, M. Holtzapple, C. Patterson and J. Wagner attended the SAE ICES annual meeting in San Francisco. F. Little made a presentation to the AIAA Technical Committee on RECON activities and a visit was made to NASA/ARC.
6. July 12, 1988: T. Rogers was at NASA/JSC and visited with Clete Booher to obtain NASA Standards Doc. #3000 and other related documents. Meetings were also held with Gene Winkler of Crew Systems about the Shuttle Waste Management System and with Don Price and Charles Verotsko about ongoing studies on the Water-Waste Management system in the RECON Lab.
7. August 26, 1988: Malcolm Smith and Stan Morehead, ILC Space System Division, Houston, Texas, visited our campus and O. Nicks led discussions about cooperative relationships with industry partners who are already involved in life support systems activities with NASA. Several labs were toured and brief descriptions of activities were provided by various team members.
8. September 28, 1988: Bill Crump, M.D., University of Alabama Medical School, Huntsville, and Melvin Kilgore, Johnson Engineering, Huntsville, Alabama, were at TAMU where they explained the activities of the Consortium for the Space Life Sciences and how they are becoming involved with MSFC in Space Station activities. RECON team members provided discussions about specific research tasks in progress and how these investigations were complementary to their efforts. Plans for

further discussions are being made and at least two research proposals will be jointly developed with the Consortium in early 1989.

9. October 4-6, 1988: Some 25 Texas A&M faculty, staff and students attended the NASA/JSC Engineering Expo held at the Gilruth Center.
10. October 25-26, 1988: O. Nicks attended a Space Station Symposium and Users Workshop in Denver. Workshops included Bioscience-Life Support topics.
11. October 31, 1988: Mel Averner and Gary Coulter, NASA Headquarters and Mike Duke, NASA/JSC were at TAMU. O. Nicks led discussions on RECON program plans with various team members providing briefings emphasizing biological systems. These included:
  - Dynamic Modeling - M. Makela, H. Preisig
  - Controlling Atmospheric CO<sub>2</sub> by Regulating Plant Metabolism - B. Wright
  - Lunar Soil Simulants - R. Drees
  - Higher Plant Food Processing and Algae Processing for Edibility - J. Wagner, D. Spence, C. Patterson
  - Physical Properties of Algae Solutions for Engineering Design Studies - C. Patterson
  - Plant Physiology Experiments - T. Rogers, D. Spence, P. Sharpe, H. Wu, H. Slater
12. November 2, 1988: Al Brouillet, Harlan Brose, Jim McElroy and Dick Johnston from Hamilton Standard were at TAMU. O. Nicks presented a briefing on "Developing the University-Industry Cooperative Relationship to Support Advance Life Support Systems Technology." This material described the need for and importance of establishing a university-industry relationship, how it could be implemented, and provided five mini-proposals for work we believe might complement their task responsibilities for life support systems work at MSFC. Tours of labs emphasized physical/chemical systems and included:
  - Organic Reaction Kinetics and Catalysis - M. Holtzapple, A. Akgerman, R. Anthony
  - Evaporative Water Recovery with Catalytic Purification - T. Rogers, B. Moses
  - Electrochemistry of Organic Waste Processing - Biofuel Cells - D. Hitchens
  - Dynamic Modeling - M. Makela, H. Preisig
  - Discussions about interaction and partnership - Nicks, Little, Johnson
13. November 18, 1988: M. Makela and T. Rogers were at NASA/JSC where M. Makela made a presentation on "Models of Human Physiology for use in Space Life Sciences Research" to Laurie Webster and Frank Kutonya, Medical Sciences Div. and to S. Srinivasan, Krug International. T. Rogers provided overview discussions of how the RECON efforts will require integrations with life sciences.
14. December 6-9, 1988: F. Little attended the In-Space Technology Experiments Symposium and Workshop in Atlanta, as a member of the Life Support Working Group
15. December 16, 1988: Walter Olstad of Lockheed Missiles and Space Company was at TAMU to review status of RECON activities and to visit the RECON Lab.

## 3. COMPUTER BASED MODELING DEVELOPMENT

### 3.1 Intelligent Design Support Environment for Space Station System Engineering

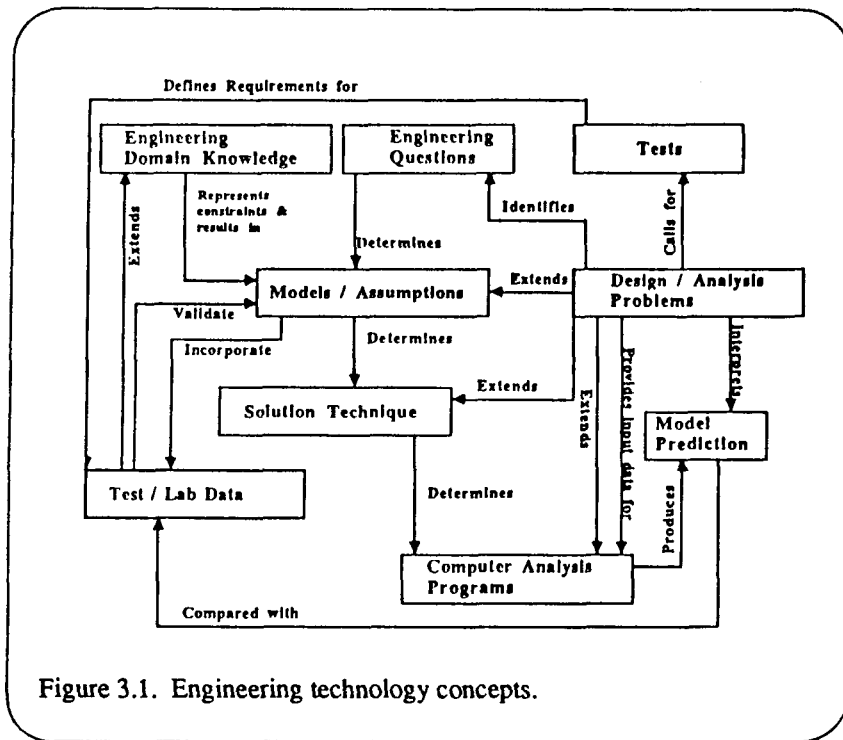
The goal of this phase of the Intelligent Design Support Environment (IDSE) component of the RECON project was to investigate the use of intelligent user interfaces for the parametrization of engineering analysis programs and the conceptualization of the IDSE requirements for engineering modeling development support. Due to near term needs of the RECON project for a steady state analysis program for the evaluation of life support system configurations, the focus of the intelligent user interfaces activities were centered around the Closed Environment Life Support System Analyzer (CELSS). The first section of this chapter addresses some of the key issues for model development support in a large scale, long term engineering project (such as the Space Station initiative). This section also establishes some basic terminology for describing the requirements for intelligent design support. The second section of this chapter documents the basic concepts behind an operational intelligent user interface for CELSS.

#### Meta-Models of the Engineering Modeling Process

The engineering process is distinguished from the scientist or technician process by the use of modeling, experimentation and analysis processes in the design process. In considering the development of an IDSE, one must consider what types of support are needed in order to facilitate the engineering modeling process as well as what types of support are needed to facilitate the construction and configuration control of designs. Understanding the engineering modeling process involves establishing a terminological basis for distinguishing at least the following:

- 1) The definition of state variables and the correspondences and relations between these state variables.
- 2) The definition of the solution process that is designed for a particular analysis need (i.e., given a set of independent and dependent variables, a set of available and unavailable variable data, and a desired set of answers; how can the correspondences and relations be manipulated mathematically or computationally to result in the desired answers.)
- 3) The software code which implements a solution process or a part of a solution process.
- 4) The definition of the design or analysis problem at hand.

Figure 3.1 displays a gross conceptual view of a part of the terminology necessary to discuss the design modeling support issues. We use the term "model" to refer to the collection of information characterized in item #1. We will use the term "solution technique" to refer to the collection of information characterized by item #2, and the term "computer analysis programs" to refer to the information characterized by item #3. Within this terminology framework the focus of the experimental software developed in this phase of the



RECON project focused on enhancing the link between the "design/analysis problems" and the "computer analysis program" (e.g. CELSS). The focus of the investigative research component of this phase of the RECON project has been on the ontology of the "model" component and on the development of a method for describing the "solution technique" component. Due to the limited time and funds available and the need for an effective CELSS modeler by the rest of the RECON team, little

progress has been made on the ontology effort.

### Complexity of the Stoichiometric Model of the CELSS

The stoichiometric model of the CELSS was designed by Dr. Mark Holtzaple. The complexity of the stoichiometric model is reflected in the complexity of the solution technique developed to describe it. The model components behind the CELSS capability include chemical reactors, storage tanks of various types, and system regulators. The chemical reactors in the system are the crew members, a waste combustor, a Bosch reactor, an ammonia synthesizer, water electrolyzer and plant growth. The system includes storage tanks for food, hydrogen, carbon dioxide, oxygen, and water. There are regulatory systems for removing nitrogen, carbon dioxide, and water from the cabin atmosphere and for purifying urine. These components are each dependent upon the other; the output of one or more will be input to one or more of the other components. To add to this complex problem, the storage tanks must be able to store any excesses to provide input to the reactors. The basic relations / correspondences between the system's components revolve around the human component in the system. The rate at which food and oxygen are used is determined by the total metabolic rate of the crew. The rate at which food is consumed determines the flow of carbon dioxide and water into the plant growth chamber. These relationships cascade down. The ammonia synthesizer produces only enough ammonia to satisfy the needs of the plant growth chamber. The waste combustor requires oxygen to burn all waste products, human or otherwise. This oxygen supply is regulated to assure that the contents of the waste combustor are burned completely. The water electrolyzer separates water into oxygen and hydrogen, and it

performs its function based upon the oxygen and hydrogen demands by the system. The analysis problem being addressed is the determination of the effect of the crew's diet on this system; e.g., what effect does a particular diet have on various reactors, separators, and storage tanks in the space station. The diets include foods taken from food stores supplemented by plants and/or algae grown in the plant growth chambers. This information would allow for the re-sizing of the various reactors and other components in the environment and/or inclusion of certain plants in the plant production component of the space station.

The solution technique whose components are described above is applied, for instance, to a particular diet. It requires extensive input in regard to the content of the diet. This input includes:

- (a) The composition of each food taken from food stores.
- (b) The composition of each plant that is provided by plant production in the growth chamber.
- (c) What percentage of the total diet is taken from food stores.
- (d) What percentage of the total diet is taken from plant production.
- (e) What percentage of the food stores is represented by each food item.
- (f) What percentage of the plant production total is provided by each individual plant.
- (g) The chemical makeup of each food and plant included in the diet.

The input to the analysis technique described above relates only to the diets to be tested. There are other parameters in the system as well. The system parameters include:

- (a) Metabolic rate of the crew.
- (b) Size of the crew.
- (c) Trash production, drink, and sweat rates of the crew.
- (d) Cabin temperature and relative humidity.
- (e) An additional six parameters that specify physical relations.

The validity of the steady state solution process was proven and a computerized implementation of the solution was written. It required the input of each of the parameters listed above, along with the composition of each of the plants and food store items present in the diet. Calculations were performed to determine the composition of the foods, plant residue, food consumed, and trash. All of this was then used to calculate the sixty sequential equations required in the steady state model. This computer program was implemented on a PC using a one shot flat user interaction style. This user interface style proves to be nearly as complicated as the problem it is designed to solve. The design of an intelligent interface to the model can make a computerized implementation of a complex analysis model much easier to use, more reliable, and produce more usable results.

## **Intelligent User Interface for the CELSS Steady State Model**

Requirements of the Interface:

The purpose of an intelligent interface to an engineering analysis program is not to produce a new solution technique, but to provide among other things easier access to, more efficient and reliable input to, and increased

output from an already proven solution technique. In short, an intelligent interface should take a complex engineering analysis method and hide the complexity from the user.

An intelligent user interface for the CELSS steady state model has been implemented on the Symbolics Lisp Machine using the Symbolics implementation of common Lisp windows and flavors. This provided the tools necessary to accomplish the goal of the project.

The primary input requirement for the CELSS analysis model is the diet. An intelligent interface should assist the diet composition and description process. The system should know the composition of the various foods and plants that compose the diet. Regarding plant production, the system should be able to separate the edible part of a plant from the residue. An intelligent interface would not have to ask for such things as the residue coefficient of the individual plants that are part of a diet. An intelligent system (where the concept of a "diet" is treated as a complete object), can automatically calculate the composition and energy content of any diet that it is given. The same applies to the composition of the trash items that are associated with a given diet. The system can calculate the composition of the trash that is to be produced by a diet unaided by the user of the system.

The system will have to obtain some information about the diet from the user. This includes the percentage of the diet to be taken from food stores. Once this information is known, the system can calculate the percentage from plant production. At a more detailed level for each plant in the diet, the system would have to be told what percentage of the total plant production the plant represents. If the food item comes from food stores, it will be necessary for the system to be told what percentage of the total food stores it represents.

Closely associated with the diet is the metabolic rate. One of the points made previously is that the stoichiometric model of the CELSS is driven by the food consumption that is necessary to maintain a given metabolic rate. Since the metabolic rate of the crew is so important in the calculations involved in the system, a user should not have to calculate this variable. The daily metabolic rate is calculated based upon a complex equation involving the time spent performing such activities, as sleeping, sitting, and light to heavy work. If the time spent in each of these activities is known, the system will be able to calculate the required metabolic rate. In the intelligent interface, the system calculates the individual metabolic rate and the total metabolic rate for the entire crew regardless of the crew size.

In an intelligent user interface, changes to the independent variables in the system should automatically be reflected in the dependent variables. This update should not be required of the user of the system. The solution technique for the CELSS steady state model requires a large number of input variables. Some of these variables, such as the total metabolic rate of the crew, depend upon the metabolic rate for each crew member as well as the size of the crew. Changes made to either of the second two variables should automatically update the total metabolic rate of the crew.

Other Input Requirements met by the CELSS system are:

Almost any computer can execute a series of equations in sequential order given the correct input. The CELSS user interface, an intelligent user interface, does more than just execute equations. One of the first

requirements of the CELSS user interface was to place some intelligence into the selection of a diet.

The higher plant model requires not just a list of available foods but two lists: one for the plant production and one for the food stores. (The food stores are the foods that are prepackaged.) The CELSS user interface allows the entry of an almost unlimited number of each of these types of food. The composition of each of the food items, whether of type food store or plant, would be entered. For the plants the composition of the non-edible residue would be entered along with the residue component for each plant. Each of these lists would exist in the computer until it is cold-booted (reinitialized). These two lists are used to select food items to make up a test diet. A list of trash types will also be defined in the same way. These lists will be referred to as the Food Stores List, the Plant Production List, and the Trash List. Each item in each list knows its identity and its chemical composition. These lists may have items added to them at any time, but the composition of the foods and trash items will not have to be reentered until the system is rebooted. For the system user, this input will be the most complex aspect of the analysis. The system depends upon its user for accurate data entry of these values. Once defined, the items in each of these three lists exist in the system as independent objects that may or may not be used during the course of a session. It is from this input that the system gets its data about the foods used in a diet. Thus, setting up a test diet has become a process that is separated from the input of the list of possible foods and plants. The user can rapidly compare several diets for a specific set of test conditions such as crew size, cabin temperature, etc.

A diet to be tested is selected from the Food Stores List and the Plant Production List. The trash associated with the diet is selected from the list of possible trash items in the Trash List. Because the system is an intelligent system it will automatically calculate the energy content for any diet it is given without additional prompting. In a step analysis, the percentage of the diet taken from food stores must also be entered.

If the expected daily schedule of activities is entered, the system will automatically calculate the crew's metabolic rate; otherwise the metabolic rate defaults to a set rate. The crew's metabolic rate is related to the size of the crew. The system will maintain all variables based upon the crew size. When the size of the crew changes, the other variables will be automatically recalculated.

In addition to meeting the special needs of the CELSS solution technique, the CELSS Intelligent User Interface meets the requirements for an intelligent interface for any engineering analysis system. This basic set of requirements for an intelligent user interface to any engineering analysis system includes the following items:

- (a) Simplify data input and eliminate user input errors if at all possible.
- (b) When possible the same input data should not have to be repeatedly reentered.
- (c) System variables should have reasonable, usable, and changeable defaults.
- (d) Minimize the number of commands that are necessary to run a system.
- (e) Graphical as well as textual displays should be provided.
- (f) Printed output should be available.
- (g) A system should provide easily accessible on-line help.

Those requirements from above as applied in the CELSS system are:

Data input should be simplified to prevent user input errors. In the intelligent CELSS interface this has been accomplished in several ways. One of the ways that an interface can prevent user input errors can be described by examining the input of the daily schedule. (The daily schedule is used in the calculation of the individual metabolic rate.) The CELSS interface knows that a daily schedule will consist of not more or less than 24 hours. In the input of a daily schedule the input a of number of hours not equal to 24 is not allowed. The command will not complete unless the total number of hours equals 24. The system knows what a reasonable or acceptable answer is and will not accept input that falls outside the predetermined range of acceptability. Another means of assuring correct or acceptable input is to check the state of the system before allowing certain commands to execute. Although the user of a system can "abort" a command if he or she determines that the required data is not present in the system, this means of obtaining correct input is not satisfactory. A secure system should not require this of the user. In the CELSS user interface the commands check to determine if the necessary information is present before attempting to execute. In this manner, the system will not get an abnormal termination because of insufficient or invalid data.

User data entry errors can also be decreased by commands that are easy to issue to the system. One of the most helpful features implemented in the CELSS analyzer was a mouseable menu (See Figure 3.2). At the top of the screen, there, is a menu that lists the necessary commands in alphabetical order. This has the effect of having the available commands easily visible and quickly accessible by the user at all times.

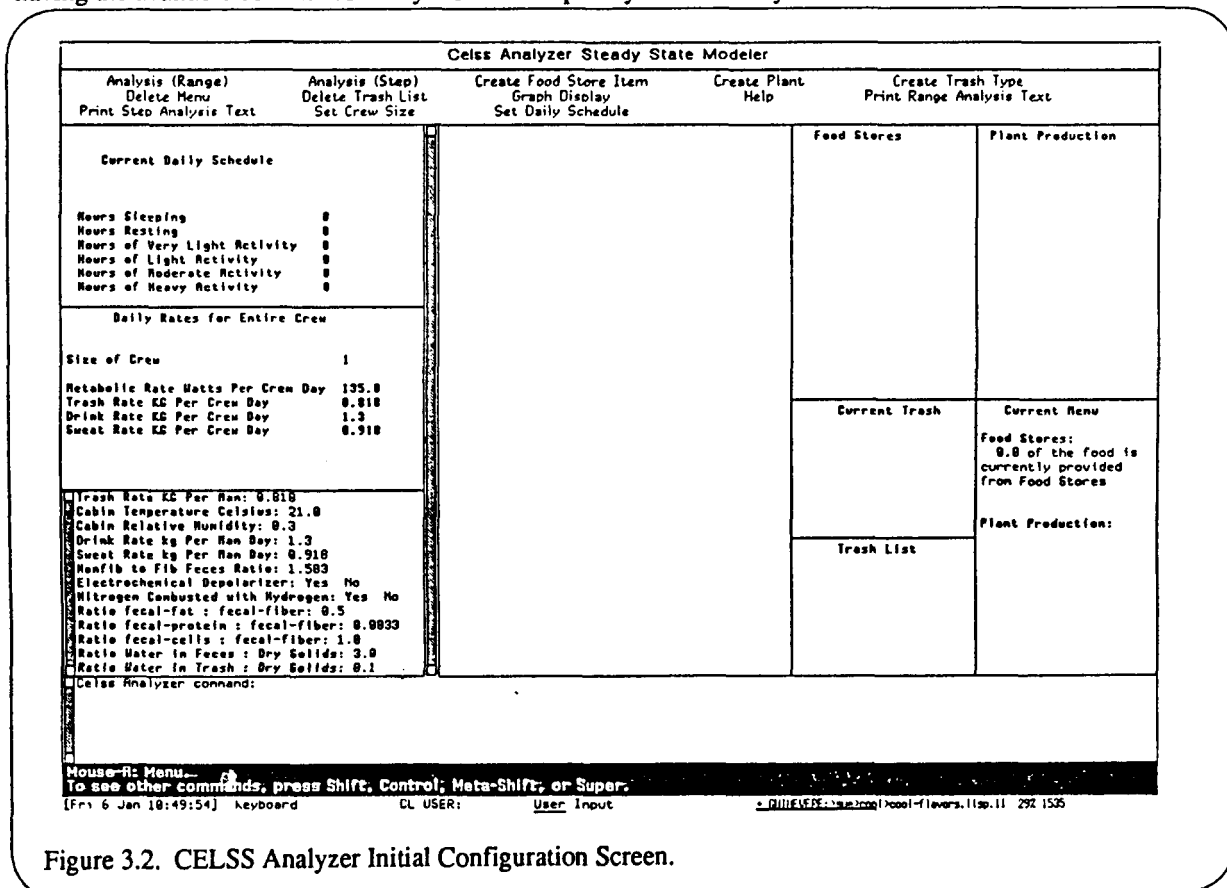


Figure 3.2. CELSS Analyzer Initial Configuration Screen.

When possible, the same input data should not have to be reentered. Using the intelligent CELSS system it is possible to keep a diet and change some or all of the other parameters in the system. The user of the CELSS solution technique may wish to test the same diet several times changing different variables each time. For instance, compare the results for a particular diet with and without an electrochemical depolarizer. The intelligent CELSS user interface remembers its previous diet and all of the other system variables, including whether or not it used an electrochemical depolarizer. To test the effect of the electrochemical depolarizer on the system, the CELSS analyzer user changes one variable and issues the command to run the analysis.

System variables should have reasonable, usable, and changeable defaults. Most of the system parameters are constantly visible and accessible to the CELSS interface user. Examples of these are the metabolic rate of a crew member, crew size, cabin temperature, and approximately fifteen other parameters of this type. The system has defaults for each of these, and the user may choose to change some, but not others. Those that are not changed by executing some command in the main menu are available directly in a smaller on-line menu. Changes to any of these variables will result in an automatic update of any dependent variables in the system.

An intelligent user interface minimizes the number of commands that are necessary to run a system to prevent errors. In the CELSS interface this was done by combining several commands into one. The analysis commands are those that represent the combining of several commands into one. There are two analysis commands "Analysis(Range)" and Analysis(Step)". The analysis requires one or more diets and a set of trash items associated with the diets. As part of the execution of each of these commands, the system will prompt for the diets to test, the percentages represented by each food item, trash associated with the diet, and, in the case of the step analysis the percentage of food taken from food stores. The system does not rely on the user to remember to enter this data, it knows it will need the information so it asks for it. The range command will execute the steady state process model ten times for the diets input. The analysis makes the calculations for each diet consisting of from 0% to 100% plant production in increments of 10%. The Step Analysis executes the steady state process model once and for only one diet.

The CELSS solution technique is first and foremost an analysis program. Analysis programs should provide graphical as well as textual displays. The intelligent interface to the CELSS solution technique provides both. The textual displays are provided for the step analysis and graphical for the range analysis. Printed output is available for the results produced by each of these two commands.

In the CELSS user interface there are two different configurations. These are the initial configuration and the range configuration. The initial configuration is used to obtain the input for the analysis, and for the display of the results when a step analysis is performed. (See Figure 3.2). All of the user input is handled in this configuration.

The range configuration is used for graphical display only and is automatically displayed when the range analysis command is executed. When the command "Range Analysis" completes execution the system switches to the range configuration (See Figure 3.3). In this configuration there are six small screens. In one of these screens the diet or diets under investigation are displayed, and in the others the graphs of the results of the range

ORIGINAL PAGE IS  
OF POOR QUALITY

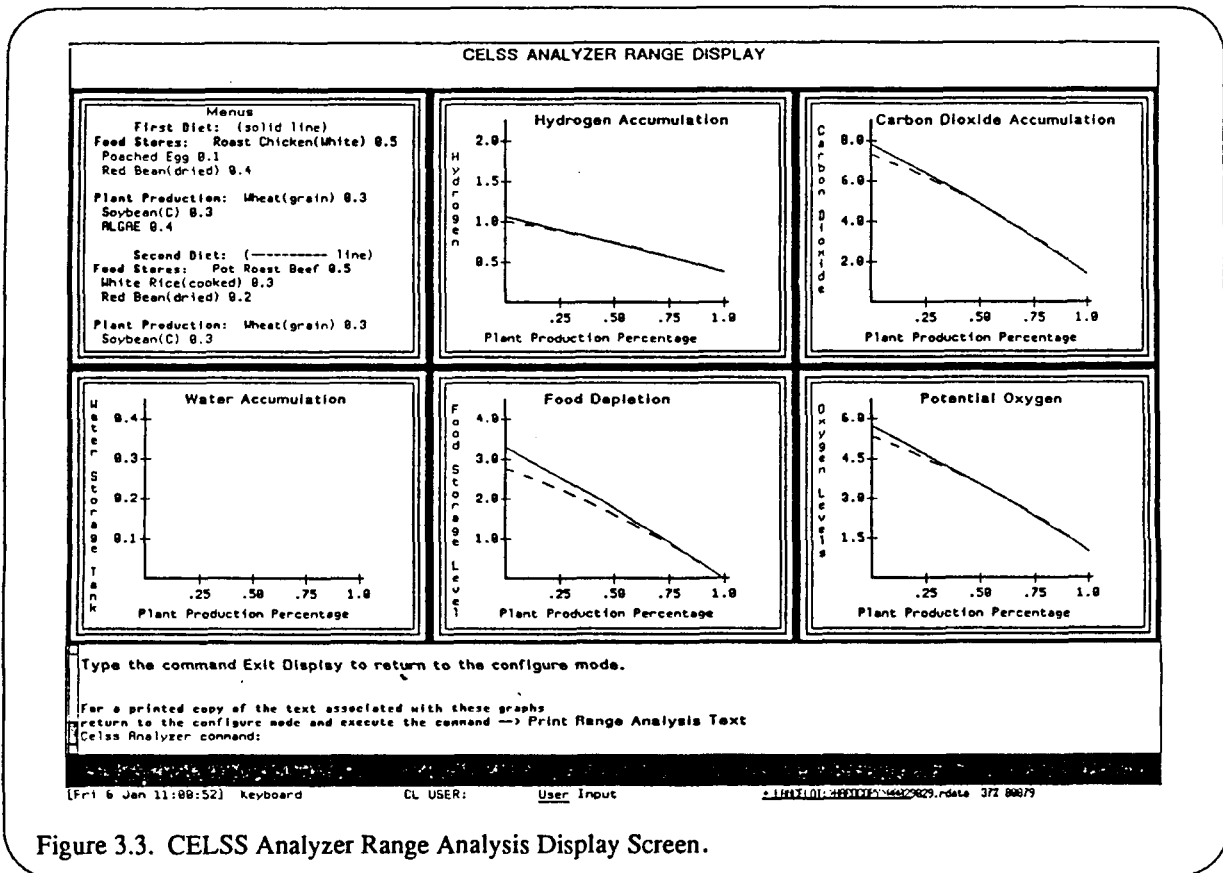


Figure 3.3. CELSS Analyzer Range Analysis Display Screen.

analysis are displayed. The graphs are as follows: Hydrogen Accumulation, Carbon Dioxide Accumulation, Water Accumulation, Good Depletion, and Potential Oxygen.

With any computer program, the new or infrequent user has difficulty remembering or knowing what process to follow. This more than any thing can keep the user from using a more efficient method for approaching the solution to the task. An intelligent user interface should address this issue with context sensitive and user tailorable help. One of the commands available in the Command Menu is "Help"(See Figure 3.4). This Help facility, accessible from the main menu, provides a listing of the available commands and instructions on how to run the system. The instructions remain on the screen. The screen, in which the help is displayed is scrollable. Once the help has been displayed it remains readily available on the screen.

## Conclusions

In the course of this phase of the Recon project we designed, verified and implemented an intelligent user interface for the stoichiometric model of the CELSS. This effort required rehosting and revisions/extensions to the basic solution method. The resulting product represents a usable engineering analysis capability for use in the design of environmentally closed life support systems. We also characterized the features and requirements

ORIGINAL PAGE IS  
OF POOR QUALITY

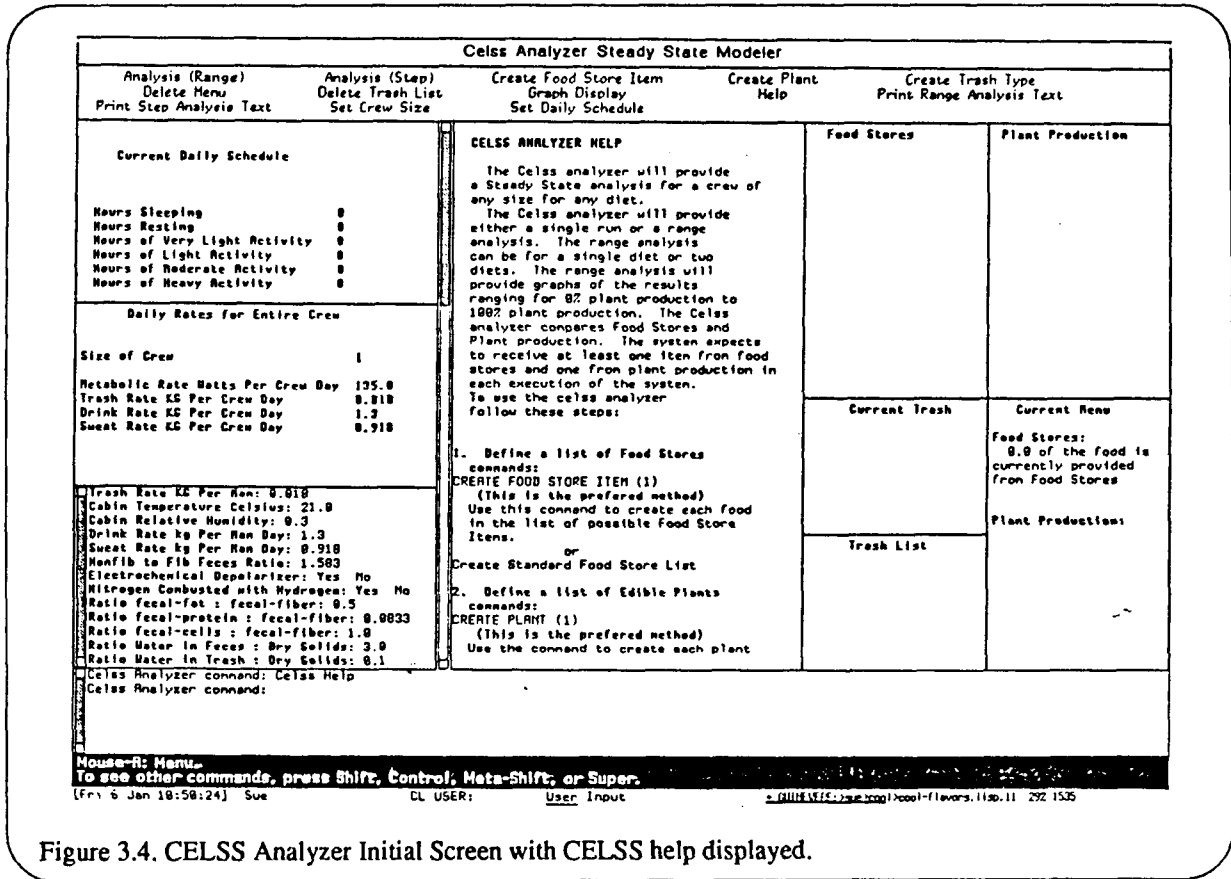


Figure 3.4. CELSS Analyzer Initial Screen with CELSS help displayed.

for such engineering analysis system intelligent interfaces. This characterization can be used to guide future engineering modeling and analysis support interfaces. It also establishes some of the basic support requirements of the IDSE. Finally, during this project we initiated the development of the IDSE architecture and the engineering modeling ontology needed to populate the conceptual schema of that architecture. The system architecture which has evolved from this effort is referred to as a "design knowledge management system" (DKMS). This environment has the facilities to support knowledge based design support tools (e.g., CELSS) as well as design data integration and design data management and control. A conceptual view of this DKMS is illustrated in Figure 3.5. The primary focus of the next phase of this effort will be the development of a prototype of that concept.

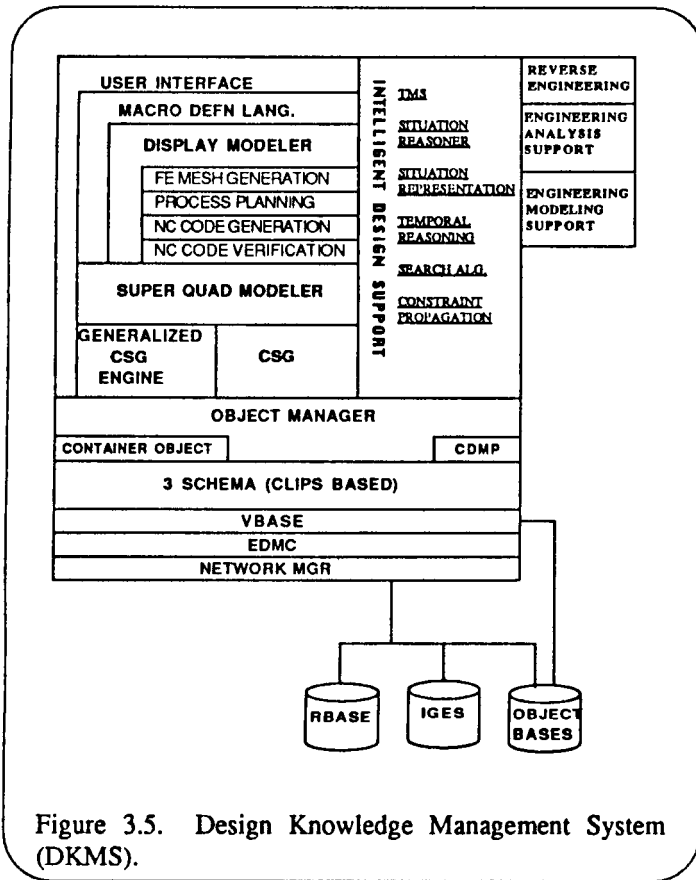


Figure 3.5. Design Knowledge Management System (DKMS).

## 3.2 Representation of Physical-Chemical-Biological Systems (PCBS)

### Introduction

The ultimate objective of designing life support systems is to regenerate all matter required to sustain human life in space. The main recycle streams are air, water and food. Since these systems are designed for long-term missions, the major design objective is to close the space unit with respect to mass importing energy only. However, this ideal goal is not the only one. Other requirements which affect the design are reliability, controllability and robustness.

Reproduction of air, water and food from the waste produced by the humans requires a number of different units. In general, the system will include separation units, chemical reactors of various types, biochemical reactors and plant chambers. It can also be expected that the various reproducing recycle loops are not independent but to the contrary, a very high degree of integration must be expected because the regenerative task could be regarded as the task of inverting the highly integrated human being.

A number of subsystems have not only been designed in the past, but have also been realized and tested in the laboratory, such as the celebrated RITE system described in this and previous reports. The development of a fully integrated system is still in its infancy; one of the main problems being to select a number of units which come closest to the ultimate objective of closing the system. No systematic approach to generating alternatives has yet been attempted, but the number of alternatives can be expected to be extremely large. The means of generating alternative model systems is currently quite primitive. Basically every model system is fully coded into a program for simulation. Correspondingly time consuming is the selection process. The situation becomes even worse if the selection process is refined by examining the systems from other, different viewpoints, such as requiring not only the highest possible closure or closure with respect to certain components, but also criteria related to the operation of life support systems, such as greater reliability, controllability or robustness. To investigate these properties of each alternative requires dynamic models with more or less details. Even on the level of very primitive model systems with only a moderate number of base units (20 to 30), documentation becomes progressively more difficult and extensive as the number of units increases. It is correspondingly difficult for the user to maintain a survey of his work. The approach of specialized code becomes very quickly unmanageable. Consequently, the objective of generating a modeling tool has been formulated: tools should aid the user in defining complex model systems quickly, achieve a high level of documentation, and generate desired target codes that can then be embedded into different environments such as existing simulation or design packages.

The existing commercial tools which are used to simulate the behavior of chemical plants are called flow sheeting programs. Most of them are designed to solve steady-state mass and energy balances which in the long run, for above mentioned reasons, will not be sufficient for the design of life support systems. Also, these systems are unit oriented, meaning a software module will generally represent a physical unit such as a reactor or separation unit. No real hierarchical modeling tool has yet been generated in this commercial environment.

The degree of flexibility is therefore low. Also, the user interfaces are very specific and in most instances very user unfriendly. Most large programs actually require a specialist to operate them. Depending on the selection criteria, detailed dynamic process models will be required which will very quickly cause an increase of complexity to the extent that it will not be possible to maintain and document the models without supporting tools such as data bases and a modeling aid which helps to build complex hierarchical models from simple generic building blocks. Based on these views and arguments, the objectives for a modeling and design package have been derived which for the current period were defined as follows in the next section.

## **Objectives for this Period**

By their nature, life support systems are PCB systems of considerable complexity. One of the major problems is to find basic building blocks which are suitable for describing these complex systems. This type of generic approach is found in Systems Theory, an applied mathematics discipline which, as its main object, seeks to investigate and design systems, mostly dynamic systems, of any kind. State space representation is one of the very well accepted mathematical forms used to represent dynamic systems. Established in the late fifties and mostly developed during the sixties and early seventies, it is based on generalized principles such as generalized Newtonian physics and axiomatic thermodynamics. These approaches were used in our research.

In the first few periods of research on life support systems (LSS), modeling was mainly done in two ways, namely the classical chemical engineering approach and the knowledge-based approach. The chemical engineering effort was based on formulating and solving steady-state mass balances of a hypothetical topology of units and the knowledge-based approach resulted mainly in a discrete time-step using the IDEF0 tool. The latter two simulations were both based on the chemical engineering steady-state model. The three approaches, even though they look quite different, produce--from the technical point of view--very similar results. The objective of the effort reported here was to carefully examine the three approaches and to establish a solid theoretical base for future work in this field.

Research concentrated on representing physical-chemical-biological systems PCBS in two ways, namely a generalized discipline specific representation, referred to as the engineering representation (ER), and a system theoretical representation, referred to as the state space representation (SSR).

The software tools to be developed will use the ER to interface with the user "engineer" since it is the language the engineer talks and the SSR will be used as the basis for the internal representation to manipulate the mathematical model objects because the design and interpretation of the manipulations is better supported in the more abstract SSR.

## **Achievements in This Period**

The main goals have been achieved, namely:

- The engineering representation (ER) has been clarified and generalized to the degree that a very wide class of systems fits into the resulting framework. This work has been developed to the

extent that first thought experiments have been undertaken towards a design of a formal language which could be used to adequately represent the basic objects in a computer-oriented language.

- Mappings for the transition of ER into state-space representation (SSR) have been defined based on system theoretical principles. The maps consist of a definition of a state, input and output vector for every subsystem. Since these definitions are not unique, they have been chosen such that the resulting SSR matches a particular mathematical structure which for lumped systems is the standard first order dynamic systems:

$$\text{state propagation: } V \{ \dot{x} \} = V \{ f \} (V \{ x \}, V \{ u \}),$$

$$\text{the dynamic equation output: } V \{ y \} = V \{ g \} (V \{ x \}, V \{ u \}),$$

the stationary equation

- The chemical system has been separated as a separate system from the physical flow system.
- The steady-state model reported in the previous progress reports has been analyzed for completeness. Conditions for the existence of solutions to steady-state mass balance systems have been examined.

## Some Problems with PCB System Representation

Some of the problems one faces when representing PCB systems are best explained by a simple example. Let us assume that the prototype (the system to be modeled) consists of two ideally stirred tanks standing side-by-side. The two tanks are connected by a pipe attached at the bottom of both tank 1 and tank 2. Tank 1 receives its supply from a pipe discharging fluid into the top of the tank. Tank 2 has an outlet in its bottom. For simplicity, both tanks are cylindrical with constant cross sectional area. By formulating simple total mass balances for each tank and the coupling equation, the model describing the levels in the two tanks is easily found:

$$\text{mass balance tank 1} \quad \dot{m}_{1,0} = \dot{m}_{11} + \dot{m}_{12}$$

$$\text{mass balance tank 2} \quad \dot{m}_{2,0} = \dot{m}_{21} + \dot{m}_{22}$$

$$\text{connection equation} \quad \dot{m}_{12} = - \dot{m}_{21}$$

where

$\dot{m}_{k,0}$  :: the accumulation of mass in the tank  $k \in \{1,2\}$

$\dot{m}_{kj}$  :: the mass flow rate in stream  $j \in \{1 :: \text{inflow}, 2 :: \text{outflow}\}$  of tank  $k$

Providing the following assumptions hold for the mass transfers:

$$(I) \quad \dot{m}_{k,0} = \rho h_k A_k$$

$$(II) \quad \dot{m}_{12} = -\alpha_2 (h_1 - h_2)$$

$$(III) \quad \dot{m}_{21} = -\alpha_3 h_2$$

where

- $\rho$  :: density of the fluid
- $h_k$  :: level in tank  $k$
- $A_k$  :: cross sectional area of tank  $k$
- $\alpha_k$  :: proportionality constant

one finds that the transfer of fluid from one tank to the other depends on the levels in the two tanks. Modeling the tanks as individual units and connecting them together would therefore depend on the knowledge of the nature of the particular connection and could not be done independently of the other system. At first, it seems that the two other streams, namely the streams 1 and 3, are different. Stream 1 seems to be given and seems not to depend on the level in tank one whereas stream 3 depends only on the level in tank 2. Examining the nature of these two transfers in more detail reveals that intrinsic assumptions have been made about the nature of the connecting systems, namely that the pressure at the end of these pipes has no effect on the flow rate or, in other words, that the pressure difference between the two ends of each pipe is given for the stream 1 and, in case of stream 3, is only related to the level in tank 2.

Applying this point of view to other systems and different transfer phenomena one finds that each transfer is in general a function of the states on both sides of the system boundary. Two disciplines, thermodynamics and transport phenomena, deal with this subject. In particular axiomatic thermodynamics emphasizes the systems approach which will be the approach followed when generalizing the modeling of PCBS.

## Generalized Engineering Representation of PCBS

For reasons of simplicity of the following treatise, the discussion shall be limited to lumped systems. The extension into distributed systems is straightforward and will be discussed in a later report.

**Definition-Simple Lumped System:** Finite spatial domain separated from the universe by a closed boundary. The conditions and properties inside the closed boundary are uniform and independent of the location in the domain of the system. The system shall be physically realizable and non-anticipatory.

The models for lumped PCBS are based on the conservation of extensive properties which is formulated in the following postulate:

**Postulate:** All extensive quantities of a system are conserved.

Since the extensive properties are additive, the mathematical form of the conservation of the extensive quantity<sup>1</sup>  $\phi_e$  of subsystem  $s$  on level  $l$ , which ultimately is composed of simple lumped systems on level  $l = 1$ , is represented by the equation:

$$\dot{\phi}_{e,0,s,l} = \sum_{j \in \mathcal{S}} \dot{\phi}_{e,j,s,l} + \sum_{r \in \mathcal{R}} \dot{\phi}_{e,r,s,l}$$

where

$\dot{\phi}_{e,j,s,l}$	:: Extensive quantity $e$ in stream $j$ of system $s$ on level $l$
$\dot{\phi}_{e,0,s,l}$	:: Accumulation of extensive quantity in the system (stream 0)
$\dot{\phi}_{e,j,s,l}$	:: Flow of extensive quantity associated with stream $j$
$\dot{\phi}_{e,r,s,l}$	:: Production rate of extensive quantity associated with reaction $r$
$\mathcal{E}$	:: Index set of extensive quantities; $e \in \mathcal{E}$
$\mathcal{S}$	:: Index set of streams; $j \in \mathcal{S}$
$\mathcal{R}$	:: Index set of reactions; $r \in \mathcal{R}$
$\mathcal{F}$	:: Index set of sub-systems; $s \in \mathcal{F}$
$\mathcal{L}$	:: Index set of levels; $l \in \mathcal{L}$

The left-hand side of this equation describes the accumulation of the extensive quantity in the system defined as the hierarchical level  $l$ . The terms in the first summation represent the different transfer rates of  $\phi_e$  across the boundary defining the system and the terms in the second summation describe the net rate-of-production associated with reaction  $r$ .

As was demonstrated in the introductory example, the transfer of the extensive quantity is in general a function of the states of the two connected systems. From this fact a major question arises, namely how should a software tool support a modular approach to system modeling; do the modules, which each represents a sections of an overall PCBS model, pre-define the possible connections or are they only defined at the time the connections with another subsystem are actually established? Choosing an approach which defines an exchange of extensive quantities with the environments before the actual connection to that environment is established would mean that prefabricated, typed connections are defined which could only be matched by an identical connection defined in another subsystem. Libraries of such modules would consequently be of limited use, which can be seen from the following example. Assume that we have a set of building blocks which connect to each other by the means of connectors. Now assume additionally that not only one type of connectors is defined but a set of incompatible connectors. It is obvious that the set of structures that can be built with a set of blocks equipped with different incompatible connectors is smaller than the set of structures that could be constructed from a set of blocks with compatible connectors. This suggests choosing a different approach which defines the transfer description, namely the connection, only at the time the connection is

---

1. Note that the sign of the extensive quantities indicates the direction of flow relative to the system.

actually established between the different modules.

As implied above, the tool is intended to support a hierarchical modeling approach in which a group of connected modules could be assigned to constitute a new object on the next higher level. Applying this idea recursively, a general, arbitrary hierarchical system structure is obtained which consists of primitive models, namely simple lumped and simple distributed systems, as its base. Analysis of this approach reveals the fact that the formation of higher-hierarchical modules does not affect the mechanism of connecting. The links are always introduced on the lowest level because ultimately every module, independent of its definition level, consists of base systems. These ideas form a consistent framework for system internal connections but raise the question of how to define the inputs and outputs of the global system. In view of the use of the model for simulation, optimization and other purposes, the system inputs and in some applications also the system outputs are predefined as a function of time, or manipulated by a mechanism that depends on the particular application. In any case, the relevant connections to the environments are, so-to-speak, connected to other blocks or modules which either generate a function to be used as a system input or output or are connected to a method specific module which provides this information.[1] Again, the suggested approach would apply. No generic problem arises in the definition of the system inputs and outputs since they are connected to the base simple models in the same way as are all the other internal connections.

Examining the existing tools such as flow-sheeting programs, which are used to represent and simulate chemical plants, one finds that they follow the approach of prefabricated modules with given connectors. As a matter of fact only a very few types of connectors are usually supported, the main one being a connection representing a physical pipe. The modules included in the libraries shipped with these packages are for these reasons usually describing a set of process units with more or less details. This is in contrast with our suggested approach which would support any connection that can be expressed in the ER and no assumption is therefore made about the relation between the type of physical system that is mapped into one base module. (Again, the lumped and distributed simple systems are the base module.)

## Extensive Properties and States

So far the discussion on modeling a PCBS has been based on general extensive properties. But in practice, what are these extensive properties? The main extensive properties utilized for modeling PCBS are mass, energy, momentum and charge which are listed in decreasing frequency of use. The conservation principles form the core of a PCBS model which is then supplemented with the transfer laws, empirical correlations for physical properties, kinetic laws and other mostly empirical relationships that complete the overall picture. Even though the state is in general an artifact that can be chosen to meet defined needs, it is quite common to choose physical variables such as pressure, temperature and composition to capture the information about the present state of the system. These variables shall also be the choice in the following discussion. The transfer of information shall be discussed later.

The ER shows nicely the connection between the different elements related to the real-world connections. However, the mathematical structure stands out more when mapping this ER into a SSR which has a long tradition in serving as the base representation for analysis, synthesis and design. The mapping between the two representations is defined by the definition of the *state*, *input*, *output* and *parameters*.<sup>2</sup> The state of a system incorporates the quantities affected by changes in the environment of the system. Inputs are the quantities of the environment that, by changing, affect the state of the system. The outputs are those variables in the system that, by changing, affect the state of the environments and additionally those variables of the system that are connected in any other way to an information system such as an outside observer.

The state concept of mathematical system theory is based on a generalization of the classical physics and thus, the initial choice of a set of state variables that make up the state vector of a system is a set of physical variables as already mentioned, namely, pressure, temperature and composition. Although Thermodynamics actually uses the term *state* in this connection, state space theory has not caught on in thermodynamic circles.

The state representation of the introductory example is found easily: The state of the two tanks with respect to their contents is either described by the mass or the volume in the tanks. Since it was indicated that the level is of interest, the two levels can be chosen as the state variables and because of the assumption of a constant cross sectional area of each tank and the assumptions(i)-(iii), the result is a very simple set of equations

$$\begin{aligned} \dot{x}_1 &= -p_1(x_1 - x_2) + p_2 u_1 \\ \dot{x}_2 &= p_1(x_1 - x_2) + p_3 x_2 \end{aligned}$$

where

$$\begin{aligned} \mathbf{x} &:= [h_1, h_2]^T \\ \mathbf{u} &:= [V] \\ \mathbf{y} &:= \mathbf{x} \\ \mathbf{p} &:= [\alpha_2/A_1, \alpha_2/A_2, \alpha_3/A_2]^T \end{aligned}$$

In this particular case the notation can be compressed further because this model is linear in the states. In matrix notation the model is

$$\begin{aligned} \dot{\mathbf{x}} &= \underline{\mathbf{A}}\mathbf{x} + \underline{\mathbf{B}}\mathbf{u} \\ \mathbf{y} &= \mathbf{x} \end{aligned}$$

Let us now turn our attention to another example chosen to illustrate the mapping of a system with chemical reactions. The example is a classic: the ideally-stirred jacketed tank reactor.

---

2. Note that the two terms *input* and *output* are used in two ways, in the ER as flows of extensive property and in SSR as flows of information.

The model of the contents in the ER consists of a set of component mass balances and the energy balance which is usually reduced to the enthalpy balance since the change in potential and kinetic energy is negligibly small compared to the other terms. For a general set of reactions, the mass balance for the species  $i$  is

$$\dot{n}_{i,0} = \sum_{\forall j \in \mathcal{M}} \dot{n}_{i,j} + \sum_{\forall r \in \mathcal{R}} \dot{n}_{i,r} \quad ; \forall i \in \mathcal{A}$$

where

- $\dot{n}_{i,0}$  :: accumulation of molar mass in the system
- $\dot{n}_{i,j}$  :: molar flow of species  $i$  in stream  $j$
- $\dot{n}_{i,r}$  :: molar production rate of species  $i$  from reaction  $r$
- $\mathcal{M}$  :: index set of mass streams;  $j \in \mathcal{M}$
- $\mathcal{A}$  :: index set of species;  $i \in \mathcal{A}$

and the enthalpy balance:<sup>3</sup>

$$\dot{H}_0 = \sum_{\forall j \in \mathcal{M}} \dot{H}_j + \sum_{\forall j \in \mathcal{Q}} \dot{q}_j + \sum_{\forall j \in \mathcal{W}} \dot{w}_j$$

where

- $\dot{H}_0$  :: accumulation of enthalpy in the system
- $\dot{H}_j$  :: enthalpy flow associated with the mass flow stream  $j$
- $\dot{q}_j$  :: heat stream  $j$
- $\dot{w}_j$  :: work stream  $j$
- $\mathcal{Q}$  :: index set of heat streams;  $j \in \mathcal{Q}$
- $\mathcal{W}$  :: index set of work streams;  $j \in \mathcal{W}$

The flows represent the connections to the environments in the form of flow through pipes. The production rate of molar mass is the reaction rate per unit volume times the volume of the contents. The reaction rates are usually given in the form of power laws with one or two concentrations being raised to powers of 0 through 2. The proportionality constant is called the reaction constant and is known to be a strong nonlinear function of the temperature. The Arrhenius function is frequently applicable: it relates the reaction constant with an exponential function to the temperature.

For the sake of modularity, we have tried to find a state-space representation which retains the separation of reaction kinetic equations and the mass and energy balance of the contents. It is hoped this approach will increase the flexibility of manipulating the objects later in the project.

---

3. Note again that the signs of all directional quantities are relative to the system.

Returning to the example and limiting the discussion to the standard case by assuming ideal solutions and constant volume in the tank, the mass and enthalpy balances can be rewritten as follows :<sup>4</sup>

$$V_0 \dot{c}_{i,0} = \sum_{\forall j \in \mathcal{M}} V_j \dot{c}_{i,j} + \sum_{\forall r \in \mathcal{R}} n_{i,r}$$

$$\dot{H}_0(T_0, \underline{c}_0) = \sum_{\forall j \in \mathcal{M}} \sum_{\forall i \in \mathcal{A}} V_j h_{i,j}(T_j) \dot{c}_{i,j} + \sum_{\forall j \in \mathcal{Q}} \dot{q}_j + \sum_{\forall j \in \mathcal{W}} \dot{w}_j$$

where

- $\dot{c}_{i,0}$  :: change of concentration of specie  $i$  in the system
- $V_0$  :: volume of the system
- $V_j$  :: volumetric flow rate of mass stream  $j$
- $\underline{c}_0$  :: concentration vector, system
- $T_0$  :: temperature of system
- $T_j$  :: temperature in mass stream  $j$
- $h_{i,j}$  :: specific enthalpy of specie  $i$  in mass stream  $j$

Introducing the standard enthalpies (enthalpies at some standard conditions), and the enthalpy differences as the difference between the enthalpy at the process conditions and the standard enthalpies, the enthalpy balance can be reformulated to yield:

$$\Delta \dot{H}_0(T_0, \underline{c}_0) = \sum_{\forall j \in \mathcal{M}} \sum_{\forall i \in \mathcal{A}} V_j \Delta h_{i,j}(T_j) \dot{c}_{i,j} + \sum_{\forall j \in \mathcal{Q}} \dot{q}_j + \sum_{\forall j \in \mathcal{W}} \dot{w}_j + \sum_{\forall r \in \mathcal{R}} (-\Delta h_r(T^0)) \xi_{i,r}$$

Now define the equations describing the chemical stoichiometry and the reaction kinetics occurring in the tank:

$$\sum_{\forall i \in \mathcal{A}} \nu_{i,r} A_i = 0$$

and

$$r_{i,r} = \frac{\nu_{i,r}}{|\nu_{i,r}|} k_r \prod_{\forall i \in \mathcal{A}} (c_{i,0})^{\alpha_{i,r}}$$

and represent the Arrhenius relation as a differential equation:

$$\frac{dk_r}{d1/T} = \gamma k_r \quad ; k_r(0) = k_r^0$$

where

- $\nu_{i,r}$  :: Stoichiometric coefficient for species  $i$  in reaction  $r$
- $A_i$  :: specie  $i$
- $r_{i,r}$  :: reaction rate for species  $i$  in reaction  $r$

---

4. Again, the flow direction is relative to the system.

$k_r$	:: reaction constant for reaction $r$
$\alpha_{i,r}$	:: power coefficient for composition of species $r$ in reaction $r$
$\Delta h_r$	:: reaction enthalpy
$\gamma$	:: exponential factor
$k_r^0$	:: pre-exponential factor
$\xi_{i,r}$	:: extent of reaction for specie $i$ in reaction $r$

By expanding the left-hand side of this equation, the time derivative of the temperature can be isolated. Defining the extent of reaction  $\xi$  by

$$\xi_r := \frac{r_{i,r}}{v_{i,r}} V_0$$

The production rate of species  $i$  in reaction  $r$  is then

$$\begin{aligned} n_{i,r} &= \xi_r v_{i,r} \\ &= V_0 r_{i,r} \end{aligned}$$

Assuming that the enthalpy accumulation is only a function of the temperature or, in other words, the effect of changing concentration is negligible, the change of the system temperature can be readily calculated. Since thermodynamics defines the derivative of the enthalpy with respect to temperature at constant pressure as the heat capacity of the system (if normalized the specific heat capacity) the enthalpy balance reads:

$$T_0' = \frac{1}{V_0 C_p} \sum_{\forall j \in \mathcal{X}} \sum_{\forall i \in \mathcal{A}} V_j \Delta h_{i,j}(T_j) c_{i,j} + \sum_{\forall j \in \mathcal{Q}} q_j + \sum_{\forall j \in \mathcal{W}} \dot{w}_j + \sum_{\forall r \in \mathcal{R}} (-\Delta h_r(T^0)) \xi_{i,r}$$

where

$C_p$  :: heat capacity of the contents

For simplicity, it is further assumed that no work stream crosses the system's surface and that only one heat transfer occurs in the system namely between the jacket and the contents. The heat transfer is modeled by:

$$q' := -a(T_0 - T_j)$$

where

$T_j$  :: jacket temperature

$a$  :: heat transfer parametric

The number of flow streams is also limited to one in and one out for the same reasons. Thus the enthalpy balance becomes

$$T_0' = \frac{1}{V_0 C_p} \sum_{\forall j \in \mathcal{M}} \sum_{\forall i \in \mathcal{R}} V_j \Delta h_{i,j}(T_j) c_{i,j} + a(T_0 - T_j) + \sum_{\forall r \in \mathcal{R}} (-\Delta h_r(T^0)) \xi_{i,r}$$

At this point the physical and the chemical system can be mapped into the state space. Both systems assume the same mathematical form (one of the objectives), namely:

$$\begin{aligned} \dot{\mathbf{x}} &= \mathbf{f}(\mathbf{x}, \mathbf{u}, \mathbf{p}) \\ \mathbf{y} &= \mathbf{g}(\mathbf{x}, \mathbf{u}, \mathbf{p}) \end{aligned}$$

• **Physical System:**

**Description:** Ideally-stirred tank with a jacket, one inflow and one outflow

**Assumptions:**

- (i) ideally stirred : one uniform internal system
- (ii) no change in potential energy
- (iii) no change in kinetic energy
- (iv) constant volume
- (v) accumulation term in enthalpy is a function of temperature only
- (vi) only one in and one out flow
- (vii) overall heat transfer law
- (viii) ideal mixtures
- (ix) no volume effects (in flow = out flow)

**Notation:**

- $V_0$  :: system volume
- $\mathbf{c}_0$  :: concentration vector, system
- $T_0$  :: system temperature
- $V'$  :: volumetric flow rate in and out
- $\mathbf{c}_{in}$  :: concentration vector, input stream
- $T_{in}$  :: temperature of input stream
- $T_j$  :: jacket temperature
- $\xi_r$  :: extent of reaction
- $C_p$  :: heat capacity of contents
- $h_{i,j}$  :: specific enthalpy of specie  $i$  in stream  $j$
- $\Delta h_r$  :: heat of reaction

$$\begin{aligned}\underline{\xi} &:= [\xi_r]_{\forall r} \\ \underline{H} &:= [h_{i,j}(T_j)]_{\forall i;\forall j} \\ h_r &:= [-\Delta h_r]_{\forall r}\end{aligned}$$

**Mappings:**

$$\begin{aligned}\text{State} &: \mathbf{x} := [T_0, \underline{c}_0]^T \\ \text{Input} &: \mathbf{u} := [V, \underline{c}_{in}^T, T_{in}, T_J, \underline{\xi}^T]^T \\ \text{Output} &: \mathbf{y} := [\underline{x}^T, V]^T \\ \text{Parameters} &: \mathbf{p} := \{V_0, C_p, \underline{H}, h_r^T, \alpha\}^s\end{aligned}$$

• **Chemical System:**

**Description:** General irreversible chemical reaction system

**Assumptions:**

- (i) power law for kinetic rates
- (ii) Arrhenius for temperature dependency of reaction constants
- (iii) homogeneous reaction system

**Notation:**

$$\begin{aligned}V_0 &:: \text{system volume} \\ \underline{c}_0 &:: \text{concentration vector, system} \\ T_0 &:: \text{system temperature} \\ V &:: \text{volumetric flow rate in and out} \\ \xi_r &:: \text{extent of reaction} \\ \underline{\xi} &:= [\xi_r]_{\forall r} \\ \underline{N} &:= [N_{i,r}]_{\forall i;\forall r} \\ \mathbf{k} &:= [k_r]_{\forall r}\end{aligned}$$

**Mappings:**

$$\begin{aligned}\text{State} &: \mathbf{x} := [\underline{\xi}^T, \underline{k}^T]^T \\ \text{Input} &: \mathbf{u} := [\underline{c}_0^T, T_0]^T \\ \text{Output} &: \mathbf{y} := \underline{\xi} \\ \text{Parameters} &: \mathbf{p} := \left\{ \{N_{i,r}\}_{\forall i;\forall r}, \{k_r^0\}_{\forall r}, \underline{N}, V_0 \right\}\end{aligned}$$

5. The parameter "vector" should be regarded as a record structure.

## Design Considerations

Any programmatic approach to PCBS model building based on general principles, such as energy and mass balances for simple systems, will have to simulate exactly the operations exercised in the last section in the stirred tank example. Defining that unknown model parts are of arbitrary complexity, any of the assumptions, which result in the declaration of certain model parts, can be considered as an act of model simplification the same as additional assumptions will further reduce the degree of complexity. Nine assumptions were applied to the general energy balance of a simple lumped system in our example:

(i) ideally stirred

→ mathematical form of the model: ODEs

→ conditions in the output flow = conditions in the contents denoting

$\mathbf{x}_0$  :: state of the contents

$\mathbf{y}_j$  :: output describing the outflow conditions

$\mathcal{M}^-$  :: set of output mass streams

then

$$\mathbf{x}_0 = \mathbf{y}_j \quad \forall j \in \{\mathcal{M}^-\}$$

(ii),(iii) The general energy balance is reduced to an enthalpy balance.

(iv),(v) Simplify the description of the accumulation term, the isolation of the time derivative of the temperature is very simple.

(vi),(vii) Define the connections with the environments a flow source, a flow sink and an alternative heat sink and source.

(viii) Allows specification of the functional relation between the enthalpy and the composition.

(ix) Density remains constant and with (iv) a relation between the input flow and the output flow can be established (in this case both are equal).

The relatively large number of major assumptions which were applied to simplify the model in this case indicates that a correspondingly large number of different physical structures can be generated by changing the assumptions. In comparison, the degree of complexity seems to be smaller for the chemical system, because it has less structural elements.

In principle, all the assumptions introduce new equations such as shown in the discussion on the assumption of the ideally stirred model. Any implementation will therefore have to provide the means of introducing new equations and as a consequence also the means for manipulating these equations. In view of the project's goal to minimize modeling errors by automating and guiding the process, the user should interact with the system on the high level such as "ideally stirred" in contrast to defining the equations in mathematical form that represent the effects the assumption has expressed.

Different scenarios are possible, in terms of technical implementation. Any of them has its advantages and disadvantages. A first prototype will probably use a menu-type of approach in which the different assumptions are listed, this includes such things as lumped, distributed, negligible kinetic and potential energy, transfer laws, relations for calculating physical properties, to mention a few. This implementation could either be done in one of the commonly available languages such as ADA or Modula which enforce structured programming techniques or in a knowledge-based shell. In any case, the result of these operations shall be a set of equations in an internal format that allows manipulating the equations in an algebraic manipulator and that allows translating sets of equations representing a PCBS into any language used by computational tools such as simulation packages. In this sense, the suggested software can be regarded as an intelligent interface to computational tools.

One of the keys to the above approach is the internal representation of the PCBS models. The next effort shall concentrate on designing a context-free formal language for representing PCBS models. This language will be the base on which the whole system will be built and must therefore be carefully designed. First thought experiments showed that this approach uncovers naturally a number of problems that when not properly solved result in very common modeling mistakes. It is for example important to define the unit system properly, include unit conversion as a natural to the system and define ranges of validity for different variables. Also the relation between the different relevant quantities will have to be formulated explicitly and clearly so as to allow for the necessary manipulations.

### **State Space Representation**

The mapping into the state space needs some more thinking. The concept is clear and is well understood. The only problem being that the research done during this period resulted in a suggestion of a fixed state vector for the elements of the PCBS. Before this suggestion is implemented, more examples need to be worked to further justify the suggested approach. At this time it seems reasonable to define a state vector which includes pressure, temperature, concentration and extent of reaction as the main elements. The question of how this concept applies to living plants and micro organisms need more analysis.

## **Research Plans for the Next Period**

### **State Space Representation**

Extend analysis to other elements such as distributed systems, electro-chemical systems and biological systems.

### **Design of a Formal Language**

First experiments shall be solidified. More literature research is needed to explore possible alternatives.

## Design of a First Prototype

The prototype shall be designed based on the theoretical results. At the same time a thorough analysis of the different technological approaches is to be made; decide on the technology and implement. Possibilities include an approach from scratch using ADA, Modula-2 or C++ or KEE or any other similar development tools.

### Notation

The notation follows the following conventions:

:: means "defined as" in a word definition

:= means 'defined as' in a mathematical definition

$\dot{x}$  is the time derivative of  $x$

$\forall$  is "for all"

$\in$  is "included in"

$\mathbf{x}$  is a vector

$\underline{\mathbf{X}}$  is a matrix

$A_i$	::	specie $i$
$A_k$	::	cross sectional area of tank $k$
$C_p$	::	heat capacity of the contents
$T_0$	::	system temperature
$T_{in}$	::	temperature input stream
$T_j$	::	temperature in stream $j$
$T_J$	::	jacket temperature
$V_0$	::	system volume
$h_{i,j}$	::	specific enthalpy of specie $i$ in stream $j$
$h_k$	::	level in tank $k$
$k_r$	::	reaction constant for reaction $r$
$k_r^0$	::	pre-exponential factor
$\underline{c}_0$	::	concentration vector, system
$\underline{c}_{in}$	::	concentration vector, input stream
$h_r$	:=	$[-\Delta h_r]_{\forall r}$
$k$	:=	$[k_r]_{\forall r}$

$\underline{x}_0$	:: state of the contents
$\underline{y}_j$	:: output describing the outflow conditions
$\underline{H}$	::= $[h_{i,j}(T_j)]_{\forall i; \forall j}$
$\underline{N}$	::= $[V_{i,r}]_{\forall i; \forall r}$
$\dot{H}_0$	:: accumulation of enthalpy in the system
$\dot{H}_j$	:: enthalpy flow associated with the mass flow stream $j$
$V$	:: volumetric flow rate in and out
$\dot{m}_{k,0}$	:: the accumulation of mass in the tank $k$
$\dot{m}_j$	:: the mass flow rate in stream $j$
$\dot{n}_{i,0}$	:: accumulation of molar mass in the system
$\dot{n}_{i,j}$	:: molar flow of species $i$ in the stream $j$
$\dot{n}_{i,r}$	:: molar production rate of species $i$ from reaction $r$
$\dot{q}_j$	:: heat stream $j$
$\dot{r}_{i,r}$	:: reaction rate for specie $i$ in reaction $r$
$\dot{w}_j$	:: work in stream $j$
$\Delta h_r$	:: reaction enthalpy
$\alpha_{i,r}$	:: power coefficient for composition of specie $i$ in reaction $r$
$\alpha_k$	:: proportionality constant
$\rho$	:: density of the fluid
$\gamma$	:: exponential factor
$v_{i,r}$	:: stoichiometric coefficient for specie $i$ in reaction $r$
$\phi_{e,j,s,l}$	:: Extensive quantity in stream $j$ of system $s$ on level $l$
$\xi_r$	:: extent of reaction
$\dot{\phi}_{e,0,s,l}$	:: Accumulation of extensive quantity in the system (stream 0)
$\dot{\phi}_{e,j,s,l}$	:: Flow of extensive quantity associated with stream $j$
$\dot{\phi}_{e,r,s,l}$	:: Production rate of extensive quantity associated with reaction $r$
$\underline{\xi}$	::= $[\xi_r]_{\forall r}$
$\mathcal{A}$	:: index set of species; $i \in \mathcal{A}$
$\mathcal{E}$	:: index set of extensive quantities; $e \in \mathcal{E}$
$\mathcal{F}$	:: index set of subsystems; $s \in \mathcal{F}$
$\mathcal{L}$	:: index set of levels; $l \in \mathcal{L}$
$\mathcal{M}$	:: index set of mass streams; $j \in \mathcal{M}$
$\mathcal{M}^-$	:: set of output mass streams

$Q$  :: index set of heat streams;  $j \in Q$   
 $\mathcal{R}$  :: index set of reactions;  $r \in \mathcal{R}$   
 $S$  :: index set of streams;  $j \in S$   
 $\mathcal{W}$  :: index set of work streams;  $j \in \mathcal{W}$

### 3.3 ANALYSIS OF STEADY STATE MODEL

#### Introduction

Complex models are almost always built in a hierarchical fashion. An example is a distillation column, which is built up of trays, flash units, splitters, mixers, heat exchangers, pumps, etc. A flash unit itself is in fact a hierarchical structure. Embedded in it is the need to evaluate K-values and enthalpies, so in concept it uses a library of models that already exist to evaluate the needed physical properties. To create complex models, one needs, therefore, the ability to combine previously written models with the extra defining equations for the complex model. It is here that "language" considerations become important.

Object-oriented programming tools support hierarchical construction. An overall system can be assembled by coupling subsystems recursively. Every subsystem is to be represented as an object composed of a set of objects which may include other model-representing objects due to this recursive approach. Coupling is to be performed by using connection relations which relate inputs of an object with outputs of the other objects. Therefore, mathematical representation of objects becomes important to support the object-oriented approach to modeling because each object should have inputs and outputs. A system can be represented with inputs, outputs, and states with state space system representation. A dynamic model can be written in the form of a mixed set of ordinary differential equations and algebraic equations:

$$\dot{x} = f(x, u)$$

$$y = g(x, u)$$

$$x(0) \text{ given,}$$

where  $x$  are "state" variables,  $u$  are "input" variables, and  $y$  are "output" variables.

A steady-state mathematical model is a special case of a dynamic model when  $\dot{x} = 0$ . Hence, a steady-state model can be represented by the equation

$$f(x) = 0$$

where  $f(x)$  is a set of  $n$  equations in  $n + m$  unknowns. To solve the equations requires that  $m$  of the unknowns be specified by other means and the remaining found by solving the  $n$  nonlinear algebraic equations in  $n$  unknowns.

The problem facing the steady-state system analyst is the setting up and solving of the hundreds to thousands of linear and/or nonlinear algebraic equations that are needed to model various processes. The three major problems to be faced are:

1. Write a correct set of  $n$  equations in  $n + m$  unknowns. It is entirely too easy to include a redundant equation or to miss an equation that is needed.
2. Select a correct set of  $m$  unknowns to be independently specified so that the problem remaining is nonsingular and can be solved, in principle, for some reasonable values of the selected independent variables.
3. Solve.

The project is not intended to re-invent all the solution methods, rather the extensive use of existing solution methods is recommended. For this purpose, mapping procedures which are basically compilers are needed which translate the models represented in the internal meta-language into the language of the solution methods. This mapping should be bidirectional because the user should also be able to view the results in his/her own terminology.

### Degree-of-Freedom Analysis

The question of whether the algebraic model we have constructed will yield a physically realistic solution is in general determined by the degree-of-freedom analysis. In order to solve a set of equations in, say,  $n$  unknowns, it is necessary that the set consist of  $n$  independent equations. If less than  $n$  independent equations are available, no solution is possible. If more than  $n$  equations are available, then one could choose any  $n$  for solution. The degree-of-freedom-analysis is simply a systematic mechanism for counting all the variables, balance equations, and relations that are involved in the problem. The degree of freedom of a system is defined as follows:

$$\begin{aligned} \text{Degree of freedom} &= \text{total number of independent stream variables} \\ &\quad - \text{total number of independent balance equations} \\ &\quad - \text{total number of specified independent stream variables} \\ &\quad - \text{total number of subsidiary relations.} \end{aligned}$$

The following system is shown as an example of the application of degree of freedom analysis on a typical life support system. The system presented was previously developed by the RECON team. In addition to air, water, and waste treatment units, it incorporates an algae reactor for food production and oxygen regeneration. The system is represented in Figure 3.6. Table 3.1 shows the degree of freedom of the system. As is evident from Table 3.1, the process is completely specified. Since the degree of freedom of crew cabin (Unit 1) is 2, the balances associated with this unit can be solved if the stream variables (compositions) of stream 27 are specified. With the completion of crew cabin calculations, the stream variables of stream 11 have been determined, hence the degree of freedom of Unit 3 will have been reduced to 3. Streams 16 and 17 have already been specified, so the completion of Unit 1 calculations has no effect on the degree of freedom of Unit

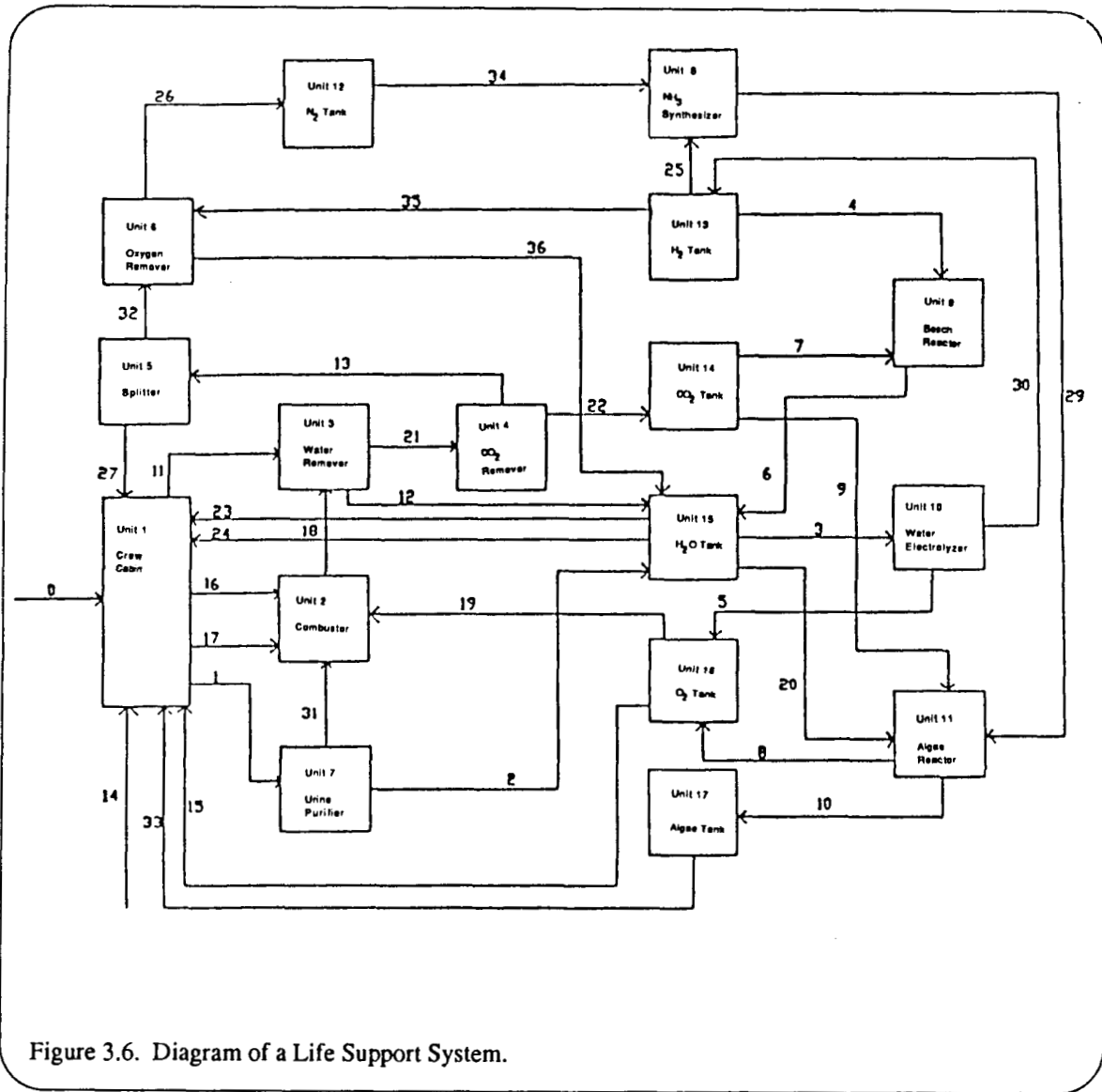


Figure 3.6. Diagram of a Life Support System.

2, (combustor). Specification of stream 27 reduces the degree of freedom of Unit 5 by 2. Similarly, the flows of streams 23 and 24 have been determined, so that the degree of freedom of Unit 15 will be reduced to 3. Finally, the stream variables of stream 1 have been determined, so that the degree of freedom of Unit 7 will be reduced to zero. These considerations indicate that mass balances for Unit 7 (urine purifier) should be calculated next. With the completion of calculations for the urine purifier, streams 2 and 31 have been determined, hence the degree of freedom of Unit 15 will be reduced to 2 and the degree of freedom of Unit 2 will be reduced to zero. Therefore, the balances for Unit 2 should be calculated next.

As in the preceding examples, the order in which unit balances were solved was determined by updating the degree of freedom of the individual process units after each set of unit balances was complete. This updating can be conveniently carried out by augmenting the degree-of-freedom table with one additional row

Table 3.1. Degree-of-freedom table.

	Unit																	process
	1	2	3	4	5	6	7	8	9	10	11	12	13	14	15	16	17	
Number of variables	30	14	11	6	6	6	4	4	5	4	6	3	5	4	9	5	5	79
Number of balances	9	10	4	3	2	4	2	3	4	3	5	1	1	1	1	1	54	
Number of specified compositions	11	7															3	1
flows	6							1			1	1					2	7
Number of auxiliary relations	2								1	1			3	2	3	2		5
Degree of freedom	2	1	7	3	4	2	2	0	0	0	0	1	1	1	5	2	0	2
Specification of stream #27	<u>-2</u>																	<u>-2</u>
	0																	0

for each unit balances. These additional rows can be used to record the new information that is obtained as each set of unit balances are completed. Table 3.2 shows complete degree-of-freedom updating table.

Table 3.2. Degree-of-freedom updating table.

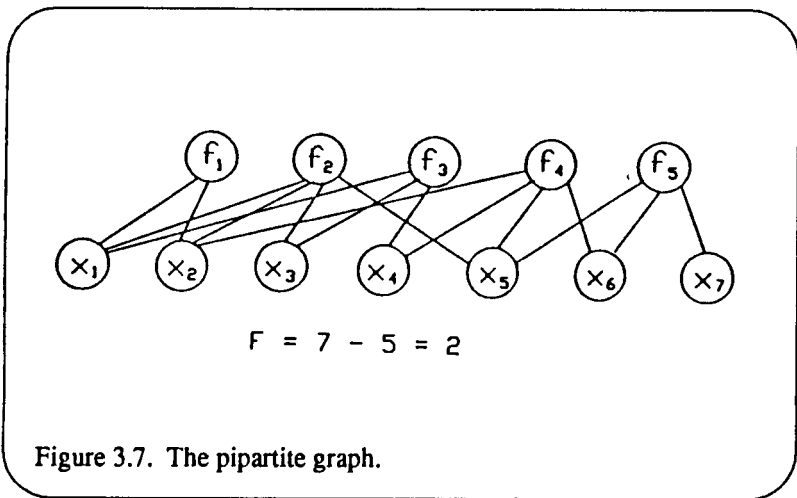
	Unit																
	1	2	3	4	5	6	7	8	9	10	11	12	13	14	15	16	17
Initial degree of freedom	0	1	7	3	4	2	2	0	0	0	0	1	1	1	5	2	0
Unit 1 balances			-4		-2		<u>-2</u>								-2	-1	
Unit 7 balances		<u>-1</u>													-1		
Unit 2 balances			<u>-3</u>													<u>-1</u>	
Unit 3 balances				<u>-3</u>											-1		
Unit 4 balances					<u>-2</u>									<u>-1</u>			
Unit 5 balances						<u>-2</u>											
Unit 6 balances											<u>-1</u>	<u>-1</u>		<u>-1</u>			

### On the Selection of Unknown Variables

Generally, it is necessary to specify the numerical values of certain of the variables in the system equations before solution can be obtained. The number of such variables is equal to the degree of freedom of the equations, that being the excess of variables over equations. However, the degree-of-freedom analysis does not give any information as to which  $m$  variables should be chosen in order to get a solution. A necessary and sufficient condition for the solution of a set of equations is that the Jacobian determinant be non-zero. While of considerable mathematical significance, this condition is of little direct use to the process engineers, since it is extremely difficult to compute the Jacobian determinant for a large system.

In a logically consistent set of  $n$  equations there will be  $n$  unspecified variables, and for each equation it will be possible to denote one variable as the output variable for that equation. And, no variable will be an output variable for more than one equation. If such an output assignment is possible, the equations are said to satisfy the diversity condition of Hall,[2] a necessary but not sufficient condition for the existence of a solution.

We represent the system of equations by a special graph which exposes the structure of the equations. This notation is the bipartite graph of topology (Figure 3.7). Consider the following system of equations:



$$f_1(x_1, x_2) = 0$$

$$f_2(x_1, x_2, x_3, x_5) = 0$$

$$f_3(x_1, x_3, x_4) = 0$$

$$f_4(x_2, x_4, x_5, x_6) = 0$$

$$f_5(x_5, x_6, x_7) = 0$$

Figure 3.7. The bipartite graph.

If a variable  $x_j$  is assigned as the output variable of equation  $f_i$ , then the edge connecting nodes  $f_i$  and  $x_j$  will be oriented from  $f_i$  to  $x_j$  and all other edges associated with  $f_i$  will be oriented to  $f_i$ . Selected variables are not candidates for the output set and their edges must be oriented to the equations. If  $x_2$  and  $x_3$  are selected, the graph in Figure 3.8 might result.

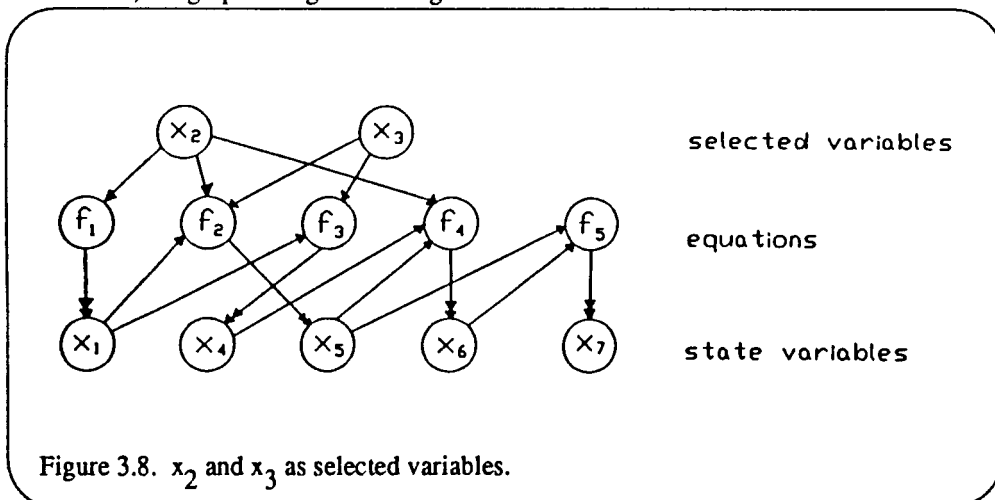


Figure 3.8.  $x_2$  and  $x_3$  as selected variables.

An output set denoted by the double-headed arrows indicates that the diversity condition is satisfied. In addition, an order of solution is suggested by the direction of the arrows. Figure 3.9 shows the rearranged graph. Starting from the left and proceeding to the right, the set of five equations can be solved one at a time. If

selection of  $m$  variables to solve the system equations satisfies the diversity condition, then the variables are properly specified. This algorithm can be used to decide whether selections are properly made or not.

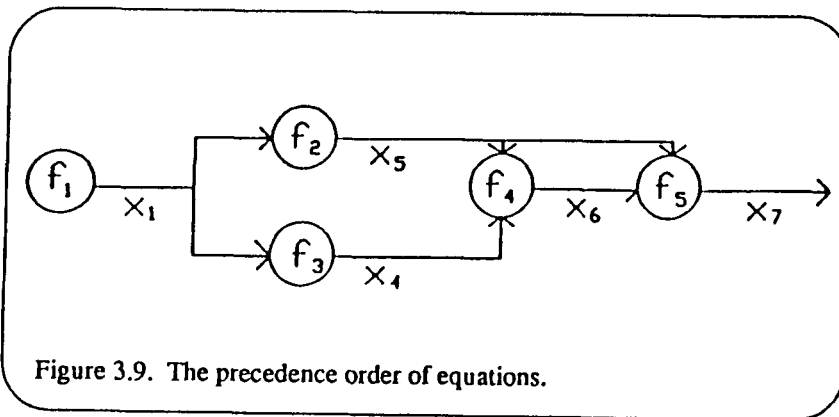


Figure 3.9. The precedence order of equations.

### 3.4 STATE SPACE SIMULATION

#### Dynamic model

A crew model has been constructed by utilizing the object-oriented concept and state space notation of a system. In this report, only a human being was simulated, but entire life support system can be similarly simulated. The human being has been decomposed into five subsystems: lung, blood, stomach, colon, and bladder. Blood, in turn, is composed of two subsystems, a physical system and a metabolic reaction system. Each subsystem was represented with inputs, outputs, and state variables. For example, the material balances, input, output, and state vectors of lung and blood are as follows:

#### $\Sigma_1$ : LUNG

Assumptions: (i) Stirred-tank, equilibrium with blood

Component Mass Balances:

$$\begin{aligned} \text{O}_2 &:: V_1 \frac{dc_{101}}{dt} = v_1 c_{111} - k_1(c_{101} - k_2 c_{201}) - v_4 c_{101} \\ \text{N}_2 &:: V_1 \frac{dc_{102}}{dt} = v_1 c_{112} - v_4 c_{102} \\ \text{CO}_2 &:: V_1 \frac{dc_{103}}{dt} = v_1 c_{113} - k_3(c_{103} - k_4 c_{203}) - v_4 c_{103} \\ \text{H}_2\text{O} &:: V_1 \frac{dc_{104}}{dt} = v_1 c_{114} - k_5(c_{104} - k_6 c_{204}) - v_4 c_{104} \end{aligned}$$

Notation:

- $c_{ijk}$  :: Composition of  $k^{\text{th}}$  component in the  $j^{\text{th}}$  stream of  $i^{\text{th}}$  unit ( $j=0$  means the content of a unit)
- $k_1, k_3, k_5$  :: Mass transfer coefficients
- $k_2, k_4, k_6$  :: Equilibrium constants
- $v_1, v_4$  :: Air flow rates
- $V_1$  :: Lung volume

Definitions:

$$\begin{aligned} \text{Input} &:: [c_{111}, c_{112}, c_{113}, c_{114}, c_{201}, c_{203}, c_{204}]^T \\ \text{State} &:: [c_{101}, c_{102}, c_{103}, c_{104}]^T \\ \text{Output} &:: [c_{101}, c_{102}, c_{103}, c_{104}]^T \end{aligned}$$

#### $\Sigma_2$ : BLOOD

Assumptions: (i) Stirred-tank, equilibrium with lung and colon

### Component Mass Balances:

$$\begin{aligned} \text{O}_2 &:: V_2 \frac{dc_{201}}{dt} = k_1(c_{101} - k_2 c_{201}) - R_{21} \\ \text{CO}_2 &:: V_2 \frac{dc_{203}}{dt} = R_{23} - k_3(c_{103} - k_4 c_{203}) \\ \text{H}_2\text{O} &:: V_2 \frac{dc_{204}}{dt} = R_{24} + R_{ab} V_6 c_{604} - k_5(c_{104} - k_6 c_{204}) - R_{fil} c_{204} - R_{sweat} \\ \text{Carbo} &:: V_2 \frac{dc_{205}}{dt} = R_{ab} V_6 c_{605} - R_{25} \\ \text{Protein} &:: V_2 \frac{dc_{206}}{dt} = R_{ab} V_6 c_{606} - R_{266} \\ \text{Fat} &:: V_2 \frac{dc_{207}}{dt} = R_{ab} V_6 c_{607} - R_{27} \\ \text{Urea} &:: V_2 \frac{dc_{209}}{dt} = R_{29} - R_{fil} V_2 c_{209} \end{aligned}$$

### Notation:

$$\begin{aligned} R_{ab} &:: \text{Absorption rate of food from colon to blood} \\ R_{fil} &:: \text{Filtration rate of water and urea from blood to bladder} \\ R_{sweat} &:: \text{Water evaporation as sweat} \\ V_2 &:: \text{Blood volume} \\ V_6 &:: \text{Colon volume} \\ R_{ij} &:: \text{Metabolic reaction rate} \end{aligned}$$

### Definitions:

$$\begin{aligned} \text{Input} &:: [c_{101}, c_{103}, c_{104}, c_{604}, c_{606}, c_{607}]^T \\ \text{State} &:: [c_{201}, c_{203}, c_{204}, c_{205}, c_{206}, c_{207}, c_{209}]^T \\ \text{Output} &:: [c_{201}, c_{203}, c_{204}, c_{205}, c_{206}, c_{207}, c_{209}]^T \end{aligned}$$

## Simulation

The simulation of a human being was performed using ACSL (Advanced Continuous Simulation Language). All the material balances and input, output, and state vectors of each subsystem of a human being are in the simulation program. The remaining problem is to get reasonable parameter values such as mass transfer coefficients, equilibrium constants, and volumes of each subsystem, etc.

## 3.5 Biophysics of Plant Growth: Algae and Higher Plants

### Introduction

In the first report for Project NAG 9-253, we presented a generalized model of algal growth as a function of light, CO<sub>2</sub> and O<sub>2</sub> availability. We stated our plans to develop the algal model further and extend the applications for higher plants. The revised model presented here is a generic model which, with a few specified qualifications concerned largely with higher plant structure, are applicable to both algae and higher plants.

The generalized algal model is developed from the same fundamental growth process as the higher plant model. The major difference between the algal and the higher plant models is that algae do not have a complex system of stomatal valves regulating gaseous exchange with the ambient environment. They also lack the necessity for a complex transport and allocation system.

In addition, due to the low solubility of oxygen in water, algae do not have a photorespiration problem of the magnitude of higher plants. However, high levels of oxygen such as used by hydroponic plant growth cause algae to produce glycolate which must be excreted to the surrounding nutrient solution. Higher plants recycle glycolate using the Tolbert pathway, because they do not have the option of glycolate excretion to the surrounding media.

### Objective

The objective of this study was to develop a mathematical model of plant growth applicable to both algae and higher plants, which can be incorporated into a larger model simulating a regenerative life support system. This plant growth model must be sufficiently general to account for all likely responses in space environments. The model can be used for four purposes:

1. To provide a base for comparison of plant-based systems with physical, chemical and other biological systems which could be used for regenerative life support.
2. To optimize the design of such a system.
3. To manage and control a plant growth component with a CELSS system.
4. To provide guidance in emergency procedures to ensure survival of algal and phyto-cultures and reestablishment of steady-state function.

The objectives of the biophysical plant model complement and serve to provide direction to experimental plant growth studies related to regenerative life support. Environmental factors include changes in water, light, temperature, humidity and nutrients as well as interactions of these changing environments with exposures to trace gases that may develop in CELSS such as ozone and nitrous oxides. The model is to be used to propose and test alternative mechanisms of plant growth and pollutant interference. Eventually, the model should demonstrate and explain how pollutants in closed environments change metabolic cycle dynamics and alter compensatory growth responses.

## Justification

A plant growth model is needed as part of the larger regenerative life support system for the following reasons:

1. Various engineering designs need to be investigated. Plants have internal control systems, and cannot simply be turned off and on by external valves. If such a system is to be used and controlled, the system must be designed to take advantage of all capabilities.
2. Recently, knowledge of mechanisms has increased rapidly, but information is fragmentary and should be brought together in a quantitative framework.

The report is divided into sections dealing with (1) model design, (2) modeling methodology, (3) detailed description of model components, and (4) linkages between components.

## Model Design

The model design must be sufficiently detailed to include the mechanisms of compensatory adjustments in physiological processes. To facilitate compensatory interactions among biophysical processes and resource acquisition structures, the model is structured in terms of three processes:

- (1) Autotrophic biosynthesis of C<sub>6</sub> carbon skeletons and amino acids.
- (2) Storage and distribution of photosynthate.
- (3) Heterotrophic growth and maintenance of different plant parts (in the case of higher plants) and biomass.

The model is currently at the conceptual stage of development where we consider all possible model inputs and outputs. In this way, the design structure can be built with the flexibility to anticipate inclusion of possible additional components as the model evolves. The model as documented is not complete, but further development will be facilitated by the building of a strong foundation.

The scope of possible model inputs and outputs for a simplified higher plant is summarized in Figure 3.10. Crown inputs consist of solar radiation (PAR light, hv), relative humidity (RH), carbon dioxide (CO<sub>2</sub>), gaseous pollutants such as ozone (O<sub>3</sub>), sulfur dioxide (SO<sub>2</sub>) and various nitrous oxides (NO<sub>x</sub>). Outputs from the crown are oxygen, water vapor and volatile secondary metabolites. During the night, a reversal of CO<sub>2</sub> and O<sub>2</sub> fluxes may occur, depending on degree of stomatal closure.

The root surfaces exchange a large number of chemical elements and organic compounds with the soil environment. These complex exchange processes are divided into: (1) primary nutrients (NO<sub>3</sub>, NH<sub>4</sub>, PO<sub>4</sub>, SO<sub>4</sub>), (2) soluble salts (K, Na, Ca, Mg, Cl), (3) trace and toxic elements (Mn, Fe, Co, Cu, Mo, Zn, B, V, Al, Pb, Hg, As, Cd, Cr, Ni), (4) pH, (5) water, (6) O<sub>2</sub> and CO<sub>2</sub> exchange and (7) organic root exudates. The interactive effects of pH are numerous, particularly on primary nutrients, as well as on trace and toxic elements. Trace elements and toxic metals are included in the same submodel because trace elements in excess usually exhibit toxic effects. There are also numerous interactions between trace and toxic elements, necessitating coupling these process components. The bio-physical process components of the growth model are shown in Figure

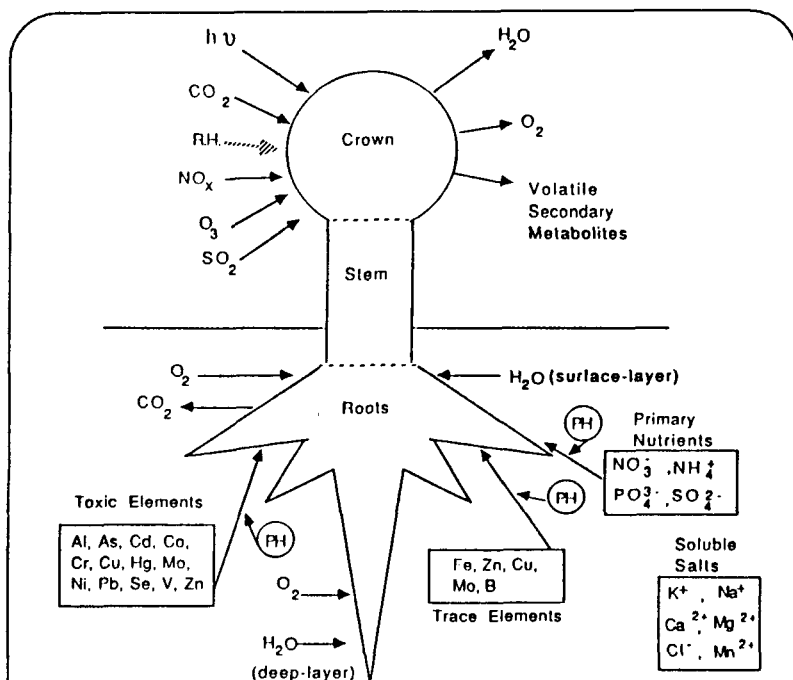


Figure 3.10. Overview of complexity of factors determining plant growth. Imbalances between factors stimulate compensatory adjustments. Toxic elements inhibit metabolic and transport processes.

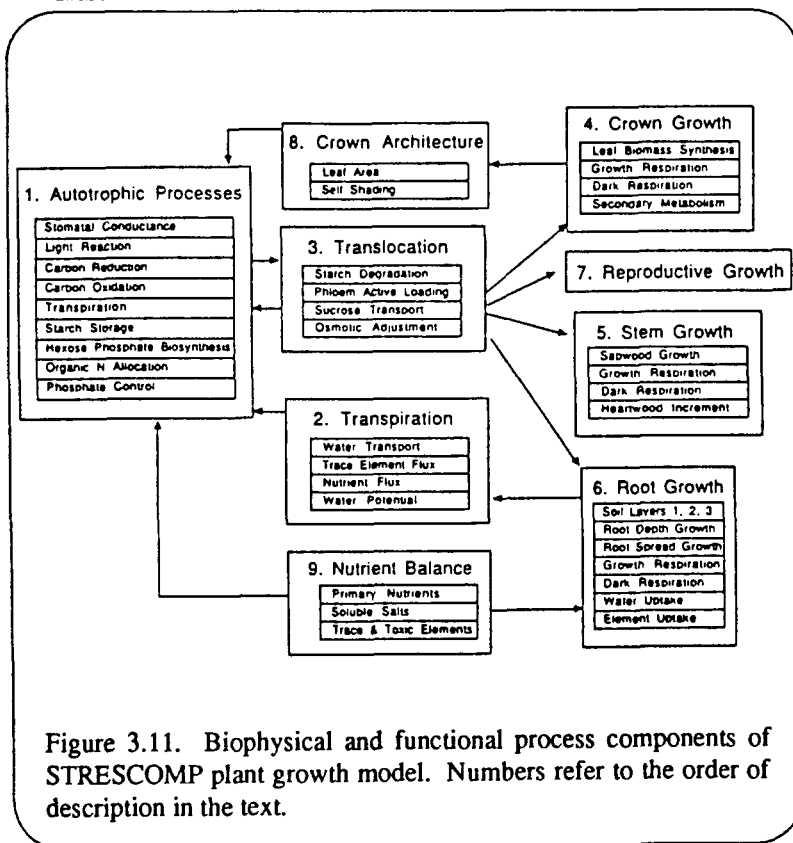


Figure 3.11. Biophysical and functional process components of STRESCOMP plant growth model. Numbers refer to the order of description in the text.

3.11. These processes are not represented as separated subroutines, but are linked together using the integrated rate method, which as its name implies, couples dissimilar rates with different units.

At the whole-plant level of organization, autotrophic production processes are physically separated from heterotrophic growth processes. These processes are linked by two transport systems, the phloem translocation system which distributes photosynthate, and the water transpiration system, which supplies mineral nutrients to both autotrophic and heterotrophic metabolic processes. These subprocesses are coupled by environmental driving factors and compartments representing resources, metabolic intermediates and biomass products.

## Modeling Methodology

The appropriate mathematical forms for biochemical processes are enzyme kinetics of the type presented by Farquhar *et al.*[3] describing  $C_3$  photosynthesis. In scaling up from photosynthesis to growth, however, some simplification is required.

Each higher level of biological organization involves self-simplification because the hierarchy imposes a new system of constraints.[4] Two problems arise from this solution to

the hierarchical problem. First, abstract thermodynamic concepts are less concrete than corresponding enzyme pathway representations. Second, the mathematics describing transitions between thermodynamic aggregates in physiological systems is not established. Integrated rate theory (IRT) is proposed as a formal biophysical methodology to represent the macroscopic behavior of physiological processes.

The concept underlying IRT is that components of free energy, particularly thermal energy and configuration entropy, provide a natural representation of biosystems states for model building. Particular integrated rate models (IRM) based on aggregate states defined in thermodynamic terms are simpler and therefore likely to be much more easily transferred between hierarchical levels than models representing detailed biochemical pathways.

## Description of Model Components

The hierarchical structure of the plant growth model is based upon two levels of subsystem organization. The specific subsystems are:

### 1. Autotrophic Biosynthesis

In terms of model design, the crown is composed of a population of leaves of variable age and size. This population is divided into heterotrophic growing leaves and mature autotrophic nongrowing leaves. Leaf population dynamics are controlled by leaf initiation, development and senescence rates.

#### a. Photosynthetic carbon reduction

The autotrophic photosynthetic carbon reduction subsystem of the crown is hypothesized to operate by the same mechanisms as individual chloroplasts and peroxisomes of algal cells, but at a higher scale. The crown photosynthesis system is assumed to move between two energy levels, termed the regenerative state  $E^0$  and the activation state  $E^\ddagger$ , respectively. Examples of regenerative states at the microscopic level include P680, P700, ADP, NADP and Ribulose-5 Phosphate. All these regenerative entities are represented at the macroscopic level by a single regenerative state (O). Examples of activated states at the microscopic level include Z (Photosystem I), Q (Photosystem II), ATP and NADPH. These activated entities are represented at the macroscopic level by a single activated state (1).

The calculation of maintenance costs of the autotrophic photosynthesis system is problematic. Maintenance energy in nongrowing cells is primarily used to sustain (1) active configurations of enzymes and membranes (by continuous breakdown and resynthesis of proteins) and (2) ion concentration gradients. In heterotrophic cells, this cost can be calculated in terms of glucose equivalents. It can also be measured in terms of  $CO_2$  evolution. In autotrophic cells, however, maintenance energy can be harvested directly from light energy. When light intensity is nonlimiting, more energy in the form of ATP and reducing power is available than is consumed in carbon skeleton biosynthesis. It is therefore incorrect to compute  $CO_2$  evolution as an estimate of photosynthesis system maintenance because light, rather than hexose, supplies this energy during daylight. At night, or during artificial darkness, oxidative phosphorylation supplies energy for maintenance, causing release of  $CO_2$ . For simplicity and convenience, it is assumed that the 1% to 4% maintenance energy cost calculated by Penning de

Vries[5] in autotrophic cells is supplied entirely by light energy and is represented by a reduction in quantum yield.

In the energy activation diagram shown in Figure 3.12, absorption of light quanta alters the energy status of the photosynthesis system, which is reflected in a change in its activation free energy.[6; 7; 8] The transition 0 to 1 therefore reflects all the light reaction processes in a single transition.

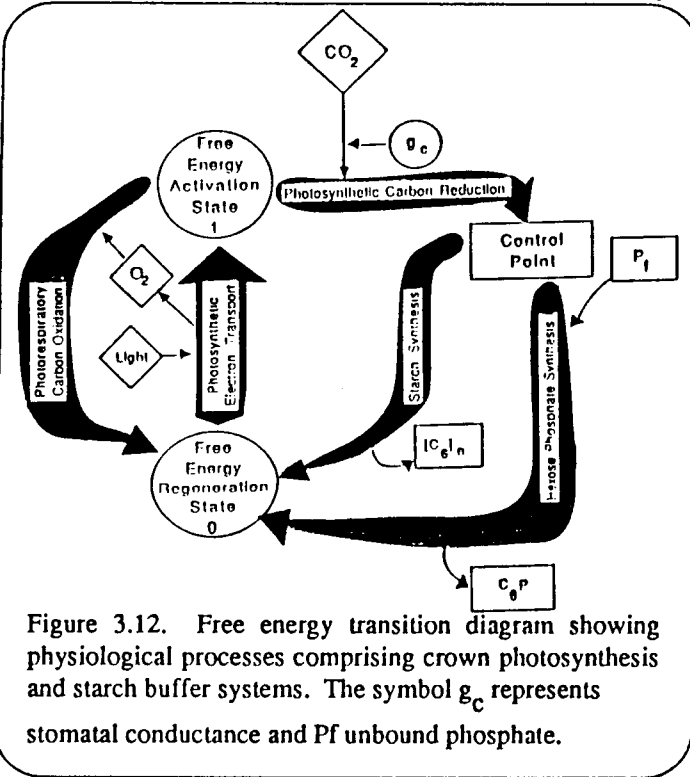


Figure 3.12. Free energy transition diagram showing physiological processes comprising crown photosynthesis and starch buffer systems. The symbol  $g_c$  represents stomatal conductance and  $P_i$  unbound phosphate.

The competition between carbon photosynthetic reduction and oxidation processes for transitions leaving state 1 depend not only on the relative concentrations of  $CO_2$  and  $O_2$  at the rubisco fixation site but also on leaf temperature. The temperature dependence transition function for photosynthetic carbon oxidation (PCO) with respect to photosynthetic carbon reduction (PCR) is denoted by  $\phi(T)$ :

$$\phi(T) = \exp\left[\frac{1}{R}\left(\frac{1}{T^*} - \frac{1}{T}\right)(\Delta E_o^\ddagger - \Delta E_c^\ddagger)\right], \quad (1)$$

where  $E_o^\ddagger$  is the energy of activation for PCO,  $E_c^\ddagger$  is the energy of activation for PCR,  $T^*$  is the projected temperature at which the rate of carbon oxidation is equal to the rate of carbon reduction.

Organic nitrogen is allocated by the compensatory control system of the plant to either light harvesting (transition 0 ---> 1) or carbon reduction (transitions 1 ---> 0) reductions. This is the primary compensation mechanism available for overcoming discrepancies in the proportional balance between light and  $CO_2$  availability. The proportional allocation mechanism must operate within the genetic limits of the species. The relative concentrations of organic nitrogen allocated to light harvest and carbon reduction are denoted by  $\sigma_{NL}$  and  $\sigma_{NR}$ . The relative allocation of organic nitrogen is therefore given by the relationship:

$$\sigma_{NL} + \sigma_{NR} = \sigma_{NO} \quad (2)$$

If  $\sigma_{NL}$  increases,  $\sigma_{NR}$  must decrease and *vice versa*, because organic nitrogen must be conserved. Control of organic nitrogen allocation is structured to be a function of the long-term average light intensity. Low average light intensities shift allocation of organic nitrogen towards  $\sigma_{NL}$ , whereas high average light intensities shift the balance toward  $\sigma_{NR}$ . A reduction in total nitrogen availability reduces both  $\sigma_{NL}$  and  $\sigma_{NR}$ , thereby reducing both the rate of light energy generation and carbon reduction.

Because plants acclimate and adjust their response to light intensity, and different species may have unique light response curves, light intensity levels must also be defined in terms of a phytocentric reference standard. The relative intensity is denoted by  $\sigma_I$ .

Self-shading due to increasing leaf area index (LAI) reduces the total light interception by the crown. A self-shading factor  $\sigma_{ss}$  is defined:

$$\sigma_{ss} = \frac{1}{1 + \exp[\gamma_{ss} (LAI - LAI_{1/2})]} \quad (3)$$

where  $LAI_{1/2}$  is the leaf area index at which the light interception is reduced to half, and  $\gamma_{ss}$  is a crown geometry parameter. The crown geometry factor can be determined either from theoretical analysis or experimental measurement.

Following the same argument outlined above, we denote the phosphate concentration by  $P$ . During the course of a day, phosphate can exist in either free  $P_f$  or substrate bound  $P_b$  form; therefore:

$$P_f + P_b = P. \quad (4)$$

The proportional control of synthesis of sugar phosphate  $C_6P$  and starch  $[C_6]_n$  is determined by the availability of free phosphate  $f$ , which is defined:

$$f = \frac{P_f}{P} \quad (5)$$

When  $f$  increases, synthesis of  $C_6P$  is favored, whereas when  $f$  decreases, starch synthesis is facilitated.

The autotrophic biosynthesis cycle as represented in Figure 3.12 undergoes transitions between the regenerative state (0) and the activation state (1). At any given instant of time, the steady state probability of the biosynthesis cycle being in state 0 is defined as  $\pi_0$  and in state 1 as  $\pi_1$ . Using Markovian mathematics, the steady state solution for these probabilities can be computed:

$$\pi_0 = \frac{\lambda_1 + \lambda_I}{\lambda_0 + \lambda_1 + \lambda_I} \quad (6)$$

$$\pi_1 = \frac{\lambda_0}{\lambda_0 + \lambda_1 + \lambda_I} \quad (7)$$

where

$$\begin{aligned} \lambda_0 &= \sigma_I \sigma_{NL} \sigma_{ss} \tau_L, \\ \lambda_1 &= \sigma_c \sigma_{NR} \tau_R, \text{ and} \\ \lambda_I &= \sigma_o \sigma_{NR} \phi(I) \tau_o \end{aligned}$$

with  $\tau_L$ ,  $\tau_o$  and  $\tau_r$  the *temperature inhibition functions* for the light reaction, carbon oxidation and carbon reduction processes, respectively, and the factors  $\sigma_c$  and  $\sigma_o$  are the relative internal  $CO_2$  and  $O_2$  concentrations, respectively.

b. Carbon assimilation, transpiration and stomatal conductance

Carbon dioxide concentration  $C$  within the substomatal cavity (which we assume is approximately equal to the concentration at rubisco fixation sites due to an efficient  $\text{CO}_2$  membrane transport system) can be calculated from the  $\text{CO}_2$  balance at quasi-steady state:

$$A + \alpha_{CO} \lambda_I \pi_1 - \alpha_{CR} \lambda_I \pi_1 = 0, \quad (8)$$

where  $A = g_c (C_s - C)$  is the carbon assimilation rate,  $g_c$  is the stomatal conductance for  $\text{CO}_2$ , and  $C_s$  is the  $\text{CO}_2$  concentration at the leaf surface.[9] The parameters  $\alpha_{CO}$  and  $\alpha_{CR}$  determine the relative carbon oxidation and reduction fluxes, respectively. The expression for internal carbon dioxide  $C$  can be thus obtained:

$$C = C_s + \frac{1}{g_c} [\alpha_{CR} \lambda_I - \alpha_{CO} \lambda_I] \pi_1. \quad (9)$$

Transpiration rate is computed in terms of a reference transpiration calculated for  $g_w$  equal to  $g_w^{\hat{}}$  (maximum stomatal conductance for species type) and  $h_s$  equal to 0.5. For  $h_s$  greater than 0.5, transpiration is reduced by the lowered vapor gradient. Where  $h_s$  is less than 0.5, stomatal closure reduces transpiration for humidity-sensitive plants. The transpiration index  $\sigma_T$  is therefore:

$$\sigma_T = 2\sigma_{g_w} (1 - h_s), \quad (10)$$

where

$$\sigma_{g_w} = g_w / g_w^{\hat{}}. \quad (11)$$

The actual transpiration for the entire crown is calculated from

$$T_r = \sigma_T g_w^{\hat{}} LA \sigma_{ss}, \quad (12)$$

where  $LA$  is leaf area and  $\sigma_{ss}$  is the self shading factor.

c. Hexose phosphate and starch production

The production increment of hexose ( $\Delta C_G$ ) over the time interval  $\Delta t$  is 1/6 of the rate of carbon reduction, therefore:

$$\Delta C_6 = \frac{\alpha_{CR} \lambda_1 \pi_1}{6} \quad (13)$$

Hexose is assumed to be synthesized in two forms, hexose phosphate  $C_6P$  and starch  $[C_6]_n$ . The synthesis equations for these two carbohydrates are:

$$\Delta C_6P = \frac{\alpha_{CR}^f \lambda_1 \pi_1}{6} \quad (14)$$

and

$$\Delta [C_6]_n = \frac{\alpha_{CR}^f \lambda_1 \pi_1}{6} \quad (15)$$

The relevant equations determining carbon reduction and oxidation rates, starch and hexose phosphate synthesis are shown in Figure 3.13. There are essentially three transition rate  $\lambda_0$ ,  $\lambda_1$  and  $\lambda_2$  between two free

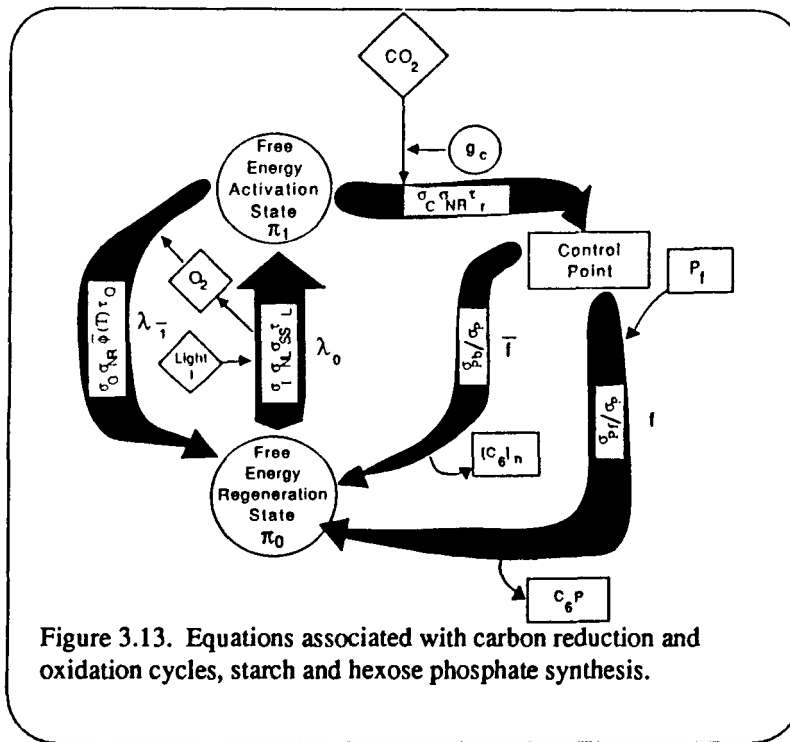


Figure 3.13. Equations associated with carbon reduction and oxidation cycles, starch and hexose phosphate synthesis.

energy states. The transition  $\lambda_1$  branches at the control point for synthesis of starch or hexose phosphate. The probability of being in either of the two free energy states is given by the values  $\pi_0$  and  $\pi_1$ . Analytic solution of these probability states defines the steady state activity of the system at any given instant of time. The autotrophic biosynthesis system is summarized in Figure 3.14. Factors controlling rates of transitions are represented in terms of actual values (boxes) and relative "measures" (circles). The integration of driving variables with dissimilar units is accom-

plished by casting them into any information form.

Similarly, the IRM output is cast into both actual and relational values. For example, starch synthesis in Figure 3.14 is calculated from assimilation rate A and relative rate of starch synthesis from IRM. Starch can be

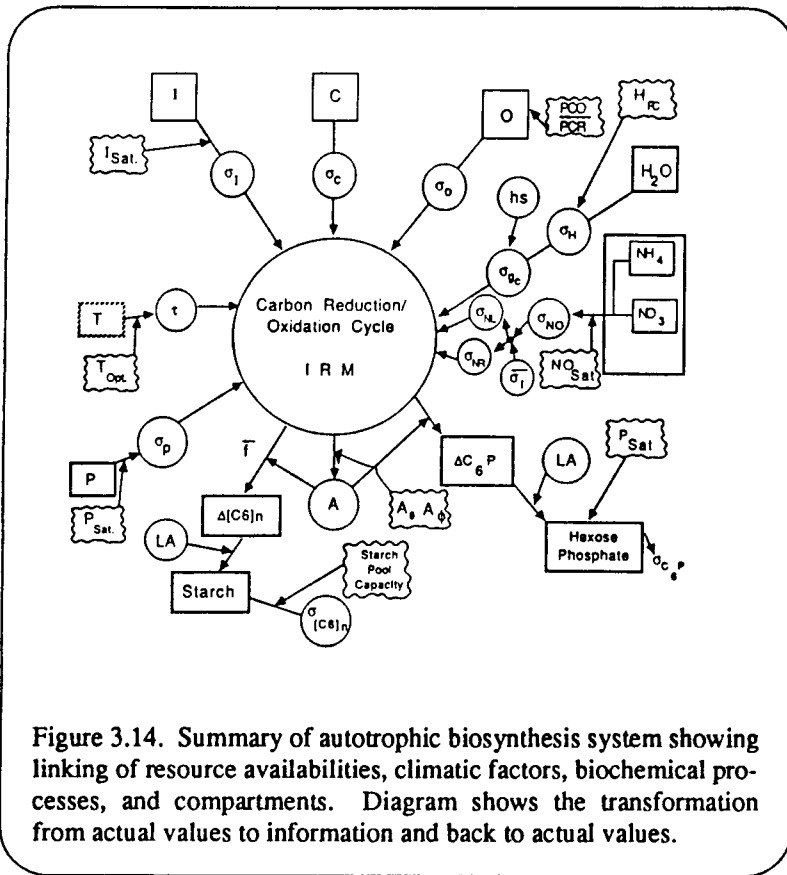


Figure 3.14. Summary of autotrophic biosynthesis system showing linking of resource availabilities, climatic factors, biochemical processes, and compartments. Diagram shows the transformation from actual values to information and back to actual values.

represented as both actual concentration and as a measure of proportional fullness of the starch pool.

## 2. Photosynthate Distribution

The growth processes of higher plants are dependent upon active loading and solute-driven transport of carbon skeletons in the form of sucrose and amino acids in phloem vessels. The increased cost of long-distance translocation in large plants is offset to some extent by a reduction in the cost of nitrate reduction.

When the light response curve is saturated, the rate of carbon assimilation  $i$  generally limited by the rate of  $CO_2$  diffusion into the leaf, light energy is thus available for nitrate and sulfate reduction.[10] For this condition, nitrate and sulfate reduction

consume much less energy from assimilates than is expected from their high reduction cost in darkness. [5]

### a. Phloem loading

Phloem loading is described as an energy transition process in which unbound sites for active transport are defined as the regenerative state. Similarly, bound active transport intermediates are defined as the activated energy state. Although this system embraces microscopic detail, its role as a key system control point gives macroscopic significance to its dynamics. Real time carbon-11 tracer studies [11; 12; 13; 14; 15; 16] and phloem transport models [17; 18; 19; 20] provide some insight into the dynamics of this subsystem. The IRT transition diagram for this subsystem is shown in Figure 3.15. Control of phloem and leaf sucrose concentrations is linked to plant water potential. Regulation of sucrose produc-

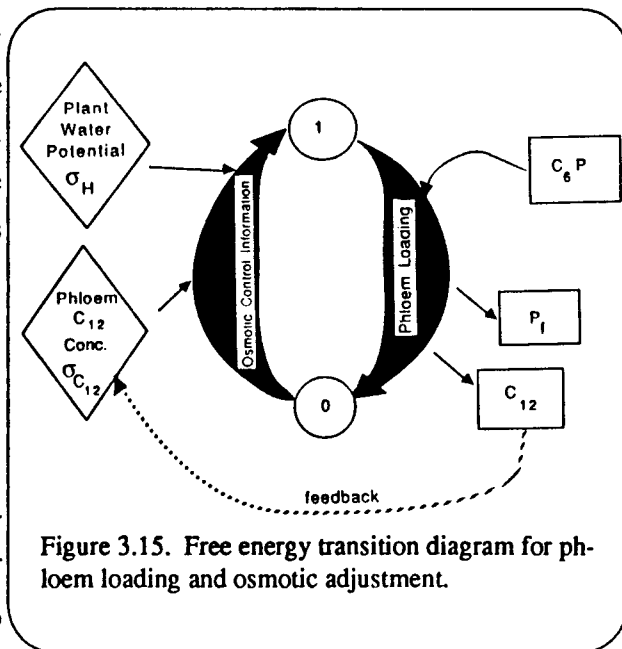
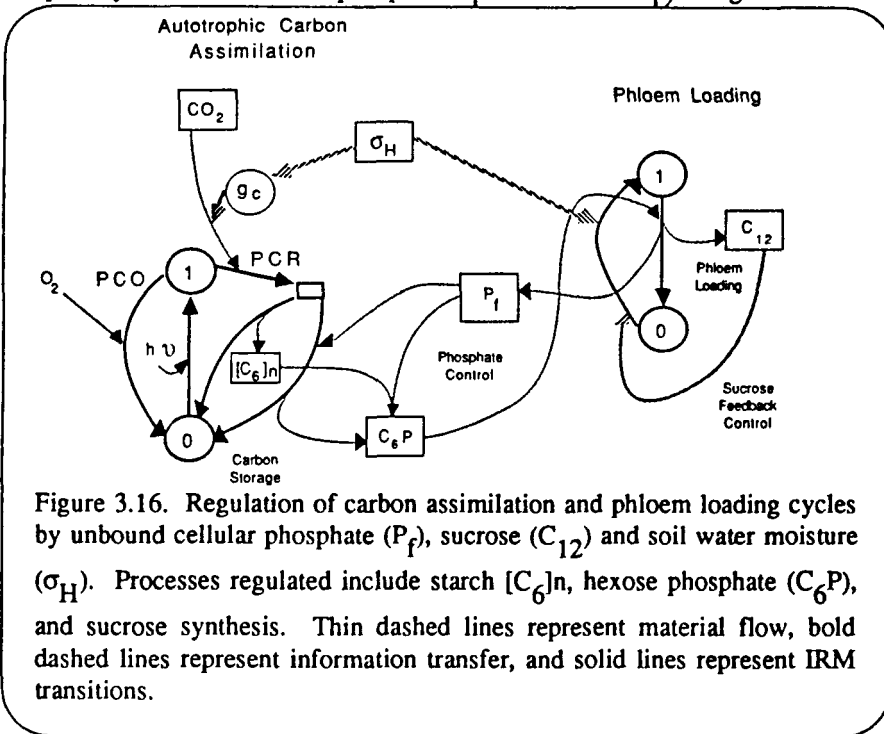


Figure 3.15. Free energy transition diagram for phloem loading and osmotic adjustment.

tion and active loading is determined by the concentration of sucrose in the phloem, modified by the plant water potential. Synthesis of sucrose leads to release of unbound phosphate which stimulates synthesis of hexose phosphate.

The linkages and feedbacks regulating autotrophic synthesis of starch and hexose phosphate, together with their coupling to sucrose synthesis and phloem loading, are shown in Figure 3.16. The major regulators of this coupled system are unbound phosphate  $P_f$  and sucrose  $C_{12}$ . High concentrations of unbound phosphate  $P_f$



stimulate the synthesis of hexose phosphate  $C_6P$  and conversion of starch  $C_n$  to hexose phosphate  $C_6P$ . High sucrose concentrations  $C_{12}$  in the phloem inhibit active loading of sucrose into the phloem. Soil water moisture  $\sigma_H$  reduction stimulates phloem loading to maintain a positive osmotic pressure gradient and sieve element turgidity for transport of photosynthate to roots, stem and emerging leaves. This framework pro-

vides a template for other control factors, including pollutants.

The coupled biosynthesis-transport system shown in Figure 3.16 is a self-regulating process that stores starch when carbon assimilation rate exceeds the rate of carbon utilization. Excess carbon stored as starch is mobilized during periods of carbon supply shortage, thereby prolonging the period available for growth. The carbon assimilation and phloem loading system compensate for water stress by simultaneously reducing water loss and carbon uptake, while increasing phloem sucrose concentration. Growth potential is reduced by these two processes, but the impact is greater on leaf growth than root growth, for reasons to be explained.

For starch to be exported from a mature leaf, it must be hydrolyzed. Hydrolysis and formation of hexose phosphate is controlled by the fraction of free phosphate  $\sigma_{P_f}$ . The rate of starch breakdown into hexose phosphate is given by the equation:

$$\Delta C_6P = \text{Min} \{ P_f, [C_6]_n \} \quad (16)$$

The phloem loading submodel shown in Figure 3.15 has an activation state (1) and a regeneration state (0). The mean transition rate between state 0 and 1, represented by  $\lambda_0$ , is controlled by the phloem sucrose level index  $\sigma_{C_{12}}$ ,

$$\lambda_0 = \frac{1}{1 + \exp [\gamma_{C_{12}}(\sigma_{C_{12}} - \sigma_{C_{12.5}})]} \quad (17)$$

where  $\sigma_{C_{12.5}}$  is the phloem sucrose operating concentration, which is a function of soil water moisture index  $\sigma_H$ . As  $\sigma_H$  decreases,  $\sigma_{C_{12.5}}$  increases, resulting in osmotic adjustment of the phloem and to a lesser extent of the whole plant. The parameter  $\sigma_{C_{12.5}}$  represents the 50% set point of the feedback control mechanism. Transition  $\lambda_0$  therefore represents the compensatory response regulating phloem sucrose concentrations.

The transition from states 1 to 0 (Figure 3.15) converts hexose phosphate  $C_6P$  into sucrose  $C_{12}$  and releases free phosphate  $P_f$ . The mean transition rate depends on the relative hexose phosphate concentration:

$$\lambda_1 = \sigma_{C_6P} \tau_P \quad (18)$$

where  $\tau_P$  is the temperature-dependent configuration function for phloem loading and transport.

The concentration of sucrose in the phloem  $C_{12}^{j+1}$  at the time period  $j+1$  is determined by the concentration  $C_{12}^j$  plus the amount corrected from  $C_6P$  to  $C_{12}$  and loaded into the phloem:

$$C_{12}^{j+1} = C_{12}^j + \Delta C_{12} \quad (19)$$

The loading rate of sucrose into the phloem is given by the equation:

$$\Delta C_{12} = \frac{P}{2} \frac{\lambda_0 \lambda_1}{\lambda_0 + \lambda_1} \quad (20)$$

where  $\frac{P}{2}$  represents the maximum concentration of  $C_6P$  that can be converted into  $C_{12}$  and  $\lambda_1$  includes the

term  $\sigma_{C_6P} = C_6P / P$  that reflects the relative concentration of hexose phosphate.

The equations regulating phloem loading and osmotic adjustment are shown in Figure 5.17. There are two transition rates  $\lambda_0$  and  $\lambda_1$  between two free energy states. The rate of transition  $\lambda_0$  is primarily controlled by the feedback sensing of current phloem sucrose concentration. The operating phloem concentrations osmotically adjust under conditions of water stress to maintain phloem turgor and thus distribution of photosynthate. Transition  $\lambda_1$  is controlled by the availability of hexose phosphate and regulated by temperature which can limit sucrose movement when temperatures fall below or rise above the low and high  $T_{1/2}$  thresholds.

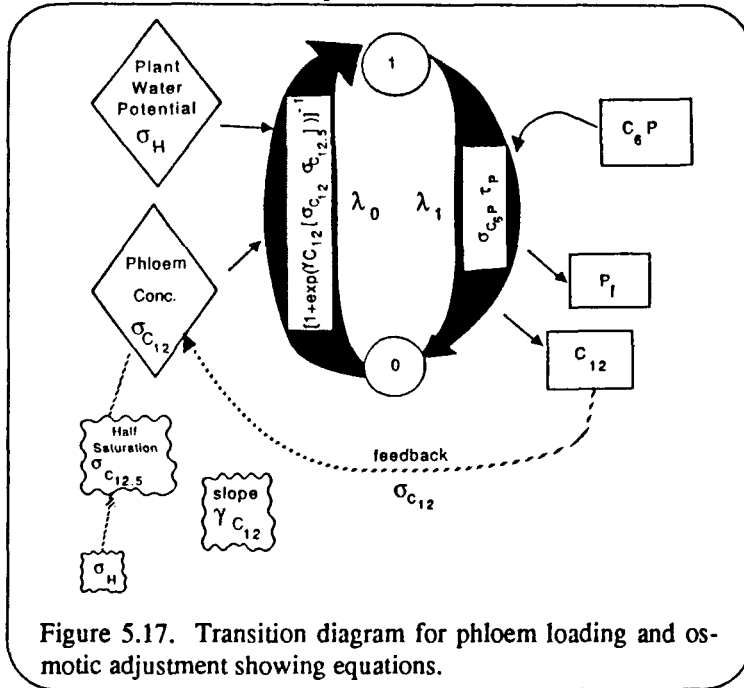


Figure 5.17. Transition diagram for phloem loading and osmotic adjustment showing equations.

### b. Phloem Transport and Distribution

To construct a simple pressure flow model, we assume that mass flow resistances  $R_i$  to growth sinks  $i$  control photosynthate distribution. The pressure gradient is assumed equal to the concentration gradient,  $C_{12} - C_{12}^i$  thus mass flow  $J_i$  to sink  $i$  is:

$$J_i = \frac{C_{12} - C_{12}^i}{R_i} \quad (21)$$

Phloem loading regulates phloem concentration to the value  $C_{12}$  as previously described in Eq. (17) through Eq. (20) to lie between these extremes.

ously described in Eq. (17) through Eq. (20) to lie between these extremes.

### 3. Heterotrophic growth and maintenance

#### a. Maintenance

Maintenance costs in higher plants are low compared to animals and micro-organisms, but both growth and maintenance compete for the same pool of substrate. Although each shows a strong temperature dependence, growth yield is independent of temperature but maintenance requirements increase with temperature. Maintenance cost of tissues consumes about 1% to 4% of the weight of the dry matter in the form of carbohydrates per day.[5]

The temperature dependence of maintenance is a well established phenomenon, though the fundamental mechanisms are not quantified. Here, the maintenance temperature response  $\phi_m(T)$  is described by a modified Eyring[6] equation with the form:

$$\phi_m(T) = \frac{\rho_m T}{T_m} \exp \left[ \frac{\Delta E_m^\ddagger}{R} \left( \frac{1}{T_m} - \frac{1}{T} \right) \right] \quad (22)$$

where  $T_m$  is a reference temperature (chosen by the experimenter) in °K,  $\rho_m$  is the observed rate at the reference temperature,  $T$  is the ambient temperature,  $R$  is the gas constant and  $\Delta E_m^*$  is the energy of activation for maintenance. The value for  $\Delta E_m^*$  can be calculated from the slope of the maintenance temperature response curve at  $\rho_m$  on a log plot. [21;8]

The maintenance model is built with two control factors, organic nitrogen and temperature. Figure 5.18 shows two free energy states for maintenance, state 0, the regenerative state, and state -1, the partial degradation state. The transition  $\lambda_0$  determines the maintenance demand:

$$\lambda_0 = \sigma_{NO} \quad (23)$$

where  $\sigma_{NO}$  is the relative nitrogen content for heterotrophic growth tissues.

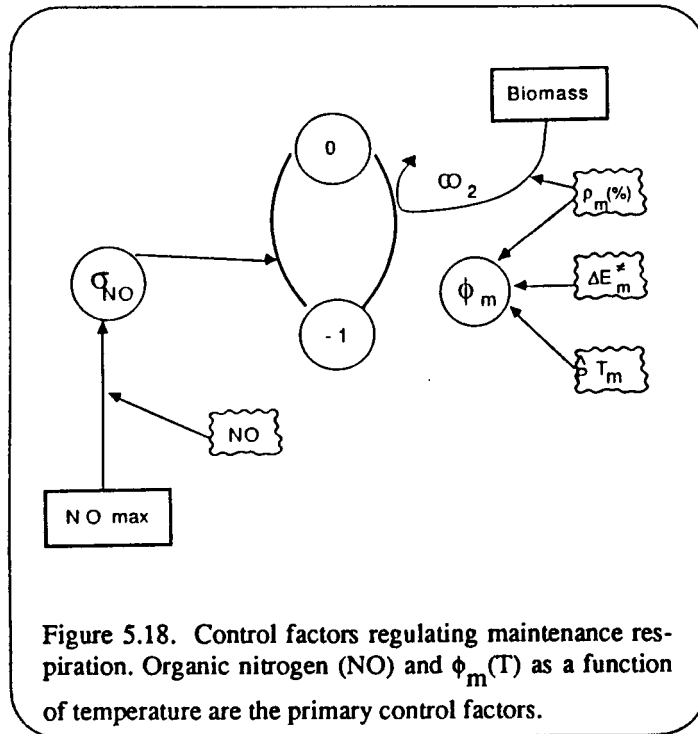


Figure 5.18. Control factors regulating maintenance respiration. Organic nitrogen (NO) and  $\phi_m(T)$  as a function of temperature are the primary control factors.

The transition  $\lambda_1$  from state -1 to the regenerative state is defined by Eq. (22),

$$\lambda_1 = \phi_m(T) / \rho_m. \quad (24)$$

The maintenance temperature function extends beyond the limits of the growth temperature threshold values for  $T_{1/2}$ , otherwise thermal damage cannot be repaired. [22]

#### b. Growth Yields

Calculation of growth involves three components, (1) growth yield calculation based upon efficiency of substrate conversion to product, (2) growth demand determined by genetic factors interacting with environment

factors and (3) photosynthate supply. Growth yield is independent of temperature and can be calculated from the chemical formula of the product. [23]

#### c. Growth Demand

Heterotrophic growth rate depends upon temperatures lying between growth threshold limits, sucrose supply in the phloem  $C_{12}$  and availability of primary nutrients NPS, soluble salts NS and trace elements  $N_2$  from the transpiration stream. Primary nutrients are essential for synthesis of protoplasm, especially proteins

and nucleotides. Soluble salts and trace elements are necessary for metabolic function. A lack of primary nutrients diverts biosynthesis towards secondary metabolites. [24;25] A plentiful supply of primary nutrients, particularly nitrogen, favors biomass growth.

## Linkages Between Components

The linkage between growth and maintenance for leaves, stems, reproductive organs and roots is shown in Figure 3.19. Maintenance proceeds regardless of the environmental conditions other than temperature. Biomass of the plant parts is the difference between the growth increment and the maintenance demand. The left-hand side of the diagram represents the supply (autotrophic) system and the right-hand side the demand (heterotrophic) system.

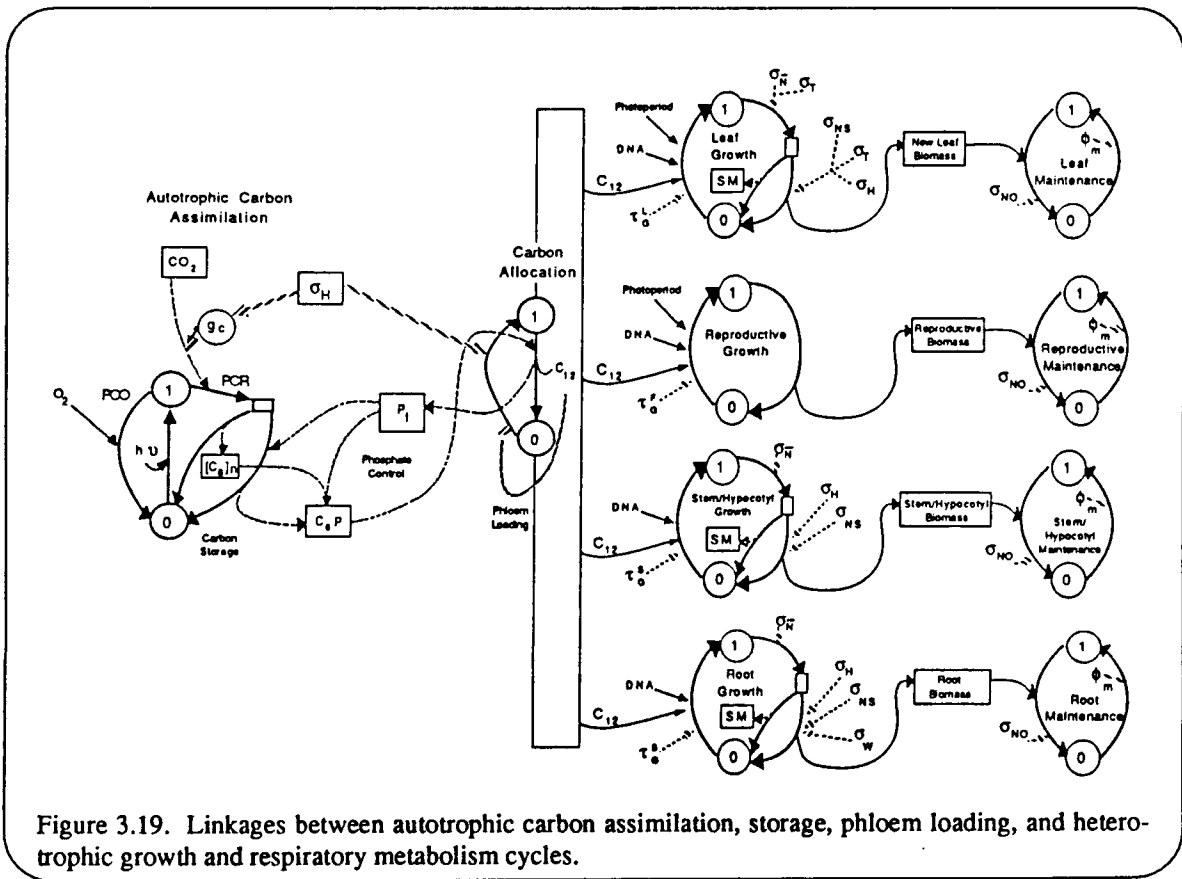


Figure 3.19. Linkages between autotrophic carbon assimilation, storage, phloem loading, and heterotrophic growth and respiratory metabolism cycles.

## 3.6. A Human Physiology Model to be Interfaced with the Life Support System (LSS)

### Introduction

The use of computer simulation in the field of medical physiology has grown tremendously in the last 20 years. In 1972, A.C. Guyton, T.G. Coleman and H.J. Granger[26] published a paper describing a systems analysis approach to regulation of whole body blood circulation. As a part of this effort they wrote a Fortran program, referred to since then as the Guyton model, which included 18 major systems and over 400 mathematical operations. The model was revolutionary in being the first application of systems analysis to a very complex natural phenomenon. For the first time researchers could perturb one part of the system and visualize responses in other parts of the system with their intricate control mechanisms and feedback loops. This model has been used and modified extensively for analyzing data in both medicine and space life sciences. Data gathered on the nine astronauts during the three manned Skylab missions has been analyzed using the Guyton model modified to accommodate the fluid shifts and cardiovascular changes brought about by extended stays in zero gravity.

The Guyton model, however, is both scientifically and technologically out of date. Our understanding of most physiological systems has advanced significantly since the Guyton model was written but most of these changes have not been incorporated. Modification of the model is cumbersome since it was written in Fortran and because of the time constants of some functions, runtime is often greater than realtime. Also, portability of the model from one computer to another is hampered by Fortran's machine specificity.

Since the Guyton model was written, numerous smaller, more specialized human physiology models have been written for both research and teaching purposes. While these models probably run faster, their applicability is limited by the incorporated physiological systems. In addition, most of the earlier of the special models are in Fortran and suffer from the same modification and portability problems as the Guyton model.

### Objectives

The proposed research will produce a dynamic simulation model of human physiology (HP) that will interface with the LSS models being developed. The HP model will have two functions: 1) it will provide the food, water and oxygen uptake rates and carbon dioxide, water and waste output rates for humans to the LSS model as these variables change with level of activity and 2) it will show the human physiological response to the variable conditions within the life support system.

The specific objectives are:

- Assessing the current state of human physiological models in medical and space life sciences research. This will insure that the model incorporates those physiological systems that are of interest to scientists concerned with astronaut health and that the systems include state-of-the-art knowledge of human physiology.

- Participation in the modeling activities of the Recon group as it builds the physical-chemical-biological LSS model to develop the best interface for the two models. This effort will also include interaction with other LSS modeling projects across the US to assess the possibility of providing modified HP models to interface with their versions of LSS models.
- Building the HP simulation model and an interface which will allow the user to vary those physiological systems or variables under observation.

## Description of Proposed HP Model

The major consideration to be taken into account in building the proposed HP model will be its compatibility with the LSS models currently under development. The purpose of a LSS is to take waste gases, liquids and solids generated by humans and convert or purify them into reusable gases, liquids and solids. A LSS is typically composed of physical and chemical components (machines, reactors and storage tanks) that are interconnected in some manner and controlled either centrally or locally. Since these functions can be accomplished by a many different sets of components, a single model will not suffice to describe all possible LSS configurations. In addition a single LSS configuration can be modeled in several different ways for different types of analysis and design purposes. Therefore, the LSS modeling efforts at this university are concentrating on building a knowledge base of LSS component machines and reactors and a user interface which will aid a researcher in building a specific type of model of a specific LSS configuration.

Each LSS model will need a human component as an integral part to supply information about what is needed and what is produced. The type of LSS model will dictate how complex an HP model is needed. For dynamic simulation LSS models a single HP model is feasible since the human interface component, namely the crew cabin, is common in all configurations and varies only in size.

LSS models that have been developed up to now have usually assumed a steady-state, non-responsive human physiology. For the purposes of designing a LSS this view is both one sided and over-simple. Even dynamic models of HP which vary the input and output according to activity level are insufficient from a space life science point of view. Humans as well as other animals have very intricate, dynamic and robust control systems of their various physiological components. These control systems react to the environment in such a way so as to keep the human functioning. Environmental conditions which may appear to be tolerable in the short run because of human compensatory control systems, may actually have invisible, cumulative or long-term adverse effects. HP models which are merely activity-level-driven gas-exchangers may be adequate for a first draft LSS design but are not adequate for fine tuning LSS control systems or for assessing the overall adequacy of a particular LSS design.

Further problems arise because humans are designed by natural selection to function in one earth gravity and in a very large open ecological life support system. Human control systems which function well on earth cause some undesirable effects in zero and low gravity, such as a shift of fluid from the lower to the upper part of the body. A well built HP model needs to incorporate these control mechanisms and their effects in zero-

gravity in order to allow the assessment of a LSS dynamics on an already compromised human system. Environmental conditions which could be tolerated in one gravity may not be tolerable in zero-gravity.

## **TAMU Personnel and Facilities**

The HP model will be built by Merry Makela, a Ph.D. in Biology, with extensive experience in modeling natural systems and in statistics and data analysis. She has participated in the Recon group during the last year and a half and has built an object-oriented dynamic LSS model with human and plant components. Dr. Makela will be assisted in the human physiological aspects of the model by faculty from the TAMU School of Medicine, Medical Physiology Department. Dr. Harris Granger, Head of this department and co-author of the Guyton model, has extensive experience in developing models of human physiology and has expressed interest in the proposed work. Dr. Thomas Rogers of the TAMU Space Research Center, who spent nearly 20 years working on contract to the Life Sciences Division at JSC, and Dr. C.O. Patterson of the Department of Biology will assist. In addition to personnel at Texas A&M, researchers on contract to NASA-JSC have expressed their interest and willingness to assist in these efforts.

## **Conclusion**

The HP model will become an integral part of the LSS modeling efforts. Traditionally Life Sciences has enjoyed a step-child status at NASA because few NASA engineers were adequately trained to understand or appreciate the role of Life Sciences in space exploration. By providing an HP model that will interface with LSS models, the odious task of incorporating humans into LSS models may become more tolerable. The engineers designing LSS may come to rely on the HP model to represent the human input and response without actually having to understand how the model works. In addition space life and medical scientists will have a vehicle for evaluating proposed LSS designs at a very early stage.

- [1] Preisig, H.A., On the Design of a Block Diagram Based Signal Processing and Simulation Package, AIChE Annual Meeting, Miami, 1986
- [2] Hall, P., *J. London Math. Soc.*, 10, 26 (1934)
- [3] Farquhar, F.D., S. von Caemmerer and J.A. Berry. (1980). A biochemical model of photosynthetic CO<sub>2</sub> assimilation in leaves of C<sub>3</sub> species. *Planta*, 149:78-90.
- [4] O'Neill, R.V., D.L. deAngelis, J.B. Waide and T.F.H. Allen (1986). *A Hierarchical Concept of Ecosystems*. Princeton University Press, Princeton, N.J. 253 p.
- [5] Penning de Vries, F.W.T. (1974). Substrate utilization and respiration in relation to growth and maintenance in higher plants. *Neth. J. Agric. Sci.*, 22:40-44.
- [6] Eyring, H. (1935). The activated complex in chemical reactions. *J. Chem. Physics*, 3:107.
- [7] Sharpe, P.J.H. and D.W. DeMichele (1977). Reaction kinetics of poikilotherm development. *Journal of Theoretical Biology*, 64:649-670.
- [8] Sharpe, P.J.H. (1983). Responses of photosynthesis and dark respiration to temperature. *Annals of Botany*, 52:325-343.
- [9] Ball, J.T., I.E. Woodrow and J.A. Berry (1987). A model predicting stomatal conductance and its contribution to the control of photosynthesis under different environmental conditions. *Progress Photosynthesis Research*, 4:221-224.
- [10] Wellburn, A.R. (1985). SO<sub>2</sub> effects on stomatal and thylakoid function. pp. 133-147. In: (eds. W.E. Winner, H.A. Mooney, and R.A. Goldstein) *Sulfur Dioxide and Vegetation: Physiology, Ecology and Policy Issues*.
- [11] Fares, Y., D.W. DeMichele, J.D. Goeschl and D.A. Baltuskonis (1978). Continuously produced, high specific activity <sup>11</sup>C for studies of photosynthesis, transport, and metabolism. *International Journal of Applied Radiation and Isotopes*, 29: 431-441.
- [12] Goeschl, J.D., C.E. Magnuson, Y. Fares, C.H. Jaeger, C.E. Nelson and B.R. Strain (1984). Spontaneous and induced blocking and unblocking of phloem transport. *Plant, Cell and Environment*, 7:89-100.
- [13] Magnuson, C.E., J.D. Goeschl and Y. Fares (1986). Experimental tests of the Munch-Horwitz model of phloem transport: Effects of loading rates, *Plant, Cell and Environment*, 9:103-109.
- [14] Goeschl, J.D., Y. Fares, C.E. Magnuson, H.W. Scheld, B.R. Strain, C.E. Nelson and C.H. Jaeger (1988). Short-lived isotope kinetics: A window to the inside, pp. 21-53. In: (Gary R. Beecher, ed) *Research Instrumentation for the 21st Century*. Beltsville Symposium in Agricultural Research.
- [15] Sharpe, P.J.H., R.D. Spence and E.J. Rykiel (1988). Diagnosis of sequential ozone effects on carbon assimilation, translocation, and allocation in cottonwood and loblolly pine. *NCASI Technical Bulletin* (in press).
- [16] Spence, R.D., P.J.H. Sharpe and E.J. Rykiel (1989)., Ozone alters carbon allocation in loblolly pine without visible damage: Assessment with carbon-11 dating. *Oecologia* (in review).
- [17] Goeschl, J.D., C.E. Magnuson, D.W. DeMichele and P.J.H. Sharpe (1976). Concentration-dependent unloading as a necessary assumption for a closed form mathematical model of osmotically driven pressure flow in phloem. *Plant Physiology*, 58:556-562.
- [18] Goeschl, J.D., C.E. Magnuson and Y. Fares (1986). Physiological implications of the Munch-Horwitz model of phloem transport: Effects of loading rates, *Plant, Cell and Environment*, 9:95-102.
- [19] Magnuson, C.E., J.D. Goeschl, P.J.H. Sharpe and D.W. DeMichele (1979). Consequences of insufficient equations in models of the Munch hypothesis of phloem transport. *Plant, Cell and Environment*, 2:181-188.

- [20] Smith, K.C., C.E. Magnuson, J.D. Goeschl, and D.W. DeMichele (1980). A time-dependent mathematical expression for Munch type phloem translocation in plants. *Journal of Theoretical Biology* 86:493-505.
- [21] Schoolfield, R.M., P.J.H. Sharpe and C.E. Magnuson (1981). Non-linear regression of biological Arrhenius functions. *Journal of Theoretical Biology*, 99:719-731.
- [22] Alexandrov, V. Ya. (1964). Cytophysiological and etoecological investigations of heat resistance of plant cells towards the action of high and low temperature. *Quart. Rev. Biol.*, 39:35-77.
- [23] McDermitt, D.K. and R.S.Loomis (1981). Elemental composition of biomass and its relation to energy content, growth efficiency and growth yield. *Ann. Bot.*, 48:275-290.
- [24] Sharpe, P.J.H., H. Wu, R.G. Cates and J.D. Goeschl (1975a). Energetics of pine defense systems to bark beetle attack. In: *Proceedings, Integrated Pest Management Research Symposium*, (S.J. Branham and R.C. Thatcher, eds.). Southern Forest Experimental Station, New Orleans, Louisiana, General Technical Report, 50-56. pp. 206-223.
- [25] Lorio, P.L., Jr., (1986). Growth-differentiation balance: a basis for understanding southern pine beetle - tree interactions. *For. Ecol. Manage.*, 14:259-273.
- [26] Farquhar, F.D., S. von Caemmerer and J.A. Berry. (1980). A biochemical model of photosynthetic CO<sub>2</sub> assimilation in leaves of C<sub>3</sub> species. *Planta*, 149:78-90.
- [27] O'Neill, R.V., D.L. deAngelis, J.B. Waide and T.F.H. Allen (1986). *A Hierarchical Concept of Ecosystems*. Princeton University Press, Princeton, N.J. 253 p.
- [28] Penning de Vries, F.W.T. (1974). Substrate utilization and respiration in relation to growth and maintenance in higher plants. *Neth. J. Agric. Sci.*, 22:40-44.
- [29] Eyring, H. (1935). The activated complex in chemical reactions. *J. Chem. Physics*, 3:107.
- [30] Sharpe, P.J.H. and D.W. DeMichele (1977). Reaction kinetics of poikilotherm development. *Journal of Theoretical Biology*, 64:649-670.
- [31] Sharpe, P.J.H. (1983). Responses of photosynthesis and dark respiration to temperature. *Annals of Botany*, 52:325-343.
- [32] Ball, J.T., I.E. Woodrow and J.A. Berry (1987). A model predicting stomatal conductance and its contribution to the control of photosynthesis under different environmental conditions. *Progress Photosynthesis Research*, 4:221-224.
- [33] Wellburn, A.R. (1985). SO<sub>2</sub> effects on stomatal and thylokoid function. pp. 133-147. In: (eds. W.E. Winner, H.A. Mooney, and R.A. Goldstein) *Sulfur Dioxide and Vegetation: Physiology, Ecology and Policy Issues*.
- [34] Fares, Y., D.W. DeMichele, J.D. Goeschl and D.A. Baltuskonis (1978). Continuously produced, high specific activity <sup>11</sup>C for studies of photosynthesis, transport, and metabolism. *International Journal of Applied Radiation and Isotopes*, 29: 431-441.
- [35] Goeschl, J.D., C.E. Magnuson, Y. Fares, C.H. Jaeger, C.E. Nelson and B.R. Strain (1984). Spontaneous and induced blocking and unblocking of phloem transport. *Plant, Cell and Environment*, 7:89-100.
- [36] Magnuson, C.E., J.D. Goeschl and Y. Fares (1986). Experimental tests of the Munch-Horwitz model of phloem transport: Effects of loading rates, *Plant, Cell and Environment*, 9:103-109.
- [37] Goeschl, J.D., Y. Fares, C.E. Magnuson, H.W. Scheld, B.R. Strain, C.E. Nelson and C.H. Jaeger (1988). Short-lived isotope kinetics: A window to the inside, pp. 21-53. In: (Gary R. Beecher, ed) *Research Instrumentation for the 21st Century*. Beltsville Symposium in Agricultural Research.
- [38] Sharpe, P.J.H., R.D. Spence and E.J. Rykiel (1988). Diagnosis of sequential ozone effects on carbon assimilation, translocation, and allocation in cottonwood and loblolly pine. *NCASI Technical Bulletin* (in press).
- [39] Spence, R.D., P.J.H. Sharpe and E.J. Rykiel (1989)., Ozone alters carbon allocation in loblolly

- pine without visible damage: Assessment with carbon-11 dating. *Oecologia* (in review).
- [40] Goeschl, J.D., C.E. Magnuson, D.W. DeMichele and P.J.H. Sharpe (1976). Concentration-dependent unloading as a necessary assumption for a closed form mathematical model of osmotically driven pressure flow in phloem. *Plant Physiology*, 58:556-562.
- [41] Goeschl, J.D., C.E. Magnuson and Y. Fares (1986). Physiological implications of the Munch-Horwitz model of phloem transport: Effects of loading rates, *Plant, Cell and Environment*, 9:95-102.
- [42] Magnuson, C.E., J.D. Goeschl, P.J.H. Sharpe and D.W. DeMichele (1979). Consequences of insufficient equations in models of the Munch hypothesis of phloem transport. *Plant, Cell and Environment*, 2:181-188.
- [43] Smith, K.C., C.E. Magnuson, J.D. Goeschl, and D.W. DeMichele (1980). A time-dependent mathematical expression for Munch type phloem translocation in plants. *Journal of Theoretical Biology* 86:493-505.
- [44] Schoolfield, R.M., P.J.H. Sharpe and C.E. Magnuson (1981). Non-linear regression of biological Arrhenius functions. *Journal of Theoretical Biology*, 99:719-731.
- [45] Alexandrov, V. Ya. (1964). Cytophysiological and ecophysiological investigations of heat resistance of plant cells towards the action of high and low temperature. *Quart. Rev. Biol.*, 39:35-77.
- [46] McDermitt, D.K. and R.S. Loomis (1981). Elemental composition of biomass and its relation to energy content, growth efficiency and growth yield. *Ann. Bot.*, 48:275-290.
- [47] Sharpe, P.J.H., H. Wu, R.G. Cates and J.D. Goeschl (1975a). Energetics of pine defense systems to bark beetle attack. In: *Proceedings, Integrated Pest Management Research Symposium*, (S.J. Branham and R.C. Thatcher, eds.). Southern Forest Experimental Station, New Orleans, Louisiana, General Technical Report, 50-56. pp. 206-223.
- [48] Lorio, P.L., Jr., (1986). Growth-differentiation balance: a basis for understanding southern pine beetle - tree interactions. *For. Ecol. Manage.*, 14:259-273.
- [49] Guyton, A.C., T.G. Coleman, and H. J. Granger; "Circulation: Overall Regulation", *Annual Review of Physiology* pp 13-46, 1972.

## 4. Conceptual Modeling Studies for Waste Electrolyzer

### Model Development

Figure 4.1 shows a schematic representation of a CELSS approach which incorporates plants or algae to supplement the diet of the astronauts. This is based on our earlier model [1]: but wastes are electrolyzed rather than combusted. Reactors are represented as square boxes, separators as circles, and storage tanks as rounded boxes. Table 4.1 indicates the composition of each stream. Many of the streams have well defined chemical compositions (e.g.,  $H_2$ ,  $O_2$ ,  $CO_2$ ,  $N_2$ ,  $H_2O$ , and  $HNO_3$ ) while some of the streams are not well defined (e.g., edible plants, inedible plants, food, feces, urine, trash.)

A stoichiometric model of the CELSS system shown in Fig. 4.1 is necessary to define the capacities of the various reactors and separators. These capacities allow sizing of the components for weight, volume, and power trade-off studies. Also, the stoichiometric model will allow the daily accumulation (or depletion) of each of the tanks to be calculated. It will then be possible to determine if certain components must be supplied or if there will be a net production of some chemicals which may be used for other purposes. To be useful, the stoichiometric model must allow for various compositions of food and trash. There will be no attempt to model the system exactly since this would be too cumbersome. Instead, the stoichiometric model will be a "first-order" analysis of the system which sacrifices some accuracy in favor of simplicity. As with all models, some assumptions must be made.

The algae, food, and feces are assumed to be composed of carbohydrate, protein, fat, and fiber. Although there is an ash component in each of these items, the ash is inert so it is neglected in this first-order analysis. Table 4.2 shows the assumed chemical formulae and energy content for carbohydrates, protein, fat, and fiber, and lignin. The chemical reactions occurring in each of the reactors of Fig. 4.1 are shown in Table 4.3.

Table 4.2. Chemical formulae for carbohydrate, protein, fat, fiber, and lignin.[2]

Code	Compound	Formula	Molecular Weight	Energy Value (kcal/g)
C	Carbohydrate	$C_6H_{12}O_6$	180	4
P	Protein	$C_4H_5ON$	83	4
F	Fat	$C_{16}H_{32}O_2$	256	9
B	Fiber	$C_6H_{10}O_5$	162	0
L	Lignin	$C_{10}H_{11}O_2$	163	0

Urine contains about 60% organic substances (e.g., urea, uric acid, creatinine, and ammonia) and 40% inorganic salts.[3] For simplicity, the salt fraction will be considered inert and will be neglected. The organic fraction is assumed to be urea which is derived from ingested protein.

The trash contains a number of items such as waste paper, plastic wrap and food scraps. It

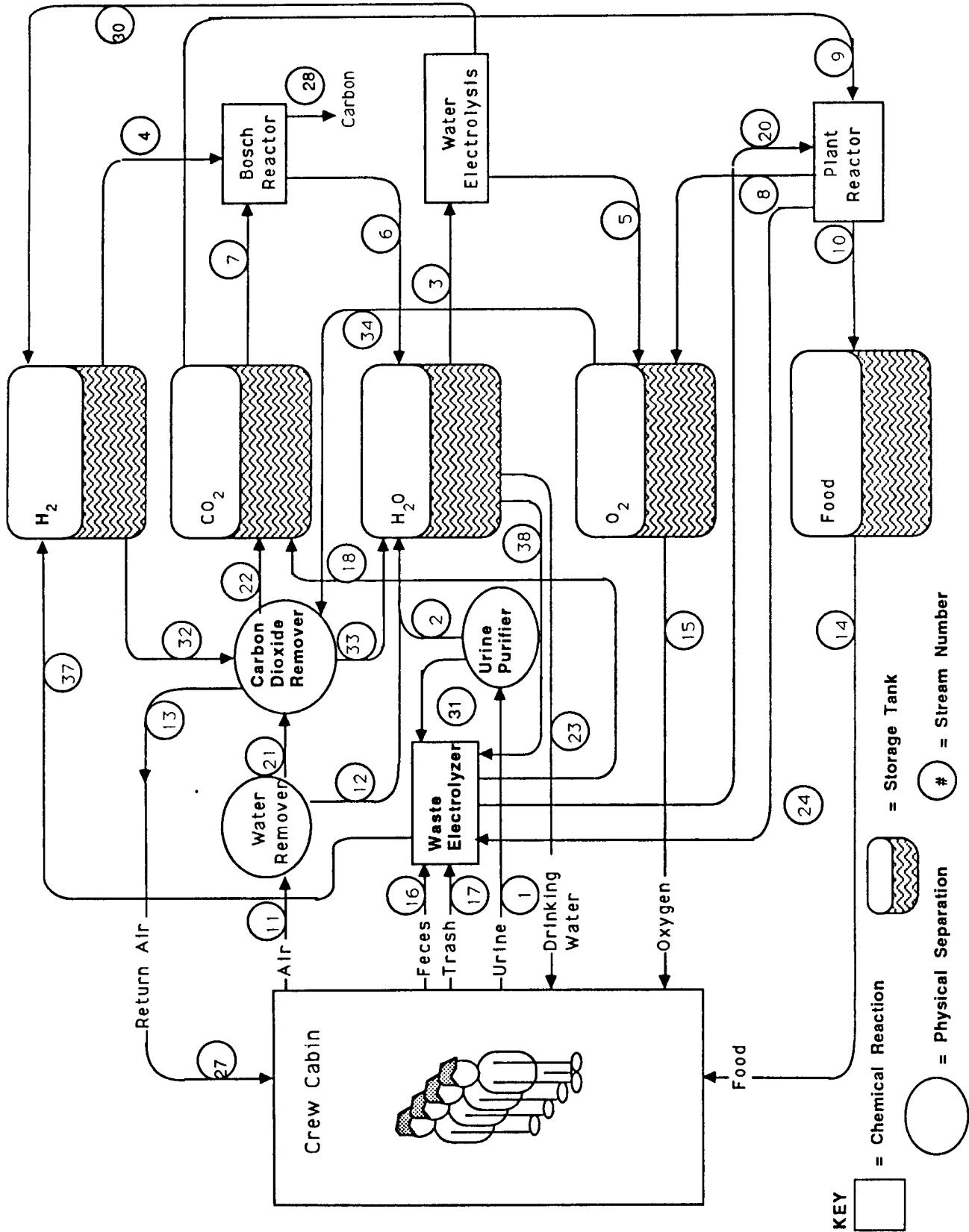


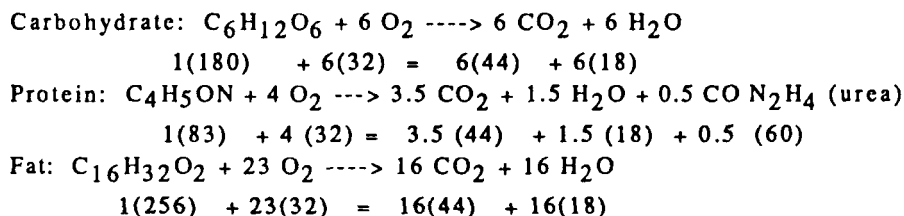
Figure 1. CELSS schematic using higher plants or algae for food and oxygen production.

Table 1. Composition of the streams shown in Figure 1.

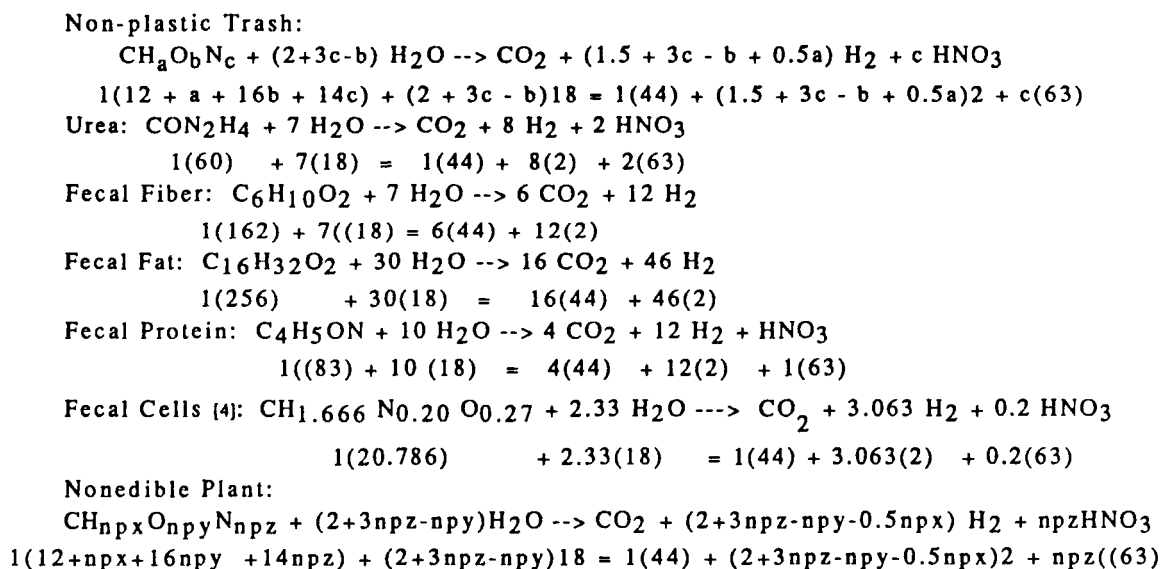
Stream	H <sub>2</sub>	O <sub>2</sub>	CO <sub>2</sub>	N <sub>2</sub>	H <sub>2</sub> O	C	HNO <sub>3</sub>	Edible Plants (Dry)	Food (Dry)	Feces (Dry)	Urine (Dry)	Trash (Dry)	Inedible Plants (Dry)
1					x						x		
2					x								
3					x								
4	x												
5		x											
6					x								
7			x										
8		x											
9			x										
10					x			x					
11		x	x	x	x								
12					x								
13		x		x									
14					x				x				
15		x											
16					x					x			
17					x							x	
18			x	x	x								
19		x											
20					x								
21		x	x	x									
22			x										
23					x								
24													x
25	x												
26				x									
27		x		x									
28						x							
29							x						
30	x												
31											x		
32	x												
33					x								
34		x											
35	x												
36					x								

Table 4.3. Chemical reactions occurring in the CELSS system.

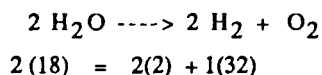
Crew Cabin



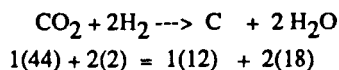
Waste Electrolyzer



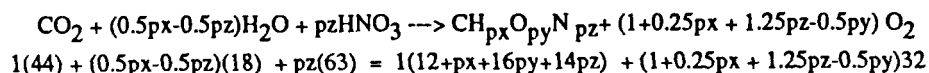
Water Electrolyzer



Bosch Reactor



Plant Growth



is assumed that metallic items have not been deposited in the trash, since they may foul the waste treatment process. The electrolyzer does not break down plastics. It will be assumed that all non-plastic trash sent to the electrolyzer will consist of C, H, O, and N atoms.

Although a number of control strategies may be devised to regulate the operation of the chemical reactors, the strategy shown in Table 4.4 was designed to minimize the capacity of each reactor. For example, the Bosch reactor could operate at higher than the minimum rate required to meet the water needs and produce more water which could then be split to produce extra oxygen. This would make the equipment larger than necessary for achieving the basic water balance and increase power consumption.

---

Table 4.4. Control Strategies for Chemical Reactors.

Crew Cabin

The metabolic rate of the crew members determines the rate of oxygen and food delivered to the cabin. The metabolic rate represents the "load" on the life support system.

Plant/Algae Reactor

The CO<sub>2</sub> and H<sub>2</sub>O flow to the plant/algae reactor will be determined by food consumption rate. The light intensity will be adjusted for the most efficient production of biomass at the required output.

Waste Electrolyzer

The electric current to the waste electrolyzer will be regulated to completely break down all nonplastic trash, feces, and urine solids fed to the reactor.

Water Electrolyzer

The rate of the electrolyzer may be governed by the oxygen demand or the hydrogen demand, whichever is greater. Generally, the oxygen demand is controlling.

Bosch Reactor

The Bosch reactor will be regulated by the level in the water tank. The rate is adjusted so there is no depletion in the water tank. The Bosch reactor would be shut off if water were accumulating in the tank.

---

The food eaten by the astronauts is composed of plants or algae plus items from the food stores. Tables 4.5, 4.6 and 4.7 show the method for determining the total composition of the food eaten by the astronauts. Table 4.8 lists the composition of some food items which might be used to supplement the plant/algal diet. Tables 4.9 and 4.10 show the method for calculating the composition of plant residues and Table 4.11 shows the method for calculating the composition of the entire plant. The elemental composition of the trash is calculated as shown in Table 4.12. The generalized chemical formula for trash is CH<sub>a</sub>O<sub>b</sub>N<sub>c</sub>. Table 4.12 also shows how the constants a, b, and c are calculated.

Table 4.5. Method for calculating composition of food store items.

Item	Composition of Food Item					
	Fraction of Food Store Items (mass fraction)	Carbohydrate (mass fraction)	Protein (mass fraction)	Fat (mass fraction)	Fiber (mass fraction)	Water (kg water/kg dry food)
1	$x_1$	$FSC_1$	$FSP_1$	$FSF_1$	$FSB_1$	$FSW_1$
2	$x_2$	$FSC_2$	$FSP_2$	$FSF_2$	$FSB_2$	$FSW_2$
3	$x_3$	$FSC_3$	$FSP_3$	$FSF_3$	$FSB_3$	$FSW_3$
.	.	.	.	.	.	.
.	.	.	.	.	.	.
.	.	.	.	.	.	.
n	$x_n$	$FSC_n$	$FSP_n$	$FSF_n$	$FSB_n$	$FSW_n$
	$\Sigma x_n$	$\Sigma x_n FSC_n$	$\Sigma x_n FSP_n$	$\Sigma x_n FSF_n$	$\Sigma x_n FSB_n$	$\Sigma x_n FSW_n$

$$1 = FSC_n + FSP_n + FSF_n + FSB_n \text{ (condition)}$$

$$FSF_t = \Sigma x_n FSF_n$$

$$1 = \Sigma x_n \text{ (condition)}$$

$$FSB_t = \Sigma x_n FSB_n$$

$$FSC_t = \Sigma x_n FSC_n$$

$$FSW_t = \Sigma x_n FSW_n$$

$$FSP_t = \Sigma x_n FSP_n$$

Table 4.7. Method for calculating composition of food eaten.

$$C_t = x_{\text{food stores}} FSC_t + (1 - x_{\text{food stores}}) EPC_t$$

$$P_t = x_{\text{food stores}} FSP_t + (1 - x_{\text{food stores}}) EPP_t$$

$$F_t = x_{\text{food stores}} FSF_t + (1 - x_{\text{food stores}}) EPF_t$$

$$B_t = x_{\text{food stores}} FSB_t + (1 - x_{\text{food stores}}) EPB_t$$

$$w_{\text{food}} = x_{\text{food stores}} FSW_t + (1 - x_{\text{food stores}}) EPW$$

Table 4.6. Method for calculating composition of edible plants.

Item	Fraction of Plant Production (mass fraction)	Composition of Food Item					Water (kg water/ kg dry plant EPW <sub>n</sub> )
		Carbohydrate (mass fraction)	Protein (mass fraction)	Fat (mass fraction)	Fiber (mass fraction)		
1	j <sub>1</sub>	EPC <sub>1</sub>	EPP <sub>1</sub>	EPF <sub>1</sub>	EPB <sub>1</sub>	EPW <sub>1</sub>	
2	j <sub>2</sub>	EPC <sub>2</sub>	EPP <sub>2</sub>	EPF <sub>2</sub>	EPB <sub>2</sub>	EPW <sub>2</sub>	
3	j <sub>3</sub>	EPC <sub>3</sub>	EPP <sub>3</sub>	EPF <sub>3</sub>	EPB <sub>3</sub>	EPW <sub>3</sub>	
.	.	.	.	.	.	.	
.	.	.	.	.	.	.	
n	j <sub>n</sub>	EPC <sub>n</sub>	EPP <sub>n</sub>	EPF <sub>n</sub>	EPB <sub>n</sub>	EPW <sub>n</sub>	
	$\Sigma j_n$	$\Sigma j_n EPC_n$	$\Sigma j_n EPP_n$	$\Sigma j_n EPF_n$	$\Sigma j_n EPB_n$	$\Sigma j_n EPW_n$	

$$1 = EPC_n + EPP_n + EPF_n + EPB_n \text{ (condition)}$$

$$EPF_t = \Sigma j_n EPF_n$$

$$1 = \Sigma j_n \text{ (condition)}$$

$$EPB_t = \Sigma j_n EPB_n$$

$$EPC_t = \Sigma j_n EPC_n$$

$$EPW_t = \Sigma j_n EPW_n$$

$$EPP_t = \Sigma j_n EPP_n$$

$$EPCarbon = \frac{6(12)}{180} EPC_t + \frac{4(12)}{83} EPP_t + \frac{16(12)}{256} EPF_t + \frac{6(12)}{162} EPB_t$$

$$= 0.4 EPC_t + 0.578 EPP_t + 0.75 EPF_t + 0.444 EPB_t$$

$$EPHydrogen = \frac{12}{180} EPC_t + \frac{5}{83} EPP_t + \frac{32}{256} EPF_t + \frac{10}{162} EPB_t$$

$$= 0.0667 EPC_t + 0.0602 EPP_t + 0.125 EPF_t + 0.0617 EPB_t$$

$$EPOxygen = \frac{6(16)}{180} EPC_t + \frac{1(16)}{83} EPP_t + \frac{2(16)}{256} EPF_t + \frac{5(16)}{162} EPB_t$$

$$= 0.5333 EPC_t + 0.1927 EPP_t + 0.125 EPF_t + 0.4938 EPB_t$$

$$EPNitrogen = \frac{1(14)}{83} EPP_t = 0.1687 EPP_t$$

$$epx = \frac{12}{1} \frac{EPHydrogen}{EPCarbon} = 12 \frac{EPHydrogen}{EPCarbon}$$

$$epy = \frac{12}{16} \frac{EPOxygen}{EPCarbon} = 0.75 \frac{EPOxygen}{EPCarbon}$$

$$epz = \frac{12}{14} \frac{EPNitrogen}{EPCarbon} = 0.857 \frac{EPNitrogen}{EPCarbon}$$

Table 4. 8. Composition of some food items.[5]

Item	Composition (dry, ash-free basis)				
	Carbohydrate (mass fraction)	Protein (mass fraction)	Fat (mass fraction)	Fiber (mass fraction)	FSW (g H <sub>2</sub> O/g dry food)
Pot Roast Beef	0	0.521	0.479	0	1.01
American Cheese	0.034	0.422	0.544	0	0.73
Roasted Chicken (white meat)	0	0.903	0.097	0	1.82
Poached Egg	0.032	0.506	0.462	0	2.92
Baked Flounder	0	0.785	0.215	0	1.52
Shrimp (raw)	0.074	0.887	0.039	0	3.83
Red Bean (dried)	0.672	0.262	0.017	0.049	0.12
Cashew Nut	0.303	0.187	0.495	0.015	0.05
Corn	0.801	0.134	0.038	0.027	2.80
White Rice (cooked)	0.916	0.076	0.004	0.004	2.76

Table4. 9. Residue coefficients.

Item	Fraction of Plant Production (mass fraction)	Residue Coefficient (kg dry residue/kg dry edible plant)
------	--	---

1	j <sub>1</sub>	RC <sub>1</sub>
2	j <sub>2</sub>	RC <sub>2</sub>
3	j <sub>3</sub>	RC <sub>3</sub>
.	.	.
.	.	.
.	.	.
n	j <sub>n</sub>	RC <sub>n</sub>
		$\overline{\Sigma j_n RC_n}$

$$PW = \Sigma j_n RC_n$$

$$k_1 = \frac{j_1 RC_1}{PW}$$

$$k_2 = \frac{j_2 RC_2}{PW}$$

$$k_3 = \frac{j_3 RC_3}{PW}$$

$$k_n = \frac{j_n RC_n}{PW}$$

Table 4.10. Method for calculating composition of nonedible plant residue.

Item	Fraction of Nonedible Plant Production (mass fraction)	C (mass fraction)	P (mass fraction)	F (mass fraction)	B (mass fraction)	L (mass fraction)	W (g water/g dry matter)
1	$k_1$	$NPC_1$	$NPP_1$	$NPF_1$	$NPB_1$	$NPL_1$	$NPW_1$
2	$k_2$	$NPC_2$	$NPP_2$	$NPF_2$	$NPB_2$	$NPL_2$	$NPW_2$
3	$k_3$	$NPC_3$	$NPP_3$	$NPF_3$	$NPB_3$	$NPL_3$	$NPW_3$
.	.	.	.	.	.	.	.
.	.	.	.	.	.	.	.
.	.	.	.	.	.	.	.
n	$k_n$	$NPC_n$	$NPP_n$	$NPF_n$	$NPB_n$	$NPL_n$	$NPW_n$
	$\Sigma k_n$	$\Sigma k_n NPC_n$	$\Sigma k_n NPP_n$	$\Sigma k_n NPF_n$	$\Sigma k_n NPB_n$	$\Sigma k_n NPL_n$	$\Sigma k_n NPW_n$

$$1 = NPC_n + NPP_n + NPF_n + NPB_n + NPL_n \text{ (condition)} \quad NPF_t = \Sigma k_n NPF_n$$

$$1 = \Sigma k_n \text{ (condition)} \quad NPB_t = \Sigma k_n NPB_n$$

$$NPC_t = \Sigma k_n NPC_n \quad NPL_t = \Sigma k_n NPL_n$$

$$NPP_t = \Sigma k_n NPP_n \quad NPW_t = \Sigma k_n NPW_n$$

$$NPC_{Carbon} = 0.4 NPC_t + 0.578 NPP_t + 0.75 NPF_t + 0.444 NPB_t + 0.736 NPL_t$$

$$NPHydrogen = 0.0667 NPC_t + 0.0602 NPP_t + 0.125 NPF_t + 0.0617 NPB_t + 0.0675 NPL_t$$

$$NPOxygen = 0.5333 NPC_t + 0.1927 NPP_t + 0.125 NPF_t + 0.4938 NPB_t + 0.1963 NPL_t$$

$$NPNitrogen = 0.1687 NPP_t$$

$$np_x = \frac{12}{1} \frac{NPHydrogen}{NPC_{Carbon}} = 12 \frac{NPHydrogen}{NPC_{Carbon}}$$

$$np_y = \frac{12}{16} \frac{NPOxygen}{NPC_{Carbon}} = 0.75 \frac{NPOxygen}{NPC_{Carbon}}$$

$$np_z = \frac{12}{14} \frac{NPNitrogen}{NPC_{Carbon}} = 0.857 \frac{NPNitrogen}{NPC_{Carbon}}$$

Table 4.11. Method for calculating composition of entire plant.

$$PCarbon = \frac{12}{12 + ep_x + 16ep_y + 14ep_z} + \frac{12(PW)}{12 + np_x + 16np_y + 14np_z}$$

$$PHydrogen = \frac{ep_x}{12 + ep_x + 16ep_y + 14ep_z} + \frac{np_x(PW)}{12 + np_x + 16np_y + 14np_z}$$

$$POxygen = \frac{16ep_y}{12 + ep_x + 16ep_y + 14ep_z} + \frac{16np_y(PW)}{12 + np_x + 16np_y + 14np_z}$$

$$PNitrogen = \frac{14ep_z}{12 + ep_x + 16ep_y + 14ep_z} + \frac{14np_z(PW)}{12 + np_x + 16np_y + 14np_z}$$

$$p_x = \frac{12 PHydrogen}{PCarbon} = 12 \frac{PHydrogen}{PCarbon}$$

$$p_y = \frac{12 POxygen}{16 PCarbon} = 0.75 \frac{POxygen}{PCarbon}$$

$$p_z = \frac{12 PNitrogen}{14 PCarbon} = 0.857 \frac{PNitrogen}{PCarbon}$$

Table 4.12. Calculation of the elemental composition of trash.

Item	Fraction of Total Trash (mass fraction)	Composition of Trash Item			
		C (mass fraction)	H (mass fraction)	O (mass fraction)	N (mass fraction)
1	y <sub>1</sub>	TC <sub>1</sub>	TH <sub>1</sub>	TO <sub>1</sub>	TN <sub>1</sub>
2	y <sub>2</sub>	TC <sub>2</sub>	TH <sub>2</sub>	TO <sub>2</sub>	TN <sub>2</sub>
3	y <sub>3</sub>	TC <sub>3</sub>	TH <sub>3</sub>	TO <sub>3</sub>	TN <sub>3</sub>
.	.	.	.	.	.
.	.	.	.	.	.
.	.	.	.	.	.
n	y <sub>n</sub>	TC <sub>n</sub>	TH <sub>n</sub>	TO <sub>n</sub>	TN <sub>n</sub>
	$\Sigma y_n$	$\Sigma y_n TC_n$	$\Sigma y_n TH_n$	$\Sigma y_n TO_n$	$\Sigma y_n TN_n$

Table 4.12. Continued.

$$1 = TC_n + TH_n + TO_n + TN_n \text{ (condition)}$$

$$1 = \sum y_n \text{ (condition)}$$

$$TC_t = \sum y_n TC_n$$

$$TH_t = \sum y_n TH_n$$

$$TO_t = \sum y_n TO_n$$

$$TN_t = \sum y_n TN_n$$

Trash Formula =  $C H_a O_b N_c$

$$a = \frac{12}{1} \frac{TH_t}{TC_t} = 12 \frac{TH_t}{TC_t}$$

$$b = \frac{12}{16} \frac{TO_t}{TC_t} = 0.75 \frac{TO_t}{TC_t}$$

$$c = \frac{12}{14} \frac{TN_t}{TC_t} = 0.857 \frac{TN_t}{TC_t}$$

With the preliminary information described thus far, it is possible to calculate the flow rates,  $R$ , of the various process streams and the accumulation,  $A$ , or depletion,  $D$ , of materials in the various tanks. The procedure for making these calculations will be presented in a stepwise manner. When the calculations are performed in the following order, there is no need for trial-and-error solutions to a series of simultaneous equations; that is, this system of equations can be solved in a sequential, stepwise manner. Most of these equations were developed using simple material balances around each of the pieces of equipment shown in Figure 4.1.

### 1. Energy content of food

The energy content of food is commonly measured in kcal/g. This is converted to J/g using the conversion factor of 4190.

$$E = (4C_t + 4P_t + 9F_t) 4190 = 16,760 C_t + 16,760P_t + 37,710F_t \quad (1)$$

### 2. Rate of food metabolism

The food required for metabolism is easily calculated from the energy content of the food. The conversion factor 86.4 is required to convert g/s to kg/d.

$$R_{food,met} = \frac{M}{E} 86.4 \quad (2)$$

Table 4.13 lists some metabolic heats for various activities.

### 3. Rate of $CO_2$ production by metabolism

The components of  $R_{food,met}$  which can be metabolized (carbohydrate, protein and fat) are converted to carbon dioxide according to the following relationship

$$R_{C O_2}^{met} = \left( \frac{6(44)}{180} C_t + \frac{3.5(44)}{83} P_t + \frac{16(44)}{256} F_t \right) R_{food,met} \quad (3)$$

$$= (1.467 C_t + 1.855 P_t + 2.75 F_t) R_{food,met}$$

#### 4. Rate of O<sub>2</sub> consumption by metabolism

The amount of oxygen required to metabolize the food is given by

$$R_{O_2}^{met} = \left( \frac{6(32)}{180} C_t + \frac{4(32)}{83} P_t + \frac{23(32)}{256} F_t \right) R_{food,met} \quad (4)$$

$$= (1.067 C_t + 1.542 P_t + 2.875 F_t) R_{food,met}$$

#### 5. Rate of H<sub>2</sub>O production by metabolism

The rate of water production by metabolism is given by

$$R_{H_2O}^{met} = \left( \frac{6(18)}{180} C_t + \frac{1.5(18)}{83} P_t + \frac{16(18)}{256} F_t \right) R_{food,met} \quad (5)$$

$$= (0.6 C_t + 0.325 P_t + 1.125 F_t) R_{food,met}$$

#### 6. Rate of urea production by metabolism

Urea is produced by the metabolism of proteins.

$$R_{urea}^{met} = \frac{0.5(60)}{83} P_t R_{food,met} = 0.361 P_t R_{food,met} \quad (6)$$

#### 7. Rate of food consumption

The rate at which food is consumed is larger than the rate of food which is metabolized. A portion of the food is fiber and exits in the feces. (See Table 4.14 for the composition of feces.) The human small intestine is not able to recover all the nutrients in the food since some of them are adsorbed onto the fiber. Some of these nutrients are utilized by microbes in the latter part of the large intestine. Also, some of the protein and fat is nondigestible and exits in the feces. Some fat also sluffs off of the intestinal lining. Thus, it can be seen that the digestion process is very complex. For this first-order analysis, it will be assumed that the food consumed can be partitioned into two fractions of identical composition (see Figure 4.2). The first fraction of the food is used for metabolism ( $R_{food,met}$ ) and the other fraction ( $R_{food,feces}$ ) results in feces production. The fiber fraction of  $R_{food,met}$  also will ultimately end up in the feces. The ratio,  $r$ , will be defined as the amount of nonfibrous fecal matter to the fibrous fecal matter

$$r \equiv \frac{\text{nonfibrous fecal matter}}{\text{fibrous fecal matter}}$$

Table 4.13. Metabolic heat associated with various activities.[6]

Activity	Metabolic Heat (W)
Sleep	84
Resting (sitting)	118
Very Light Activity (taking notes)	140
Light Activity (vehicle repair)	237
Moderate Activity (cycling 8 mi/h)	398
Heavy Activity (cycling 23 mi/h)	683
Very Heavy Activity (rowing 3.5 mi/h)	767

Table 4.14. Composition of \*Dry Feces.[7]

	Mass Fraction
Bacteria	0.3
Fat	0.1-0.2
Inorganic Matter	0.1-0.2
Protein	0.02-0.03
Fiber	0.3

\*Note: wet feces contain about 75% water.

For simplicity, this ratio is calculated on a mineral-free basis and is assumed to be constant. From the data shown in Table 4.14, a typical value is  $r=1.583$ . Examination of Figure 4.2 shows that the ratio  $r$  may be written explicitly as

$$r = \frac{(1 - B_t) R_{\text{food, feces}}}{B_t R_{\text{food, cons}}}$$

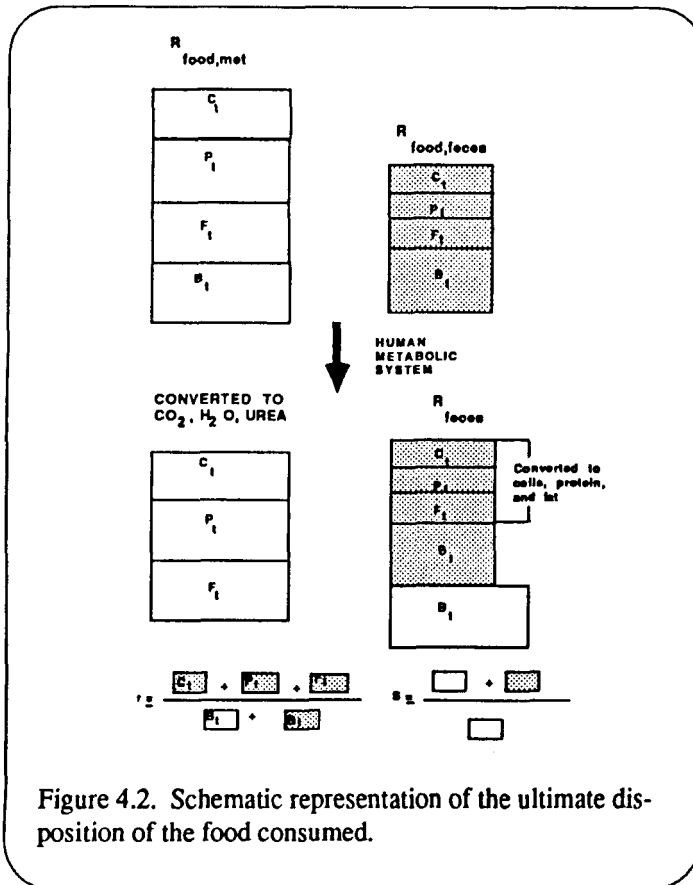


Figure 4.2. Schematic representation of the ultimate disposition of the food consumed.

This may be solved for  $R_{\text{food,feces}}$ . The ratio,  $s$ , is defined as the ratio of food consumed to food eaten for metabolism

$$s \equiv \frac{R_{\text{food, cons}}}{R_{\text{food, met}}}$$

This may be solved for  $R_{\text{food,met}}$ . The total food consumed is the sum of food used for metabolism and the food used for feces production

$$R_{\text{food, cons}} = R_{\text{food, met}} + R_{\text{food, feces}}$$

Substituting expressions for  $R_{\text{food,met}}$  and  $R_{\text{food,feces}}$  and solving for  $s$  gives

$$s = \frac{1 - B_t}{1 - (1 + r)B_t} \quad (7)$$

This value of  $s$  may then be used to calculate the food consumed from the food metabolized

$$R_{food, cons} = s R_{food, met} \quad (8)$$

It should be noted that Equation 7 has a singularity when  $(1+r)B_t=1$  and that  $s$  is negative when  $(1+r)B_t > 1$ . This results from the assumption that  $r$  is a constant. In actuality,  $r$  is a function of  $B_t$ . This functional relationship is not known, so the assumption that it is constant is used as a starting point. Further refinement will require experimental feeding trials.

#### 8. Rate of feces production

The feces are composed of fibrous and nonfibrous matter. The rate of fecal production can be calculated from

$$R_{feces} = (1 + r) B_t R_{food, cons} \quad (9)$$

#### 9. Rate of water loss in breath

During the act of breathing, air is brought into the lungs, where it is heated to body temperature and becomes saturated with moisture. The rate at which water evaporates from the lungs,  $R_{breathing}$ , is given by

$$R_{breathing} = Q (g_{out} - g_{in})$$

where  $Q$  is the volumetric flow of air through the lungs and  $g$  is the water content of the air going into and coming out of the lungs. The volumetric flow of air is related to the metabolic rate of the astronaut. A man at rest (118W) breathes about 18 breaths per minute with a volume of 0.75 L per breath.[6; 8] This translates to 19,400 L/d of air. Guyton [9] gives figures of 12 breaths per minute and 0.5 L per breath which translates to 8,640 L/d. We have chosen the higher estimate as a more conservative approach in estimating the required size of the water separator. Assuming the breathing rate is linear with metabolic rate, the breathing rate for other metabolic rates is given by

$$Q = 164 M$$

The water content of air is given by

$$g = \frac{p^{vap}}{RT} 18 \phi$$

where  $p^{vap}$  is the vapor pressure of water at temperature  $T$ . The parameter  $\phi$  is the relative humidity of the air expressed as a fraction which varies from 0 to 1.

An empirical expression for the vapor pressure of water is

$$p^{vap} = B - \frac{A}{C + t}$$

where  $p^{vap}$  is in mm Hg and  $t$  is in °C. The constants

are  $A = 1750.286 \text{ }^\circ\text{C}$ ,  $B = 8.10765$ , and  $C = 235.0 \text{ }^\circ\text{C}$ .

Substituting the above expressions,  $g$  may be calculated as

$$g = \frac{8.10765 - \frac{1750.286}{235.0 + t}}{10} \quad 18 \phi = \frac{8.10765 - \frac{1750.286}{235.0 + t}}{t + 273.15} \quad 0.2886 \phi$$

$$\left( 0.08205 \frac{\text{atm L}}{\text{gmole } ^\circ\text{K}} \right) \left( 760 \frac{\text{mmHg}}{\text{atm}} \right) (t + 273.15)$$

The air exiting the lungs is assumed to be saturated with moisture (i.e.,  $\phi = 1$ ) at  $37^\circ\text{C}$ . Therefore, it has a water content  $g_{\text{out}}$  of  $0.0438\text{g/L}$ . The water content of the air entering the lungs is dependent on the cabin temperature and relative humidity. The water loss by breathing,  $R_{\text{breathing}}$  (in  $\text{kg/day}$ ), is given by

$$R_{\text{breathing}} = 0.164M \left( 0.0438 - 0.2886 \frac{10}{t + 273.15} \phi \right) \quad (10)$$

#### 10. Rate of urine water produced

The sources of water for an astronaut are the water he drinks, the water produced from the metabolism of food, and the water in the food he eats. The astronaut loses water in urine, by sweating, in his breath, and in his feces. An expression for urine water may be obtained as follows:

$$R_{\text{urine}} = R_{\text{drink}} + R_{\text{H}_2\text{O}}^{\text{met}} + w_{\text{food}} R_{\text{food,cons}} - R_{\text{sweat}} - R_{\text{breathing}} - w_{\text{feces}} R_{\text{feces}} \quad (11)$$

where  $w_{\text{food}}$  is the ratio of food water to dry food and  $w_{\text{feces}}$  is the ratio of fecal water to dry feces.

#### 11. Rate of hydrogen production in waste electrolyzer

The waste electrolyzer breaks down non-plastic trash, urea from urine, and feces according to the stoichiometries shown in Table 4.3. The rate of water production for each component is shown below.

a. non-plastic trash

$$R_{\text{H}_2, a}^{\text{elec}} = \frac{(1.5 + 3c - b + 0.5a)2}{12 + a + 16b + 14c} R_{\text{trash}} \quad (12)$$

b. urea

$$R_{\text{H}_2, b}^{\text{elec}} = \frac{8(2)}{1(60)} R_{\text{urea}}^{\text{met}} = 0.267 R_{\text{urea}}^{\text{met}} \quad (13)$$

c. fecal fiber

$$R_{\text{H}_2, c}^{\text{elec}} = \frac{12(2)}{1(162)} B_t R_{\text{food,cons}} = 0.148 B_t R_{\text{food,cons}} \quad (14)$$

d. fecal fat

$$R_{H_2,d}^{elec} = \frac{46(2)}{1(256)} B_t F_f R_{food,cons} = 0.360 B_t F_f R_{food,cons} \quad (15)$$

where  $F_f$  is the ratio of fecal fat to fecal fiber.

e. fecal protein

$$R_{H_2,e}^{elec} = \frac{12(2)}{1(83)} B_t F_p R_{food,cons} = 0.289 B_t F_p R_{food,cons} \quad (16)$$

where  $F_p$  is the ratio of fecal protein to fecal fiber.

f. fecal cells

$$R_{H_2,f}^{elec} = \frac{3.063(2)}{1(20.786)} B_t F_c R_{food,cons} = 0.295 B_t F_c R_{food,cons} \quad (17)$$

where  $F_c$  is the ratio of fecal cells to fecal fiber.

g. plant wastes

$$R_{H_2,g}^{elec} = \frac{(2 + 3npz - npy - 0.5npx) 2}{12 + npz + 16npy + 14npz} PW (1 - x_{foodstores}) R_{food,cons} \quad (18)$$

The total hydrogen produced by the electrolyzer is given as the sum of the above rates..

$$R_{H_2}^{37} = R_{H_2,a}^{elec} + R_{H_2,b}^{elec} + R_{H_2,c}^{elec} + R_{H_2,d}^{elec} + R_{H_2,e}^{elec} + R_{H_2,f}^{elec} + R_{H_2,g}^{elec} \quad (19)$$

## 12. Rate of carbon dioxide production in the electrolyzer

The reaction stoichiometries shown in Table 4.3 may be used to calculate the  $CO_2$  production in the electrolyzer.

a. non-plastic trash

$$R_{CO_2,a}^{elec} = \frac{44}{12 + a + 16b + 14c} R_{trash} \quad (20)$$

b. urea

$$R_{CO_2,b}^{elec} = \frac{1(44)}{1(60)} R_{urea}^{met} = 0.733 R_{urea}^{met} \quad (21)$$

c. fecal fiber

$$R_{CO_2,c}^{elec} = \frac{6(44)}{1(162)} B_t R_{food,cons} = 1.630 B_t R_{food,cons} \quad (22)$$

d. fecal fat

$$R_{CO_2,d}^{elec} = \frac{16(44)}{1(256)} B_t F_f R_{food,cons} = 2.75 B_t F_f R_{food,cons} \quad (23)$$

e. fecal protein

$$R_{CO_2,e}^{elec} = \frac{4(44)}{1(83)} B_t F_p R_{food,cons} = 2.12 B_t F_p R_{food,cons} \quad (24)$$

f. fecal cells

$$R_{CO_2,f}^{elec} = \frac{1(44)}{1(20.786)} B_t F_c R_{food,cons} = 2.117 B_t F_c R_{food,cons} \quad (25)$$

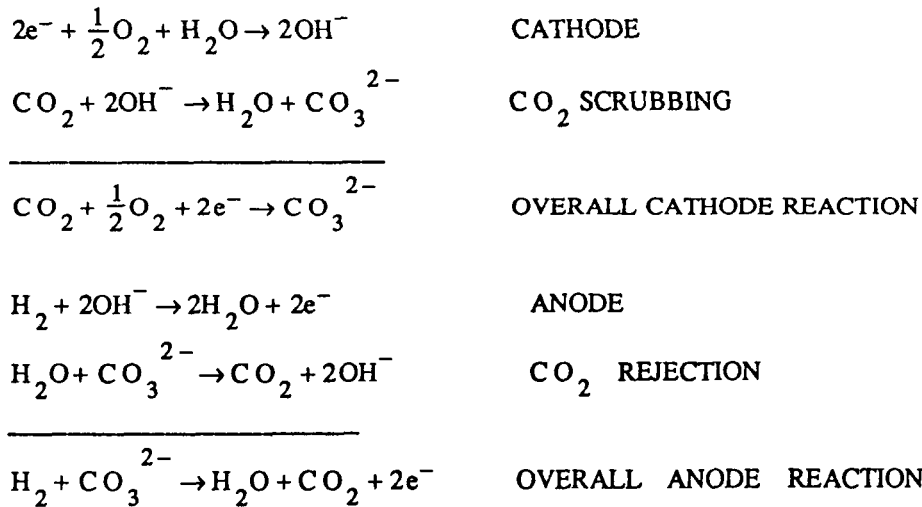
g. plant waste

$$R_{CO_2,g}^{elec} = \frac{1(44)}{12 + npx + 16npy + 14npz} PW (1 - x_{foodstores}) R_{food,cons} \quad (26)$$

The total carbon dioxide production from the combustor will be the sum of the above rates

$$R_{CO_2}^{18} = R_{CO_2,a}^{elec} + R_{CO_2,b}^{elec} + R_{CO_2,c}^{elec} + R_{CO_2,d}^{elec} + R_{CO_2,e}^{elec} + R_{CO_2,f}^{elec} + R_{CO_2,g}^{elec} \quad (27)$$

Carbon dioxide may be removed from the cabin atmosphere by an electrochemical depolarizer. The electrochemical depolarizer is essentially a fuel cell which allows carbon dioxide to be transferred from one electrode to another. It has the following stoichiometry.



The following equations must be used if the electrochemical depolarizer is used:

$$R_{H_2}^{32} = \frac{1(2)}{1(44)} \left( R_{CO_2}^{met} \right) = 0.04545 \left( R_{CO_2}^{met} \right) \quad (28)$$

$$R_{O_2}^{34} = \frac{0.5(32)}{1(44)} \left( R_{C O_2}^{met} \right) = 0.3636 \left( R_{C O_2}^{met} \right) \quad (29)$$

$$R_{H_2 O}^{33} = \frac{1(18)}{1(44)} \left( R_{C O_2}^{met} \right) = 0.409 \left( R_{C O_2}^{met} \right) \quad (30)$$

If a purely physical method, such as a membrane, is used to separate CO<sub>2</sub>, then the above rates would be zero

$$R_{H_2}^{32} = 0 \quad (28')$$

$$R_{O_2}^{34} = 0 \quad (29')$$

$$R_{H_2 O}^{33} = 0 \quad (30')$$

### 13. Water required for waste electrolysis

The reaction stoichiometries shown in Table 4.3 allow the water required for electrolysis to be calculated.

a. non-plastic trash

$$R_{H_2 O, a}^{elec} = \frac{(2 + 3c - b)18}{12 + a + 16b + 14c} R_{trash} \quad (31)$$

b. urea

$$R_{H_2 O, b}^{elec} = \frac{7(18)}{1(60)} R_{urea}^{met} = 2.1 R_{urea}^{met} \quad (32)$$

c. fecal fiber

$$R_{H_2 O, c}^{elec} = \frac{7(18)}{1(162)} B_t R_{food, cons} = 0.778 B_t R_{food, cons} \quad (33)$$

d. fecal fat

$$R_{H_2 O, d}^{elec} = \frac{30(18)}{1(256)} B_t F_f R_{food, cons} = 2.109 B_t F_f R_{food, cons} \quad (34)$$

e. fecal protein

$$R_{H_2 O, e}^{elec} = \frac{10(18)}{1(83)} B_t F_p R_{food, cons} = 2.169 B_t F_p R_{food, cons} \quad (35)$$

f. fecal cells

$$R_{H_2O,f}^{elec} = \frac{2.33(18)}{1(20.786)} B_t F_c R_{food,cons} = 2.018 B_t F_c R_{food,cons} \quad (36)$$

g. plant waste

$$R_{H_2O,g}^{elec} = \frac{(2 + 3npz - npy)18}{12 + npz + 16npy + 14npz} PW (1 - x_{foodstores}) R_{food,cons} \quad (37)$$

The total oxygen required is determined by summing the above equations

$$R_{H_2O}^{19} = R_{H_2O,a}^{elec} + R_{H_2O,b}^{elec} + R_{H_2O,c}^{elec} + R_{H_2O,d}^{elec} + R_{H_2O,e}^{elec} + R_{H_2O,f}^{elec} + R_{H_2O,g}^{elec} \quad (38)$$

#### 14. Nitrate production in waste electrolyzer

a. urea

$$R_{HNO_3,a}^{elec} = \frac{2(63)}{1(60)} R_{urea}^{met} = 2.1 R_{urea}^{met} \quad (39)$$

b. fecal protein

$$R_{HNO_3,b}^{elec} = \frac{1(63)}{1(83)} B_t F_p R_{food,cons} = 0.759 B_t F_p R_{food,cons} \quad (40)$$

c. fecal cells

$$R_{HNO_3,c}^{elec} = \frac{0.2(63)}{1(20.786)} B_t F_c R_{food,cons} = 0.606 B_t F_c R_{food,cons} \quad (41)$$

d. nonedible plant waste

$$R_{HNO_3,d}^{elec} = \frac{npz(63)}{12 + npz + 16npy + 14npz} PW (1 - x_{foodstores}) R_{food,cons} \quad (42)$$

The total nitrate production is

$$R_{HNO_3}^{20} = R_{HNO_3,a}^{elec} + R_{HNO_3,b}^{elec} + R_{HNO_3,c}^{elec} + R_{HNO_3,d}^{elec} \quad (43)$$

#### 15. Rate of water removal by the water remover

In order to prevent a build-up of moisture in the cabin, the water remover must remove the water produced by breathing, sweating, and combustion of wastes.

$$R_{H_2O}^{12} = R_{breathing} + R_{sweat} \quad (44)$$

## 16. Plant/Algal growth chambers

The stoichiometry of plant growth is shown in Table 4.3. Each component will be considered in sequence.

### a. carbon dioxide consumption

$$R_{CO_2}^9 = \frac{1(44)}{12 + px + 16py + 14pz} (1 - x_{\text{foodstores}}) R_{\text{food,cons}} (1 + PW) \quad (45)$$

### b. water consumption

$$\begin{aligned} R_{H_2O}^{20} = & \frac{(0.5px - 0.5pz)18}{12 + px + 16py + 14pz} (1 - x_{\text{foodstores}}) R_{\text{food,cons}} (1 + PW) \\ & + NPW_t (1 - x_{\text{foodstores}}) R_{\text{food,cons}} PW \\ & + EPW_t (1 - x_{\text{food stores}}) R_{\text{food, cons}} \end{aligned} \quad (46)$$

### c. nitrate consumption

$$R_{HNO_3}^{\text{plant}} = \frac{63pz}{12 + px + 16py + 14pz} (1 - x_{\text{foodstores}}) R_{\text{food,cons}} (1 + PW) \quad (47)$$

### d. oxygen production

$$R_{O_2}^8 = \frac{(1 + 0.25px + 1.25pz - 0.5py)32}{12 + px + 16py + 14pz} (1 - x_{\text{foodstores}}) R_{\text{food,cons}} (1 + PW) \quad (48)$$

## 17. Waste Electrolyzer water requirement

$$R_{H_2O}^{38} = R_{H_2O}^{20} - w_{\text{trash}} R_{\text{trash}} - w_{\text{feces}} R_{\text{feces}} - NPW_t (1 - x_{\text{foodstores}}) R_{\text{food,cons}} PW \quad (49)$$

The water requirement for the waste electrolyzer cannot go below zero. If  $R_{H_2O}^{38} < 0$ , then  $R_{H_2O}^{38} = 0$ .

## 18. Water Electrolyzer

The water electrolyzer produces both oxygen and hydrogen. The required capacity of the electrolyzer will be determined by which demand is greater. If the demand for oxygen is greater (i.e., oxygen control), then an excess of hydrogen will be produced. If the demand for hydrogen is greater (i.e., hydrogen control), then there will be an excess of oxygen produced. Assuming that the electrolyzer is controlled by the oxygen demand, the following analysis is used. If this assumption is in error, the hydrogen storage tank would have to be depleted in order to supply the excess demand for hydrogen.

### a. oxygen production

The electrolyzer must produce oxygen for human metabolism and waste combustion. The plant/algae reactor will supplement this requirement.

$$R_{O_2}^5 = R_{O_2}^{met} - R_{O_2}^8 + R_{O_2}^{34} \quad (50)$$

b. hydrogen production

$$R_{H_2}^{30} = \frac{2(2)}{1(32)} R_{O_2}^5 = 0.125 R_{O_2}^5 \quad (51)$$

c. water consumption

$$R_{H_2O}^3 = \frac{2(18)}{1(32)} R_{O_2}^5 = 1.125 R_{O_2}^5 \quad (52)$$

## 19. Bosch Reactor

a. water production

According to the control strategy described in Table 4.4, the Bosch reactor will produce only enough water to prevent the level in the water tanks from being depleted. The depletion in the water tanks, is found by performing a balance around the tank.

$$D_{H_2O} = OUT - IN$$

$$D_{H_2O} = R_{H_2O}^3 + w_{food} R_{food,cons} + R_{H_2O}^{20} + R_{drink} - R_{urine} - R_{H_2O}^{12} - R_{H_2O}^6$$

The condition that the depletion is zero allows the water produced by the Bosch reactor to be calculated

$$R_{H_2O}^6 = R_{H_2O}^3 + R_{H_2O}^{38} + R_{drink} - R_{urine} - R_{H_2O}^{12} - R_{H_2O}^{33} - R_{H_2O}^{36} \quad (53)$$

This formula is subject to the condition that  $R_{H_2O}^6$  would not go negative. If it does go negative, then  $R_{H_2O}^6 = 0$ .

b. carbon production

$$R_C^{28} = \frac{1(12)}{2(18)} R_{H_2O}^6 = 0.3333 R_{H_2O}^6 \quad (54)$$

c. hydrogen consumption

$$R_{H_2}^4 = \frac{2(2)}{2(18)} R_{H_2O}^6 = 0.1111 R_{H_2O}^6 \quad (55)$$

d. carbon dioxide consumption

$$R_{CO_2}^7 = \frac{1(44)}{2(18)} R_{H_2O}^6 = 1.2222 R_{H_2O}^6 \quad (56)$$

## 20. Storage tanks

The various tanks have inputs and outputs. If inputs are greater than outputs, the tank will accumulate material. If the outputs are greater than the inputs, the tank will lose material.

a. hydrogen accumulation

$$A_{H_2} = R_{H_2}^{30} - R_{H_2}^4 - R_{H_2}^{32} + R_{H_2}^{37} \quad (57)$$

b. carbon dioxide accumulation

The carbon dioxide tank is supplied with carbon dioxide from metabolism and waste combustion and is depleted by the algae reactor and Bosch reactor.

$$A_{CO_2} = R_{CO_2}^{met} + R_{CO_2}^{18} - R_{CO_2}^9 - R_{CO_2}^7 \quad (58)$$

c. water accumulation

$$A_{H_2O} = R_{H_2O}^{12} + R_{urine} + R_{H_2O}^6 - R_{H_2O}^3 - R_{H_2O}^{38} - R_{drink} + R_{H_2O}^{33} + R_{H_2O}^{36} \quad (59)$$

Typically,  $A_{H_2O} = 0$  since the Bosch reactor rate  $R_{H_2O}^6$  is adjusted so the tank level stays constant.

d. oxygen accumulation

It has been assumed that the oxygen production requirements control the electrolyzer. In this case, the production rate is regulated so there is no accumulation of oxygen in the tank

$$A_{O_2} = 0 \quad (60)$$

If this assumption were wrong, it would cause  $A_{H_2}$  to be negative. For the case of a hydrogen-controlled electrolyzer, it would be necessary to implement a control strategy where the electrolyzer is regulated so there is no accumulation of hydrogen in the storage tank. In this case, oxygen would accumulate in its storage tank.

e. food depletion

Any food consumption not met by plants/algae must be met by depleting the food stores

$$D_{food} = x_{foodstores} R_{food,cons} \quad (61)$$

f. nitrate accumulation

Excess nitrates will be produced from protein-containing stored foods.

$$A_{HNO_3} = R_{HNO_3}^{20} - R_{HNO_3}^{plant} \quad (62)$$

## Calculational Procedure

The required capacity for each of the reactors and separators and the level of each of the tanks may be calculated by the following procedure:

### 1. Specify independent inputs

Typical values of the independent inputs are listed below:

- a. metabolic rate [10] = 135 W/man
- b. trash production rate [10] = 0.818 kg/man d
- c. cabin temperature = 21°C
- d. cabin relative humidity = 0.3
- e. drink rate [10] = 1.3 kg/man d
- f. sweat rate [10] = 0.918 kg/man d

### 2. Specify physical relations

- a.  $r = 1.583$  [7]
- b.  $F_f = 0.5$  [7]
- c.  $F_p = 0.0833$  [7]
- d.  $F_c = 1$  [7]
- e.  $w_{feces} = 3$  [7]
- f.  $w_{trash} = 0.1$

3. Calculate composition of food store items- see Table 4.5
4. Calculate composition of edible plants - see Table 4.6
5. Input residue coefficients - see Table 4.9
6. Calculate composition of nonedible plant residue - see Table 4.10
7. Calculate composition of entire plant - see Table 4.11
8. Calculate composition of food eaten - see Table 4.7
9. Calculate elemental composition of trash - see Table 4.12
10. Calculate equations 1 to 62 sequentially

(Note: equation 53 is subject to the condition that it not go negative. If it does,  $R_{H_2O}^6 = 0$  .)

Equation 49 is also subject to the condition that it not go negative. If it does,  $R_{H_2O}^{38} = 0$  .)

### 11. Report results

## Conclusions

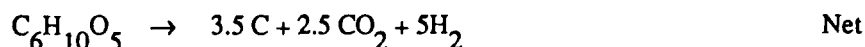
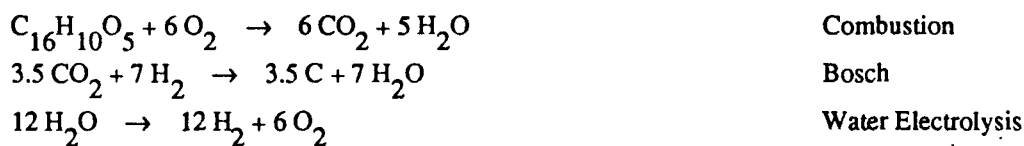
A "stoichiometric model" has been presented which calculates the required capacities of each unit operation in a CELSS which incorporates plants/algae and chemical methods to process air and wastes. Most of the equations in the model are linear. The equations may be solved sequentially rather than simultaneously which makes it easy to implement in a computer program.

The model is driven primarily by the human metabolic rate; therefore, it may be used to determine the effect of astronaut exercise levels on the required capacity of each unit operation in the CELSS. This is important if exercise is used to counter the adverse effects of low gravity on humans.

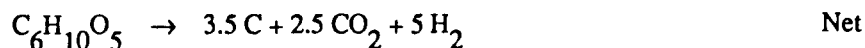
The first-order model presented in this paper is not an exact representation of reality. The major simplification of the model is the manner in which food is divided into fractions which are used for metabolism and feces production. The model assumes that nonfiber fractions allocated to metabolism are completely metabolized. This is not completely correct since some food components (e.g., protein and fat) cannot be completely metabolized, some would end up in the feces. Also, the non-fiber food fraction allocated to feces production is assumed to be completely transformed into microbes. This is a gross simplification since some of the most readily available fractions (e.g., carbohydrate) would be used by human metabolism. Another simplification was that the composition of the feces was independent of the food composition. This simplifying assumption can lead to mismatches in elemental composition between the food allocated for feces production and the actual feces composition. Thus the model may not predict closure when in fact closure would be possible. The errors caused by the simplifying assumptions are relatively minor. The model should give reasonable approximations to reality except in the case of very high fiber diets.

## Comparison of Waste Combustion to Waste Electrolysis

The stoichiometric relationships for the combustion of waste were developed in the previous report.[1] The combustion of wastes requires that oxygen be produced by the electrolysis of water. For example, the net reaction involved in the combustion of paper is as follows:



If the paper were electrolyzed, the following stoichiometry is required:



Waste electrolysis produces the same net reaction as waste combustion, but there is no load placed on the water electrolyzer which reduces system weight.

With waste combustion, the two products ( $\text{CO}_2$  and  $\text{H}_2\text{O}$ ) are produced together, so separators are required. In the case of waste electrolysis, the two products ( $\text{CO}_2$  and  $\text{H}_2$ ) are produced in separate chambers so no separation equipment is required. This also leads to a reduction in system weight.

With waste combustion, nitrogen present in the waste will be converted to dinitrogen and various forms of nitrogen oxide. Although the dinitrogen can be safely vented to the cabin, the nitrogen oxides must be removed. This requires a separator and a reactor which can convert the nitrogen to a form usable by plants. With waste electrolysis, nitrogen in the waste material is converted to nitric acid (or nitrate salts, depending on the pH) which can be used directly by plants as a nitrogen source. No separator is required since the liquid effluent from the waste electrolyzer may be directly added to plants. System weight savings are achieved by eliminating the separator and the reactor to fix nitrogen in a form usable by plants.

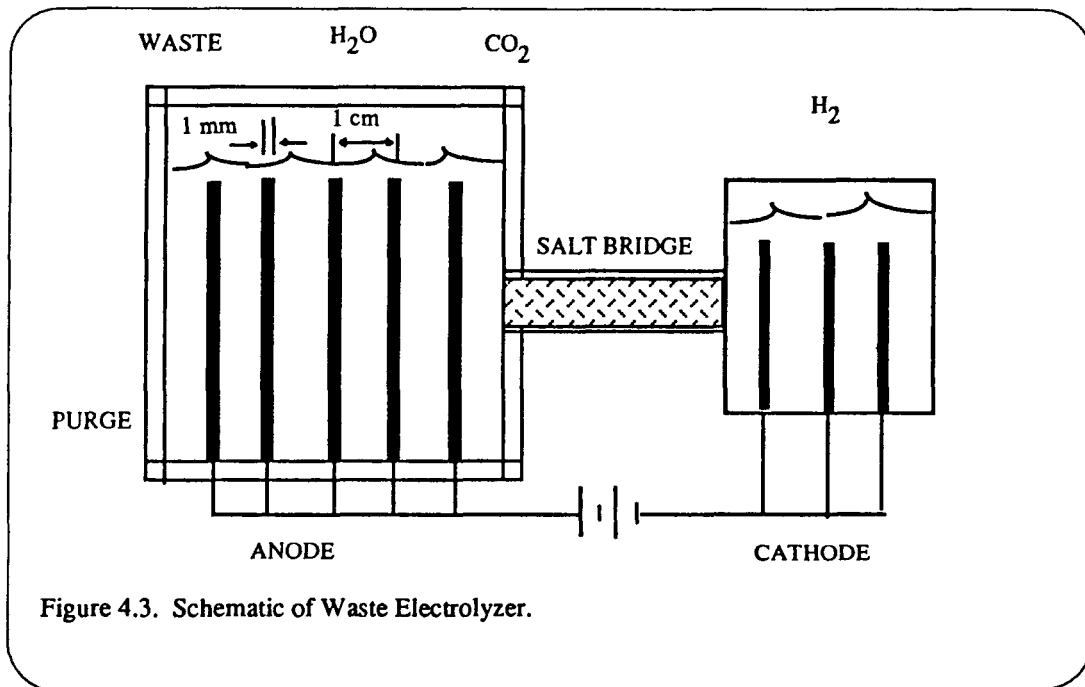


Figure 4.3. Schematic of Waste Electrolyzer.

Figure 4.3 shows a schematic of the waste electrolyzer. Water and waste are added to the anode chamber where the waste oxidation occurs. Since much of the waste is in polymeric form, it is necessary to hydrolyze it to monomers before it can react. This is accomplished by allowing the nitric acid to build up to a high concentration before it is purged. The hydrolysis reaction rate is increased by raising the temperature of the anode chamber. The anodes are composed of 1-mm thick lead spaced by 1 cm. A salt bridge or membrane (not shown) separates the anode chamber from the cathode chamber where hydrogen is produced. Platinum electrodes are used as the cathodes. This reaction is extremely rapid compared to the waste oxidation reaction. It has been experimentally determined[11] that an anode with a  $25 \text{ cm}^2$  geometric area ( $50 \text{ cm}^2$

real area) can produce 3 g/day of carbon dioxide. Using this production rate, Table 4.15 shows the estimated component weights for a system which produces 2 kg/day of carbon dioxide.

Table 4.15. Estimated component weights for a waste electrolyzer which produces 2 kg CO<sub>2</sub>/day.

	Estimated Weight (kg)
Lead Anodes	10
Casing/Support Structure	15
Grinder	25
Pump	5
Hydrogen Cell	5
Urinal	20
Liquid	9
Power Supply/Controls	20
Miscellaneous	<u>15</u>
	124

A comparison of waste combustion and waste electrolysis was performed using the stoichiometric equations developed here (for waste electrolysis) and in the previous report[1] (for waste combustion). The stoichiometric equations allow the rates of each piece of life support equipment to be determined. Table 4.16 shows the estimated weight of each life support component at a given capacity. The weight for other capacities was determined by linear extrapolation.

Table 4.16. Estimated weights of life support equipment.

Device	Function	Capacity	Weight
Electrochemical Depolarizer[12]	CO <sub>2</sub> removal	6.0	265
Bosch Reactor[12]	CO <sub>2</sub> reduction	6.0	257
Dehumidifier[12]	H <sub>2</sub> O removal	11.0	46
Static Feed Generator[12]	H <sub>2</sub> O electrolysis	5.0	485
Nitrogen Separator/ Ammonia Synthesizer[13]	NH <sub>3</sub> production	0.5	58
RITE System Combustor[14]	Waste combustion	1.1	140
RITE System Water Purifier[14]	H <sub>2</sub> O evaporation	25.5	186
Waste Electrolyzer	Waste electrolysis	2.0	124

Tables 4.17 and 4.18 show computer printouts for a four-person crew which is eating stored food and potatoes which are grown in the life support system. The status of the humans, equipment, and storage tanks is reported. The weight of the life support system (exclusive of the potato production facility) is also reported. Figure 4.4 shows the life support system weight (exclusive of the potato production

facility) as a function of the percentage of potato in the diet. The system weight when waste combustion is employed ranges from 2100 to 4500 kg depending on how much of the diet is potato. As the amount of potato is increased, the system weight increases, because of the need to process the plant wastes. The system

Table 4.17. Life support system using a waste combustor.

THIS SYSTEM CONTAINS A BOSCH REACTOR  
THIS SYSTEM CONTAINS PLANTS  
THIS SYSTEM CONTAINS A COMBUSTOR  
THIS SYSTEM CONTAINS AN ELECTROCHEMICAL DEPOLARIZING CELL  
THIS SYSTEM SEPARATES N2 BY COMBUSTION

CREW SIZE	4
METABOLIC RATE (WATTS)	135.5
TRASH PRODUCTION RATE (kg/d)	.8175
CABIN TEMPERATURE (C)	21
CABIN RELATIVE HUMIDITY (fraction)	.3
DRINK RATE (kg/d)	1.3
SWEAT RATE (kg/d)	.9175

NUMBER OF FOOD ITEMS IS 2

FOOD COMPOSITION

ITEM	MASS FRAC	CARB	PROT	FAT	FIBER	WATER
potato	.5	.84	.13	0	.03	4
stored food	.5	.7	.14	.15	.01	3
	1	.77	.135	.075	.02	3.5

INEDIBLE PLANT COMPOSITION

ITEM	RES COEFF	CARB	PROT	FAT	FIBER	LIGNIN	WATER
potato	.275	0.3	0.19	0	0.45	0.06	19
	.275	0.3	0.19	0	0.45	0.06	19

NUMBER OF TRASH ITEMS IS 1

TRASH ELEMENTAL COMPOSITION

ITEM	MASS FRAC	CARBON	HYDROGEN	OXYGEN	NITROGEN
paper	1	.441	.062	.494	0
	1	.441	.062	.494	0

STATUS OF HUMANS

FOOD CONSUMPTION (kg dry food/d)	2.68901856
FOOD CONSUMPTION/PERSON (kg/dry food/d)	0.6722564
FECES PRODUCTION (kg dry feces/d)	0.138914784
URINE PRODUCTION (kg urine water/d)	8.6556384
CARBON DIOXIDE PRODUCTION (kg/d)	4.12785504
OXYGEN CONSUMPTION (kg/d)	3.24009504
WATER PRODUCTION (kg/d)	1.53602784
RESPIRATORY QUOTIENT (CO2/O2)	.92653960938358

STATUS OF EQUIPMENT

CARBON DIOXIDE REMOVER (kg H2O/d)	17.037648
CARBON DIOXIDE REMOVER (kg CO2/d)	10.44576
WASTE COMBUSTOR (kg dry matter/d)	03.9056397074355
URINE PURIFIER (kg urine water/d)	8.6556384
BOSCH REACTOR (kg CO2/d)	0
ELECTROLYZER (kg O2/d)	9.5514012672002
PLANT FOOD PRODUCTION (kg dry food/d)	1.34450928
AMMONIA PRODUCTION (KG NH3/DRY)	0.0501846624

STATUS OF STORAGE TANKS

CARBON DIOXIDE ACCUMULATION (kg/d)	7.71018912
WATER ACCUMULATION (kg/d)	0
OXYGEN ACCUMULATION (kg/d)	0.0000020736
HYDROGEN ACCUMULATION (kg/d)	0.717527808
NITROGEN ACCUMULATION (kg/d)	0.0060103296
PLANT GROWTH NITROGEN ACCUMULATION (kg/d)	0.0377764992
FOOD DEPLETION (kg dry food/d)	1.3445136
CARBON ACCUMULATION (kg C/d)	0

SYSTEM WEIGHT (kg)

3166.86

Table 4.18. Life support system using a waste electrolyzer.

THIS SYSTEM CONTAINS A BOSCH REACTOR  
 THIS SYSTEM CONTAINS PLANTS  
 THIS SYSTEM CONTAINS A WASTE ELECTROLYZER  
 THIS SYSTEM CONTAINS AN ELECTROCHEMICAL DEPOLARIZING CELL

CREW SIZE 4  
 METABOLIC RATE (WATTS) 135.5  
 TRASH PRODUCTION RATE (kg/d) .8175  
 CABIN TEMPERATURE (C) 21  
 CABIN RELATIVE HUMIDITY (fraction) .3  
 DRINK RATE (kg/d) 1.3  
 SWEAT RATE (kg/d) .9175

NUMBER OF FOOD ITEMS IS 2

FOOD COMPOSITION

ITEM	MASS FRAC	CARB	PROT	FAT	FIBER	WATER
potato	.5	.84	.13	0	.03	4
stored food	.5	.7	.14	.15	.01	3
1	1	.77	.135	.075	.02	3.5

INEDIBLE PLANT COMPOSITION

ITEM	RES COEFF	CARB	PROT	FAT	FIBER	LIGNIN	WATER
potato	.275	0.3	0.19	0	0.45	0.06	19
	.275	0.3	0.19	0	0.45	8.06	19

NUMBER OF TRASH ITEMS IS 1

TRASH ELEMENTAL COMPOSITION

ITEM	MASS FRAC	CARBON	HYDROGEN	OXYGEN	NITROGEN
paper	1	.444	.062	.494	0
1	1	.444	.062	.494	0

STATUS OF HUMANS

FOOD CONSUMPTION (kg dry food/d) 2.68901856  
 FOOD CONSUMPTION/PERSON (kg/dry food/d) 0.67225464  
 FECES PRODUCTION (kg dry feces/d) 0.138914784  
 URINE PRODUCTION (kg urine water/d) 8.6556384  
 CARBON DIOXIDE PRODUCTION (kg/d) 4.12785504  
 OXYGEN CONSUMPTION (kg/d) 3.24009504  
 WATER PRODUCTION (kg/d) 1.53602784  
 RESPIRATORY QUOTIENT (CO2/O2) .92653960938358

STATUS OF EQUIPMENT

WATER REMOVER (kg H2O/d) 7.07520096  
 CARBON DIOXIDE REMOVER (kg CO2/d) 4.12785504  
 WASTE ELECTROLYZER (kg dry matter/d) 03.9056397074355  
 URINE PURIFIER (kg urine water/d) 8.6556384  
 BOSCH REACTOR (kg CO2/d) .585435168  
 ELECTROLYZER (kg O2/d) 2.6022432  
 PLANT FOOD PRODUCTION (kg dry food/d) 1.34450928  
 NITRATE REQUIRED FOR FOOD PRODUCTION (kg HNO3/d) .185995872  
 EXCESS NITRATE PRODUCTION (kg HNO3/d) .169941888

STATUS OF STORAGE TANKS

CARBON DIOXIDE ACCUMULATION (kg/d) 7.15116384  
 WATER ACCUMULATION (kg/d) 0  
 OXYGEN ACCUMULATION (kg/d) 0.  
 HYDROGEN ACCUMULATION (kg/d) 0.582999552  
 NITROGEN ACCUMULATION (kg/d) 0.0060103296  
 PLANT GROWTH NITROGEN ACCUMULATION (kg/d) 0.0377712288  
 FOOD DEPLETION (kg dry food/d) 1.3445136  
 CARBON ACCUMULATION (kg C/d) 1.5953328

SYSTEM WEIGHT (kg)

1184.49

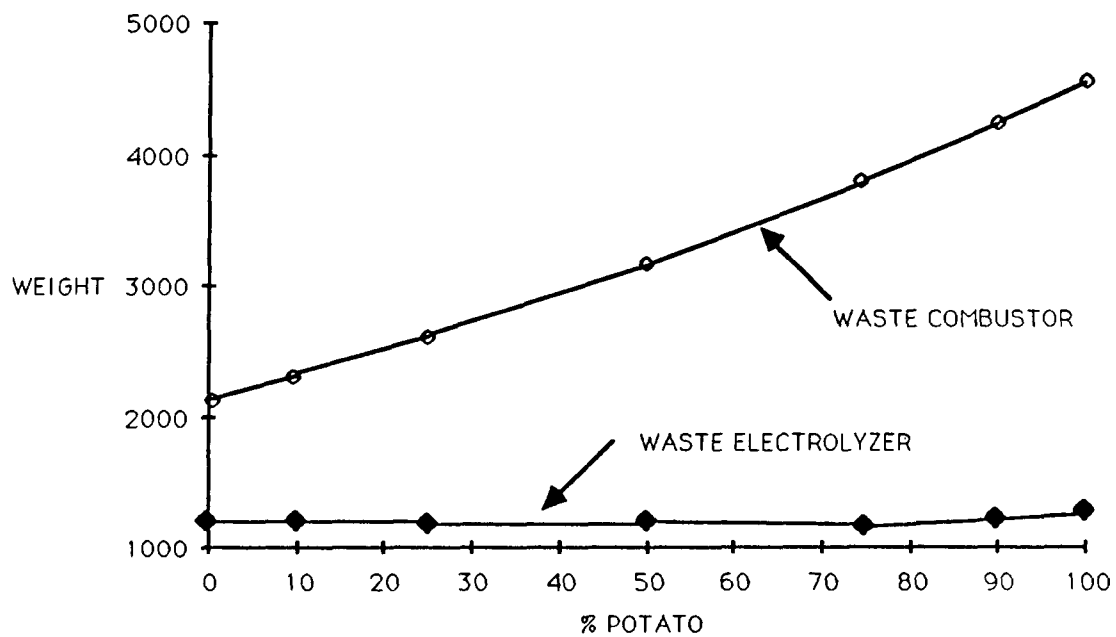


Figure 4.4. Life support system weight (exclusive of potato production facilities) for a waste combustor and waste electrolyzer.

weight when the waste electrolyzer is employed is about 1200 kg and stays approximately constant. Although the waste electrolyzer weight increases with more potato in the diet, this is counterbalanced by a reduction in the weight of the water electrolyzer since more of the human oxygen metabolic needs are supplied by the plants. The use of a waste electrolyzer reduces the life support system weight of a four-person crew by 1000 to 3000 kg, depending on the percentage of potato in the diet.

### Nomenclature

- A = accumulation kg/d
- a = molar ratio of hydrogen to carbon in trash, dimensionless
- B = fiber, mass fraction
- b = molar ratio of oxygen to carbon in trash, dimensionless
- C = carbohydrate, mass fraction
- c = molar ratio of nitrogen to carbon in trash, dimensionless
- D = depletion, kg/d
- E = energy content of food, J/g
- F = fat, mass fraction

$F_c$  = ratio of fecal cells to fecal fiber, dimensionless  
 $F_f$  = ratio of fecal fat to fecal fiber, dimensionless  
 $F_p$  = ratio of fecal protein to fecal fiber, dimensionless  
 $g$  = water content of air, g/L  
 $M$  = metabolic rate, W  
 $P$  = protein, mass fraction  
 $p^{vap}$  = vapor pressure of water, mmHg  
 $Q$  = volumetric breathing rate, L/d  
 $R$  = rate, kg/d  
 $R$  = universal gas constant, 0.08205 atm L/gmole °K  
 $r$  = ratio of nonfibrous fecal matter to fibrous fecal matter, dimensionless  
 $s$  = ratio of total food consumed to food for metabolism, dimensionless  
 $T$  = absolute temperature, °K  
 $t$  = temperature, °C  
 $TC$  = trash carbon, mass fraction  
 $TH$  = trash hydrogen, mass fraction  
 $TO$  = trash oxygen, mass fraction  
 $TN$  = trash nitrogen, mass fraction  
 $w$  = ratio of water to dry solids, dimensionless  
 $x$  = fraction of total food eaten, mass fraction  
 $y$  = fraction of total trash, mass fraction  
 $\phi$  = relative humidity, fraction (NOT percent)

- [1] The Regenerative Concepts Team, Texas A&M University "Regenerative Life Support System Research During the Period September 1987 - March 1988" Research Report, NASA Grant No. NAG 9-253 (March 1988)
- [2] T. Volk, Modeling the Growth Dynamics of Four Candidate Crops for Controlled Ecological Life Support Systems (CELSS), Final Report, Contract No. NGT 44-001-800 (Aug 1987).
- [3] *McGraw-Hill Encyclopedia of Science and Technology*, 4th Ed., Vol. 14, p. 263 (1977).
- [4] B. Atkinson and F. Mavituna, *Biochemical Engineering and Biotechnology Handbook*, The Nature Press, New York, p. 120 (1983).
- [5] P.L. Altman and D.W. Dittmer, *Metabolism*, Federation of American Societies for Experimental Biology, Bethesda, MD (1968).
- [6] W.E. Woodson, *Human Factors Design Handbook*, McGraw-Hill, New York, p. 804 (1981).
- [7] A.C. Guyton, *Textbook of Medical Physiology*, 6th Ed., Saunders, Philadelphia, p. 825 (1981).
- [8] W.E. Woodson, *Human Factors Design Handbook*, McGraw-Hill, New York, p.705 (1981).
- [9] A.C. Guyton, *Textbook of Medical Physiology*, 6th Ed., Saunders, Philadelphia, p. 483 (1981).
- [10] NASA Lyndon B. Johnson Space Center, "Space Station Systems Requirements and Characteristics," Book 3 (Strawman), p. 56 (August 30, 1982).
- [11] Duncan Hitchens, Department of Chemistry, Texas A&M University, personal communication.
- [12] Hall, J.B., M.J. Ferebee, and K.H. Sage, "Environmental control and life support systems technology options for Space Station Application," 15th Intersociety Conference on Environmental Systems, San Francisco (1985).
- [13] Holtzapple, "Conceptual Design of an Ammonia Synthesizer for Space Applications," in preparation.
- [14] Schelkopf, J.D., F.J. Witt, and R.W. Murray, "Integrated Waste Management - Water System Using Radioisotopes for Thermal Energy," General Electric Document No. 74SD4201, Contract No. AT(11-1)-3036, U.S. Atomic Energy Commission (May, 1974).

## 5. RESEARCH RESULTS

### 5.1 Electrochemistry

#### Decomposition of Waste Experiments

The report describes the investigation of a (non-thermal) method for waste oxidation on manned space missions utilizing electrochemical oxidation. The work was sponsored by Johnson Space Center, Houston, Texas under grant number NAG9-192. The technical monitor for this project during 1987 was Cinda Chullen; during 1988, the technical monitor was David Thompson. Initial results and trade studies described in this report warrant the transfer of this process to engineering demonstration stage.

- High temperatures are not required in this process (100 - 150°C max).
- Electrolysis of waste at low temperatures will not give rise to significant amounts of CO and NO<sub>x</sub> which would otherwise be evolved from conventional incineration.
- The technique represents a means of oxidizing organic waste without the consumption of atmospheric oxygen thus does not diminish the available oxygen supply.
- The electrical energy consumed in the electrolysis can be recovered. Hydrogen is produced during the reaction in large quantities and can thus be utilized to regenerate electricity in a conventional oxygen/hydrogen fuel cell.
- This waste treatment process will form the basis for recycling of waste. The process will provide CO<sub>2</sub> for oxygen regeneration by the Bosch or Sabatier processes.
- The technology may be used for all types of organic waste including human waste but may be extended to inedible plant biomass and plastic food packages made of biodegradable polymers etc.

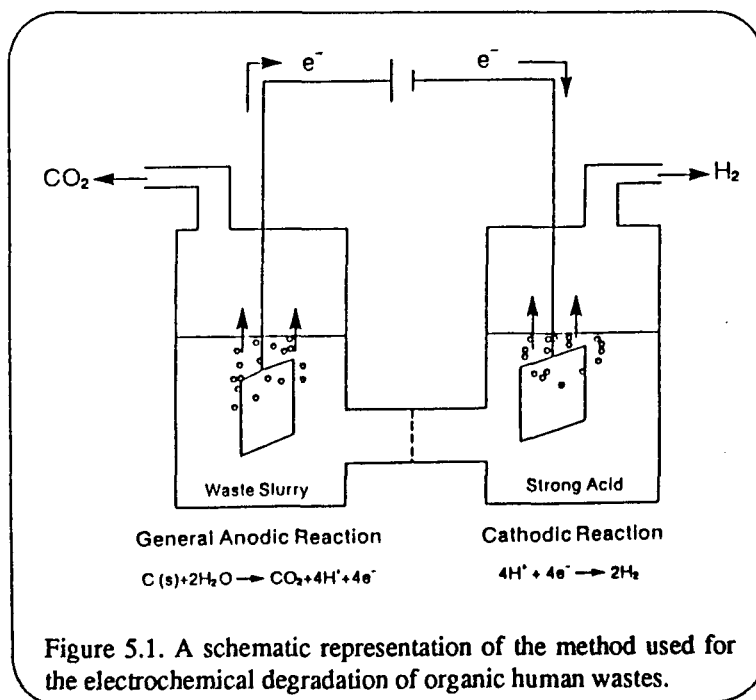
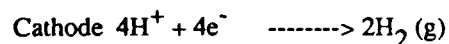
#### Summary of Research Results:

- Electrolysis was performed on a waste mixture consisting of 33% fiber, 32% microorganisms, 10% protein, 20% fat, 5% inorganic material, to represent the chemical constituents of human waste.
- On platinum, the limiting current density for anodic oxidation of waste was greatest in 70% H<sub>2</sub>SO<sub>4</sub> at 150°C, and attained a value of 7 mA cm<sup>2</sup> (3.5 mA cm<sup>2</sup> taking into account electrode roughness)
- On platinum, current efficiency after 30 minutes at 1.64 V was 116%.
- The limiting current of Pt was increased from 7.0 mA cm<sup>-2</sup> to 30 mA cm<sup>-2</sup> in the presence of 5.10<sup>-2</sup> M Ce<sup>3+</sup>/Ce<sup>4+</sup>
- Waste electrolysis was performed on platinum (25 cm<sup>2</sup> geometric area, roughness factor 2) for 24 hours at 150°C. Rate of TOC oxidation was 1.7 g/24 hours. In the presence of 5.10<sup>-2</sup> M Ce<sup>3+</sup>/Ce<sup>4+</sup> TOC oxidation was 3.0g/24 hours. In the absence of redox couples the mean current density was 1.12 mA cm<sup>-2</sup> after 24 hours.

- Waste electrolysis on lead dioxide at 2.0 V at 80°C (electrode area 3.5 cm<sup>2</sup>, 350 cm<sup>2</sup> taking surface roughness into account). In the absence of redox couples, the mean current density was 0.57 mA cm<sup>-2</sup> (real area) after 1 hour 0.47 mA cm<sup>-2</sup> after 24 hours; the CO<sub>2</sub> production rate was 0.4x10<sup>-3</sup> moles hour<sup>-1</sup> cm<sup>-2</sup> after 1 hour and 0.5x10<sup>-3</sup> moles hour<sup>-1</sup> cm<sup>-2</sup> after 24 hours.
- No carbon monoxide was detected in the off gases by GC (allowing for minimum detection limit, CO is less than 0.2% total volume of the off-gas).
- Predicted device operational features based on standard values of waste for a 4-man crew are: electrode area 0.43 m<sup>2</sup>, power 0.049 kW, the power from byproduct hydrogen is 0.022 kW indicating that a low power requiring compact flow- through reactor may be practical for waste treatment in space.

### Introduction

The aim of this project is to degrade organic waste materials by oxidation at the surface of catalytic electrodes. It is anticipated that carbon dioxide and nitrogen will be the product of the anodic oxidation and hydrogen will be evolved from the cathode. The process is illustrated schematically in Figure 5.1. In general terms, the overall reactions will take the following form: Anode C(s) + 2H<sub>2</sub>O (l) -----> CO<sub>2</sub> (g) + 4H<sup>+</sup> + 4e<sup>-</sup>



It should be stressed that the bulk of the carbon undergoing oxidation will not be in its elemental state. These reactions simulate the overall reactions and do not go into specific detail. It is indeed likely that there will be products of the oxidation other than those implied by the above formula especially since much of the waste material will be in the form of complex biological polymers derived from undigested food and micro-organisms of the intestinal flora.

During biomass electrolysis, hydrogen will be evolved continuously from the cathodic compartment. It is

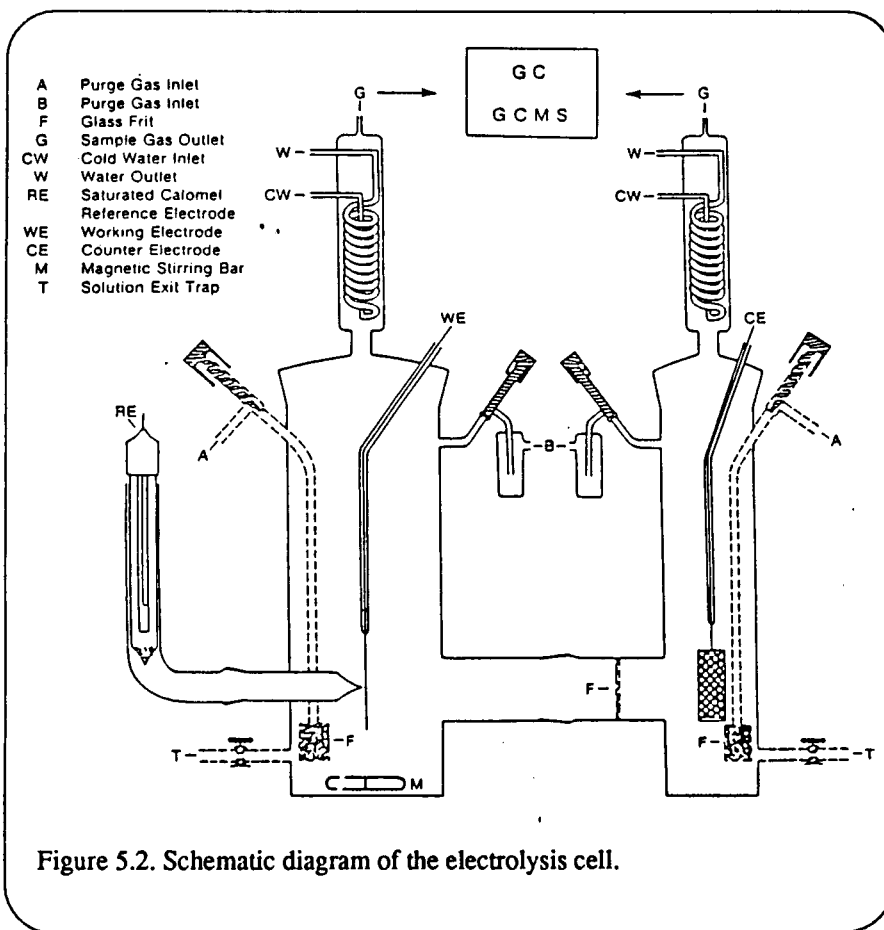
likely that hydrogen can be obtained in this manner at lower cell potentials than the reversible potential for the electrolysis of water. Indeed hydrogen can be obtained at cell potentials as low as 0.8V using lignite slurry as anodic depolarizer in contrast to 1.5V for vigorous H<sub>2</sub> evolution from water. Thus, the supply of hydrogen, which can be used to generate electricity in efficient hydrogen/oxygen fuel cells, will off-set considerably the

energy consumed in the electrolysis. The research background to this approach can be found in literature describing biomass electrolysis [1; 2; 3; 4], fecal waste electrolysis [5; 6; 7] coal electrolysis [8; 9; 10; 11; 12; 13; 14; 15] and electrochemical urine treatment [16; 17; 18].

## Methodology

### Apparatus

These experiments have been performed in a single compartment reactor made of glass schematically shown in Figure 5.2. Both the working and counter electrodes are of platinum sealed in glass and fitted through the top of the cell using ground glass joints. The area of the working electrode was 25 cm<sup>2</sup>. A saturated calomel



electrode was used as reference. The cell was continuously supplied with nitrogen as a means of sparging the CO<sub>2</sub> from the electrolyte and additional stirring was by a magnetic follower. The outlet gas was carried through a tube packed with glass wool and then to a water trap and finally to a barium hydroxide solution. The CO<sub>2</sub> produced was determined by back titration with a standardized quantity of HCl. Parallel experiments were sometimes performed on the GC to confirm the accuracy of the barium hydroxide analysis. Tempera-

ture could be raised by placing the reaction cell on a hot plate. A modified Pine Instrument RDE4 potentiostat was used for voltage sweep experiments and for galvanostatic and potentiostatic electrolysis.

### G.C. Measurement

Gaseous phase CO<sub>2</sub>, as well as the concentration of other gaseous products, were determined using a VARIAN (model 3400) gas chromatograph with a carbo sieve II column with thermal conductivity detector.

Helium or argon was used as the carrier gas at a flow rate of 30ml/min. Chromatograms were recorded using a HP3390A integrator which provided digital readouts of the retention times and integrated areas of the different peaks. Calibration curves for CO<sub>2</sub> was performed on a regular basis. The CO<sub>2</sub> calibration graph gave a slope of  $4.62 \times 10^{-4} \mu\text{l CO}_2$  per integrated count; this is equivalent to  $2.06 \times 10^{-4}$  moles of CO<sub>2</sub> per integrated count.

### Instrumentation

A modified PINE Instrument RDE 4 potentiostat was used for voltage sweep experiments and for galvanostatic and potentiostatic electrolysis. Current versus potential curves, and current versus time curves were recorded on a Hewlett Packard XY recorder (model 7044B). Most of the experiments on artificial waste have been performed a three-compartment cell (Figure 5.2).

### Total Organic Carbon (TOC) Analysis

Carbon, associated with organic compounds in the solution prior and after electrolysis, was determined by means of a model 700 TOC Analyzer Infrared instrument in conjunction with a persulfate oxidation CO<sub>2</sub> trapping technique, according to EPA method 415 by O.I. Corp., College Station, Texas.

### Electrodes

Anodes were of Pt plate, area (20 cm<sup>2</sup>), Pt gauze area 25 cm<sup>2</sup> (50 cm<sup>2</sup> real area), lead rod (PbO<sub>2</sub>) area 3.5 cm<sup>2</sup>. The counter electrode was a Pt wire. A calomel electrode served as reference. Platinum electrodes were flame-cleaned and then immersed in aqua regia, followed by rinsing with triply distilled water.

Lead Dioxide electrodes were prepared electrolytically. A lead rod, 0.9 cm diameter was electrolyzed for 12 hours in a 1.0M sulfuric acid solution with a current of 1A (the electrode area was 3.5cm<sup>2</sup>). The counter electrode was platinum and the reference was saturated calomel. Cyclic voltammograms of the electrode were performed to confirm that lead dioxide had been formed.

### Electrolyte Solutions

Solutions were made using millipore or triply distilled water, and analytical grade chemical H<sub>2</sub>SO<sub>4</sub> and H<sub>3</sub>PO<sub>4</sub>.

### Artificial Fecal Waste Preparation

The mixture was made up entirely from material from the Sigma Chemical Company. Dried *Escherichia coli* and Torpulina was used to mimic the microbial content of fecal waste since these items can be purchased in the large quantities needed at reasonable cost. Cellulose was used to represent the indigestible material of fecal waste and oleic acid was present to represent the fat material. The remainder was made up of proteins and inorganic material. The exact content of the mixture is given in Table 5.1; a 4.6 kg mixture was made and was sufficient for all the fecal waste experiments. The mixture had a paste-like consistency and gave off a strong

odor probably due to the microbes present. Between experiments, the mixture was kept frozen. For the experiments described below, the minimum of pretreatment was given. The material was weighed then given a five minute homogenization with a pestle and mortar in H<sub>2</sub>SO<sub>4</sub>.

Additional pretreatment involved sonication of homogenized mixture with a Fisher Sonics Dismembrator Model 150 for 15-20 minutes.

The conversion factor wet waste: dry weight was performed by leaving known samples of waste in the oven at 150°C and the reweighing was monitored for a number of days until a constant value was obtained; 1g wet weight of waste was shown to be equivalent to 0.39 g dry weight.

Table 5.1. Contents of artificial fecal waste.

Waste Component	Weight (kg)	% of Total Dry Weight
Cellulose	0.60	33%
Torpulina	0.43	25%
E. Coli	0.12	7%
Casein	0.17	10%
Oleic acid	0.37	20%
KCl	0.04	2%
NaCl	0.04	2%
CaCl <sub>2</sub>	0.03	1%
Water	2.9	-

### Results of Waste Electrolysis on Platinum and Lead Dioxide Electrodes

#### Potential Sweep Measurements to Determine Effect of Waste Slurry Concentration on Limiting Currents

Figure 5.3 shows potential sweep measurements performed at 1mV/s to determine limiting currents for artificial fecal waste mixture. From these experiments, appropriate potentials for the oxidation of this type of material can be obtained.

The anodic volume was 400 ml and the electrolyte consisted of 70% H<sub>2</sub>SO<sub>4</sub>. The experiments were performed using increasing amounts of waste slurry up to 80 g/liter of wet waste (corresponding to a dry weight of 32.5 g/liter). Oxidation currents were observed between 1.4 and 1.8 V (vs NHE) indicating the oxidation of organic material. A large increase in current was observed above 1.8 V indicating an increased in the amount of oxygen being evolved. From the sweep measurements, values of limiting current for each of the concentrations can be obtained and are plotted (Figure 5.4). From this graph, limiting current for the concentrations used in constant potential electrolysis experiments could be obtained.

#### Estimation of the Amount of Dissolved Material

The results on the concentration dependence of the reaction have been used to estimate the total amount of dissolved organic material at the start of the electrolysis using the following equation:  $i_L = 0.02 n C$  where  $i_L$  is the limiting current,  $n$  is the number of electrons taking part in the reaction, and  $C$  is the concentration of organic material. The organic material is of a complex nature and its molar concentration cannot be determined but has been estimated assuming oleic acid (C<sub>18</sub>) to be a typical molecular species of the waste material

(MW 282.47) and that 102 electrons are involved in its complete oxidation to CO<sub>2</sub> (see below).



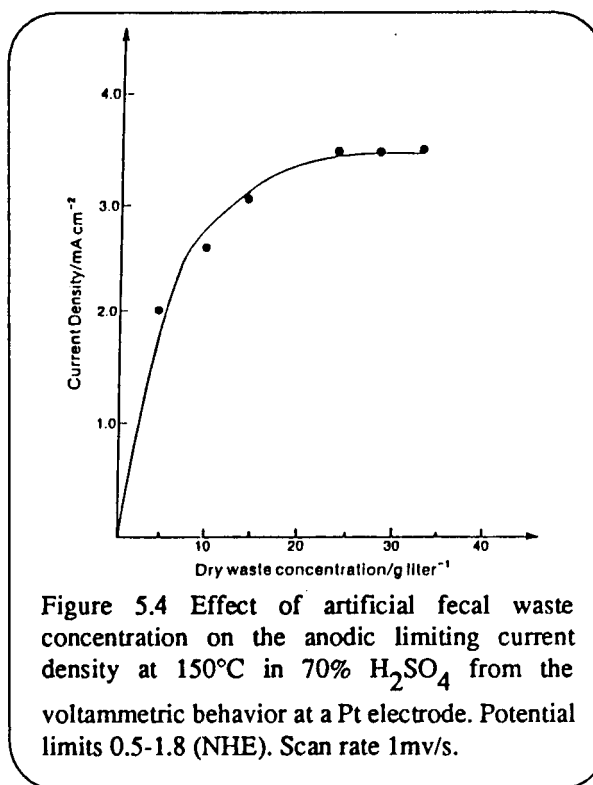
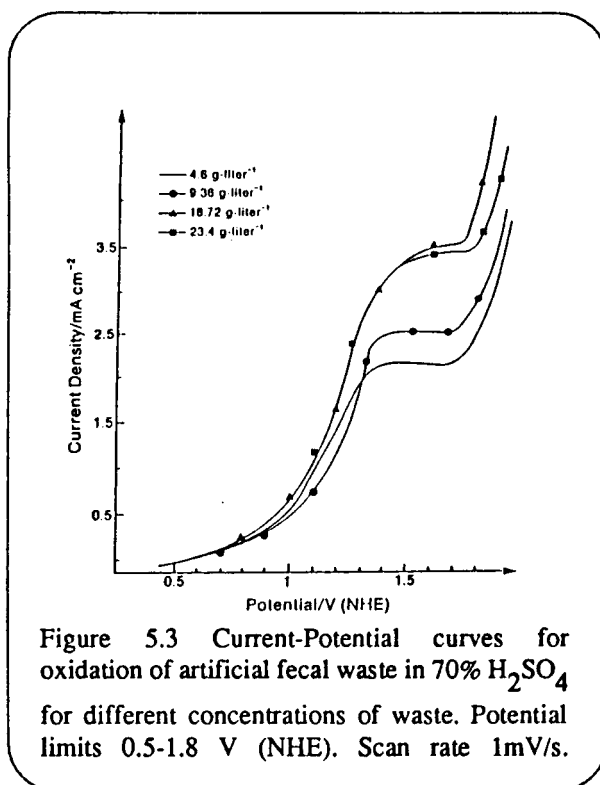
18.72 g/l dry weight = 0.066 moles oleic acid.

$$i_L = 0.02 \times 102 \times 0.066$$

$$\text{Expected } i_L = 134 \text{ mA/cm}^2$$

$$\text{Experimental } i_L = 3.5 \text{ mA/cm}^2$$

$$\frac{3.5}{134} = 3\%$$



This result indicated only 3% of biomass material has dissolved. Visual inspection of the waste slurry, however, indicated a low level of particulate material and only slight amounts of undissolved material could be separated from solution by filtration or by centrifugation (performed by O.I. Corp.) indicating a higher level of dissolved material in the solution than suggested by these results.

### Effect of Temperature and Electrolyte

The variation of the limiting current density for waste oxidation (waste slurry contained 23.4g l<sup>-1</sup> in 70% H<sub>2</sub>SO<sub>4</sub>) was performed at three different temperatures, 80°C, 120°C, and 150°C and is shown in Figure 5.5. The limiting current density increased sharply with the temperature. Experiments were performed to assess if enhanced current densities for waste oxidation can be obtained utilizing phosphoric acid as the high temperature

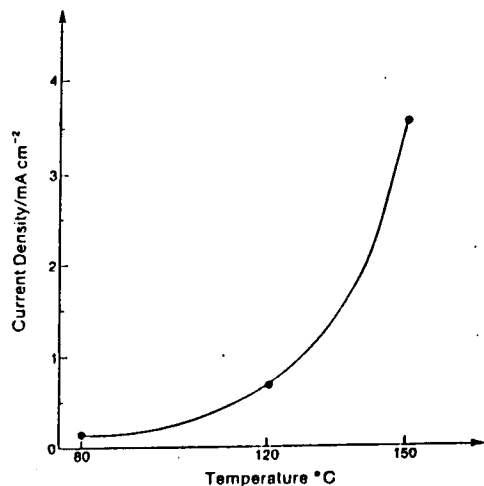


Figure 5.5. Variation of the limiting current density as a function of temperature in  $\text{H}_2\text{SO}_4$  70% from the voltametric behavior at a Pt electrode. Potential limits 0.5-18V (NHE). Scan rate 1mV/s. Dry Waste concentration 23.4 g/liter<sup>-1</sup>.

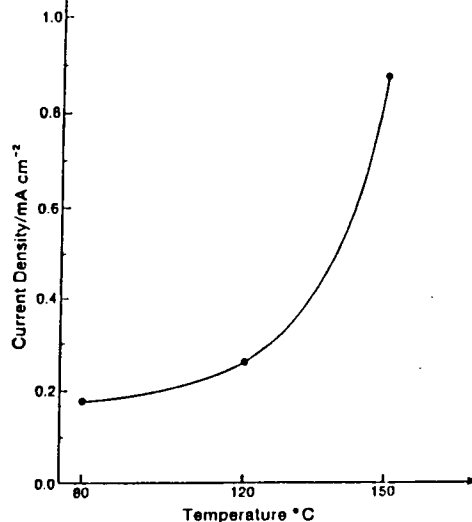


Figure 5.6. Variation of the limiting current density as a function of temperature in 85%  $\text{H}_3\text{PO}_4$  from the voltametric behavior at a Pt electrode. Potential limits 0.5-1.8V (NHE). Scan rate 1mV/s. Dry waste concentration 23.4 g/liter<sup>-1</sup>.

electrolyte. Figure 5.6 shows that the limiting current densities are approximately 10 times lower in the case of  $\text{H}_3\text{PO}_4$  than those obtained using  $\text{H}_2\text{SO}_4$  under identical conditions.

The results from Figure 5.6 and Figure 5.7 are summarized in Table 5.2 from which activation energies have been calculated; also see Figure 5.8.

### Effect of Redox Couples on Limiting Current

Addition of  $\text{Ce}^{4+}$  ions to the waste slurry gave a substantial increase in limiting currents over as shown in Fig. 5.8. The experiment were performed over a range of  $\text{Ce}^{4+}$  concentration up to  $7 \times 10^{-2}$  M; optimum current densities were achieved at  $5 \times 10^{-2}$  M which the concentration use in later experiments to assess the effect of additional oxidizing agents on the oxidation of waste.

### Determination of Current Efficiency as a Function of Platinum Electrode Potential

Details of the electrode reactions are necessary for the accurate determination of the current efficiency. Consequently, the current efficiency for the oxidation can only be obtained by making some simplifying assumptions of the typical reactions that are taking place.

Previous published investigations concerning the oxidation of waste-type materials provide a guide to the mechanism of reactions and thus can be used in these estimations. Studies of the mechanism of oxidation of cellulose have been performed under conditions near identical to those used previously [see 1] where the n value

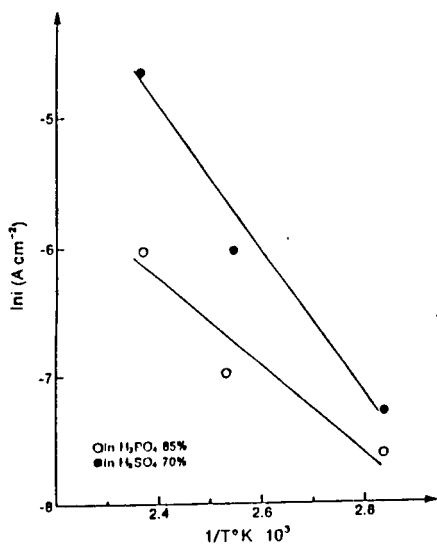


Figure 5.7 Variation of the anodic limiting current density as a function of temperature. Waste concentration  $23.4 \text{ g liter}^{-1}$

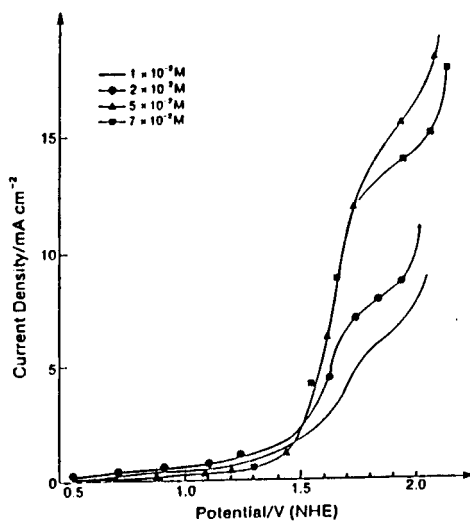


Figure 5.8 Current potential curves for oxidation of artificial fecal waste in 70%  $\text{H}_2\text{SO}_4$  using a Pt electrode for different concentrations of  $\text{Ce}^{4+}$ . Sweep rate  $1 \text{ mV/s}$ .

Table 5.2 The effect of temperature and electrolyte

$t \text{ } ^\circ\text{C}$	80	120	150
T K	353.15	393.15	423.15
$i_L (\text{A/cm}^2)$ ( $\text{H}_2\text{PO}_4$ )	$0.025 \times 10^{-3}$	$0.65 \times 10^{-3}$	$3.6 \times 10^{-3}$
$i_L (\text{A/cm}^2)$ ( $\text{H}_3\text{PO}_4$ )	$0.18 \times 10^{-3}$	$0.26 \times 10^{-3}$	$0.87 \times 10^{-3}$
$\ln(i_L)$ ( $\text{H}_2\text{PO}_4$ )	-8.29	-7.33	-5.62
$\ln(i_L)$ ( $\text{H}_3\text{PO}_4$ )	-8.62	-8.25	-7.04
$1/T \times 10^{-3}$	2.83	2.54	2.36

#### Activation Energy Calculation

$$\text{Slope} = \frac{di_L}{d(1/T)} = \frac{-\Delta H}{R}$$

$$\text{Slope } \text{H}_2\text{SO}_4 = 5.68 \times 10^{-3} \text{ deg}^{-1}$$

$$\text{Slope } \text{H}_3\text{PO}_4 = 3.36 \times 10^{-3} \text{ deg}^{-1}$$

$$R = 1.982$$

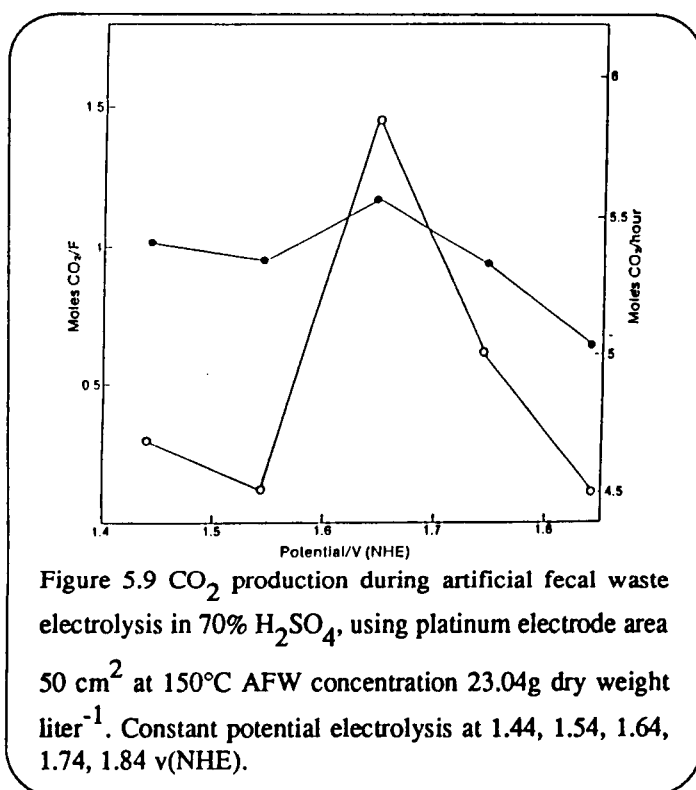
$$(\text{H}_2\text{SO}_4) \Delta H = 11.25 \text{ kcal/mole}$$

$$(\text{H}_3\text{PO}_4) \Delta H = 6.65 \text{ kcal/mole}$$

(i.e., electrons per CO<sub>2</sub>) was 2.3 and takes into account partial oxidation of cellulose under acidic conditions. In addition, n=1 was assumed in calculations of the current efficiency during coal electrolysis[15]. It therefore seems likely that assuming n=1 in the assessment of waste oxidation gives a reasonable estimate of current efficiency.

Assuming 100% current efficiency and having estimated the limiting current (see above), the ideal amounts of CO<sub>2</sub> produced can be determined and by comparison with the actual (ie measured) amount of CO<sub>2</sub> the current efficiency for the process can be assessed. The relationship given below was used to determine the ideal amount of CO<sub>2</sub> that could be produced during the reaction where I<sub>L</sub> is the limiting current, t is time of electrolysis, n is the number of electrons taking part in the reaction (ie 1) and F is the Faraday Constant.

$$\frac{I_L \cdot t}{n \cdot F} = \text{Yield assuming 100\% current efficiency}$$



Experiments were performed to establish the potential where CO<sub>2</sub> can be evolved with the maximum current efficiency. Each electrolysis was performed for 1 hour at different potentials and the total amount of CO<sub>2</sub> evolved over this time was measured. The electrolyte was 70% H<sub>2</sub>SO<sub>4</sub> at 150°C. The results are shown in Figure 5.9 in terms of total CO<sub>2</sub> production/hour per Faraday. Current efficiencies have been calculated and are given in Table 5.3. A possible explanation as to why the current efficiency decreases above 1.64 V is that oxygen evolution is occurring.

### Constant Potential Electrolysis of Artificial Waste on Platinum: The Effect of Redox Couples

Extended electrolysis (24 hours) has been performed with platinum in 70% H<sub>2</sub>SO<sub>4</sub> at 150°C. The electrode potential was 1.74 V vs NHE which is close to the potential giving the maximum rate of CO<sub>2</sub> production. The anodic volume was 400 ml and the cathodic volume 200 ml. Three sets of experiments were performed under identical conditions except for the following; (a) in the absence of current passing through the cell to establish the importance of thermal decomposition of the waste material under these conditions, (b) using

identical reaction conditions except that current was passed through the cells and, (c) the experiment was performed again in the presence of a redox couple.

Curve a in Figure 5.10 shows the CO<sub>2</sub> evolution profile obtained over 24 hours in the absence of current. Under these conditions, a large amount of CO<sub>2</sub> is evolved by thermal processes but after 10 hours this process has stopped.

The second set of experiments (curve b) concerned the electrolysis of waste with the potential of the working Pt electrode set at 1.74 V, in the absence of any redox couple. The results show a large increase in CO<sub>2</sub> evolution over the amounts evolved by heating the solution. The third set of experiments (curve c) performed in the presence of 5.10<sup>-2</sup> M of Ce (IV), CO<sub>2</sub> production was enhanced indicating redox couples can be used effectively to oxidize this type of organic biomass.

Table 5.3. Faraday current efficiencies.

E (vs NHE)	1.44	1.54	1.64	1.74	1.84
CO <sub>2</sub> moles/hour	4.7x10 <sup>-3</sup>	4.5x10 <sup>-3</sup>	5.8x10 <sup>-3</sup>	5.0x10 <sup>-3</sup>	4.5x10 <sup>-3</sup>
Total Charge C/hour	414	464	482	612	648
Current Efficiency	113%	106%	116%	79%	67%

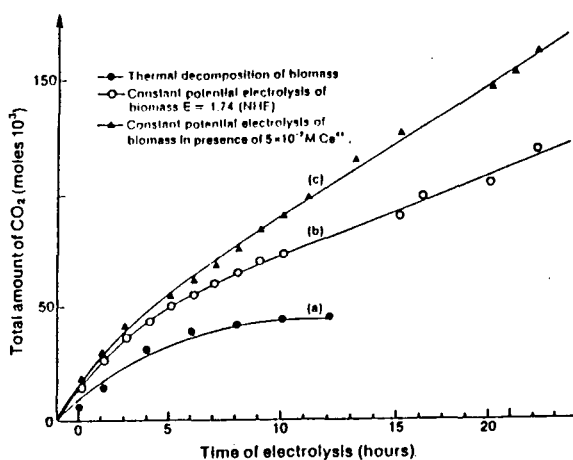


Figure 5.10 CO<sub>2</sub> production during biomass electrolysis in 70% H<sub>2</sub>SO<sub>4</sub> using a Pt electrode at 150°C. Biomass concentration 14.04 g liter.

TOC measurement were made of samples from the anodic compartment at the beginning at the end of the electrolysis. It should be noted that although the the anodic compartment contained the equivalent of 14.4 g/l of dry material, expected TOC value is lower due to the high N, O, and H content of the organic material. Since the composition of the waste is known accurately, the expected value of TOC is 45% of the total dry weight. Therefore, 14.4 g/l dry weight of waste at the start of the electrolysis which should be equivalent to 6.48 g/l TOC. The total organic carbon (TOC) before electrolysis and after 24 hours is given in Table 5.4.

Initial values of TOC are below the expected value (6.48 g/l) by 82%. Tests were run at O.I. Corporation to determine if TOC was being underestimated for any of the main components of waste (yeast, oleic acid, cellulose, and casein). Separate samples of each component were prepared at concentrations similar to those used in the waste slurry and the pretreatments usually given to the waste slurry were given to each sample. Results showed that TOC is underestimated by 10% for cellulose, 24% for yeast and 38% for oleic acid,

Table 5.4. Total organic carbon.

Conditions	Initial TOC	Final TOC
No Ce <sup>3+</sup> /Ce <sup>4+</sup>	5.0 g/l	3.3 g/l
5x10 <sup>-2</sup> M Ce <sup>3+</sup> /Ce <sup>4+</sup>	5.6 g/l	2.6 g/l

however, the TOC value for casein was determined accurately. Since the exact amounts of each component of the artificial waste is known, calculations show that the undetected portion of each component can account almost exactly for the underestimation of the TOC for the waste slurry used in the experiments. Improved methods for accurately determining TOC are being developed in collaboration with Intermountain

Laboratories. Assuming that the proportion of undetected TOC is the same at the beginning at the end of the experiment, the presence 5x10<sup>-2</sup> M Ce<sup>3+</sup>/Ce<sup>4+</sup> nearly doubled in the TOC oxidized over a 24 hour period.

In addition to TOC measurements and CO<sub>2</sub> determinations, gas chromatograph measurements were made of the gas evolved from the cathode which was confirmed to be hydrogen.

### Current Efficiency Calculations

To determine current efficiency, it is necessary to know the electrochemical reaction(s) that are taking place, however, in these complex mixtures reaction mechanisms cannot be determined at the present time. In this case, current efficiencies can be estimated by assuming 1 electron per CO<sub>2</sub>.

Data concerning CO<sub>2</sub> evolution in the presence and absence of 5x10<sup>-2</sup>M Ce<sup>3+</sup>/Ce<sup>4+</sup> is given in Table 5.5. Current efficiencies for CO<sub>2</sub> have been calculated by first subtracting the amount of CO<sub>2</sub> thermal/acid decomposition.

These data show that the presence of the redox couple that approximately doubles the amount of CO<sub>2</sub> production into account in the early stages of the electrolysis. However, the current efficiency for CO<sub>2</sub> evolution is lower in the presence of redox couple indicating cerium is acting as a current consumer. The current on Pt is markedly decreased after 10 hours of electrolysis indicating the need for electrode regeneration techniques to enhance the effectiveness of this process on platinum.

Table 5.5. Current efficiencies on platinum.

	Total moles CO <sub>2</sub>	Mean Current	Current Efficiency
No Ce <sup>3+</sup> /Ce <sup>4+</sup>			
Hour 1	1.4 x 10 <sup>-3</sup>	600mA	6.3%
Hour 10	4.0 x 10 <sup>-3</sup>	670mA	16.0%
Hour 24	1.75 x 10 <sup>-3</sup>	501mA	9.4%
5x10 <sup>-2</sup> M Ce <sup>3+</sup> /Ce <sup>4+</sup>			
Hour 1	4.05 x 10 <sup>-3</sup>	1080mA	10.0%
Hour 10	6.2 x 10 <sup>-3</sup>	770mA	21.6%
Hour 24	3.75 x 10 <sup>-3</sup>	680mA	14.8%

## Long Term Electrolysis on Lead Dioxide: The Effect of Redox Couples

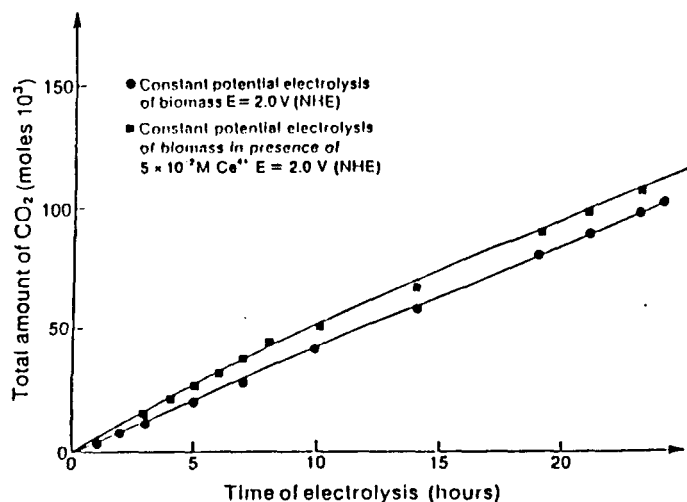


Figure 5.11.  $CO_2$  production during biomass electrolysis in 5M  $H_2SO_4$  using a  $PbO_2$  electrode ( $3.5 \text{ cm}^2$ ) at  $80^\circ\text{C}$  Biomass concentration  $14.04 \text{ g-liter}^{-1}$ .

Extended electrolysis (24 hours) was performed with  $PbO_2$  as anode in 5M  $H_2SO_4$  at 2V (NHE) at  $80^\circ\text{C}$ . The area of the  $PbO_2$  rod was  $3.5 \text{ cm}^2$  (geo-metric). The evolution rate of  $CO_2$  is shown in Figure 5.11. Current efficiencies have been calculated as described above (see Table 5.5) and are shown in Table 5.6; however, since these experiments were at  $80^\circ\text{C}$ , the amount of  $CO_2$  from thermal decomposition of the organic material is not

significant. The electrode potential was 2.0 V vs NHE.

Under these conditions cerium significantly improves the total yield of  $CO_2$  and enhances the current efficiency for  $CO_2$  evolution. The current efficiencies for lead dioxide are significantly below those obtained on platinum.

Table 5.6. Current efficiencies on lead electrode.

	Total moles $CO_2$	$CO_2$ from Thermal Decomposition	Mean Current	Current Efficiency
$No \text{ Ce}^{3+}/\text{Ce}^{4+}$				
Hour 1	$15.87 \times 10^{-3}$	$9.05 \times 10^{-3}$	56mA	330%
Hour 10	$4.0 \times 10^{-3}$	$2.0 \times 10^{-3}$	45mA	119%
Hour 24	$2.75 \times 10^{-3}$	0.0	66mA	112%
$5 \times 10^{-2} \text{ M } \text{Ce}^{3+}/\text{Ce}^{4+}$				
Hour 1	$18.0 \times 10^{-3}$	$9.05 \times 10^{-3}$	760mA	31.6%
Hour 10	$8.0 \times 10^{-3}$	$2.0 \times 10^{-3}$	600mA	27.6%
Hour 24	$3.5 \times 10^{-3}$	0.0	245mA	38.8%

## Solid Waste Electrolyzer: Predicted Operational Characteristics

### A Model for Waste Materials in a CELSS

In assessing the operational characteristics of an electrolyzer for waste oxidation it is necessary to have an accurate assessment of the composition of waste in a CELSS; the values used in these calculations are taken from Wydeven[19]. These calculations will not include the large amount of inedible biomass that would accumulate if plants are included in the system.

### Electrode Area

Rates of biomass electrolysis have been determined from TOC (Total Organic Carbon) analysis of the experiments described in Section 5.6.

Assumptions:

- a) each crew member will produce 128g dry weight  $\text{man}^{-1} \text{day}^{-1}$ .
- b) an electrode of 25  $\text{cm}^2$  geometric area (50  $\text{cm}^2$  real area) will convert 3g TOC  $\text{CO}_2 \text{ day}^{-1}$ .
- c) the waste materials are given in terms of TOC though in reality will contain large amounts of O and N.

Therefore, for 1-man crew required electrode area

$$\frac{1 \times 128 \times 25}{3 \text{ CO}_2/24 \text{ hours (4.26 m}^2/4\text{-man crew)}} = 1.06 \text{ m}^2 \text{ is the needed electrode area to convert all solid waste to}$$

### Power Requirements

Number of Crew = 1

Electrode Area = 1.06  $\text{m}^2$

Current Density = 7mA  $\text{cm}^{-2}$  (apparent area)

Cell Voltage = 2.0 V

Calculation:

Total Current = 0.007 x 1060  
= 7.42 A

Power = 7.42 x 2  
= 14.84 W

Power Required

4-Man Crew = 14.84 x 4  
= .059 kW

### Energy Obtained from By-Product Hydrogen

Hydrogen will be evolved in a separate compartment (ie at the cathode) during the electrolysis and can be used in a hydrogen/oxygen fuel cell to regenerate electrical energy.

Cathode Current = 7.2 x 4

= approx 30.0 A

$$\begin{aligned} \text{Moles } H_2 &= \frac{30 \text{ l}(24 \text{ hours})}{2 \cdot 10^5} \\ &= 12.96 \text{ moles } H_2 \\ &= 290 \text{ liters } H_2/24 \text{ hours} \end{aligned}$$

Assumption: fuel cell works at 60% efficiency

Heat of reaction for  $H_2 + 1/2 O_2 \rightarrow H_2O = 58 \text{ kcal}$

Hence, rate of energy production in Watts

$$\begin{aligned} \frac{30}{2.10} \times 58 \text{ kcal} \times 4.18 \times 0.6 &= 21.8 \text{ watts} \\ &= 0.022 \text{ kW} \end{aligned}$$

Approximately 37% of the energy used in the electrolysis can be obtained from by-product hydrogen.

## Modern Biofuel Cells for Waste Recycling in Life Support Systems

The research described here was sponsored by the Crew & Thermal Systems Division of NASA Johnson Space Center under grant number NAG9-283. The Technical Monitor was Don Price.

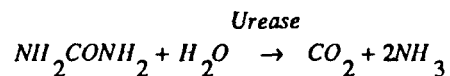
### Summary

- A biotechnology approach has been developed for treatment and recycling of waste water involving the construction of a flow-through reactor containing the enzyme catalyst urease.
- A new method for the immobilization of urease has been developed whereby the enzyme is incorporated into a polymer matrix consisting of bovine serum albumin covalently cross-linked to the enzyme with glutaraldehyde.
- The polymer has good mechanical properties for use in flow-through reactors and offers long-term stability (up to 2 months).
- An immobilized enzyme reactor containing 160 mg of urease is able to treat  $1.3 \times 10^{-4}$  mol urea/min at 25°C.
- The rate of enzyme hydrolysis can be enhanced 4-fold at 65°C.
- Design parameters for enzyme reactors or use in waste water reprocessing have been determined; to eliminate urea from 400 liters of recovered hygiene water per day containing 84000 ppb urea, an enzyme reactor of approximately 500 cm<sup>3</sup> and weighing less than 100 g is required.
- A catalyst bed has been constructed containing Ru coated Al pellets and placed for decomposition of  $NH_2$  into  $N_2$  and  $H_2$ .
- A SPE hydrogen-oxygen fuel cell has been placed in combination with the enzyme and catalytic treatment reactors for the generation of electrical from hydrogen evolved during the waste treatment process.

## Introduction

Human urine consists of inorganic ions such as  $\text{Na}^+$ ,  $\text{Cl}^-$ ,  $\text{H}_2\text{PO}_4^-$ ,  $\text{Ca}^{2+}$ ,  $\text{Mg}^{2+}$ , and organic metabolites of which urea is the main component. Urea is an important contaminant of hygiene water and is present in concentrations in the millimolar range in shower water recovery systems for manned space flight. [20; 21] Whereas the inorganic ions can be removed from urine and waste water by a variety of purification treatments,[22] urea is difficult to remove from waste water; for instance, it cannot be separated readily by chromatography or ion-exchange methods and, unlike most organic contaminants of waste water, it cannot be adsorbed onto activated carbon. Consequently, innovative ways of treating urea are important in the development of water reprocessing technology for long duration space exploration. Urea is a very stable molecule and there are few effective ways for its decomposition.[23] Super critical water oxidation can be used but this requires extreme conditions of temperature and pressures.[24] Ozone in combination with UV light has been reported to be effective in the treatment of urea,[25] as are a number of electrochemical techniques[16; 26; 27] which have attracted attention recently as a means of treating kidney failure.

One approach to urea treatment for water purification is to utilize the enzyme urease to catalyze the hydrolysis of urea to ammonia and carbon dioxide as shown below:



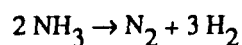
Ammonia (or ammonium ions) produced from this reaction can then be treated by a variety of methods including ion exchange.[16] Ammonia can also be utilized as a fuel in electrochemical system; thus, the treatment of urine with the enzyme urease acts as a convenient step in the purification and recycling of waste water and opens the possibility of generating electrical energy during the waste reprocessing step using a biofuel cell approach.[28; 29; 30]

The approach undertaken in the initial phase of research has been to develop an experimental reactor in which urease can be utilized for urine processing. Enzymes have advantages for use in performing chemical transformations in that they often are highly catalytic, selective for desired reactions rather than producing a large number of unwanted by-products, and are generally inexpensive to obtain. Consequently, enzymes are used extensively in many commercial and industrial processes. However, it is the ability of the enzyme to perform its catalytic hydrolysis under mild conditions (i.e., ambient temperatures and pressures), without the need for complex apparatus control mechanisms or a large outside energy source and in an aqueous environment that makes this approach attractive for use in space. A major obstacle to the use of enzymes is that they often exhibit a limited catalytic lifetime and stability; however, the lifetime of enzymes can be greatly enhanced through the use of enzyme immobilization techniques (i.e., where the enzyme molecules are attached to a solid support. (For review, see [31; 32] ) Numerous categories of techniques to effect enzyme immobilization have been developed, including: (a) ionically bonding to an inert substrate; (b) attachment to an insoluble matrix by adsorption;

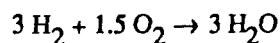
(c) physical entrapment in a gel; and (d) covalent attachment to a solid support.

### Research Plan

The system being developed during this research consists of three treatment phases: (1) urea hydrolysis; (2) ammonia catalysis to hydrogen and nitrogen; and (3) hydrogen/oxygen fuel cell for electricity production. Phase 1 has been completed and a water treatment column has been constructed for urine treatment; the research strategy has been to assess the feasibility of immobilized urease for urine treatment and waste water treatment. Phase 2 has involved taking the ammonia produced, separating it from aqueous solution to form ammonia gas, and passing it over a Ru catalyst bed to form nitrogen and hydrogen as shown below:



The performance of the catalyst bed is being investigated at the present time. Phase 3 will involve taking the mixture of hydrogen and nitrogen and passing it to a fuel cell. A solid polymer fuel cell commercially available from Electrosynthesis Company (New York) has been included as the final stage in the waste processing stream.



A schematic diagram of the apparatus set up in the laboratory is shown in Figure 5.12.

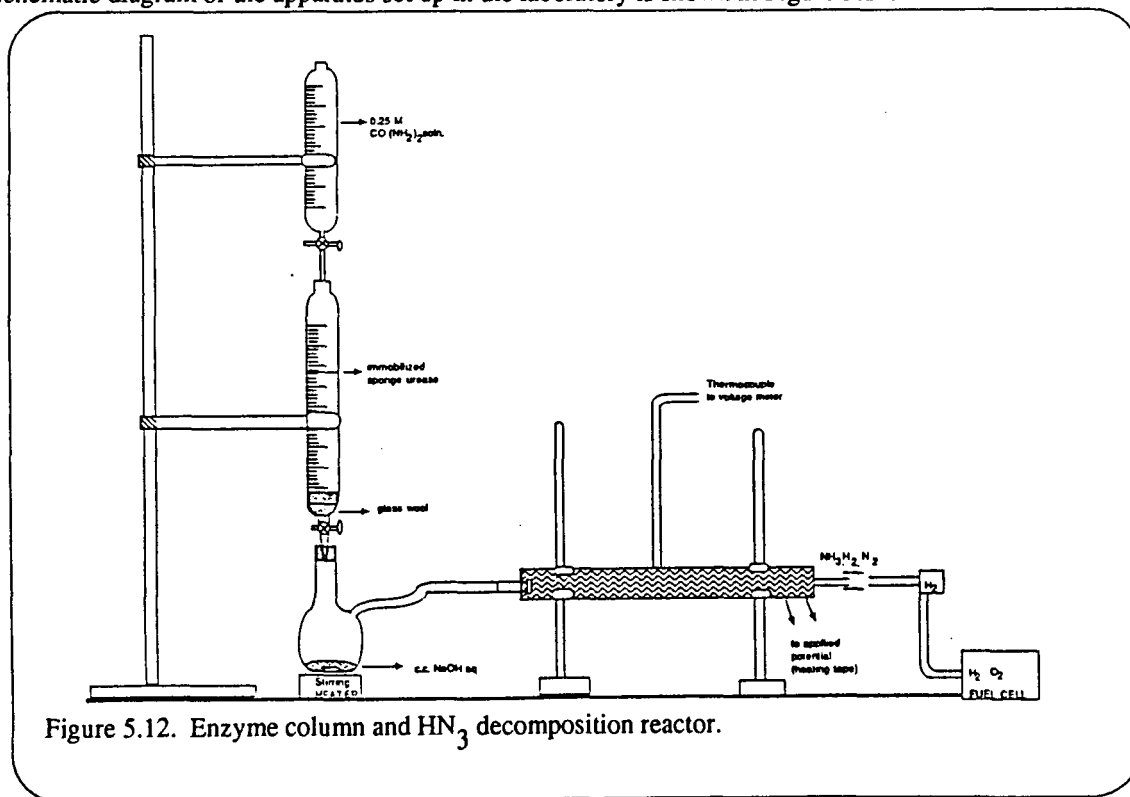


Figure 5.12. Enzyme column and HN<sub>3</sub> decomposition reactor.

## Methodology

### Enzyme Activity: Definitions

Urease activity:

1 unit can generate 1 mmol  $\text{NH}_3$  in one minute where an excess of  $\text{CO}(\text{NH}_2)_2$  is present (usually  $>0.1\text{M}$ ).

Specific activity of urease: number of active units in 1 g of enzyme protein.

The enzyme activity towards urea was assessed by determination of the  $\text{NH}_3$  that is evolved by a standard amount of enzyme in a certain period of time.

Table 5.7. Calibration of  $[\text{NH}_3]$  versus absorbance at  $\lambda=625\text{nm}$

	1.0	1.5	2.0	2.5
ABSORBANCE	1.109	1.717	2.26	2.783

Ammonia production was monitored by UV-Vis spectroscopy according to published procedures.[33] Two color developing reagents are used in this assay  $S_1$  (0.5M phenol + 0.001 sodium nitroprusside) and  $S_2$  (0.65 M NaOH + 0.03 M NaOCl).

$S_1$  and  $S_2$  form a dark blue product with  $\text{NH}_3$  and it is proportional to the absorbance at  $\lambda = 625 \text{ nm}$ . (Table 5.7) A calibration curve showing absorbance (625 nm) against concentration of  $\text{NH}_3$  is shown in Figure 5.13 This reaction sequence is summarized below:

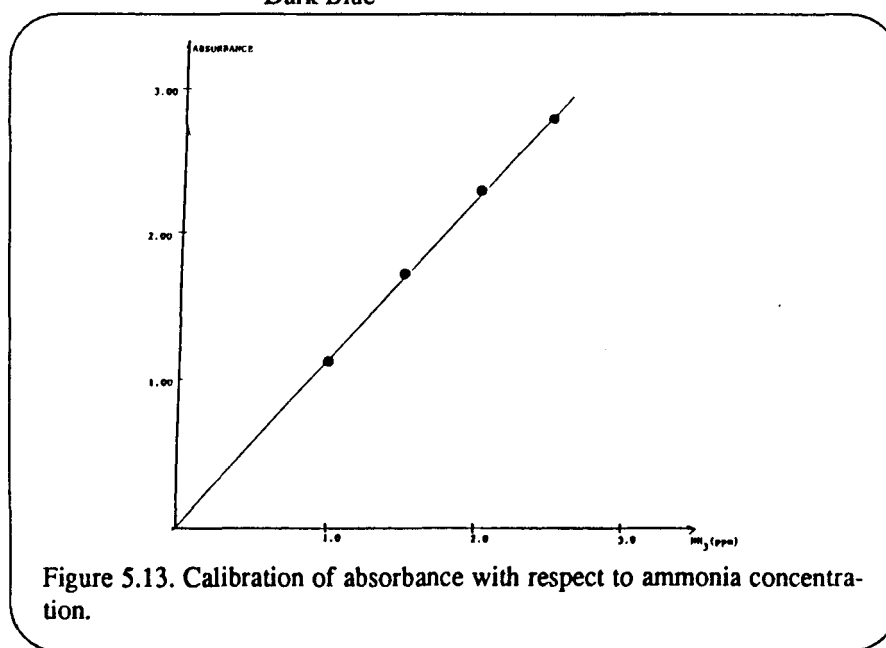
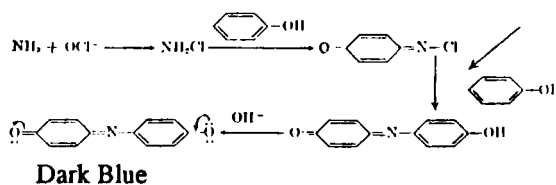


Figure 5.13. Calibration of absorbance with respect to ammonia concentration.

## Results

### Results Enzyme Activity

Sigma Type III urease was used in these experiments EC 3.5.15. (13,000  $\mu$  unit/g). Urease (79 mg) was dissolved in 100 ml of 0.02M phosphate buffer containing 1g of EDTA pH 6.36. EDTA was included to protect the enzyme from trace amounts of heavy ions eg  $\text{Cu}^{2+}$  and  $\text{Pb}^{2+}$  which can have a harmful effect on the enzyme. Urea solution contained 15 g  $\text{CO}(\text{NH}_2)_2$  in 1000 ml (0.25M). The enzyme activity was assayed at 23°C and the results are given in Table 5.8. A graph showing absorbance versus time is given in Figure 5.14.

Table 5.8. Enzyme activity measurements at 23°C.

Sample	Blank	1	2	3
Urease (ml)	0.0	0.2	0.2	0.2
Urea (ml)	1.0	1.0	1.0	1.0
Time (min)		5.27	10.53	15.9
Absorbance		0.12	0.749	1.187

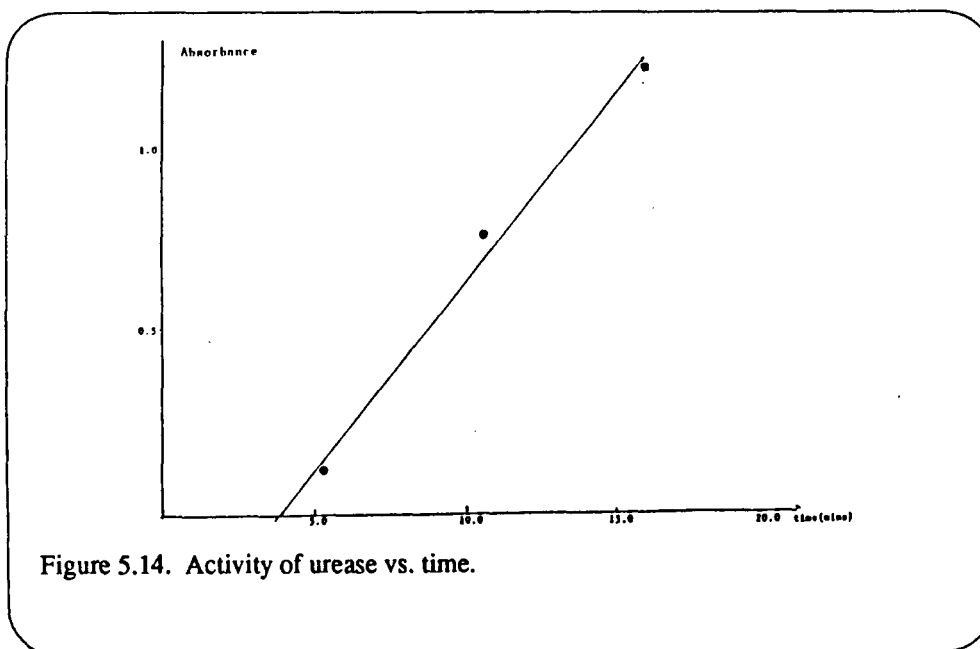


Figure 5.14. Activity of urease vs. time.

### Temperature Dependence of Urease

By making these measurements, it is possible to determine the optimal temperature for the enzyme-catalyzed hydrolysis of urea and information concerning the kinetics of the enzyme reaction. Results are given in Table 5.9. Manufacturer's specifications are 13,000 units/g of protein; however, these results indicate 1,800

Table 5.9. Activity of Urease Versus Temperature

Temperature °C	13	24	38	50	55	65	75	85	90
absorbance min	0.08	0.10	0.76	0.41	0.43	0.47	0.43	.33	.10
ppm NH <sub>3</sub> min	0.07	0.09	0.23	0.37	0.39	0.42	0.39	0.03	0.09
μmol NH <sub>3</sub> mg urease/min	0.3	0.38	0.99	1.56	1.66	1.79	1.64	1.26	0.38
relative activity versus 65°C	16.4%	21.4%	55.4%	87.3%	92.5%	100.0%	92.6%	70.0%	21.4%
1/T (10 <sup>-3</sup> K <sup>-1</sup> )	3.5	3.37	3.22	3.10	3.05	2.96	-	-	-

1. Absorbance/min was converted to ppm NH<sub>3</sub> per min using the NH<sub>3</sub> versus absorbance calibration curve shown in Figure 3 (i.e., 1.103 abs/ppm (NH<sub>3</sub>)).

2. 0.2 ml of urease solution contained  $\frac{0.2 \times 70 \text{ mg}}{100 \text{ ml}} = 0.14 \text{ mg}$

units/g. A possible explanation is that some enzyme activity has been lost either in storage or during the course of the experimental procedures. Figure 5.15 shows a plot of enzyme activity versus temperature. The activity of the enzyme increases up until 65°C; above this temperature, the enzyme activity decreases because of heat denaturation.

Figure 5.16 is a plot of  $\log V_{\max}$  versus  $T^{-1}$ . The slope of the plot is as follows:

$$\text{Slope } b. \quad \frac{d \ln V}{d 1/T} = -1.65 \times 10^3$$

Using the relationship:

$$K = A e^{-\frac{Ea}{RT}}$$

because the reaction is zero order  $V=K$  hence:

$$\ln V = \ln A - \frac{Ea}{RT}$$

$$\frac{d \ln V}{d 1/T} = \frac{-Ea}{R}$$

ORIGINAL PAGE IS  
OF POOR QUALITY

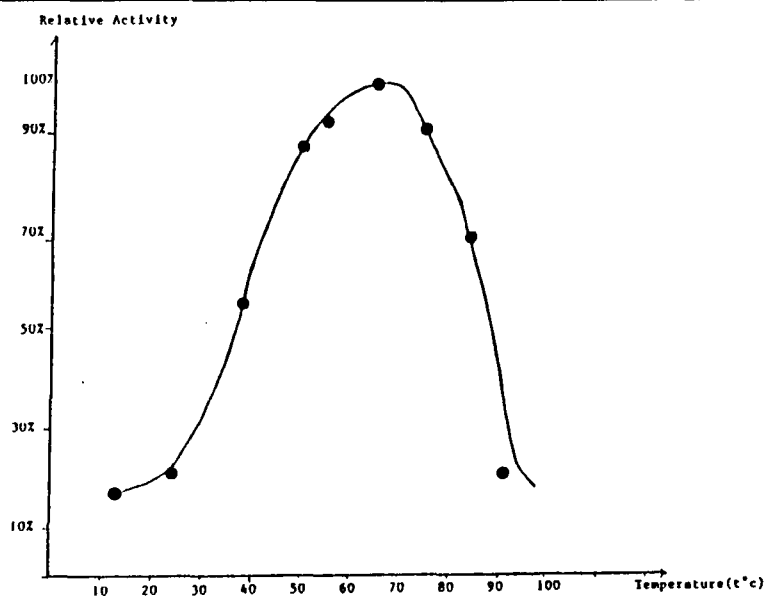


Figure 5.15. Activity of urease with respect to temperature.

$1/T(10^{-3}K^{-1})$	3.50	3.37	3.22	3.10	3.05	2.96
$\log(V)$	1.21	1.33	1.74	1.94	1.97	2.00

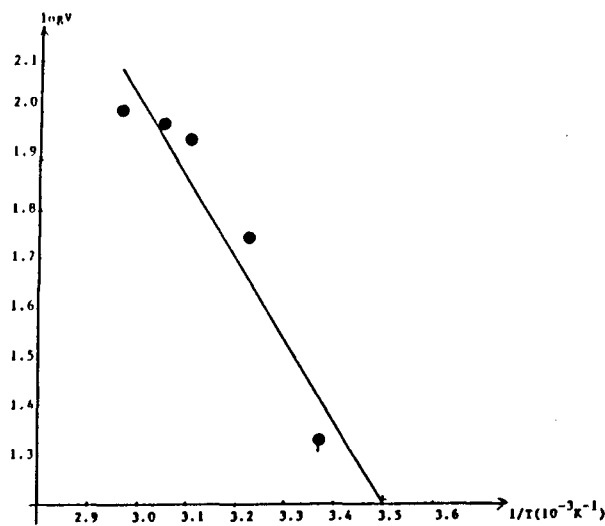


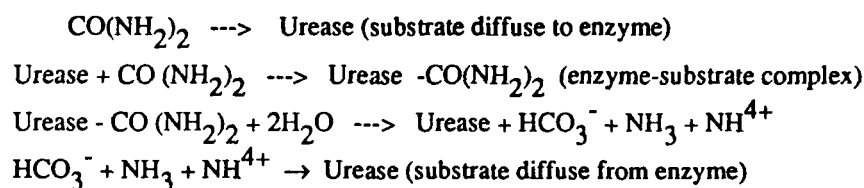
Figure 5.16.  $\log V$  vs  $1/T$ .

Thus:

$$\frac{-Ea}{R} = -1.65 \times 10^3$$

$$Ea = 13.7 \text{ kJ/mol (3.27 kcal/mol)}$$

The activation energy lies in the range expected for a diffusion-controlled process. The reaction sequence catalyzed by urease may be summarized as follows:



The results indicate that diffusion of urea to the enzyme or reaction products from the enzyme is the rate determining step for the reaction.

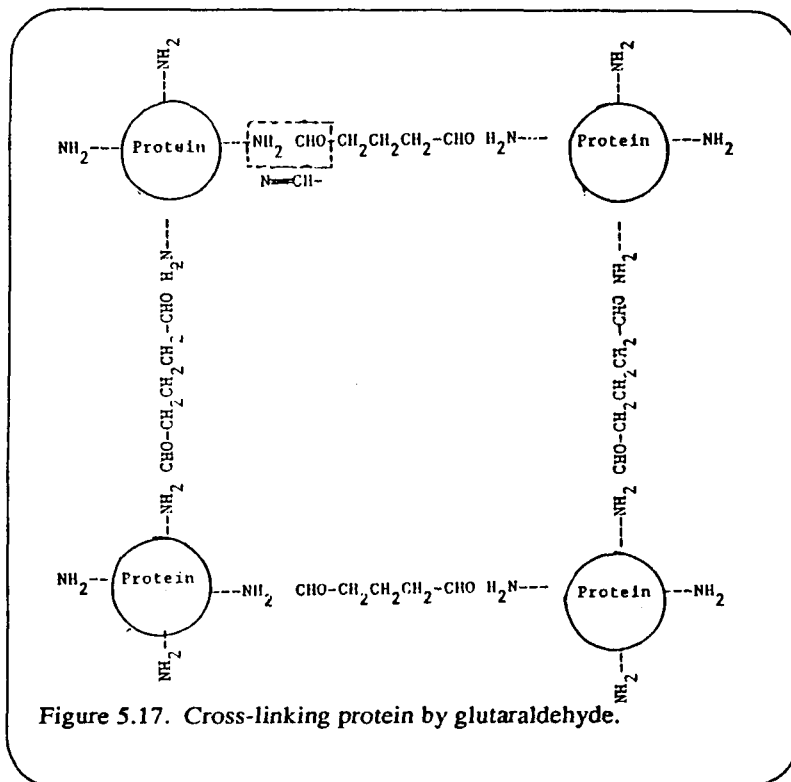
### Immobilization Procedure

A review of the literature concerning the immobilization of urease has been undertaken. A vast array of methods have been established for urease immobilization; however, most of the published literature is focused on the use of urease in clinical analysis where relatively small amounts of the enzyme are used (see [28] ) thus making many of these methods unsuitable for the bulk processing approach needed for water recycling. Consequently, other methods were assessed for their suitability for this project. The methods were assessed from the following viewpoints: (a) achieving long-term stability (i.e., activity) of the enzyme; (b) providing material with strong mechanical properties; (c) the immobilized enzyme must have low solubility for use in flow through reactor.

A proteic-polymer method described by Cocquempot, *et al.* [34; 35] was assessed to be a highly suitable approach for this work. This method involves mixing the enzyme with another protein (bovine serum albumin) then adding a chemical cross-linking reagent (glutaraldehyde) which chemically binds the urease and the BSA covalently through the -CHO groups of glutaraldehyde with the -NH<sub>2</sub> groups of the proteins such that a polymer is formed. The polymer has a sponge-like texture and is somewhat porous. The method was originally found to be effective in the enhancement of the stability of plant photosynthetic enzyme complexes and thus seemed to have good prospects for enhancing the catalytic lifetime of the enzyme urease. A copolymerization method was chosen because of its suitability for enzyme immobilization in a column reactor since the enzyme will not be washed away in a flowing urea solution and it provides a high contact surface with flowing urea solution. A schematic representation of the cross-linking process is given in Figure 5.17.

Urease was dissolved in a 100ml buffer solution containing 0.02 KH<sub>2</sub>PO<sub>4</sub>/K<sub>2</sub>HPO<sub>4</sub> and 0.2g EDTA at pH 7.0. EDTA forms a complex with contaminating heavy metal ions, thus protecting the enzyme from possible harmful effects.

The procedure for forming batches of immobilized urease involved mixing the following materials sequentially in a 15 ml test tube: 5.0 ml (400mg/100ml) urease solution 2.5 ml 24% bovine serum albumin 2.5 ml 1.5% glutaraldehyde.



The mixing was carried out at  $-25^{\circ}\text{C}$  by placing the test tubes in dry ice saturated with NaCl. The mixtures were left at this temperature for 4 hours. The tubes were then transferred to a  $-5^{\circ}\text{C}$  freezer for a further 2 hours. The material at this stage forms a brown colored polymer which is sponge-like in appearance. The material can be stored in buffer solutions at temperatures of  $-5^{\circ}\text{C}$  for extended periods of time; preliminary measurements show that the enzyme remains catalytically active after 2 months of storage. Large amounts of this material are in storage for future use.

### Enzyme Column Fabrication

The approach described above has been used to make large amounts of polymer containing immobilized enzyme. The next stage of the research has been to construct a water-treatment column containing the immobilized urease. A glass column was packed with urease-containing proteic polymer as shown schematically in Figure 5.18. Before packing the column, the mixture was taken from the freezer and placed in a refrigerator where it was left to stand for 3 hours at  $4^{\circ}\text{C}$ . This material was then broken down into small pieces and used as column packing materials. Glass wool was placed at the bottom of the reactor to prevent the escape of the enzyme material. When the column was packed with the enzyme, the volume of solution it contained was 200 ml.

### Activity of Immobilized Enzyme

The procedure to determine the catalytic activity of the immobilized enzyme first involved washing the column thoroughly with double distilled water. A liter of urea solution was made up containing 15g urea, 0.5g  $\text{KH}_2\text{PO}_4$ , 0.2g  $\text{K}_2\text{HPO}_4$ , and 0.2g EDTA at pH 7.0 and was passed through the column at a flow rate of 2 ml/min. The reacted solution was collected in 1 ml samples from the bottom of the column and assayed for the presence of  $\text{NH}_3$ . The assay was performed essentially as described above by adding 4.5 ml of  $\text{S}_1$  and 4.5 ml of  $\text{S}_2$ . A blank was obtained by collecting solution from the initial column washing.

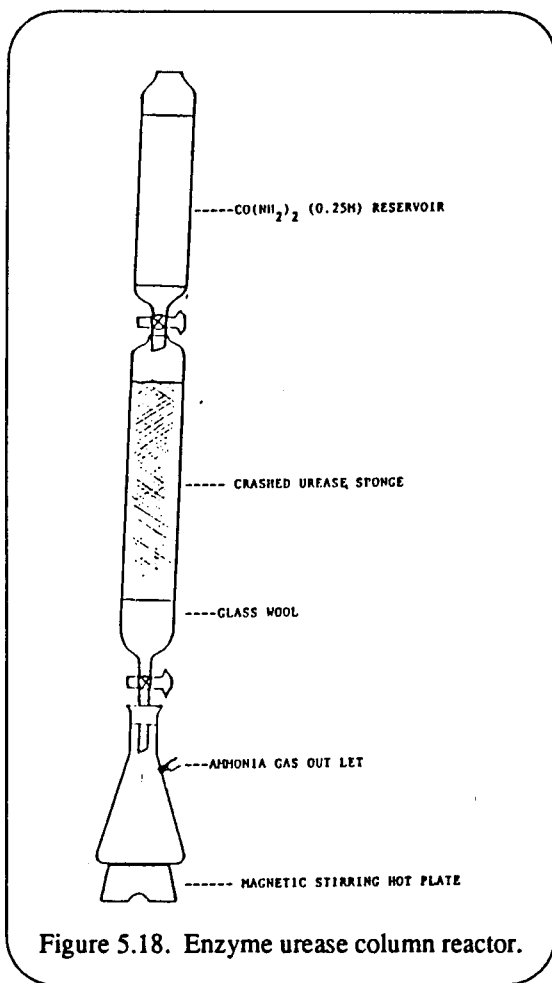


Figure 5.18. Enzyme urease column reactor.

The rate of  $\text{NH}_3$  formation under these conditions was  $2.6 \times 10^{-4}$ /min.

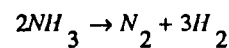
The conversion efficiency for  $\text{CO}(\text{NH}_2)_2$  is:

$$\text{conversion} = \frac{\text{CO}(\text{NH}_2)_2 \text{ decomposed per min}}{\text{CO}(\text{NH}_2)_2 \text{ input per min}}$$

$$= \frac{1/2 \times 2.6 \times 10^{-4} \times 100\%}{0.25 \times 0.002} = 26\%$$

### Decomposition of $\text{NH}_3$

The approach adopted in this phase of the research was to determine the feasibility of obtaining hydrogen from ammonia. The reaction has the following thermodynamic characteristics:



$$K_e = \frac{[\text{N}_2][\text{H}_2]^3}{[\text{NH}_3]^2}$$

$$\Delta G^\circ = 32.88 \text{ kJ/mol}$$

$$\Delta S^\circ = 197.87 \text{ J/mol}$$

$$\Delta H^\circ = 91.88 \text{ kJ/mol}$$

Table 5.10. Thermodynamic stability of ammonia.

Temperature	$\Delta G^\circ$ (kJ)	$\log K_{eq}$	$[\text{NH}_3]$ dissociated total $\text{NH}_3$
25°C (298K)	32.88	-5.76	low
100°C (373K)	18.04	-2.52	67%
200°C (473K)	-1.71	1.84	97%E

These data show that although  $\Delta G^\circ$  is positive,  $\Delta S^\circ$  is also positive, so the equilibrium constant can be increased by increasing the temperature; the effect of increasing temperature on the dissociation of ammonia is given in Table 5.10. From the table, at reaction temperatures of 350°C-400°C,  $\text{NH}_3$  can be decomposed to  $\text{H}_2$  and  $\text{N}_2$ . However,  $\text{NH}_3$

is a stable molecule and its breakdown requires a high activation energy and requires a catalyst.

Previous work[36; 37;38] has shown that Ru is a particularly good catalyst for the decomposition of ammonia; also, Fe catalysts are used because of their low cost (see Figure 5.19). A catalytic ammonia decomposer containing a Ru catalyst has been constructed in this laboratory, based on a design described else-

where, [36] and is shown in Figure 5.20. The column is packed with 1/8 inch alumina pellets coated with Ru (Ru content = 0.5%). Alumina surface area is approximately  $2400\text{cm}^2/10\text{mg}$ .

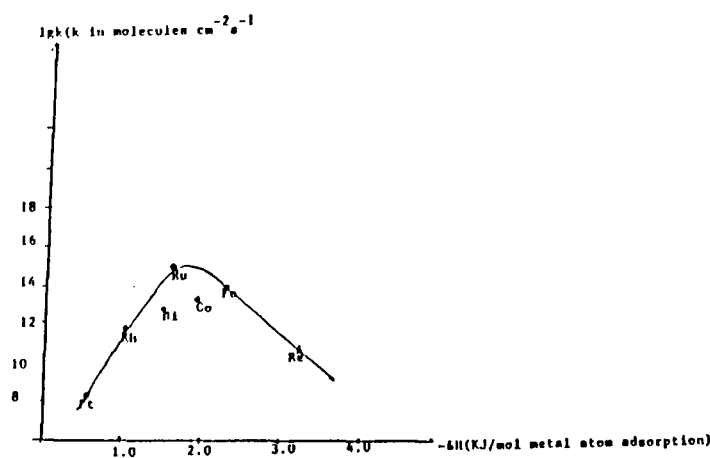


Figure 5.19. The rate constant of different catalysts of  $\text{NH}_3$  decomposition at  $t=400^\circ\text{C}$  (from reference 1).

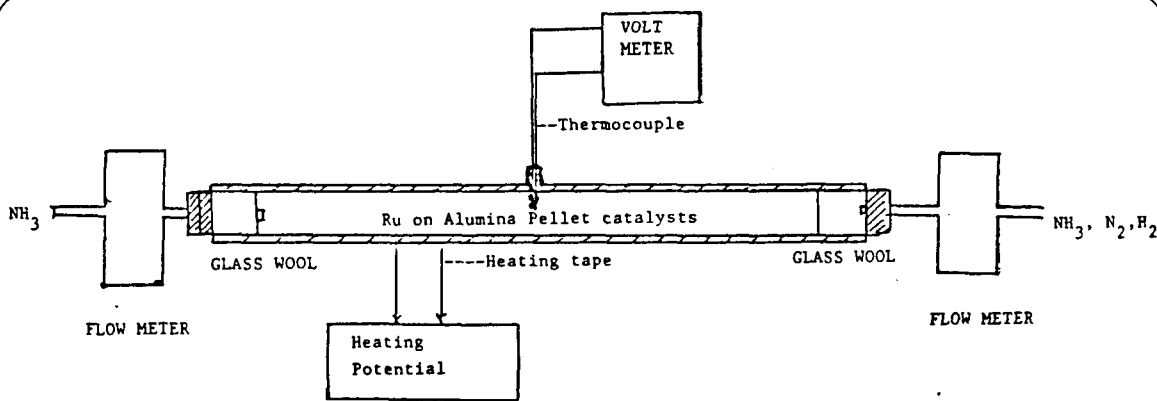


Figure 5.20. Ammonia decomposition reactor -- a flow model.

This reactor has been designed to have the following characteristics:

Operation temperature	$350^\circ\text{C}$
$\text{NH}_3$ input rate	260 ml/min (1 atm)
$\text{NH}_3$ output	172 ml/min
$\text{H}_2$ output	132 ml/min
$\text{N}_2$ output	194-259 ml/min

Under these conditions, the reactor can provide  $9.8 \times 10^{-5}$  mol  $\text{H}_2/\text{s}$ . A fuel cell working at 1A needs  $5.2 \times 10^{-6}$  mols  $\text{H}_2/\text{s}$ .

## Feasibility Study: Enzyme Technology Application for Waste Water Treatment

Preliminary calculations on the design of an enzyme bed for the treatment of waste water contaminated with urea. The size and performance of the reactor bed will be based on the following assumptions:

1. Urea concentration in typical waste water = 84000 ppb (i.e.,  $1.4 \times 10^{-3}$  M).
2. A total of 400 liters of water will be processed on a daily basis by the water recovery system.

The amount of enzyme required to maintain this amount of water free of urea can be determined as follows:

Enzyme activity is proportional to the concentration of urea and can be determined from the Michaelis Menton equation based on  $K_m = 2 \times 10^{-2}$  M urea.

$$V = \frac{V_{\max} [S]}{[S] + K_m} = \frac{V_{\max} 1.4 \times 10^{-3}}{1.4 \times 10^{-3} + 2.0 \times 10^{-2}} = \frac{1.4}{21.4} V_{\max} = 0.065 V_{\max}$$

At this low concentration of urea, the enzyme activity is 6.5% of the rate observed with 0.1M urea. Therefore, it is reasonable to that the rate of the immobilized enzyme column is reduced by 6.5% in the presence of these lower concentrations of enzyme.

It is possible to predict the rate of urea hydrolysis by the immobilized enzyme column under the lower levels of urea in solution.

$$\text{average enzyme velocity} = \frac{V_o}{2} = \frac{6.5\% V_{\max}}{2}$$

Under steady state conditions (flow rate is 2 mls/min) the measured enzyme velocity of the immobilized enzyme column was  $2.6 \times 10^{-4}$  mol  $\text{NH}_3$ /min. The amount of enzyme used to form the column was 160 mg urease and the efficiency of conversion of urea to  $\text{NH}_3$  and  $\text{CO}_2$  was 26%.

The amount of urea that this reactor can hydrolyze per day can be determined as follows:

$$\begin{aligned} &= 6.5\% \times 0.5 \times 1.3 \times 10^{-4} \times 60 \times 24 \\ &= 6.084 \times 10^{-3} \text{ mol/day} \end{aligned}$$

However, the amount of urea in 400 liters of contaminated water is:

$$400 \times 1.4 \times 10^{-3} \text{ mol} = 0.56 \text{ moles}$$

This result indicates that, under these conditions, an enzyme column that is 92 times larger than the one in the lab is necessary for the complete removal of urea from 400 liters of contaminated water on a daily basis; i.e., the reactor should include approximately 14.7 g of urease instead of 0.160 g. The volume of the present immobilized enzyme reactor is  $196 \text{ cm}^3$ ; therefore, using this technique, a reactor of volume approximately  $19600 \text{ cm}^3$  would be required, which is unacceptably large. However, the following points have to be taken into account.

1. Type III Sigma urease has a low specific activity and other types of urease having a ten times higher specific activity can be obtained commercially. This would reduce the amount of enzyme and the size of the reactor by an equivalent amount.
2. The enzyme is loosely packed into the reactor and significant volume savings can be achieved through a tighter packing of the enzyme in the column.
3. Much of the volume in the column is taken up by the BSA supporting matrix and glutaraldehyde which may not be necessary.
4. Urease is 4 times more active at 65°C than at 25°C at which the experiments were performed; therefore, a further reduction can be achieved at slightly raised temperatures (NB head pasteurization is usually performed at 62.8°C).

### Conclusions

It seems reasonable to conclude that a reduction in volume of close to 2 orders of magnitude can be achieved through simple modifications to the present reactor system. A flow-through reactor of less than 500 ml<sup>3</sup> can be highly effective in removing urea for large volumes of recovered hygiene water (i.e., up to 400 liters). The enzyme can be made more effective if it is combined with low grade heat or is used in combination with water that is higher temperatures during pasteurization. The weight of the protein contents of a 500 cm<sup>3</sup> enzyme column is approximately 30 grams.

## 5.2. Waste/Water Management System Refurbishment

Refurbishment of the waste/water management system and preliminary water quality analysis has been funded by NASA Grant #NAG 9-251. As a result of this effort, the system considered has been reconditioned to process a contaminated liquid input and provide condensate at a steady-state rate equivalent to 65% of the rate obtained during the system's original test operation. Results of the water quality assay for the condensate indicate that significant amounts of impurities, dissolved solids, and organic carbons are removed during the catalytic oxidation process, indicating that potability of the condensate can be attained.

A generalized schematic diagram of the waste/water management system is shown in Figure 5.21. More

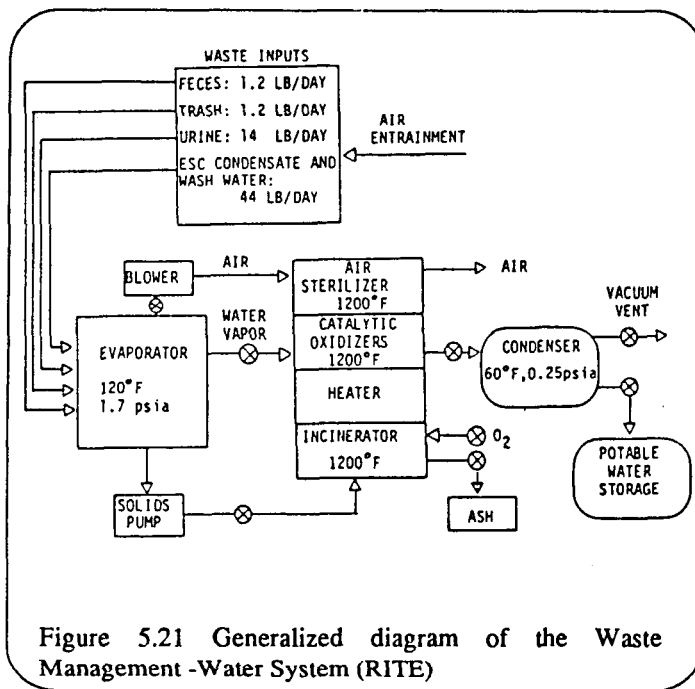


Figure 5.21 Generalized diagram of the Waste Management -Water System (RITE)

specifically, the Regenerative Concepts Laboratory staff is currently engaged in the phased refurbishment of the original system indicated in Figure 5.22. The experimental apparatus utilized for the particular set of experiments reported here is the Phase 1 sub-assembly consisting of the system evaporator, the system condenser, and a heat exchanger subsystem.

The evaporator is a stainless steel vessel, which nominally contains ports for the admission of urine, feces, trash, wash water, and oxygen, and the discharge of steam. Ports on the side of the vessel provide for the discharge of a solid slurry into the solids pump (for routing to the incinerator) and for the

readmission of liquid from the solids pump. Heat is provided to the evaporator by circulating a fluid through a 0.9525-cm diameter stainless steel coil welded to the cylindrical side of the vessel.

The condenser is constructed of stainless steel with a plexiglass top. A stainless steel manifold on the condenser top provides fittings for vapor in and vacuum attachments. A capacitance type level sensor, a thermocouple probe and water removal line are inserted through fittings in the lower portion of the bottom housing. Coolant flow is provided to the unit by circulation of a constant temperature fluid through stainless steel coil welded to the reservoir housing. A 2.54-cm thickness of foamed insulation covers the reservoir housing.

The heat exchanger subsystem is currently configured as separate heating and cooling units. These units are both Forma Scientific Model 2161 constant temperature circulators. The heating/cooling load required from this subsystem was computed from the nominal operating conditions in the evaporator and was estimated to be

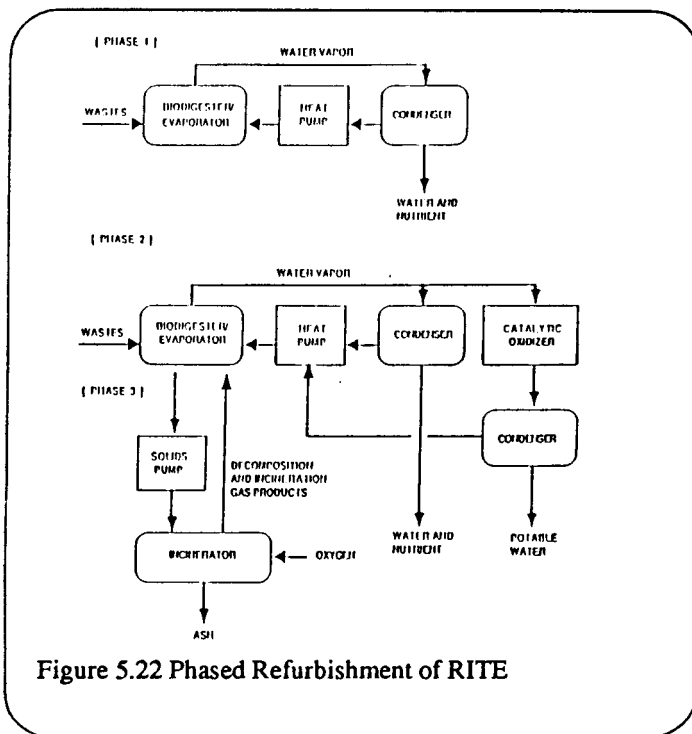


Figure 5.22 Phased Refurbishment of RITE

less than 750W.

The Phase 2 test bed, also shown in Figure 5.22, is composed of the evaporator condenser/heat exchanger system which comprised the Phase 1 test bed with the addition of the catalytic oxidizer subsystem. The catalytic oxidizer assembly processes the low pressure steam from the evaporator by heating the steam to 1100°F to 1200°F in the presence of a ruthenium catalyst.

To prevent liquid from spilling into the catalytic oxidizer from the evaporator, a cold trap has been constructed, leak-tested and installed between the evaporator and the catalytic oxidizer. A mechanical roughing pump has also been installed to evacuate the area surrounding the catalytic oxidizer

insulation jacket.

The decision to operate the catalytic oxidizer using only the mechanical roughing pump will result in a vacuum of about  $10^{-3}$  torr in the insulation jacket as opposed to  $10^{-6}$  torr available by operating both pumps in series. It is currently felt that a vacuum of  $10^{-3}$  torr should be sufficient to prevent significant conduction or convection in the insulation jacket.

The electrical resistance heating unit was inspected, reassembled, and reinstalled in the heating block. A variac has been obtained for regulation of the power input to the electric heater unit situated in the center of the heat block. The entire catalytic oxidizer subsystem was then reinstalled into the RITE system.

System operation with the catalytic oxidizer in place is evaluated using the following revised experimental test procedure:

1. Fill the evaporator with water and record the level from the level indicator.
2. Fill the condenser with 1 liter of water and close the valve between the cold trap and the evaporator.
3. Set the evaporator and condenser temperatures and allow a minimum of three hours for them to reach steady state.
4. Set the evaporator and condenser pressures by pressure regulator.
5. Once the evaporator and condenser temperatures have stabilized, record the level in the evaporator and all pressures and temperatures.
6. Open the valve between the evaporator and the cold trap.

7. Turn on the vacuum pump and open it to the condenser.
8. Allow the system to run for five hours.
9. Record the level readings from the condenser and evaporator every 30 minutes.
10. Measure the amount of fluid in the condenser and the vacuum surge tank and compare with the amount evaporated.
11. Add the required amount of water to refill the evaporator and compare it with the fluid obtained from the condenser and surge tank and determine the vacuum loss.

After repairs to the catalytic oxidizer and the cold trap were completed, experiments to establish the rate of condensation of water in the condenser were run. Condensation data for these experiments -- with the evaporator temperature set at 100°F and the condenser temperature at 60°F--are shown in Figures 5.23 through 5.25. With the vacuum leak repaired, the vacuum maintained in the evaporator was measured to be 1.2 psia, which allows for boiling in the evaporator at 108°F. These experiments, summarized in Table 5.11, represent a significant improvement in repeatability for both total condensation and average rate of condensation--plotted in Figure 5.26--over the initial phase two test bed experiments. Further, the average steady-state condensation rate for these three experiments of 11.482 ml/min is significantly greater than the 2.075 ml/min obtained initially from the phase two test bed.

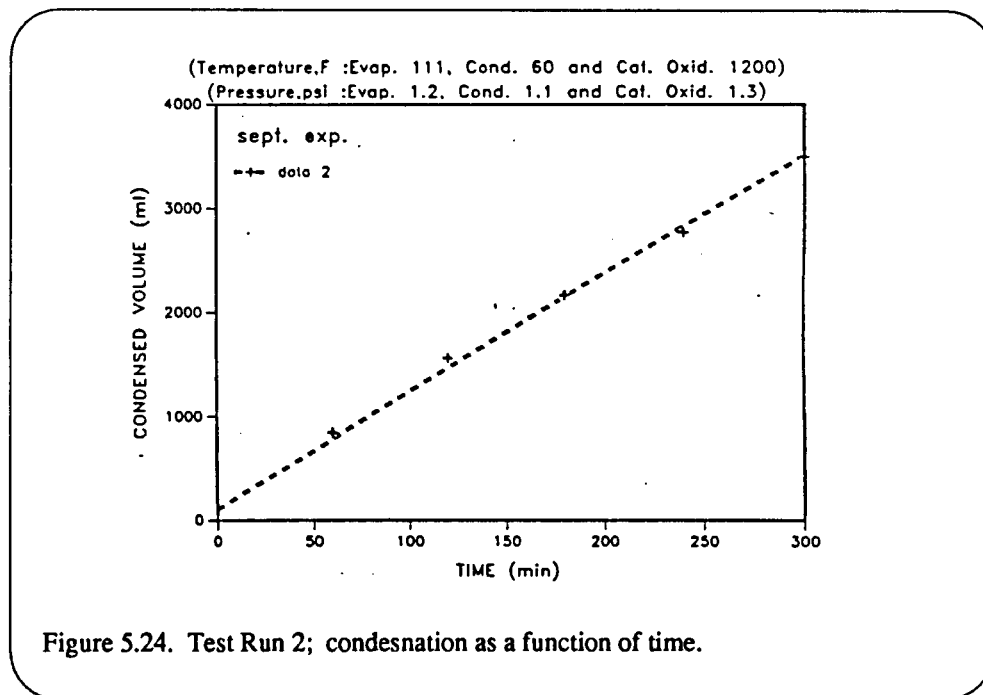
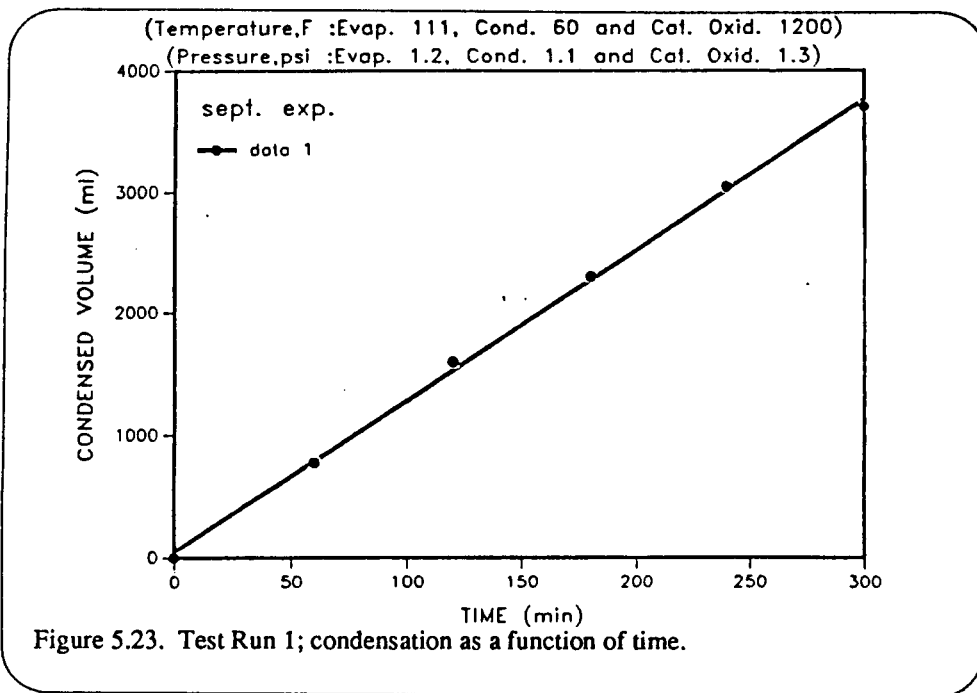
Table 5.11. Condensation Conditions for Various Evaporator and condenser Temperatures with the Catalytic Oxidizer in Place--Second Experimental Series.

Evaporator Set Temperature (°F)	Condenser Set Temperature (°F)	Total Volume Condensed after 5 Hours (ml)	Condensation Rate (ml/min)
111	60	3700	11.667
111	60	3500	10.778
111	60	3830	12.000

## Water Quality Assay

With the completion of the Phase 2 test bed refurbishment, collection of process condensate was undertaken to obtain pertinent chemical analysis data. At this point in the experimental program, the primary interest in water quality results pertains to organic content reduction.

Water samples were collected in clean polyethylene sample bottles with the sample quantity being about 250 ml. Sample #1 consisted of water taken directly from the evaporator which had previously been used for condensation rate studies in which tap water was routinely added as needed. Sample #2 was the process condensate. Next 20 ml of acetic acid (CH<sub>3</sub>COOH), 20 ml of ammonium hydroxide (NH<sub>4</sub>OH), and 20 ml of 2-propanol [(CH<sub>3</sub>)<sub>2</sub>CHOH] were added to the water in the evaporator which was equivalent to approximately 1000 parts per million for each additive. (A full evaporator contains approximately 20 liters.) Sample #3 was from the evaporator after adding the chemicals and mixing. Sample #4 was the process condensate. Assay



results are given in Table 5.12.

The total organic carbon content of Sample #3 serves as a partial reference in that the carbon fraction of the additive molecular weights is calculated to be 387 as compared to the assay result of 392. The condensate showed a ten-fold reduction in total organic carbon, but the catalytic oxidation failed to reduce the organic carbon content to potable levels.

Likewise, it appears that the ammonia nitrogen level of sample #4 (49 mg/l) is higher than might be expected. It is also noted that levels of specific conductance, total dissolved solids, nitrates, and chloride are all reduced in the catalytic oxidation process for both test samples.

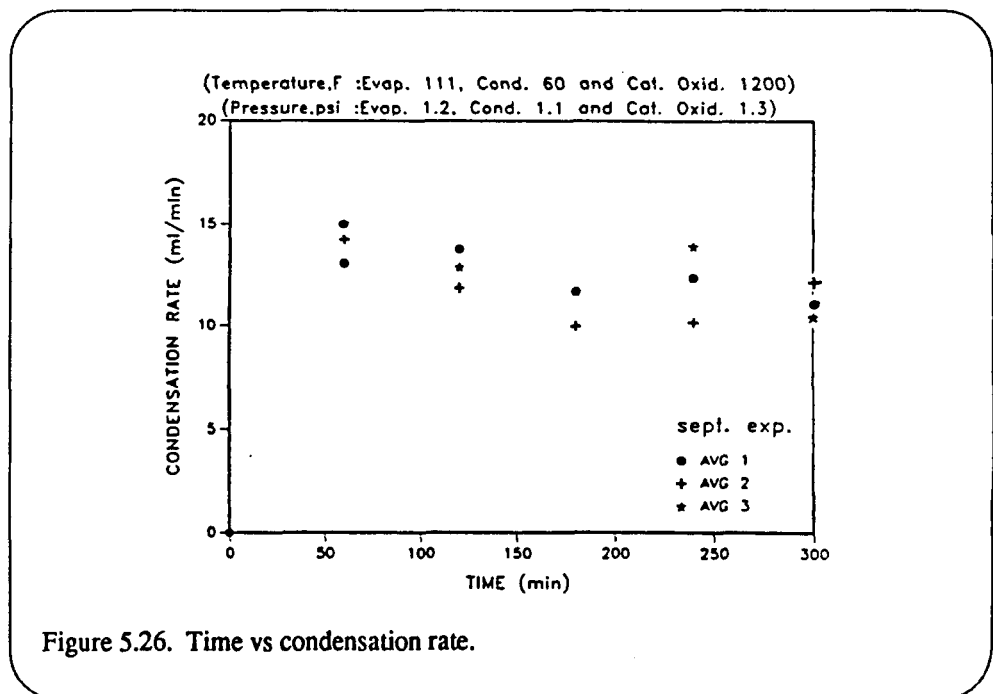
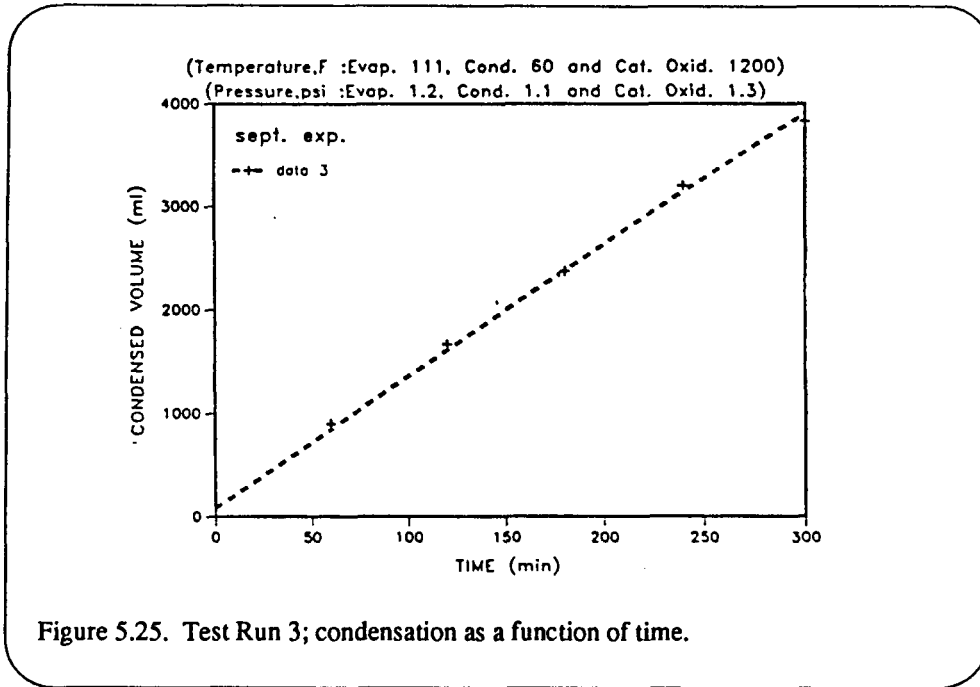


Table 5.12. Water assay of condensate, samples 1-4.

Sample No.	1	2	3	4
pH (s.u.)	9.6	6.6	8.1	8.5
Specific Conductance	1090	343	2090	589
Total Dissolved Solids 180°C	624	209	1120	354
Total Organic Carbon (mg/l)	13.3	2.82	392	31.1
Ammonia Nitrogen (mg/l)	0.04	0.07	152	49.0
Nitrate Nitrogen as "N"	0.59	<0.01	0.03	<0.01
Chloride (mg/l)	63	2.0	66	15
TRACE METALS (mg/l):				
Iron	0.09	0.22	0.08	2.60
Magnesium	0.72	0.02	1.23	<0.01

The primary cause of the excess levels of contaminants in the condensate is placed on the age of the ruthenium catalyst. While the catalyst does appear to be actively functioning, it no longer appears capable of oxidizing all of the volatile organics in the flow stream. The increase in trace metallic iron is believed to be residue from a weld required to repair the condenser after replacement of the level sensors.

Analytical data from the first set of water samples reported indicated that the catalyst bed might not be oxidizing at full capacity because of a higher than expected total organic carbon content (31.1 mg/l). It was then decided that before any action was taken to replace the catalyst with new material or change the type of catalyst, another test should be conducted using the same additives as for the first test, but increased to a 10 x concentration.

All fluid was drained from the evaporator and discarded. Next, the evaporator was rinsed with several liters of water and again drained. The evaporator was then filled with approximately 20 liters of distilled water. Six hundred ml of water was then withdrawn and 200 ml (each) of ammonium hydroxide, 2-propanol and acetic acid were added to the reservoir (this was 10 x the concentration of the previous test). Mixing was accomplished by introducing an air hose into the the evaporator fluid and allowing the air bubbling to agitate the fluid for several minutes. Next, a 250 ml sample was collected in a clean polyethylene bottle and capped. The reservoir was closed and when the temperature equilibrated, valves were set accordingly and the evaporative-condensation process was begun.

When the evaporator fluid was being changed out and rinsed, it was also decided that the manifold on the condenser side of the catalytic oxidizer should be inspected. Upon removal, corrosion-type flakes and a dark brown smudge material was noted inside the manifold. It was washed using a pressurized-water jet and most of the material was dislodged, however discoloration remained on the inside of the manifold. At this point we did not attempt to conduct an acid treatment to see if additional discoloration material could be removed. The

manifold was rinsed in distilled water and reinstalled.

Following collection of an adequate amount of condensate, the test was stopped and approximately 250 ml of process water was collected for analysis. The two samples were refrigerated overnight and delivered to Intermountain Laboratories for analysis on 03 November 1988. The results are shown in Table 5.13. Data from the control (reservoir), Sample #5 is as expected and reflects the 10 x concentration of additives previously seen in Sample #3. The water quality of the condensate, Sample #6, is significantly improved over the previous test set. The total organic carbon content of 7.5 mg/l falls within the range of Type 1 quality water which has a TOC range of 5.0 to 10.0 mg/l. At this point, residue in the manifold is suspected as the source of "contamination" for the higher than expected TOC of the previous sample (Sample #4).

Table 5.13. Water assay of condensate, Samples 5 and 6.

Sample Identification :	Sample #5	Sample #6
Date Sampled:	11-2-88	11-2-88
Date Received:	11-3-88	11-3-88
Lab Number:	0783	0784
<hr/>		
PARAMETERS:		
pH (s.u.)	5.2	5.8
Specific Conductance	8890	34
Total Diss. Solids @ 180°C	112	24
Total Organic Carbon (mg/l)	4010	7.5
Ammonia Nitrogen, (Mg/l)	1050	1.33
Nitrate Nitrogen as "N"	0.09	0.07
Chloride (mg/l)	17	2.8
TRACE METALS (Dissolved Concentration), mg/l:		
Iron	1.01	1.39
Magnesium	0.03	0.05

## Recommendations

- 1) The next step suggested is to remove the manifold, perform a mild acid wash on it to see if additional discoloration and/or corrosion can be removed and rerun the same sort of test. We might, however, drain off about half the reservoir content, refill with distilled water and collect another sample. The reservoir content of additives would be in the range of 5 x concentration or 1/2 of that for sample #5. After this test, if it is performed, we could then look at using a new mixture of additives for a couple of test series, then look at changing the catalyst type.
- 2) Should the catalyst require replacement, it is recommended that a variety of catalysts (including ruthenium) be considered. For a variety of reasons, including reduced power required for operation, a lower temperature oxidation process may be desirable.
- 3) Optimize the evaporation/condensation process with regard to catalyst selected, oxidizer temperature, evaporator temperature, and condenser temperature. The results reported here were obtained without regard for the interaction of the various system components. Increased performance should be attainable by including an assessment of the overall operating conditions.

- 4) Inspection of the two primary components of the Phase 3 test bed--the solids pump and the incinerator--reveals that near term operation of these components is not feasible. The solids pump, which was one of the most troublesome features of the original system, appears in need of extensive repair. Similarly, the incinerator shell is the only part of the incinerator capable of continued use, thus requiring refabrication of the remainder of the device.

Since analysis of the combustion products in a research environment can be carried out in a variety of other ways, it is currently recommended that the incinerator not be rebuilt in its original form. However, since the transfer of solids from one component of a processor to another will be required in any system developed, redesign of the solids pump should be strongly considered.

- 5) Consider utilizing the current waste/water management system as a post-processing system for other management/recovery technologies. As a particular example, use of an electrochemical processing scheme on basic waste products would deliver a liquid slurry, not unlike that used in these experiments, into the evaporator for processing into potable water and waste residue.

### 5.3. Algae Property Measurements for Engineering Design

Further design modifications to the algal biomass reactors currently in use in the TAMU Biology Department and in the Regenerative Concepts Lab involved fluid mechanics design considerations. This research effort revealed a tremendous lack of information relating to the fluid mechanics properties of various algal suspensions.

The limited scope of research was therefore focussed on the determination of the basic liquid properties of two particular algal strains:

- 1) *Anacystis nidulans*, strain R2
- 2) *Nostoc macrozamia*, strain MAC

Preliminary measurements with a Brookfield model LVT viscometer indicated that aqueous suspensions of each strain had viscosities which were indistinguishable from water. However, these viscosities are at the lower end of sensitivity of the viscometer. The research goals were therefore finalized into two major steps: (hypotheses)

- 1) Determine if the algal suspensions have viscosities which are significantly different from water.
- 2) If different from water, determine if the algal suspensions could be assumed to be Newtonian.

#### Methods

A long vertical pipe is a simple method for determining the viscous differences between two liquids. Each liquid is tested for flow rates in the same pipe independently. The tested liquid is first drawn into the pipe to a predetermined level. It is then allowed to flow freely down the pipe, with the elapsed time recorded at specific intervals.

The primary factors under consideration are density and viscosity (as a function of shear rate). If the two liquids can be assumed to have the same densities, then the pressure head developed by the liquids will be the same as they flow down the pipe at the same height. It should be noted that the pressure head will decrease as a decaying exponential with height (time).

If the two liquids have the same viscosities and densities, their times will be the same at these measured sites. Furthermore, if the slope of the curve is a simple first-order time exponential, the liquid(s) may be considered to be Newtonian. Similarly, if the measurement points are spaced on a logarithmic scale, the slope of the recorded times should be a straight line for a Newtonian liquid.

A 4 foot long capillary tube was used and clamped in a vertical position as indicated by Figure 5.27. The end was reduced to create a smaller orifice, thus increasing the fall times of the tested liquids. The average estimated fall time for water was 3-4 seconds, precluding reliable human measurement of fall times.

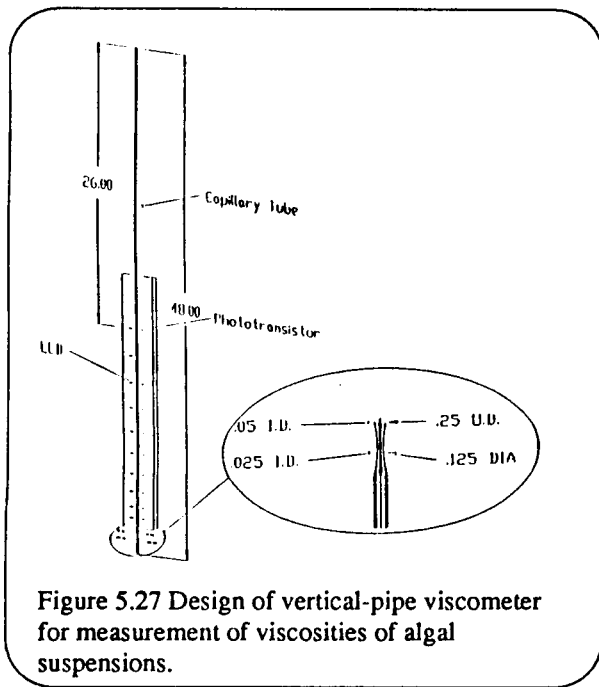


Figure 5.27 Design of vertical-pipe viscometer for measurement of viscosities of algal suspensions.

Ten LEDs and phototransistors were placed on a logarithmic scale alongside the capillary tube as indicated in Figure 5.27. The capillary tube is taller than the first detector to allow the liquid to develop a stable velocity profile. An Analog Devices model RT1800-F data acquisition board was used with a Zenith model Z200 microcomputer to send digital control signals and receive the digitized analog signals.

The digital output control circuit is indicated in Figure 5.28. CONN0 contains the coded decimal digital control signal (pins 7,13,14,15,16) which is sent to the 74154 digital multiplexer. This chip decodes the coded signal into one of sixteen states. These states represent a negative true logic: +5V=OFF GND=ON. This output is then sent to an ECG254 PNP darlington transistor pair which is used to provide the adequate

current requirements of the respective LED. The outputs of the transistor pairs are sent to CONN1 which is connected to the infrared LEDs.

The analog input circuit is indicated in Figure 5.29. CONN0 contains the same coded decimal digital control signal (pins 7,9,10,11,12) which is sent to the MUX16 analog multiplexer. This chip selects one of the 16 analog inputs in accordance with the control signal.

A positive 12 volts is supplied to the collector of each phototransistor. The base of these devices is excited by infrared photons and the emitters are connected to CONN1 as continuous inputs. A voltage representative of the received light was generated by the phototransistor emitter current which passed through each of the resistors (RA1-RA16) to ground. One of these voltages is then selected by the MUX16 for digitization by the data acquisition board.

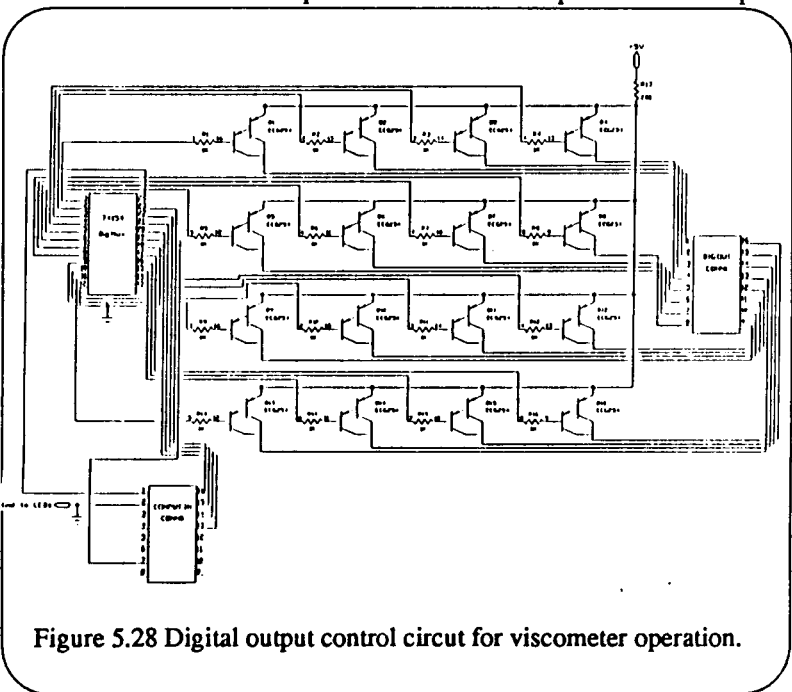


Figure 5.28 Digital output control circuit for viscometer operation.

ORIGINAL PAGE IS  
OF POOR QUALITY

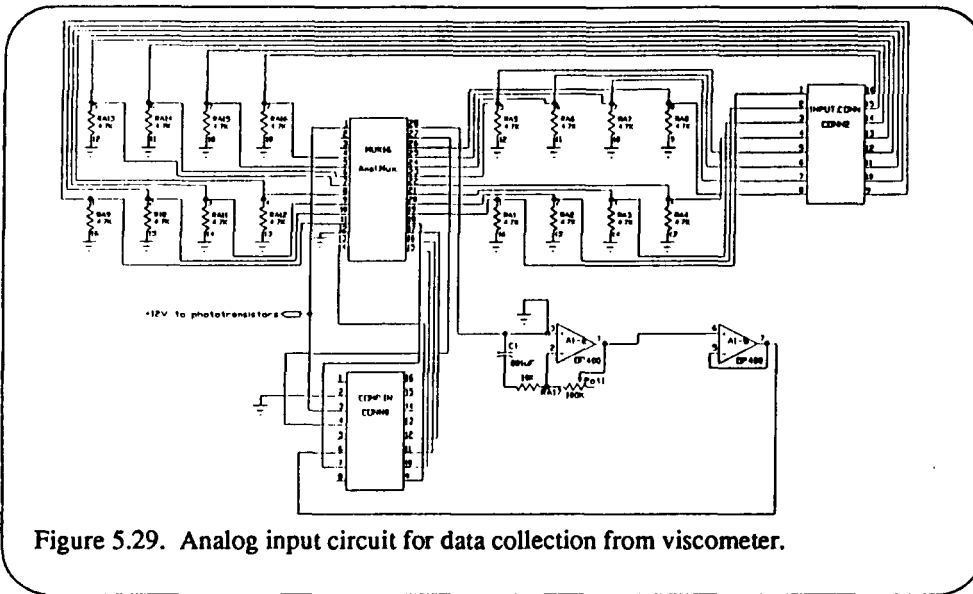


Figure 5.29. Analog input circuit for data collection from viscometer.

The logic flowchart for the controlling program is shown in Figure 5.30. The algorithm was implemented using the Microsoft 'C' language. The first three blocks initialize the hardware and software and ready the system to

store data into a designated file.

Since each of the LED-phototransistor pairs are discrete, their respective voltages vary significantly; however, the relative change in voltage due to liquid presence/absence will be the same. A scan is performed on all measurement points to record reference voltages for the empty capillary tube. These reference voltages can then be used to determine the presence of the liquid.

The user must next draw the test liquid into the tube until a specified height is achieved. The scanning process is then started and the liquid is released from

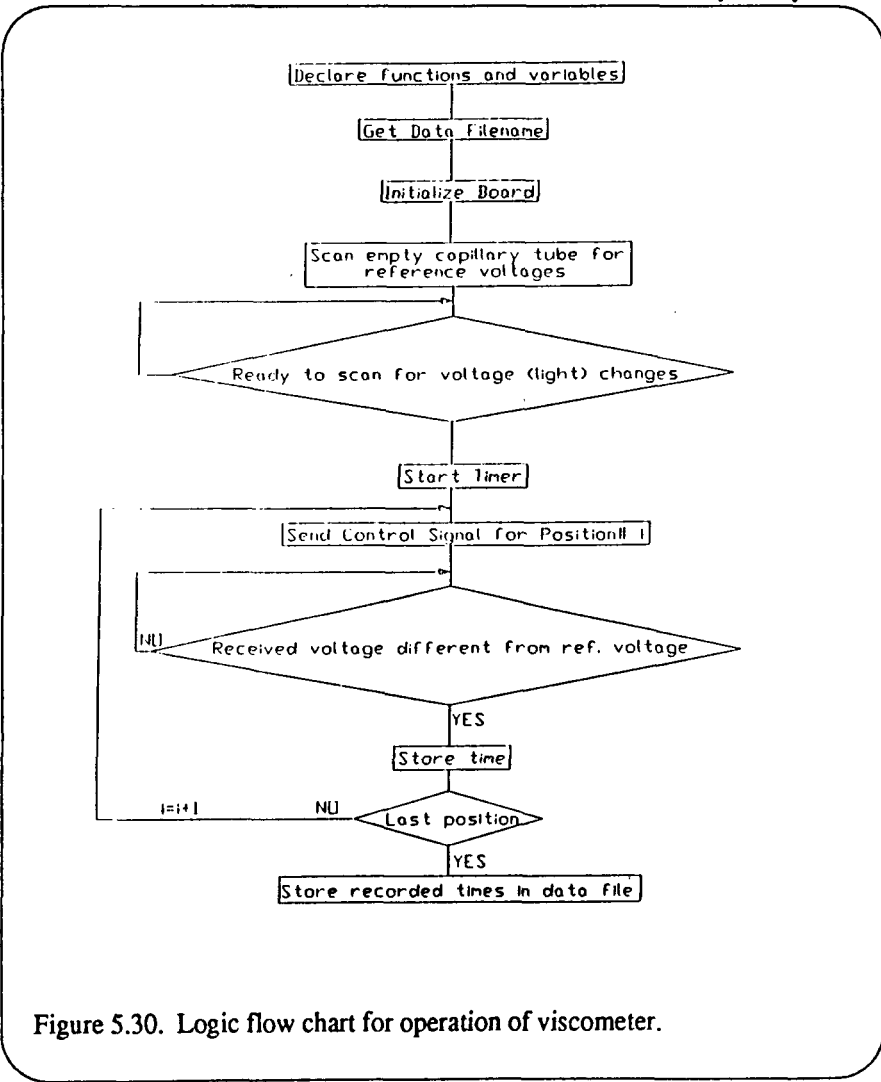


Figure 5.30. Logic flow chart for operation of viscometer.

the specified height and allowed to flow freely out of the tube.

As the liquid flows down out of the tube, the control signal for the first detector site is sent to the control circuitry. The first LED-phototransistor pair is scanned until a change in optical density is detected. When a change is detected, the time is recorded and the next detector site is activated. This process continues until the last position has been recorded.

After all data have been gathered, the information is recorded into the previously opened file.

## Results

Four different algal suspensions were tested using the test apparatus described above. Each of the tests was repeated a total of ten times. Preliminary testing indicated that the liquid did not approximate fully developed flow until the halfway point on the tube. For this reason only 10 measurement sites were used as indicated in Figure 5.27.

Samples of strain R2 and strain MAC were grown axenically on defined mineral media in previously sterilized test tubes. When the absorbance at 560nm of the growing cell suspension exceeded 99% (i.e., OD > 2), the suspensions were harvested and used for these experiments. These suspensions are designated R2clean and MACclean, respectively, in Tables 5.14 and 5.15. In addition, strain R2 was grown as a continuous, non-axenic culture in the algal biomass reactor previously described in NASA Report. Two samples were taken from this reactor culture, one week apart, and evaluated for viscosity. These samples are designated R2react1 and R2react2 in Tables 5.14 and 5.15.

Algal Suspension	Unwashed dry weight [mg/ml]	Washed dry weight [mg/ml]	Volume Concent. [u1cells/ml susp.]	Optical Density At 560nm
R2clean Axenic	6.3	3.7	13.5	>2
Macclean Axenic	6.1	2.1	7.8	>2
R2React1 Non-Axenic	3.1	1.1	4.1	>1.5
R2React2 Non-Axenic	3.9	1.4	4.6	>1.5

The four suspensions are identified and their respective physical characteristics are tabulated in Table 5.15. The data for water, methyl alcohol, and isopropyl alcohol are also given to verify the sensitivity of the test apparatus.

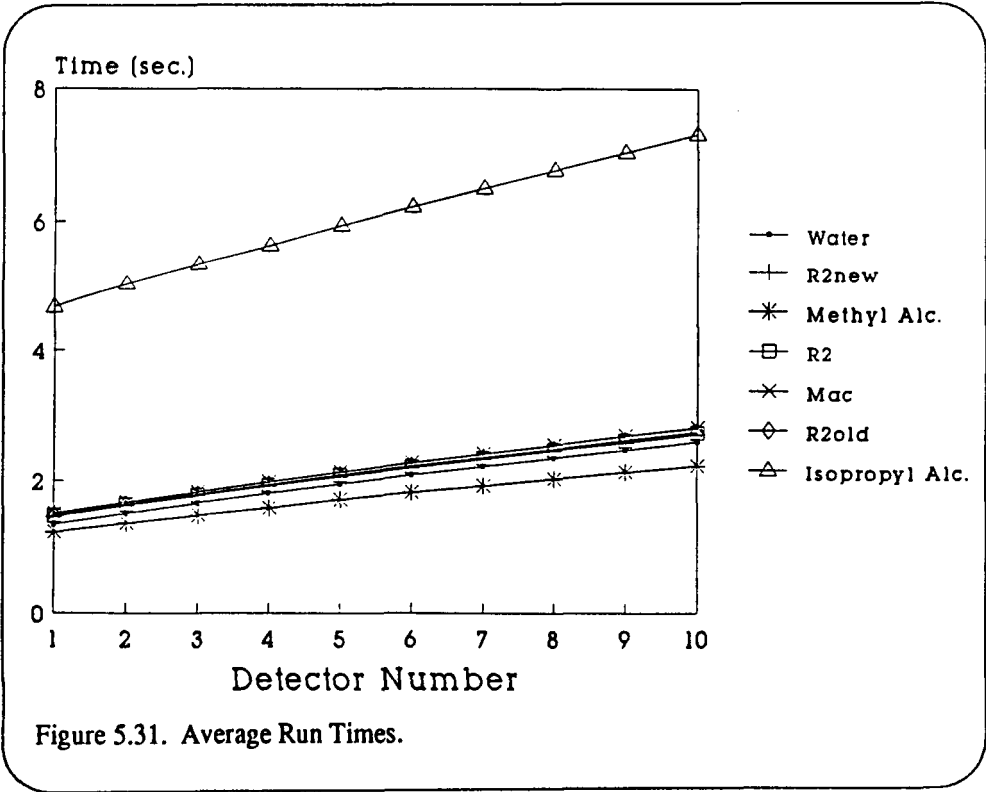
Algae	Detector site for significant time diff.	r-square coefficient for linear model
R2 clean Axenic	#3	.996
MAC clean Axenic	#1	.978
R2 REACT 1 Non-Axenic	no diff.	.998
R2 REACT 2 Non-Axenic	#2	.998

It is apparent from the data that the algae constitute a relatively small mass in the supporting media. Therefore, it is not surprising that the densities of the algal suspensions are close to that of water.

The algae and water time/ detector relationships are listed in Table 5.14. The graph of the data are shown in Figure 5.31. Qualitative inspection of the graph implies that the algal suspensions are slightly more viscous than water; however this difference

appears to be very small. The alcohols tested show a clear difference in viscosities. The small standard deviations for all tests confirm the stability of the test apparatus.

The SAS language was used to perform a statistical evaluation of the algae and water data. The alcohols were not included in any of the statistical analyses, since their viscosity differences were apparent by observation. Due to the limited scope of this research, only two statistical hypotheses were formulated:



- 1) Which algal suspensions have significantly (95% Confidence Interval) different test times from water?
- 2) Is the slope of each of the fluids (including water) linear?

A standard analysis of variance was performed to evaluate the time differences between the different algae and water. It should be noted that each of the liquids may be Newtonian (linear slopes); however if their viscosities are different, the slopes of the lines will be different from water. Therefore, it is possible for the times of the algae to deviate from the 95% confidence interval at different times. The detector points at which the different algal suspensions were considered to be significantly different are listed in Table 5.15.

It is evident that all of the algal suspensions were different except for R2react1. Table 5.14 confirms that this algal suspension is more dilute than the other suspensions. Although the lower concentration of algae is a probable factor in the resulting viscosity, the limited scope of this project did not include dilution of algal suspensions for a determination of concentration/viscosity relationships. For this reason R2react1 is confirmed to have the same viscosity as water, and will not be discussed further.

The significant time differences prove the first statistical hypothesis false. Since the times are longer than water, there is conclusive evidence that the remaining algal suspensions are more viscous than water.

A simple r-square analysis was implemented to test the goodness of fit of a linear model for each of the algal suspensions. The results are given in column two of Table 5.15. It is evident from the high r-square values (close to 1.0) that the linear model is a very good fit. These tests confirm the second hypothesis that the algal suspensions are Newtonian.

## Conclusions

Results of previous NASA projects and literature were instrumental in formulating the scope of the previously described research. The sensitivity and validity of the viscosity test apparatus has been confirmed. This test apparatus has given conclusive evidence that the algal suspensions tested are slightly more viscous than water; however they may be assumed to be Newtonian under the temperature and flow conditions simulated.

The high precision of the results indicates that the apparatus is stable, and any important controlling variables were stable during the test period. This research will be extended in future testing to evaluate the algal suspensions in different temperature and flow conditions. The need for more testing and data is indicated for varying algal concentrations, as well as diversity in different algal strains.

## 5.4. Plant Physiology Experiments

### Plant Growth at Low Atmospheric Pressure: an Experiment

Very little is known about plant growth at low atmospheric pressure, or about how atmospheric pressure interacts with environmental parameters and plant physiology to affect plant survival and biomass production. We have completed an experiment to test whether corn plants grown at 23 kPa total pressure grow, develop, and take up  $\text{CO}_2$  at the same rate as they do at 100 kPa when availability of  $\text{CO}_2$  and  $\text{O}_2$  at both pressures are identical and similar to that in atmospheric air.

#### Materials and Methods

We performed the following experiment twice at 27°C. Corn (*Zea mays*) seeds<sup>1</sup> weighing between 210 and 230 mg were selected and soaked in full strength Hoagland's solution for two hours prior to planting. The seeds were planted in PVC tubes (5.2 cm inner diameter and a length of 20 cm) whose bottoms were fiberglass screen held in place by duct tape.

The tubes were filled with wash sand and full strength Hoagland's nutrient solution was passed through them. The partially imbibed corn seeds were planted one per container at a depth of one cm. The tubes were then placed under experimental conditions in the semi-automated plant growth system described below.

The low pressure chambers were operated at a total pressure of 23 kPa. The composition of gas entering them was 98%  $\text{O}_2$ , 1.5%  $\text{N}_2$ , and 0.5 percent  $\text{CO}_2$ . At 23 kPa and 100% relative humidity this produces a density of  $\text{O}_2$  similar to that in atmospheric air.

The high pressure chambers were operated at a total pressure of 100 kPa. The densities of  $\text{O}_2$  and  $\text{CO}_2$  in them were similar to those in the low pressure chambers. Only the partial pressure of  $\text{N}_2$  in the high pressure chamber (75 kPa) was greater than that of the low pressure chambers.

The molar flow rate of gas through the high pressure chambers was almost five times that through the low pressure chambers reflecting their five times greater pressure. Thus, the volume flow rates through both the low and high pressure chambers were identical. The level of the molar flow rate through the chambers was set so that their  $\text{CO}_2$  densities were equivalent to the  $\text{CO}_2$  density in normal air.

Thirty-two plants were prepared as discussed above. Eight plants were placed in one high pressure chamber and eight plants in the other. Similarly, eight plants were placed in each of two low pressure chambers. At days 5 and 10 of growth, all 8 plants in a single low and high pressure chamber were harvested and each plant's total leaf number and area were determined, as were the dry weights of its root, seed, and shoot. In addition, the net  $\text{CO}_2$  uptake of the low and high pressure treatments were monitored throughout the 10 day experiment.

---

1. Sweet Corn seeds were of a yellow hybrid variety called "Early Sunglow" (lot 6233) which are mature in 63 days; obtained from W. Atlee Burpee Co., Warminster, PA.

## Results and Discussion

The plants of the low and high pressure treatment groups emerged late on day 2 or early on day 3. Plants in both treatment groups appeared to grow and develop similarly, and their leaf areas and dry weights at the fifth and tenth days following germination were not significantly different (Figure 5.32).

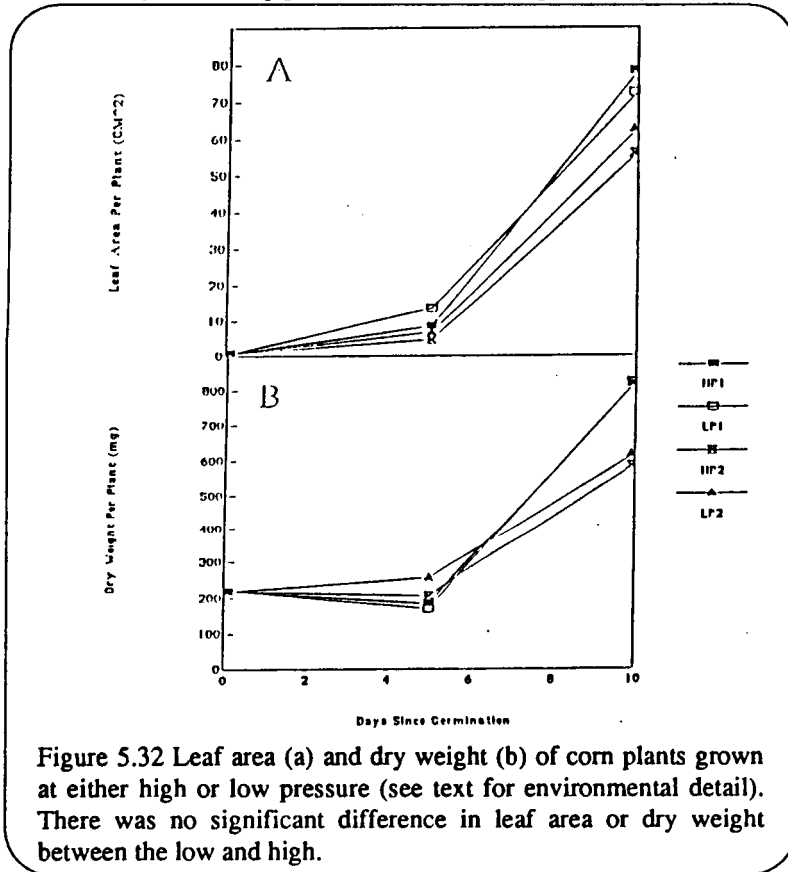


Figure 5.32 Leaf area (a) and dry weight (b) of corn plants grown at either high or low pressure (see text for environmental detail). There was no significant difference in leaf area or dry weight between the low and high.

There was no significant difference in leaf area or dry weight between the low and high pressure treatments in the first experiment (LP1 vs. HP1) or in the second experiment (LP2 vs. HP2). However, there was a significant difference between replicates (LP1 vs. LP2 and HP1 vs. HP2) at the tenth day.

These results show that corn plants grown at 23 kPa (in 98% O<sub>2</sub>) have growth rates similar to plants grown at 100 kPa (in air). This is consistent with reports in the literature for the growth of other plants under similar conditions.

Janert[39] found that oat seedlings grown in a closed illuminated system (into which CO<sub>2</sub>

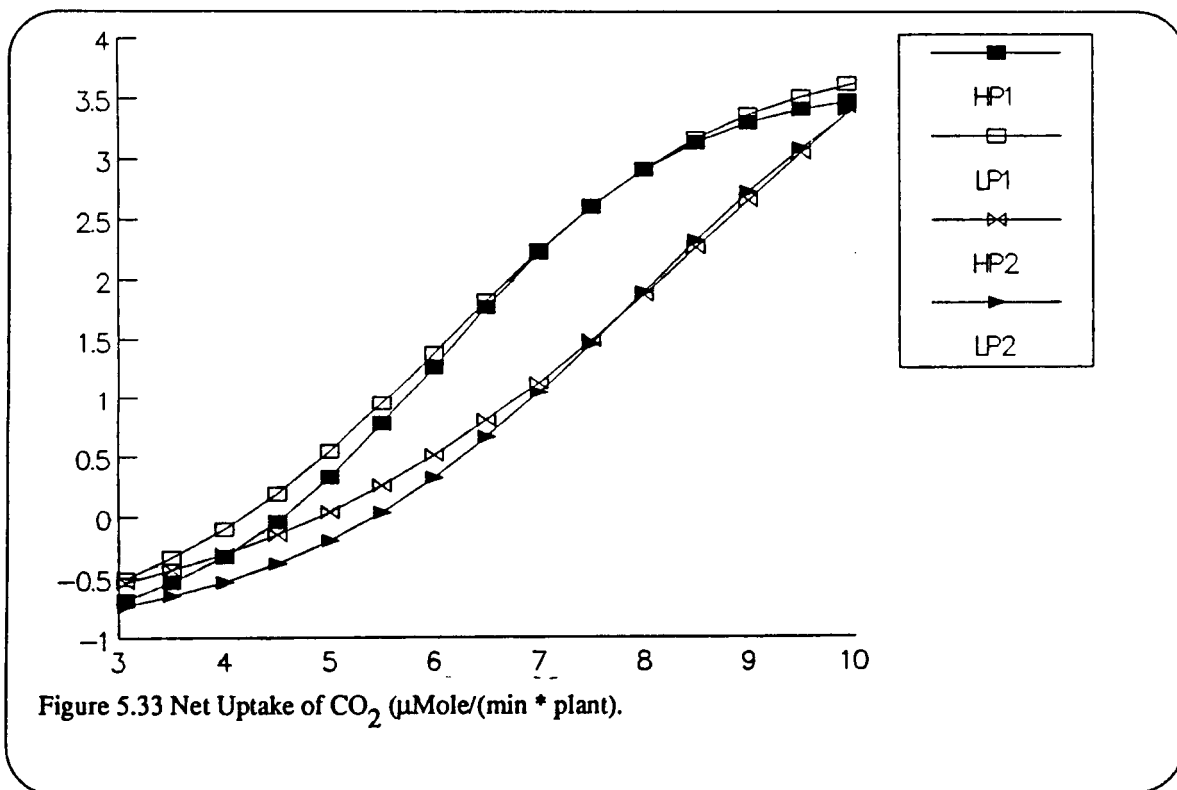
was periodically injected) were unaffected by the total atmospheric pressure at which they grew (20 kPa was the lowest pressure tested). However, he found that as the partial pressure of O<sub>2</sub> decreased below 20 kPa, there was an accelerating decrease in dry weight accumulation.

Andre and Richaud[40] grew rye-grass and barley under environmental conditions similar to Janert, except that they did not add additional CO<sub>2</sub> as Janert had. Their low pressure treatments were at 20 kPa total pressure with either 20 or 5 kPa O<sub>2</sub> and their ambient pressure treatment was 100 kPa total pressure with 20 or 5 kPa O<sub>2</sub>. All CO<sub>2</sub> in their system originated from the germinating seeds by respiration. They found that the growth of seedlings was not affected by total atmospheric pressure. However, plant growth decreased when O<sub>2</sub> partial pressure decreased to 5 kPa. They suggested that at low O<sub>2</sub> partial pressures the respiration of germinating seeds was limited, and that this resulted in a lower rate of biomass accumulation.

Musgrave *et al* [41] compared the germination of mungbean (*Phaseolus aureus Roxb.*) using an open flow-through system that was not illuminated. They found that three day old seedlings had developed normally at low pressure (20 kPa) and in fact were somewhat larger (on length and fresh weight bases) than seedlings grown at

atmospheric pressure. They also found that  $O_2$  uptake dynamics of the mitochondria differed when mungbeans were grown at low  $O_2$  partial pressure. Mitochondria from mungbeans germinated at low  $O_2$  partial pressure had a higher  $O_2$  exchange rate per unit weight, and a greater percent of cyanide resistant respiration.

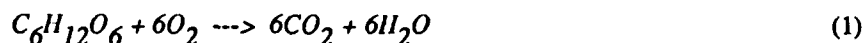
While we did not find differential growth, there was one significant difference between plants of the low and high pressure treatments after about one week, the net uptake rate of  $CO_2$  per plant in the high pressure treatment was significantly higher than in the low pressure treatment (Figure 5.33). We do not yet accept that this differential rate of  $CO_2$  uptake is due to physiological differences between plants of the two treatments. We believe that the low and high pressure treated plants took up essentially identical amounts of  $CO_2$ . However, our measured differences might have originated from other sources. An unrealized systematic error could exist in our measurement or calculation of net  $CO_2$  uptake, or maybe micro-organism populations differ in the two treatments. We are currently repeating these experiments to distinguish between these possible causes. However, our own and the above studies support the observation that the effect of reduced atmospheric pressure on the growth of the higher plants is minimal if total pressure is greater than or equal to 20 kPa, and if the partial pressure of  $O_2$  and  $CO_2$  are comparable to their values in Earth's atmosphere (20 kPa  $O_2$ , and 0.04 kPa  $CO_2$ )



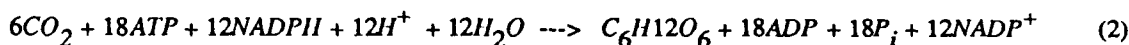
## 5.5 Artificial Chloroplast

### Introduction

The goal of this research is to develop a regenerative life support system which is required for extended missions in space. The respiration of an astronaut may be represented as



where  $C_6H_{12}O_6$  is glucose, a carbohydrate food source. To produce the glucose, the reverse of the above reaction must occur. The natural photosynthetic process uses light energy to fix the carbon dioxide as glucose. This process occurs in two phases: one requires light and the other does not. The phase which does not require light is the Calvin Cycle which converts carbon dioxide to glucose by a series of 15 reaction steps which sum to the following overall reaction:[42]



Fortunately, the Calvin Cycle has been studied since the 1950's, so this cycle is well understood. The reaction requires twelve enzymes and thirteen intermediates and occurs in the stroma of chloroplasts.[42] The affinity constant ( $K_m$ ) of the enzymes for substrates is known for virtually every enzyme. The enzymes function best around pH 8.[43] Also, the enzymes are in solution which makes them simple to use.

In nature, the energy required by the Calvin Cycle is supplied by light which is used to regenerate adenosine triphosphate (ATP) and reduced nicotinamide adenine dinucleotide phosphate (NADPH). For space applications, it is desirable to eliminate light driven reactions since the production of light from electricity is inefficient and it may be possible to use electricity directly to power the fixation of carbon dioxide as glucose. The artificial chloroplast will accomplish this goal.

Figure 5.34 shows a schematic of the proposed system. The astronaut eats glucose, breathes oxygen, and exhales carbon dioxide and water. The water is condensed from the air and is electrolyzed to produce the oxygen required for breathing. Additional water may be obtained from processing urine and other water wastes. The power source for the electrolysis unit can be envisioned as a nuclear-powered Stirling engine.

The dehumidified air is then stripped of carbon dioxide. Trace amounts of oxygen which may accompany the carbon dioxide will be removed in a catalytic combustor by reacting it with hydrogen produced in the electrolysis unit. This step is required since some of the enzymes are oxygen sensitive. Purified carbon dioxide is introduced into the Calvin Cycle reaction vessel where glucose is enzymatically produced. The glucose is removed from the reaction mixture by a membrane which passes small, uncharged molecules. Since all other species are charged or are of high molecular weight, this separation should be possible.

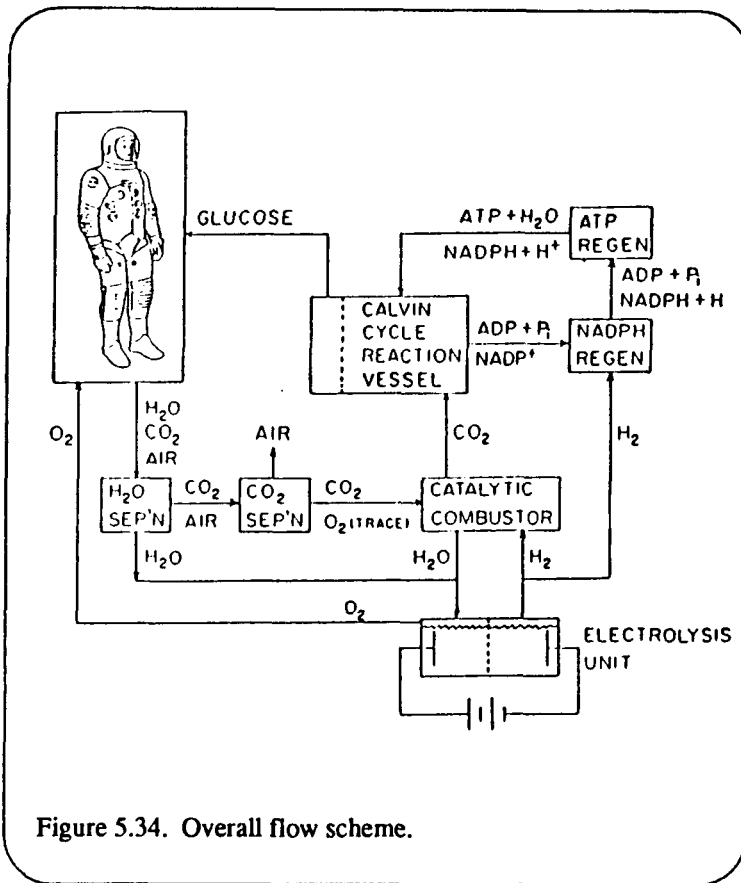
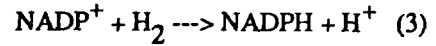


Figure 5.34. Overall flow scheme.

The NADPH required by the dark reaction is regenerated according to the following reaction[44]



using hydrogen dehydrogenase (E.C.1.1.2.1.2).

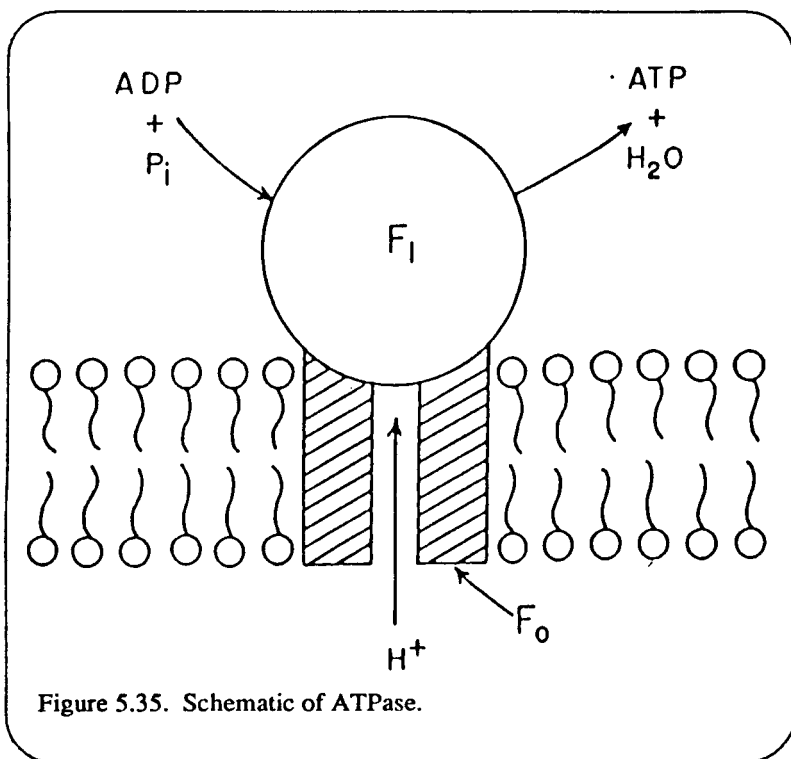
Since the Calvin Cycle is fairly well understood and NADPH regeneration has been demonstrated, the major technical barrier of this system is the regeneration of ATP. ATP molecules are synthesized naturally in the plasma membranes of bacteria and in the inner membranes of mitochondria and chloroplasts by a process known as chemiosmosis. Chemiosmotic ATP synthesis, first proposed by Peter Mitchell in 1961, requires two steps. In the first step, electrons ( $e^-$ )

and protons ( $\text{H}^+$ ) of hydrogen atoms are separated with a concentration of  $\text{H}^+$  on one side of the membrane, creating an electrochemical gradient called the protonmotive force (p.m.f.). In the second step, this build up of energy is used to power the phosphorylation of ADP



which is an endergonic reaction.

Therefore, both a chemical potential gradient  $\Delta\text{pH}$  as well as an electric potential difference  $\Delta\vartheta$  is required to synthesize ATP from ADP and  $\text{P}_i$  in nature. These gradients are vectorial, not scalar. Thus, the enzyme must be properly oriented with respect to the gradient in order to function. This orientation is accomplished by mounting the enzyme in a membrane (Figure 5.35). The  $\text{F}_0$  subunit of ATPase is embedded in the membrane and provides a passageway for electrons to flow. The  $\text{F}_1$  subunit is catalytically active and provides the site for the phosphorylation of ADP.



There is increasing evidence that the p.m.f. required to phosphorylate ADP is due to the addition of the free energy,  $\Delta G$ , stored in the  $\Delta pH$  and the  $\Delta G$  stored in the  $\Delta\psi$  and that the energy may come from one or the other if artificially induced. It is known that 7.3 kcal/gmole of free energy is required to synthesize ATP from ADP at standard conditions. If the p.m.f. is a result of a  $\Delta pH$  only, an  $H^+$  gradient across the membrane of about 3,000:1, or about 3.5 pH units, acid outside, is required. This is energetically equal to a  $\Delta\psi$  across the membrane of approximately 235 mV, with the outside positive with re-

spect to the inside.[45] Mitchell suggested that the p.m.f. generated across the membrane of mitochondria may be a combination of a  $\Delta pH$  of 1.0 and a  $\Delta\psi$  of about 150 mV. Experimentation has shown that it is possible for electron transport to generate this membrane potential.[42]

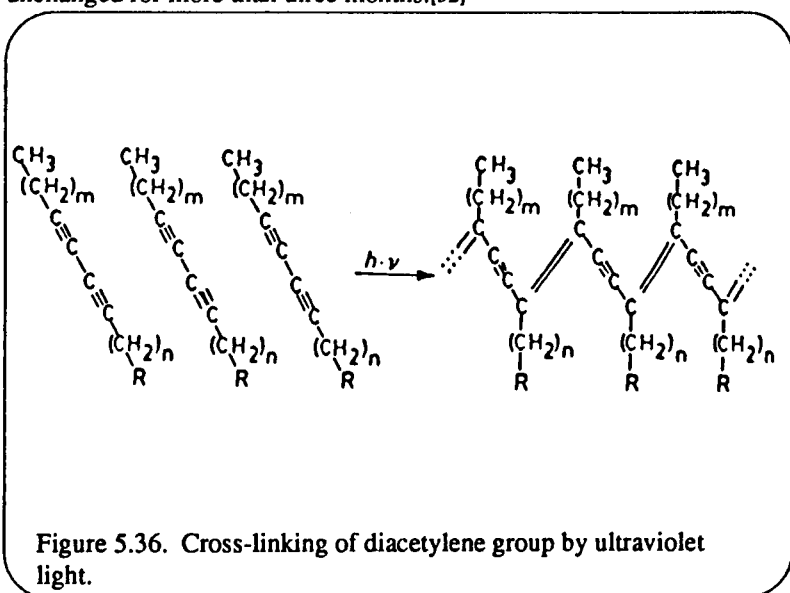
Jagendorf[46] demonstrated that phosphorylation can be induced by an artificially generated  $\Delta pH$  only. Also, Witt[47] proved that ATP synthesis can occur with an artificially generated  $\Delta\psi$  only. In their experiments isolated spinach chloroplasts were exposed to an external electric field strength (EEFS) of 1100 V/cm. To minimize deactivation of the enzyme, the applied voltage pulse was restricted to 30 ms and the system was cooled. Their results showed that the yield of ATP increases linearly with increasing number of pulses and they approximated that at least 6.5 ATP molecules were synthesized per ATPase by ten electrical pulses.

Similar experiments with rat liver mitochondria were attempted by Hamamoto;[48] however, the yield of ATP was too low to show a net turnover of the enzyme during a pulse. Their results did show that net ATP synthesis increased with increasing voltage, number of electrical pulses, and duration of electrical pulses.

Knox and Tsong[49] had greater success synthesizing ATP by electrically pulsing beef heart mitochondrial ATPase. They exposed cyanide-treated submitochondrial particles to higher voltages (EEFS=10-30 kV/cm) but shorter electrical pulses (1-100  $\mu s$ ). Maximum yield was 10-12 mol ATP per mole ATPase per pulse for a 30 kV/cm-10  $\mu s$  pulse.

## Proposed Methods

Recently, there has been an increasing interest in studying the interactions of proteins in biomembranes. Model membranes, either spherical liposomes or planar lipid membranes, may be used for resolution and reconstitution of specific proteins to investigate their functions. Problems arise with reconstituted model systems because they are not stable. To overcome this problem, Wagner[50] incorporated the ATPase from *Rhodospirillum rubrum* into the synthetic lipid 2-[bis-(2-hexacosyl-10,12-diyneoxyethyl)amino]ethanesulfonic acid. This sulfolipid contains a diacetylene group which allows it to polymerize upon UV irradiation (see Figure 5.36). These synthetic biomembranes seem to be completely stable. They cannot be destroyed by organic solvents.[51] When bacteriorhodopsin was incorporated into this sulfolipid, its activity remained completely unchanged for more than three months.[52]



Planar bimolecular lipid membranes (BLM) are formed by one of two basic methods, the brush technique and the dipping technique. An overview of methods of experimental arrangements and procedures of producing ultrathin (<100 Å) BLM in aqueous solution is presented by Tien.[53]

The formation of BLM in aqueous solution requires the creation of two coexisting solution/membrane interfaces. A thin piece of an inert material with a small hole is immersed in a dilute electrolyte. A small drop of a lipid is introduced to the hole where it will spontaneously thin by draining centrifugally to the lipid solution around the edge of the aperture, known as the Plateau-Gibbs border.

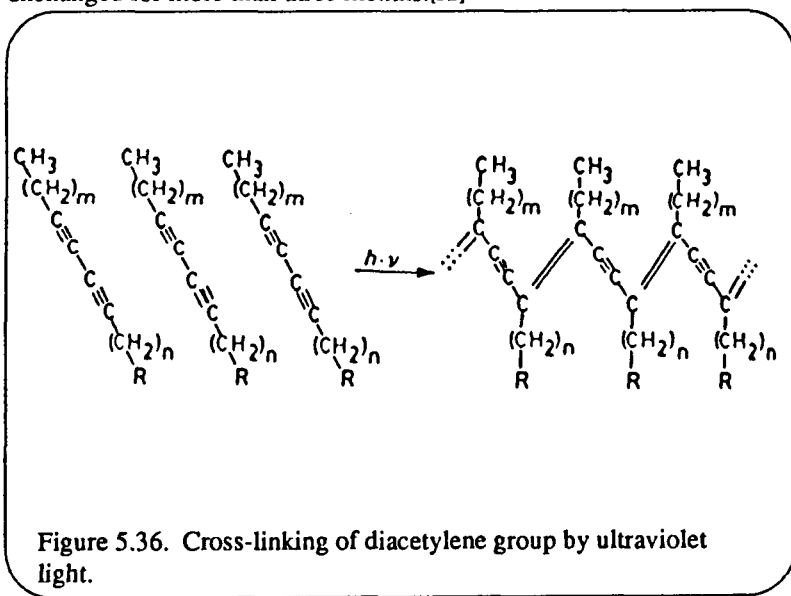
The brush technique was the original method of BLM formation. A small Teflon beaker with a small hole is set into a glass chamber and each is filled with a 0.1 M salt solution. The lipid is spread across the aperture with a fine sable hair brush.

The dipping technique may prove to be easier and to have fewer mechanical and technical problems. By the dipping technique, a metal, polyethylene, or hair loop of 1-2 mm is dipped into a lipid solution and transferred through the air to a beaker filled with an aqueous solution. If a screen is used, this method may be preferable for producing large areas of membrane.

A method described by Takagi[54] involves dipping a hydrophobic material through an air/water interface covered by a lipid monolayer. The tails of the lipids are pointed out of the water and therefore come together as the material is lowered. The surface pressure of the monolayer should be kept constant.

## Proposed Methods

Recently, there has been an increasing interest in studying the interactions of proteins in biomembranes. Model membranes, either spherical liposomes or planar lipid membranes, may be used for resolution and reconstitution of specific proteins to investigate their functions. Problems arise with reconstituted model systems because they are not stable. To overcome this problem, Wagner[50] incorporated the ATPase from *Rhodospirillum rubrum* into the synthetic lipid 2-[bis-(2-hexacosa-10,12-diynoylethyl)amino]ethanesulfonic acid. This sulfolipid contains a diacetylene group which allows it to polymerize upon UV irradiation (see Figure 5.36). These synthetic biomembranes seem to be completely stable. They cannot be destroyed by organic solvents.[51] When bacteriorhodopsin was incorporated into this sulfolipid, its activity remained completely unchanged for more than three months.[52]



Planar bimolecular lipid membranes (BLM) are formed by one of two basic methods, the brush technique and the dipping technique. An overview of methods of experimental arrangements and procedures of producing ultrathin (<100 Å) BLM in aqueous solution is presented by Tien.[53]

The formation of BLM in aqueous solution requires the creation of two coexisting solution/membrane interfaces. A thin piece of an inert

material with a small hole is immersed in a dilute electrolyte. A small drop of a lipid is introduced to the hole where it will spontaneously thin by draining centrifugally to the lipid solution around the edge of the aperture, known as the Plateau-Gibbs border.

The brush technique was the original method of BLM formation. A small Teflon beaker with a small hole is set into a glass chamber and each is filled with a 0.1 M salt solution. The lipid is spread across the aperture with a fine sable hair brush.

The dipping technique may prove to be easier and to have fewer mechanical and technical problems. By the dipping technique, a metal, polyethylene, or hair loop of 1-2 mm is dipped into a lipid solution and transferred through the air to a beaker filled with an aqueous solution. If a screen is used, this method may be preferable for producing large areas of membrane.

A method described by Takagi[54] involves dipping a hydrophobic material through an air/water interface covered by a lipid monolayer. The tails of the lipids are pointed out of the water and therefore come together as the material is lowered. The surface pressure of the monolayer should be kept constant.

Similar to the above method,[55] the hydrophobic material with the small aperture is above the air/water interface covered with a lipid monolayer. The liquid levels on each side of the partition are successively raised and the two monolayers combine to form a lipid bilayer. The last two techniques described leave little or no solvent in the resulting BLM.

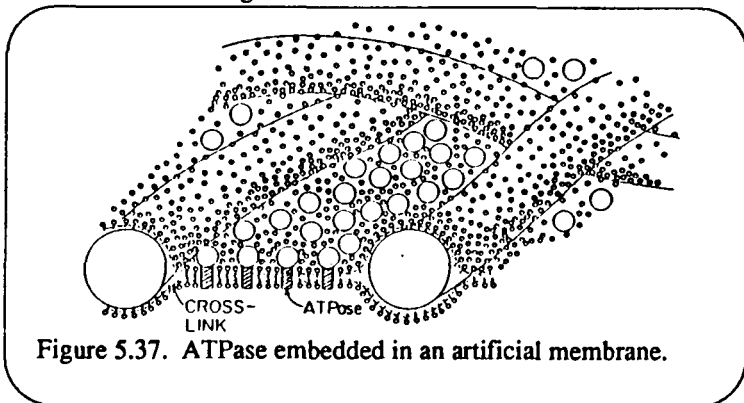


Figure 5.37. ATPase embedded in an artificial membrane.

Figure 5.37 shows a schematic of the ATPase embedded in a BLM of the synthetic lipid. The BLM is formed with the synthetic lipid by one of the techniques described above on a screen mesh made of polypropylene or stainless steel. The ATPase is then added and it spontaneously orients itself in the membrane since the  $F_0$  subunit is

hydrophobic. The sulfolipid is irradiated with ultraviolet light to induce cross-linking. Although the cross-linking is not essential to the operation of the enzyme, it is desirable since it gives strength to the membrane.

Once the ATPase is immobilized in a macroscopic membrane, the enzyme may be powered by a pH or a voltage gradient. The simplest method to establish a proton gradient is to add a volatile acid to one side of the membrane as shown in Figure 5.38. Candidate volatile acids include hydrochloric acid, trifluoroacetic acid, and acetic acid. Alternatively, a volatile base, such as ammonia, could be added to the basic side of the membrane. The acid or base would be recovered by appropriate separation procedures such as vacuum distillation or adsorption.

Figure 5.39 shows a schematic of a more elegant method of creating a pH gradient electro-chemically to power the enzyme.

A minimum potential of 1.23 V (the standard electrode potential[56]) would be applied to the electrodes. In actuality, a higher voltage of about 2 V would be needed to overcome losses in the system. At the anode, water is electrochemically split to form hydronium and oxygen. The oxygen will be added to

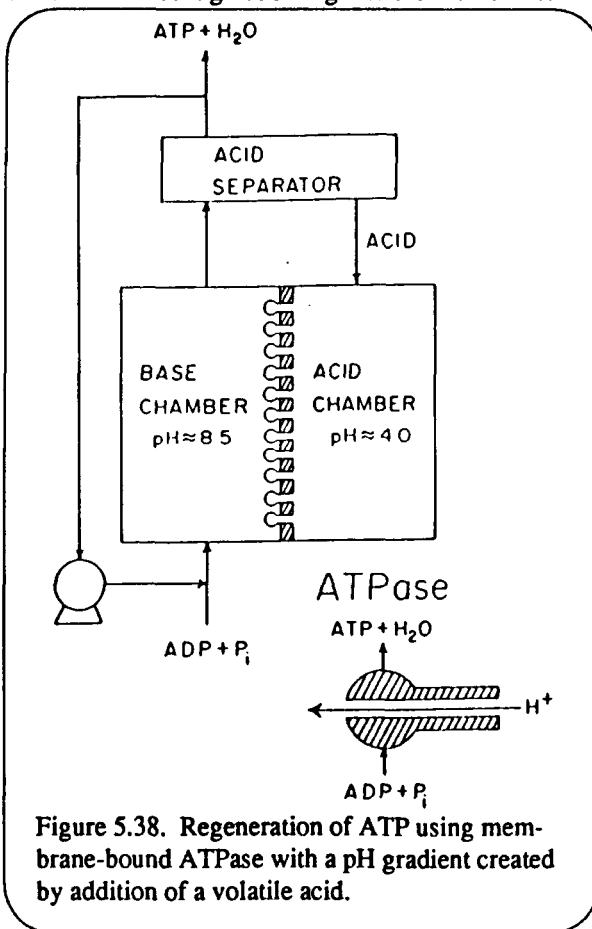


Figure 5.38. Regeneration of ATP using membrane-bound ATPase with a pH gradient created by addition of a volatile acid.

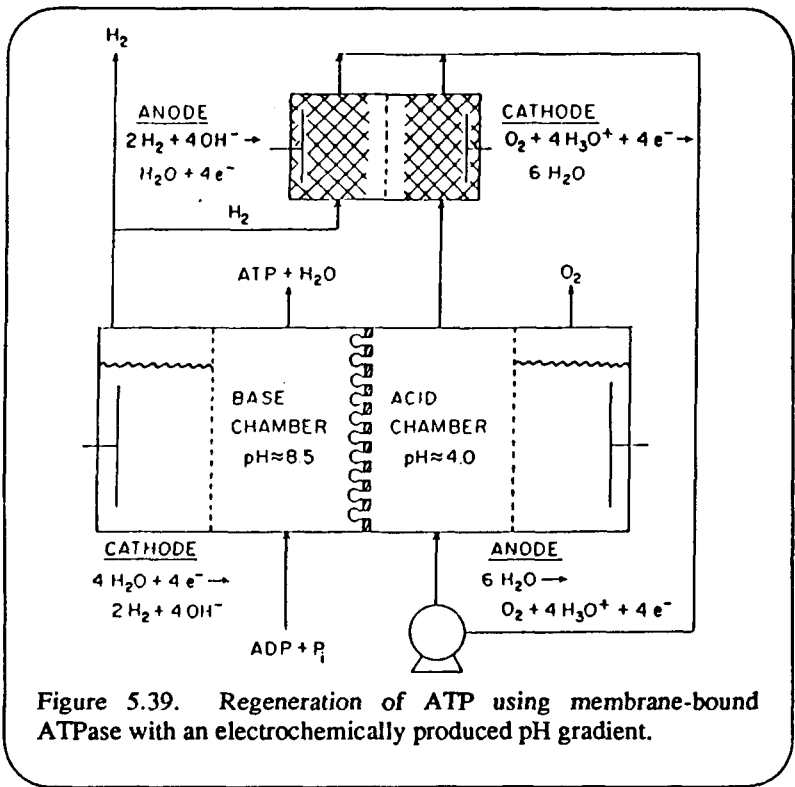


Figure 5.39. Regeneration of ATP using membrane-bound ATPase with an electrochemically produced pH gradient.

the cabin for breathing. At the cathode, water will be split to form hydrogen and hydroxide ions. The hydrogen will be used to reduce  $\text{NADP}^+$ . Thus, chamber 2 is more acidic than chamber 1. The protons (hydronium) will flow from the anode through the membrane-bound ATPase to the cathode to cause ATP to be regenerated from ADP. The electrodes are covered by ion-permeable membranes to protect the enzymes and biochemicals. The hydrogen and oxygen products could be fed to a fuel cell to help provide the electricity necessary to power the reactor.

As already mentioned, since some of the enzymes are susceptible to degradation by oxygen, the oxygen-laden liquid will be pumped through a porous catalyst which converts the oxygen and hydronium to water. Some hydrogen will have to be supplied to the anode to act as a sink for the electrons. This oxygen scavenging system will actually produce electricity since it is a fuel cell, however, it will have a relatively small power output since the oxygen is minimally soluble in water.

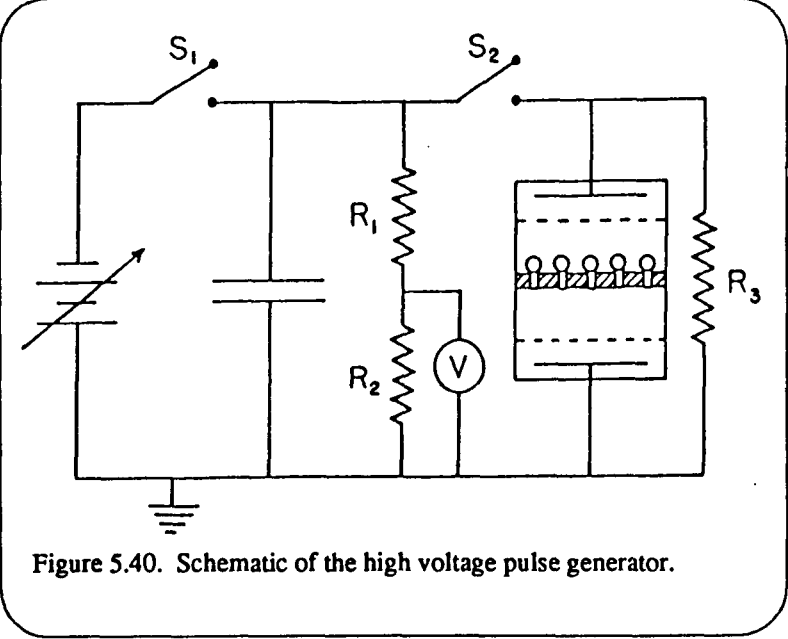


Figure 5.40. Schematic of the high voltage pulse generator.

If a voltage gradient rather than a pH gradient is used to power the ATPase, the same apparatus shown in Figure 5.39 will be used, but rather than a small voltage of about 2 V, about 1,000--20,000 V will be used. This high voltage will be supplied in pulses using an electrical circuit similar to the one shown in Figure 5.40. The variable transformer will be set to a desired voltage and switch  $S_1$  will be closed to charge the capacitor and

then reopened. Switch  $S_2$  will then be closed to discharge the capacitor through the cell and the resistors. The voltage drop across resistor  $R_2$  is a small fraction of the total voltage drop so that a conventional voltmeter or oscilloscope may be used to measure the charge on the capacitor. Resistor  $R_3$  is adjusted to control the time constant of the voltage discharge.

One of the major thrusts of the proposed research is to assess the relative merits of the two approaches to powering the ATPase. The pH gradient approach should be fairly "gentle" and easy to control compared to the use of a large voltage gradient. However, the voltage gradient approach should require the least amount of energy since a pure voltage with no current flow requires insignificant amounts of energy. In practice, however, it will not be possible to build up the voltage without some flow of current. The current flow can be minimized by reducing the ionic strength of the media and using an electrode material which has poor charge transfer properties. The studies which have been performed which apply a voltage gradient to ATPase have used platinum as the electrode material. Platinum has the best charge transfer properties of any known material,[57] so it was the worst possible choice. It would be better to choose a material with poor charge transfer properties to reduce the current flow and hence reduce power loss and ohmic heating of the media. Graphite may be a good candidate material.[58]

## Experimental Methods

### Synthesis of the Polymerizable Synthetic Sulfolipid

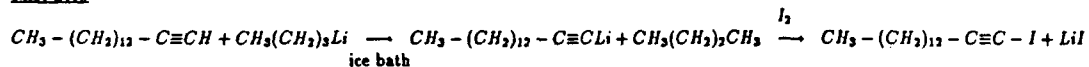
The synthetic lipid 2-[bis-(2-hexacosyl-10,12-diyndyloxyethyl)amino]ethanesulfonic acid has been successfully synthesized in our laboratory by a method described previously by Hub[51] as shown in Figure 5.41.

All reactions are performed in an atmosphere of argon under a chemical hood. The first step is to synthesize the pentadecynyl iodide. 250 mL dried petroleum ether and 35 mmoles of pentadecyne with stirring is placed in an ice bath. Add 22 mL n-butyllithium slowly, dropwise. A gel will form, so add petroleum ether if necessary. Add about 10 mg triphenylmethane as a base indicator. The mixture is now white and thick, so the precipitant may need to be broken up with a stirring bar. Let the mixture stir for 1 hour to assure complete deprotonation. The solution turns a light peach color. Add  $I_2$  in 10% excess (9.8 g) as a solid. Allow 30--40 minutes of stirring to encourage a complete reaction. Transfer the mixture to an Erlenmyer flask with 100 mL of  $H_2O$  and then into a separatory funnel. Remove the  $H_2O$  and wash consecutively with 50 mL of a concentrated solution of  $NaHSO_3$  (twice),  $H_2O$ , and brine. Dry the solution with  $Na_2SO_4$  to remove any remaining  $H_2O$ . The solution is a clear, yellow liquid. Evaporate the solvent off and the pentadecynyl iodide remains as an amber liquid. Place this product in a flask wrapped in aluminum foil and store in a freezer. Figures 5.42 and 5.43 show the  $^{13}C$  and the  $H^+$  NMR Spectra of the pentadecynyl iodide.

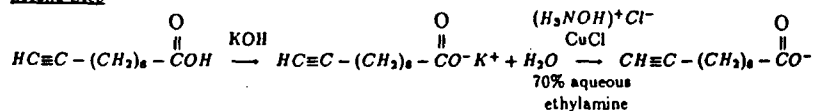
The second step of this synthesis is to make the carboxylate ion of undecynoic acid. Place 15 mmole undecynoic acid and 11.25 mL 10% KOH in a flask with stirring. Be sure the solution is basic (pH $\approx$ 10). Add

successively 75 mg hydroxylamine and a solution of 375 mg CuCl and 3 g 70% aqueous ethylamine and allow to stir for 30 minutes. This solution contains the desired carboxylate ion.

**First Step**



**Second Step**



**Third Step**

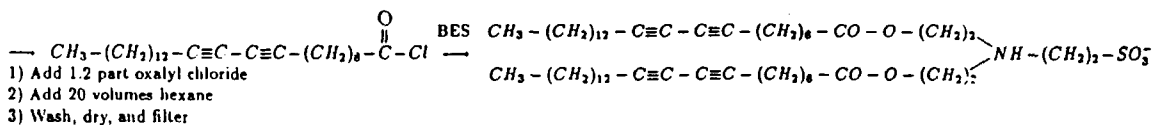
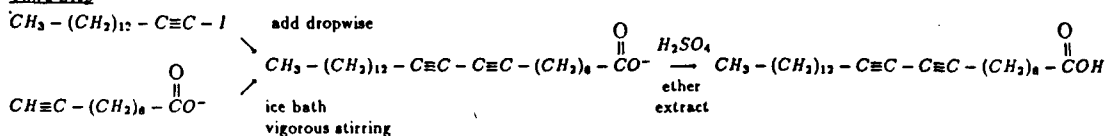


Figure 5.41. Synthesis of the polymerizable synthetic lipid.

Cool the solution containing the carboxylate ion in a water bath. Dissolve 15 mmole of the pentadecynyl iodide in 7.5 mL methanol. With vigorous stirring, add this solution to the solution containing the carboxylate

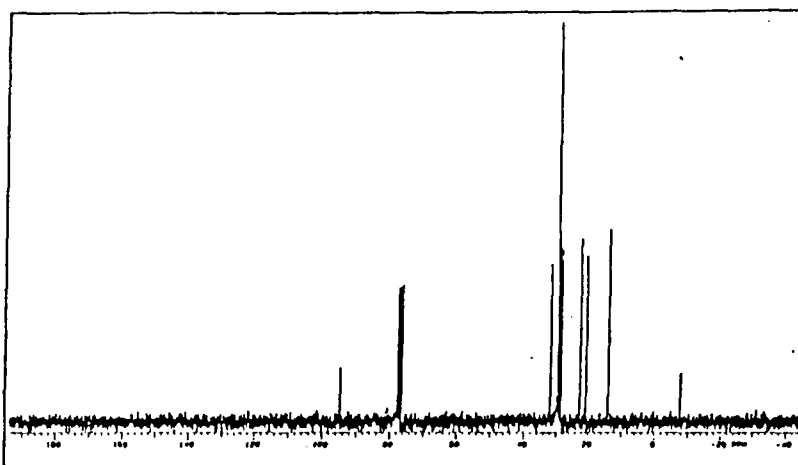


Figure 5.42. <sup>13</sup>C spectra of the pentadecynyl iodide.

ion very slowly dropwise (over a period of about 45 minutes). Allow this heterogeneous, dull yellow mixture to stir for 30 minutes. Remove the ice bath and allow the mixture to come to room temperature. Upon acidification with 2N H<sub>2</sub>SO<sub>4</sub> (about 10-15 mL) the mixture turned brown and then pink. Extract with 30

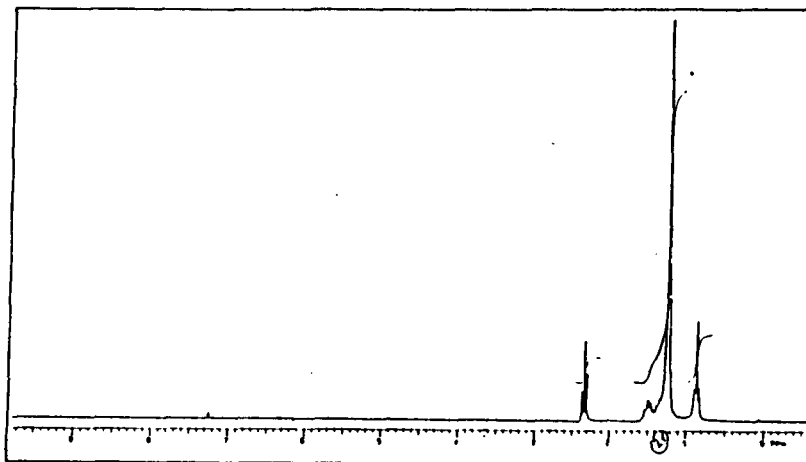


Figure 5.43.  $H^+$  spectra of the pentadecynyl iodide.

mL ether and wash the aqueous phase twice with 15-20 mL ether. Combine the organic layers and wash this solution with brine. Dry this clear yellow solution with  $Na_2SO_4$ . Filter the solution and evaporate the solvent. Figures 5.44 and 5.45 show the NMR of this acid. The melting point is 57--57.5°C (56.5°C was reported by Tieke.[59])

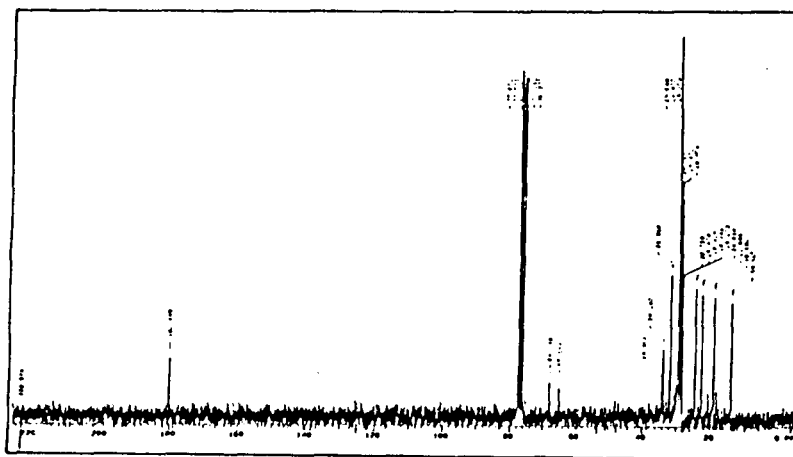


Figure 5.44.  $^{13}C$  spectra of the carboxyl acid intermediate.

Weigh the crystals (we had 1.98 g) and add about 2.38 g (1.2 times the weight of the crystals) oxalyl chloride. (Add enough oxalyl chloride to make a homogeneous mixture.) Upon addition of the oxalyl chloride HCl and CO are given off. Allow this solution to react in a flask covered with aluminum foil for 3 days with stirring.

Place in an oil bath (70--80°C) and add a water aspirator for 30 minutes. Remove from oil bath and aspirator and allow the solution to reach room temperature. Add 20 volumes of hexane and transfer the solution to a separatory funnel. Wash three times with ice cold  $H_2O$ . Emulsions will form so encourage the separation with a glass rod. Wash with a small amount of brine. If solution is not clear, wash with brine again. Dry the solution with  $Na_2SO_4$ . Allow this solution to stand for at least 15 minutes. The solution is a clear, yellow liquid. Evaporate the solvent. We have 4 mmoles of the acid chloride.

Mix the acid chloride with 0.426 g (N,N-bis[2--hydroxyethyl]-2--aminoethane-sulfonic acid (BES) and add 7 mL chloroform. The BES does not quite dissolve. Add 0.485 mL pyridine and reflux overnight. We used

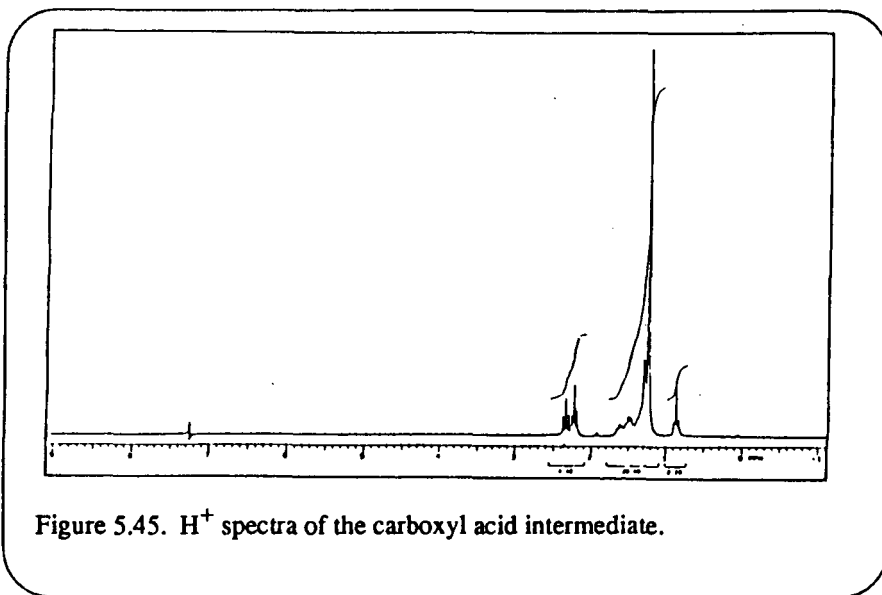


Figure 5.45.  $H^+$  spectra of the carboxylic acid intermediate.

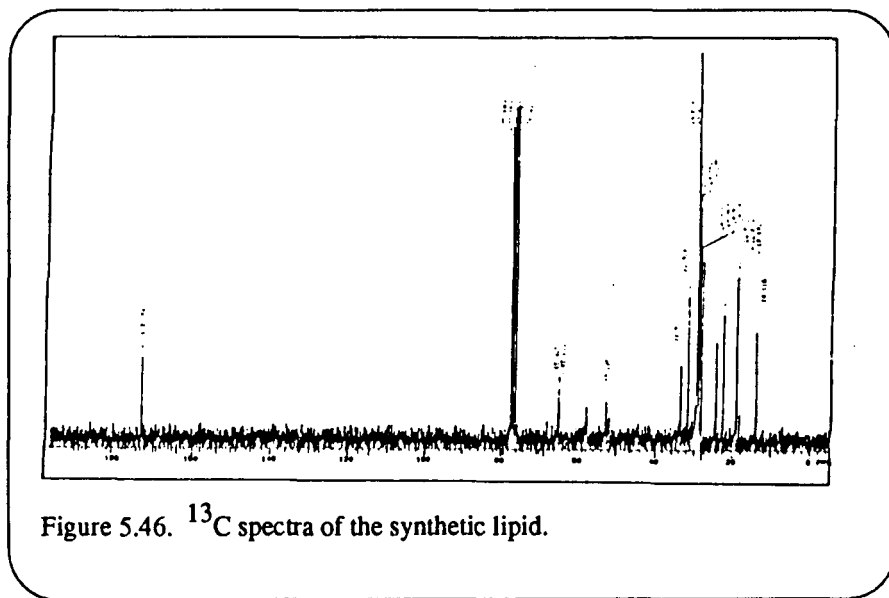


Figure 5.46.  $^{13}C$  spectra of the synthetic lipid.

an oil bath (about 60°C) and tap water for our cooling water.

Remove the oil bath and allow the solution to come to room temperature. Crystals may fall out. If crystals do not appear, evaporate part of the solvent off and place in a freezer. If crystals are reddish-brown rather than white, wash with methanol. Crystals are off white. Figures 5.46 and 5.47 show the NMR spectra of the final product.

### BLM Formation

BLM (bilayer or black lipid membrane) was successfully formed in our laboratory from lecithin. A Teflon cup with a small hole in the side was set into a glass chamber and filled with a 0.1 M sodium chloride solution. Lecithin

(phosphatidyl choline, Type XI-E, from egg yolk, chromatographically prepared) was purchased from Sigma, and the chloroform solution was evaporated by gently passing dry argon over the solution for about 30 minute. The required volume of n-decane was added to prepare a BLM-forming solution of 20 mg of lipid / 1.0 mL of decane. A 100  $\mu$ L Hamilton syringe filled with the BLM forming solution was lowered into the NaCl solution, and the syringe needle tip was positioned in front of the aperture of the Teflon cup. About 2  $\mu$ L of the lipid solution was injected. The thick lipid membrane formed in the aperture began to thin spontaneously within a couple of minutes. Interference colors appeared in reflected light as horizontal bands or swirling patterns. Finally black spots were seen in the colored membrane, either singly or several at once, and grew continuously until the whole membrane appeared black because of destructive interference. This black lipid membrane lasted

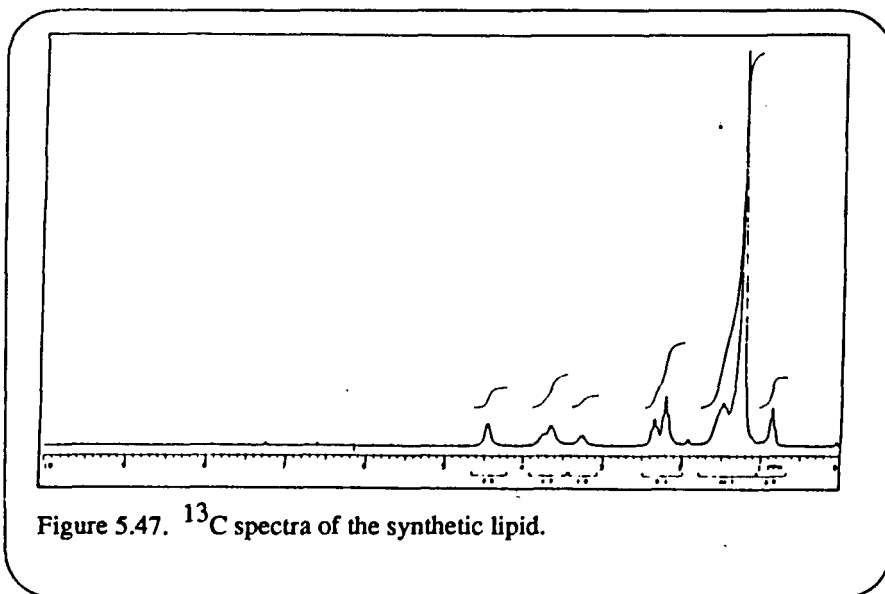


Figure 5.47.  $^{13}\text{C}$  spectra of the synthetic lipid.

for about 2 hours.

A BLM was also formed by the brush technique. A fine sable hair brush with a trimmed end was used to spread the lipid solution across the hole. The brush technique produced the colored membrane more quickly than the syringe method.

BLM formation on a polyethylene screen was easier than on the hole of a

Teflon cup. BLMs were formed just by spreading a lipid solution onto the screen immersed in 0.1 M NaCl solution by a disposable pipette. A large number of BLMs were obtained, but some were destroyed earlier than others. Statistical distribution was observed for the longevity of the BLMs. The average stability of the BLMs was dependent on the mesh size of the screen. More stable BLMs were obtained with a screen of smaller mesh size.

BLM formation with the sulfolipid was not successful as was observed by Benz *et al.*. The sulfolipid was not soluble in n-decane, which is the most widely used solvent for the BLM forming solution. Benz *et al.* succeeded in forming a BLM with some other diacetylenic compounds, but UV-initiated polymerization with them failed. Attempts to cool the BLM below the phase transition temperature of the lipids led to the rupture of the membrane. This was explained by the fact that BLM formation is possible only in the liquid analogue state. On the other hand, the polymerization of diacetylene-containing lipids is a topochemically controlled reaction and thus only takes place in the solid analogue state.

## Revised Methods of ATP Regeneration

As is evident in the foregoing description, BLMs are very unstable. Most BLMs rarely last longer than a couple of hours. In contrast, liposomes are relatively easy to prepare and can last several days. Polymerized liposomes can last a couple of months.

Liposomes are spherical or ellipsoidal, single or multicompart, closed bilayer structures composed of naturally occurring or synthetic phospholipids. Single-compartment liposomes can be formed in various ways. The most widely used method is sonication. Either a probe or a bath-type sonicator can be used. In the former, a metal probe is directly inserted into the sample. In the latter, the sample is sealed in a glass vial and suspended in an ultrasonic cleaning bath. The temperature in both types of sonication is maintained slightly above the phase

transition temperature of the lipid. Sonication below the phase transition temperature produces liposomes with structural defects.

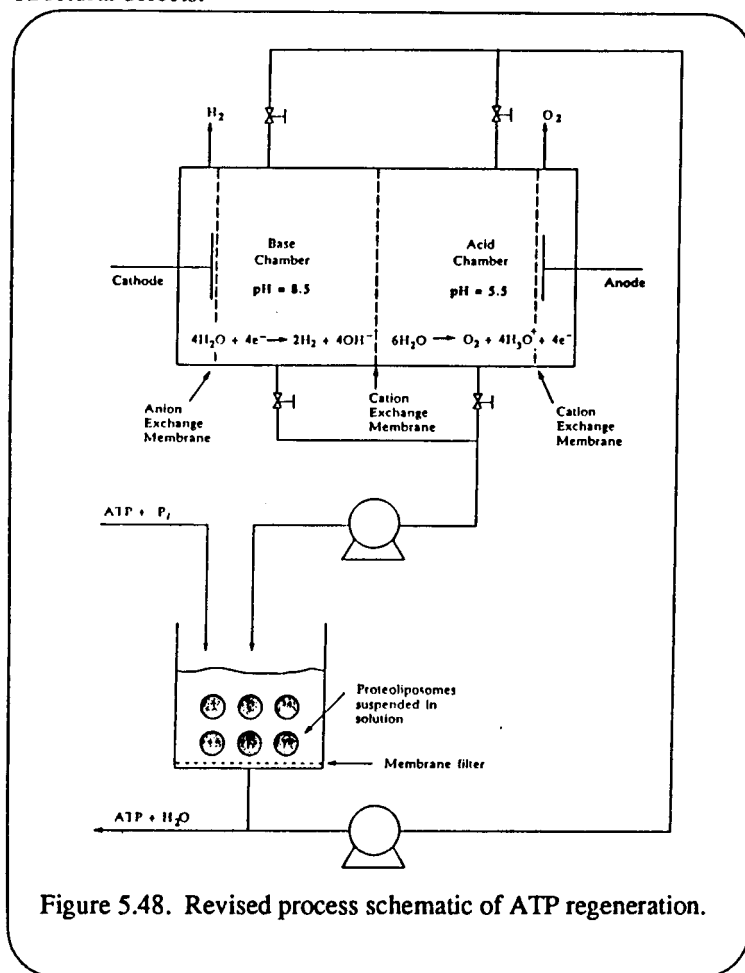


Figure 5.48. Revised process schematic of ATP regeneration.

Another advantage of using liposomes to incorporate ATPase over BLMs is the large surface area and the resulting high reaction rate. Figure 5.48 shows a schematic of the process that will be used in this project. Liposomes with incorporated ATPases may be incubated in an acidic medium (pH 5.5) to equilibrate the pH inside the liposomes to that of the medium. Most bilayer membranes are permeable to proton ions. Then, some of the acidic media is pumped back through a membrane filter to the acid chamber of the electrochemical cell. The membrane filter is used to retain the proteoliposomes (liposomes with incorporated ATPases) in the reactor. Basic medium is pumped into the reactor from the base chamber to a final pH of about 8.5. ATP is synthesized outside the liposomes due to the protonmotive force

composed of both  $\Delta pH$  and  $\Delta\psi$ . Some of the basic medium in the reactor is pumped back to the base chamber. The acid medium is supplied from the acid chamber to the reactor, and the process repeated.

### Extraction of proton ATPase

There are various kinds of ATPases in micro-organisms, plants and animal cells such as proton ATPase,  $Na^+, K^+$  ATPase, and  $Ca^{+2}$  ATPase. Proton ATPase can be classified into three types depending on its mechanism. One proton ATPase, which is mainly present in the plasma membranes of eucaryotic microorganisms and plants, forms a phosphorylated acyl intermediate and resembles the  $E_1E_2$  pumps in many respects. The second type is represented by the proton pump of mitochondria, chloroplast and plasma membranes of procaryotes. Its main function is to synthesize ATP by the protonmotive force generated during electron transport in oxidative phosphorylation and photophosphorylation. The third type exists in the intracellular organelles in animal and plant cells and differs from the mitochondrial proton pump in response to many inhibitors. Although ATP can be synthesized by any ATPase described above, the second type is considered to be the most efficient in synthesizing ATP.

Mitochondrial ATPase, chloroplast ATPase (C-ATPase), and *E. Coli* ATPase are composed of  $F_0$  (hydrophobic part) and  $F_1$  (catalytic part).  $F_0$  consists of three subunits and is embedded in the membrane by its hydrophobic property and contains the channel for proton translocation.  $F_1$  consists of five subunits, and catalyzes the ATP synthesis and hydrolysis. Mitochondrial ATPase requires two more coupling factors (OSCP and  $F_6$ ) for its synthetic activity. All of these ATPase preparations are unstable. However, Sone *et al.*[60] extracted a very stable and highly active ATPase ( $TF_0F_1$ ) from a thermophilic aerobic bacterium, PS3.

In contrast to all other  $F_1$ 's which are heat-labile and dissociate in the cold,  $F_1$  from PS3 ( $TF_1$ ) is stable when exposed to heat and cold treatment. Unlike  $F_1$  and other similar ATPases, which are inactivated in the cold,  $TF_1$  is stable for several months at 2 to 4° C in 0.1 mM EDTA, 50 mM Tris-HCl, pH 8.0.

The ATPase activity of  $TF_1$  is maximal at 75° C, and it has another peak of activity at 20° C, indicating the existence of two active forms of  $TF_1$ .  $TF_1$  has a very broad pH activity range with maximal activity at pH 9.0 and 80% of the maximal activity at pH 6.5 and pH 10.0. It is also stable in buffers of pH 3.5 to pH 12.  $F_1$  is very unstable at pH 6 or 9 in the presence of dilute dissociating agents.

$TF_0$  is more stable than  $TF_1$ . The greater stability of this ATPase ( $TF_0F_1$ ) is mainly due to an increased number of salt bridges linking residues in monomeric proteins or oligomers.[61]

The maximum level of  $P_i$  esterified in the reconstituted  $TF_0F_1$  liposomes is about 100 nmol  $P_i$ /mg  $TF_0F_1$ , while less than 2.5 nmol  $P_i$ /mg of protein is synthesized by mitochondria and other systems.[61]

Since proton ATPases are not available commercially, they must be extracted. In the extraction of ATPases, it is important to recover reconstitutable enzyme preparations, not just pure enzymes. Solubilization by a detergent, such as cholate of Triton X-100 keeps the enzyme in a biologically active state (not denatured and reconstitutable). In this project,  $TF_0F_1$  will be extracted by the procedure developed by Sone.[60] This procedure consists of membrane disruption by lysozyme, extraction of ATPase by Triton X-100 and purification of ATPase by ion exchange chromatography and gel chromatography.

#### Reconstitution of ATPase

ATPases should be incorporated into liposomes to synthesize ATP. However, simply mixing ATPases ( $F_0$ ,  $F_1$  and other coupling factors) and liposomes does not produce proteoliposomes that can synthesize ATP. A special process called reconstitution must be used. There are basically three different methods of reconstitution of membrane proteins: reconstitution of detergent-solubilized proteins, reconstitution by sonication, and reconstitution by incorporation. Reconstitution of detergent-solubilized proteins is further classified into two types, cholate dialysis and detergent dilution. The basic procedure of cholate dialysis method is to mix a suspension of sonicated phospholipids with isolated protein complex in the presence of appropriate concentration of cholate, followed by removal of the detergent by dialysis for 20 hours or longer. In the detergent dilution method, the detergent is not removed by dialysis but it is diluted. The sonication method includes direct sonication, freeze-thaw sonication, and freeze-thaw sonication in the presence of a detergent. In freeze-thaw sonication, liposomes are prepared by sonication and are added to the protein. The mixture is then quickly frozen by immersing the test tube in liquid nitrogen. After thawing at room temperature, the mixture is

exposed to brief periods of sonication. In reconstitution by incorporation, liposomes are exposed to dilute solutions of membrane proteins at 0° C for several hours in the presence of very small amount of detergent, or the mixture of liposomes and proteins are frozen and thawed. Enzyme activities of reconstituted systems are highly dependent on the reconstitution method used. Reconstitution of membrane proteins are largely empirical.

If the above mentioned methods does not work, a new reconstitution procedure should be developed.

The composition of lipids used in the liposome formation is also very important for the successful reconstitution of ATPases. Some ATPase preparations require a specific composition of lipid to be reconstituted. ATPases are critically dependent upon their lipid environments ( lipids surrounding an enzyme) for enzyme activity. This dependence is due to the conformational change when they are activated which is only possible with a certain composition of lipids.  $TF_0F_1$  could be reconstituted only in lipid derived from the thermophilic bacterium. In this project, Sone's procedure will be followed to extract lipid from PS3 and to reconstitute  $TF_0F_1$ . The cholate-dialysis method was used by Sone to reconstitute  $TF_0F_1$ .

The possibility of exchanging the PS3 derived lipid for sulfolipid will also be checked, since polymerization of the sulfolipid can increase the life of liposomes several times. Since the ATPases are active only in fluidic lipid environment (when the lipid is below the transition temperature), the amount of lipid exchangeable with sulfolipid will be limited. The transition temperature of the sulfolipid is 55° C, and the polymerized sulfolipid is rigid.

#### Thick planar membrane method

Drachev *et al.*[62] developed the so-called planar membrane system to overcome the stability problem of BLM's, and showed that bacteriorhodopsin and mitochondrial proton ATPase could be successfully reconstituted on that membrane. Soybean phospholipid solution (70 mg lipid / mL  $CH_3Cl$ ) was applied to a 1 mm aperture in a Teflon cup to form a thick planar membrane. Proteoliposomes formed by the cholate dialysis technique were added to one side of the membrane. In 15 - 30 minutes, the proteoliposomes were associated with the planar membrane.

Blok *et al.*[63] replaced the planar membrane by a lipid-impregnate Millipore filter and incorporated bacteriorhodopsin. Proton translocation by the photoeffect was observed during several days without changing the filter. Blok's method will be used to incorporate  $TF_0F_1$  in a planar lipid membrane supported on a Millipore filter. Phospholipid extracted from thermophilic bacterium PS3, diacetylenic sulfolipid synthesized, and mixture of them will be tried to form a planar lipid membrane.

#### The Reactor

Figure 5.49 shows the reactor assembly. The electrodes are placed in machined Plexiglas blocks. U-shaped Teflon spacers are inserted between the membrane and the Plexiglas. A rubber pad is placed behind the Plexiglas blocks to put some resilience in the stack. The resilience is necessary since Teflon cold-flows and will cause leaks. The entire assembly is held together by a vice to allow for easy assembly and disassembly.

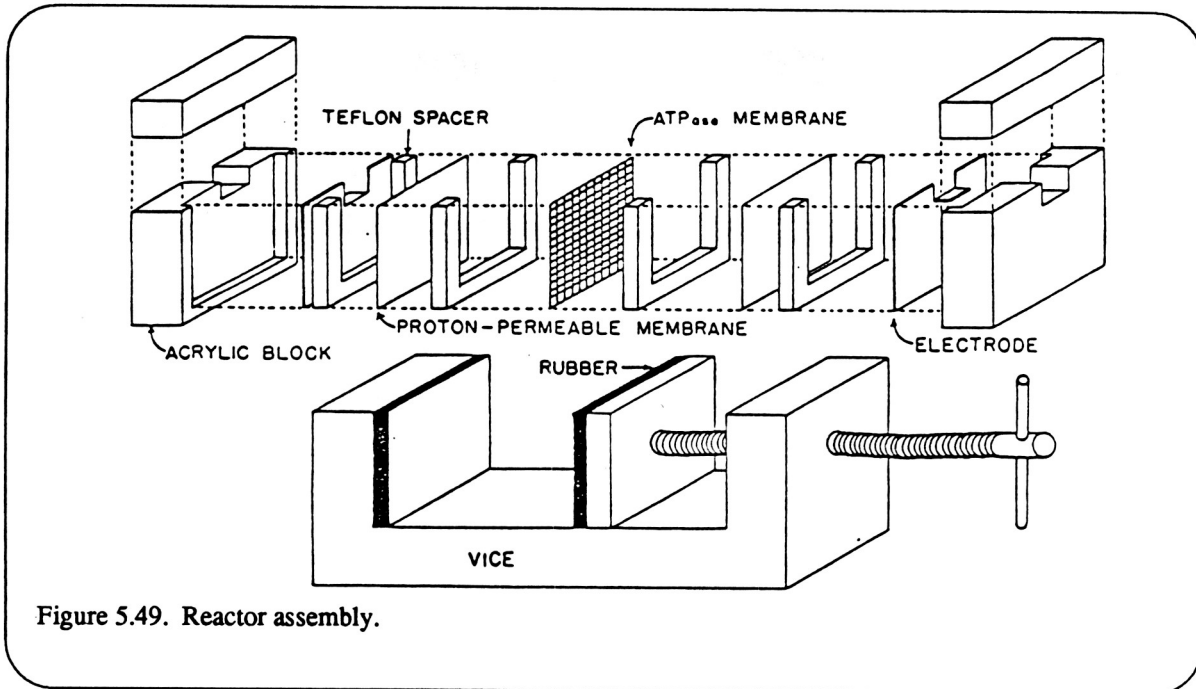


Figure 5.49. Reactor assembly.

### pH Gradient Apparatus

The reactor shown in Figure 5.49 will have platinum electrodes. Current will be supplied by a commercial power supply which regulates the voltage to about 2 V.

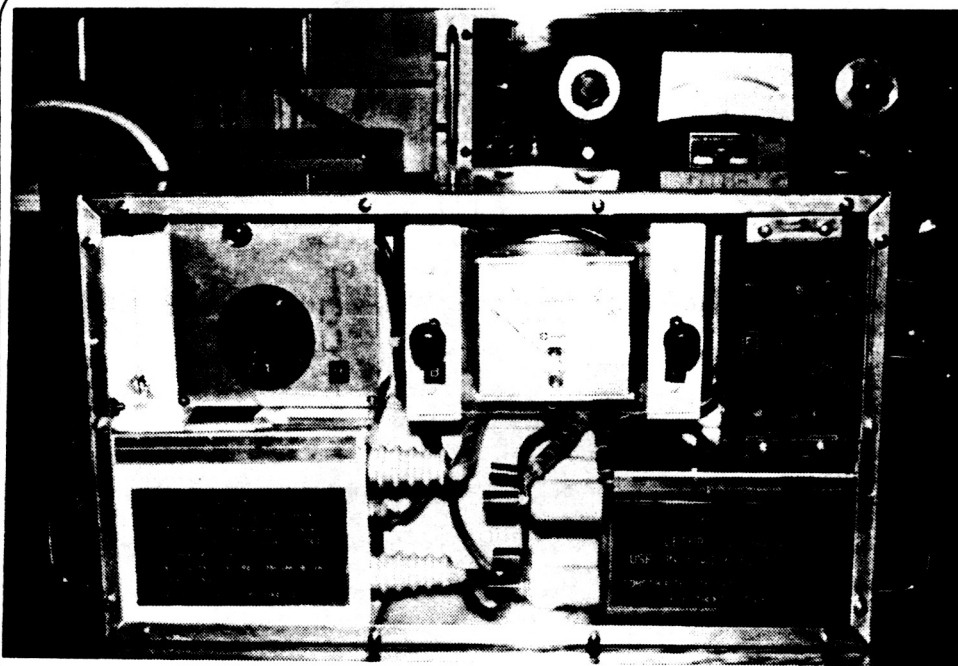


Figure 5.50. High voltage generator.

### Voltage Gradient Apparatus

The reactor shown in Figure 5.49 will have graphite electrodes. The voltage generator shown in Figure 5.50 has been custom made in the Texas A&M University Instrument Shop and is capable of supplying up to 20 kV pulses.

## Operating Procedure

Buffered hexokinase, phosphate, and ADP will be placed in the reaction chambers formed by the U-shaped cups of the Teflon spacers.

In the case of powering the enzyme with a pH gradient, the current will be adjusted so that the pH of the enzyme solution stays within acceptable limits. The side where the acid is produced will have a dilute organic acid since the pH must be low to promote proton formation at the electrode surface. The types of studies which will be conducted are the stability of the ATPase, temperature studies, and the productivity as a function of input energy.

In the case of powering the enzyme with a voltage gradient, the voltage and pulse time will be adjusted to determine the optimum productivity of the ATPase.

## Experimental Results for the Revised Methods of ATP Regeneration

### Liposomal Method

#### Formation of liposomes

Liposomes were formed from lecithin (phosphatidylcholine Type II-S from Sigma) and the sulfolipid. The sulfolipid liposomes were formed according to the procedures described by Ringsdorf.[51] Sixty mg of sulfolipid was added to 60 mL of deionized water at 60° C and sonicated under argon with a Model 300 Probe-Type Sonicator from Fisher with a large tip. A water bath was used to keep the temperature of the aqueous suspension at 60± 1° C during sonication. After sonication, the liposome solution was allowed to come to room temperature, and NaOH was added to reach a pH of about 10. The liposome solution was transferred to a 100 mL quartz round bottom flask and irradiated with UV light (General Electric RSK6 sunlamp, 275 watt) for 10 minutes. On UV irradiation, the solution changed color from colorless to red, which indicated the liposomes were polymerized. The polymerization was carried out under argon since UV light produces ozone from the oxygen in the air. The ozone would interact with the triple bonds of the sulfolipid and prevent polymerization. A water filter ( a petri dish filled with water) was placed between the UV lamp and the quartz flask to absorb infrared light. This procedure was repeated varying the power of sonication, (30%, 50% and 60%) of total power, and the time of sonication (10, 20 and 30 minutes).

Figure 5.51 shows the electronmicrograph of the sulfolipid liposomes. Negative staining with 2% phosphotungstate was used. The samples for electronmicroscopy were prepared as follows. Copper grids (400 mesh) covered with Formvar membrane then coated with carbon were floated on the surface of a droplet containing an equal volume of the liposome solution and 2% phosphotungstate, drained of excess fluid with a piece of filter paper, and dried in air.

The size distribution of the sulfoliposomes was analyzed on a Coulter Multisizer. The sample size was 0.5 mL (1 mg/mL), and the sample was diluted by 50,000 times with Isotonic II (Coulter) to a final concentration of  $2 \times 10^{-5}$  mg/mL.

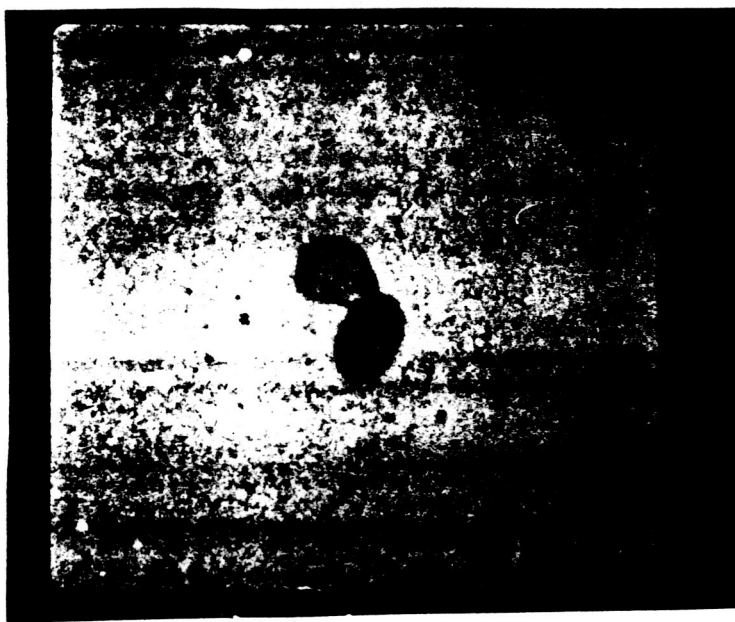
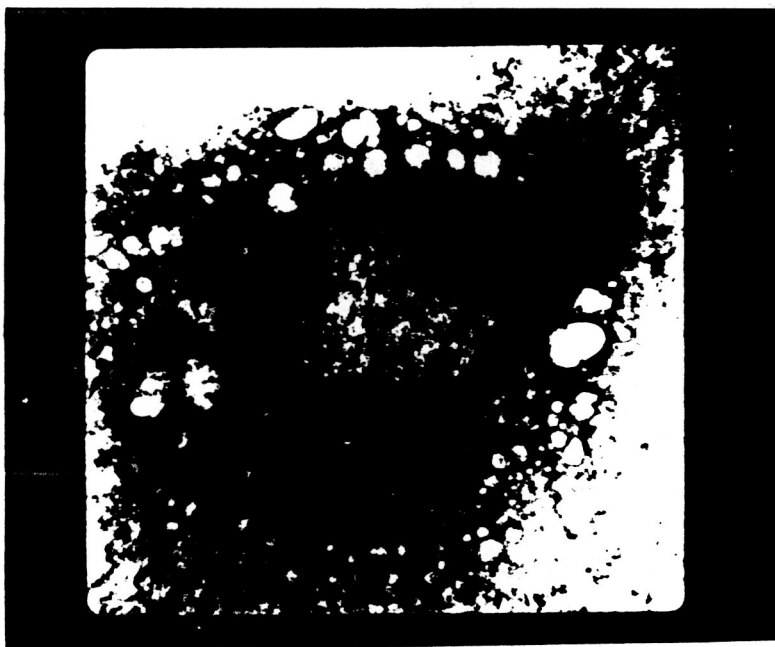


Figure 5.51. Electronmicrograph of the sulfolipid liposomes, magnification 125,000 X.

The results of the particle size distribution are shown in Figure 5.52 and Table 5.16. Liposomes provide much more surface area in a given volume than a planar membrane. For example, the screen mesh for the reactor of Figure 5.49 gives a surface area of  $2 \text{ cm}^2/\text{mL}$ , while a dilute concentration of liposomes of  $1 \text{ mg/mL}$  provides a surface area of about  $25 \text{ cm}^2/\text{mL}$ . Also, a greater concentration of synthetic lipid would increase the surface area proportionally. Knox and Tsong [49] used a phospholipid concentration of  $80 \text{ mg/mL}$  in their reconstitution experiments. If our sulfolipids were used at a concentration of  $80 \text{ mg/mL}$ , this would increase the surface area to  $2000 \text{ cm}^2/\text{mL}$ , 1000-fold increase compared to the BLM approach. This larger surface area allows more enzymes per volume and, therefore, more ATP synthesis in a given volume.

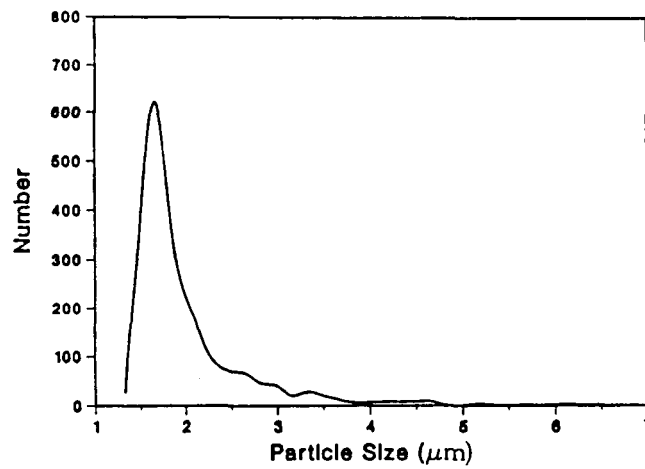


Figure 5.52. Particle size distribution for sonication at 30% power for 10 minutes.

Table 5.16. Total surface area ( $\text{cm}^2/\text{mg}$ ) varying the time of sonication and power level.

Time of Sonication (min.)	% Power		
	30	40	50
10	32.5	18.9	23.9
20	34.9	21.6	23.0
30	20.6	22.3	24.9

## 5.6 Lunar Soil Simulants

Long term space exploration and space utilization may ultimately result in the establishment of a lunar base in support of near-earth space activities or longer range projects to the planets. The moon has an inhospitable environment in terms of life support, but does have a natural regolith which may be used as a local plant growth medium to partially support a food base for lunar habitation. Due to the nature of the environment and the chemical, physical and mineralogical makeup of the lunar regolith, several important questions as to the suitability of lunar regolith as a plant growth medium must be addressed.

Currently, lunar materials are unavailable for research to determine weathering reactions, dissolution kinetics, mineral equilibrium, nutrient release, and potential for accumulation of toxic elements. Chemical reactions of lunar minerals and the fate of weathering products upon exposure to water and oxygen need to be evaluated.

An initial step in evaluating lunar materials is to evaluate terrestrial analogs. Although they would not mimic lunar materials, terrestrial materials would provide an initial starting point to develop procedures and methodologies to produce lunar simulants and finally, experiment with actual lunar materials. This report is a

summary of our efforts to characterize and evaluate several terrestrial samples as possible lunar simulants.

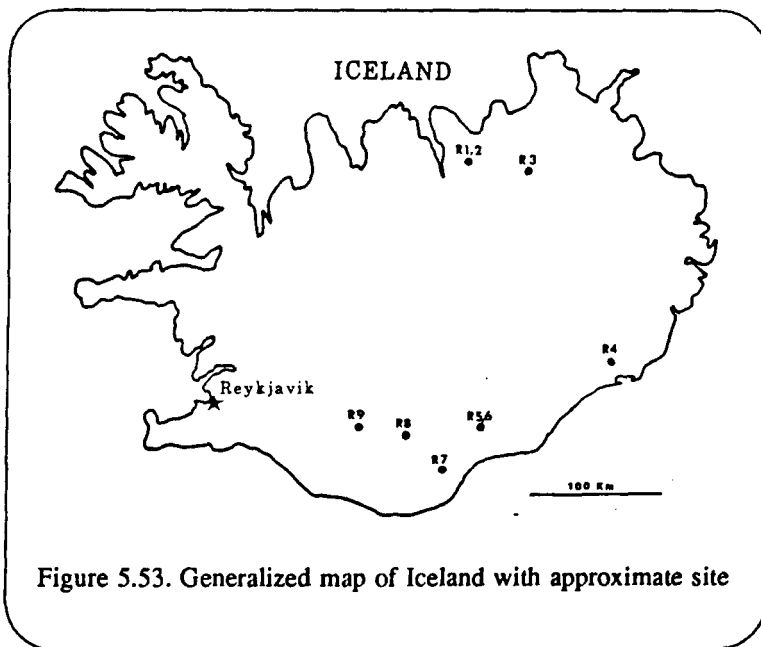


Figure 5.53. Generalized map of Iceland with approximate site

### Methods and Materials

During the summer of 1987, rock samples were collected by Dr. L.P. Wilding from nine potential locations in various portions of Iceland (Figure 5.53) These samples represent a variety of basalts, lavas, maficrich obsidians and plagonites of varying texture, mineralogy and composition. Several site locations have been documented in the literature,[64; 65] and appear to have

chemical and mineralogical composition similarities to lunar materials. Rock thin-sections were prepared for each sample to document the spatial *in situ* distribution and size of minerals within each sample. About 10 of each sample were ground in a disc mill grinder to yield a uniform mix and uniform small particle size. A powder mount of a portion of the crushed sample was prepared for X-ray diffraction analysis using a Philips XRG 3000 unit with Cu radiation and crystal monochrometer. For compositional analysis, a representative sample was sent

to Dr. Doug Ming (NASA, Johnson Space Center) for analysis. These samples were crushed, then heated to above their liquidus temperature to produce a homogeneous glass suitable for bulk chemical analysis. six to ten microprobe analyses were performed on each sample yielding an average elemental composition.

## Results

Although the samples come from a diverse group of rocks (Table 5.17), they fall into two main mineralogical groups. Samples R5 and R6 are composed primarily of a zeolite mineral, chabazite ( $\text{Ca}_2\text{Al}_4\text{Si}_8\text{O}_{24} \cdot 12\text{H}_2\text{O}$ ).

Table 5.17. Description of Samples Collected for Lunar Simulants (see Fig. 5.53 for approximate site location).

<u>SAMPLE #</u>	<u>DESCRIPTION</u>
R-1	Basalt-rich glacial till from C2 Horizon (35-60 cm). The fines were from basaltic material, little oxidized since deposition. Particle size distribution appears to approximate lunar materials.
R-2	Basalt rocks collected from C2 horizon (35-60 cm) at same site as R-1. Geological date from this area indicates basalts that are in the tholeiitic series: a relatively high content of Fe and Ti, and a low content of Al and Ca. This composition approximates lunar materials.
R-3	Mafic-rich lava with Ca-rich plagioclase phenocrysts. Site is about 10 km east of Reykjahlid. Lava field is about 3000-5000 years old. Same geologic area as R-1 and R-2.
R-4	Glacial gravel below Hoffellsjokull glacier. Samples are black, dense mafic-rich basalts with small feldspathic phenocrysts.
R-5	Base-rich and dense palagonite from landslip about 10-15 km NE Kirkjubaejarklaustur. The area from which samples of R-5 through R-9 were collected is represented by transitional alkali basalts. These rocks are characterized by a high content of Fe and Ti, and low Al. Many of the lava flows are olivine-rich tholeiites.
R-6	Less base-rich bedded rhyolite rock which has been cemented and fused into palagonite. Collected at same site as R-5.
R-7	Sample collected from an 1873 lava plain-moss covered landscape about 8 km W of Skafra bridge. Sample highly variable in composition, sharp and vesicular.
R-8	Very vesicular sample collected from 1000 year old lava field near Eldgia. Sample collected about 5 cm below zone of moss and lichen weathering.
R-9	Obsidian-like sample from columnar stack near hot goethermal spring at Landmannalaugar. Area has abundant rhyolite and other geothermally altered green rocks.

Anorthite (Ca-rich feldspar) is also present. In the other samples (R1-R4, R7-R9), the primary crystalline component is a low-Na anorthite  $[(Ca,Na)(Si,Al)_4O_8]$  with smaller amounts of pyroxene (orthoferrosilite,  $FeSiO_3$ ). In these latter samples, these two named minerals account for most of the observed diffraction peaks. In all samples, diffraction peaks were of low intensity, suggesting a portion of each sample is amorphous. This observation was confirmed by petrographic analysis.

These samples are rich in minerals anorthite (plagioclase feldspar) and pyroxenes, which are also common to lunar samples.[66] The lunar samples lack quartz, carbonates and clay minerals (phyllosilicates)[66] which is also common to these samples. Samples R5 and R6 did contain zeolites, a hydrated mineral which would not be expected to occur in lunar materials.

The bulk chemical analysis (Table 5.18) did not show the differences observed by mineralogical analysis. Sample R9 varied most from the others in terms of elemental composition. Based on the overall elemental composition these samples have similarities to lunar materials. According to a composition of lunar samples given by Mason, (1971) the samples analyzed here are about equivalent in  $SiO_2$  and  $CaO$ . However, they are slightly higher in  $Al_2O_3$ ,  $Na_2O$  and  $K_2O$ , including  $TiO$ ,  $CrO$ ,  $FeO$  and  $MgO$ . This observation, however, is not uncommon for terrestrial basalts, whose compositional characteristics are not always comparable with lunar materials.

Table 5.18. Elemental composition of rock samples by microprobe analysis. 1m.

ELEMENT	R2	R3	R4	R5	R6	R7	R8	R9
	% Elemental form							
$SiO_2$	40.83	42.59	49.32	40.86	49.39	45.66	45.64	59
.12								
$TiO_2$	1.30	1.53	2.24	2.72	2.24	2.47	2.48	0
.32								
$Al_2O_3$	28.57	24.43	16.63	29.90	17.21	23.80	20.28	26
.87								
$FeO$	9.29	10.29	12.61	11.10	11.81	10.88	12.54	3
.20								
$MnO$	0.15	0.18	0.20	0.13	0.21	0.18	0.20	0
.06								
$MgO$	6.19	6.62	6.40	3.92	5.99	4.83	5.30	0
.84								
$CaO$	10.87	10.98	10.44	7.82	10.43	8.95	9.70	1
.80								
$K_2O$	0.16	0.14	0.39	0.44	0.49	0.44	0.39	3
.61								
$Na_2O$	1.71	1.79	1.13	2.37	1.37	2.50	2.53	4
.35								
$P_2O_5$	0.15	0.17	0.23	0.32	0.24	0.28	0.30	0
.04								
$Cr_2O_3$	0.02	0.05	0.03	0.03	0.02	0.03	0.02	0
.01								
SUM	99.2	99.89	99.60	99.59	99.38	99.98	99.39	100
.23								

Micromorphological analysis shows that most of the samples are composed of fine-grained anorthite (plagioclase) feldspars and pyroxenes, as is common to lunar materials.[66] These minerals are found in a fine groundmass that ranges from opaque to translucent (Table 5.19). These minerals likely supply much of the Ca and Fe observed in elemental analyses. However, it is not possible to partition elemental concentrations to individual minerals. The groundmass likely is an important contributor to total elemental composition. Although the thin sections showed a diversity of fabrics and opacity (Figure 5.54), these differences were not evident in the elemental analyses. Despite the differences between samples, the microfabric features and mineral distributions are similar to lunar basalts[67].

Table 5.19. Brief thin section description of each sample (See Figure 5.54).

SAMPLE	DESCRIPTION
R2	Plagioclase feldspar laths about 0.2-0.4 mm long and 0.05 mm wide. Pyroxenes generally <1 mm in size. Much of the groundmass is only slightly birefringent (Figure 5.5.4A).
R3	Similar to R2 (Figure 5.54B).
R4	Dark opaque groundmass. Twined plagioclase feldspars (<0.5 mm long) and pyroxenes dispersed throughout the matrix. A few feldspars are up to 1 mm in length.
R5 & R6	File feldspar laths in a dense gray groundmass with evidence of secondary weathering products (Figure 5.54c). These samples were identified as having zeolites present.
R7	Mostly fine (<0.1 mm) with a few large (about 1 mm) plagioclase feldspars in a dark opaque matrix. Pyroxenes are generally <0.5 mm. There are many small birefringent domains in the matrix that are too small to be identified. (Figure 5.54D).
R8	Small (0.2 mm) and large (1.1.5 mm) plagioclase feldspars and pyroxenes in a black opaque matrix. Many large vughs (Figure 5.54E).
R9	Mostly fine laths (<0.1mm) of plagioclase feldspars in a glassy groundmass. Several large feldspars (2-4 mm) also present (Figure 5.54F).

## Summary

The samples collected as a part of this project have many similarities in common with lunar materials: mineral composition, grain size and elemental composition. Although there is some variance in elemental composition with average lunar material, lunar materials have a wide compositional range. Although these Icelandic samples are not lunar equivalents, there is enough in common with some of them to initiate additional studies on mineral equilibria and kinetics. With the exception of samples R5 and R6, these samples would appear to be suitable for a first approximation at developing lunar simulants.

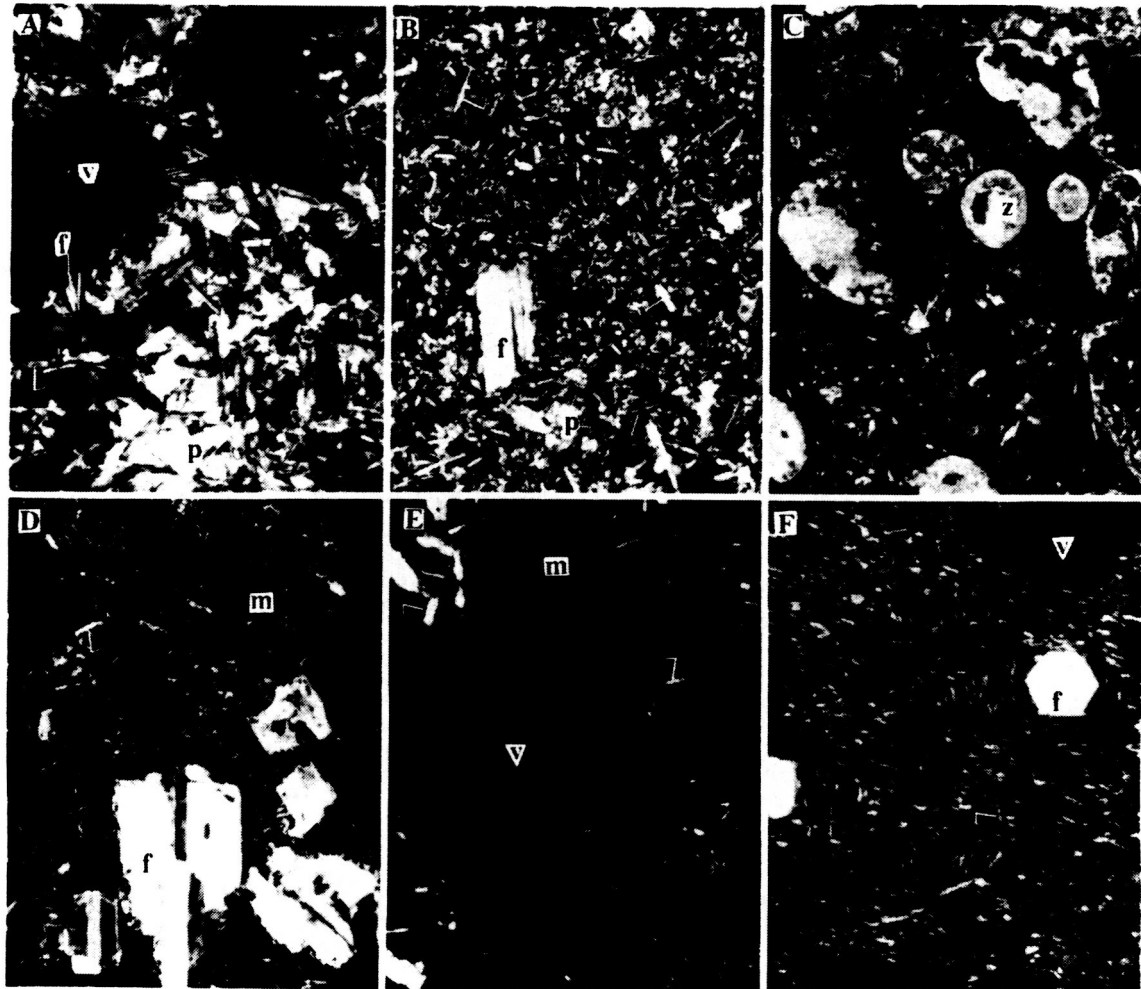


Figure 5.54. Thin section micrographs of representative rock samples. All micrographs taken under partially crossed polarized light. Bar length = 0.5 mm. A) R2, plagioclase feldspar laths (f and arrow) and pyroxene (p), v = void; B) Rd, many fine plagioclase feldspars (f and arrow and pyroxene (p) in an opaque groundmass; C) R6, altered zeolites (z) in a grey matrix, v = void; D) R7, large (f) and small plagioclase feldspars (arrow) in an opaque matrix (m), no pyroxenes in micrograph; E) R8, plagioclase feldspar (arrow) in opaque matrix (m), v = large circular void; F) R9, plagioclase feldspar (f) showing hexagonal structure, many fine feldspar laths (arrow), v = void.

ORIGINAL PAGE IS  
OF POOR QUALITY

## 5.7. Plant Growth Control Experiments

We are investigating a method to simplify the design of a CELSS. The strategy employed is to replace, as much as possible, functions in environmental control which would be done by electrical/chemical/mechanical processes with similar processes which already exist in biological components of the CELSS. One could say that we are attempting to shift the complexity of the system from the hardware to the "firmware". In this case, the firmware is higher plants. Plants will alter their biological processes in response to changes in the environment. We propose that this can be utilized to allow the plants to control certain components of the environment and that this control can be altered by appropriate changes to other environmental conditions.

Our case study involves the use of higher plants to control the concentration of  $\text{CO}_2$  in the atmosphere of the CELSS. Photosynthesis will increase and decrease with the atmospheric  $\text{CO}_2$  concentration. We are attempting to show that this response can be used as a proportional control system for  $\text{CO}_2$ . Further, this response can be modified by changes to temperature and light. We believe that this ability can be utilized to increase system reliability and to simplify the mechanical design, thereby reducing the mass of equipment needed to support plant growth. This is accomplished by allowing free interaction between the atmosphere of the crew compartment and the atmosphere of the plant growth system. The plants are allowed to react to changes in  $\text{CO}_2$  concentration caused by variation in the diet and physical activity of the crew. The trade-off of this approach with designs based upon maximizing plant productivity is a need to increase the volume of the system. The plants are not grown at their maximum rate, thus more plants are needed. We believe that more is gained from this approach than is lost.

The measurement of net carbon dioxide exchange rate (CER) by a plant in a closed plant growth chamber, that is, a plant growth chamber which is sealed air-tight and has a single inlet and a single outlet, is traditionally accomplished by measuring the difference in concentration of  $\text{CO}_2$  between the inlet and the outlet streams.[68; [69] This value is then multiplied by the flow rate to give the net carbon dioxide exchange rate of the total plant biomass in the chamber. This provides a measurement of the carbon uptake at a particular moment, provided:

1. the inlet stream  $\text{CO}_2$  concentration is held constant
2. the carbon dioxide exchange rate of the plants remains the same.

That is, the system is at steady-state.

We are interested in the response of the plants to a dynamic environment. We must, therefore, develop methods to evaluate the plants' response under unsteady-state conditions.

### Mixed Tank Reactor Model

We will begin with a very simple model of mixing called a *mixed tank reactor*. The mixed tank reactor is an engineering model with a multitude of applications. It describes a system with a closed volume which is perfectly mixed and has a single inlet and outlet.



This model assumes perfect mixing in the tank; that is, any mass entering the tank is instantly and uniformly distributed throughout the tank. Of course, this does not happen in the real world. It takes some finite amount of time for the molecules entering the tank to reach all parts of the tank volume. But, in a well-mixed tank it is a close approximation. We are interested in the amount of some component  $x$  in the tank at some given time  $t$ . The system is typically modeled with the following differential equation.

$$\frac{dx(t)}{dt} = \text{Input} - \text{Output} + \text{Production} - \text{Consumption} \quad (1)$$

That is, the change in the amount of some component in the tank with time,  $\frac{dx(t)}{dt}$ , is equal to the amount of that component in the input stream minus the amount in the output stream plus any production and minus any consumption of  $x(t)$  due to chemical reactions in the tank.

We can perform a simple analysis by beginning with the assumption that the component in question does not take part in any reaction in the tank, so the differential equation is simplified to the following form.

$$\frac{dx(t)}{dt} = \text{Input} - \text{Output} \quad (2)$$

The amount of  $x(t)$  in the input stream depends upon the input flow rate,  $F_i$ , and the concentration of  $x(t)$  in the input stream,  $C_i(t)$ . The amount of  $x(t)$  in the output stream depends upon the output flow rate,  $F_o$ , and the concentration of  $x(t)$  in the tank,  $C_t(t)$ .

$$\frac{dx(t)}{dt} = F_i C_i(t) - F_o C_t(t) \quad (3)$$

The concentration in the tank can be expressed simply as the total amount,  $x(t)$ , divided by the volume of the tank,  $V$ .

$$C_t(t) = \frac{x(t)}{V} \quad (4)$$

Furthermore, we will make the assumption that  $F_i = F_o = F$  since there is no production or consumption of  $x$  within the tank.

$$\frac{dx(t)}{dt} = FC_i(t) - \frac{F}{V}x(t) \quad (5)$$

The quantity  $F/V$  is called the mixing ratio. The reciprocal of the mixing ratio is called the residence time,  $V/F$ .

### Step Function Input

This model expresses  $x(t)$  as a continuous function and under given conditions has an analytical solution. One such condition is when we impose a step function on the input at some time  $t_0$  for example:

$$C_i(t) = \begin{cases} 0 & \text{if } t < t_0; \\ A & \text{if } t \geq t_0. \end{cases} \quad (6)$$

We are interested in the change in the amount of  $x$  in the tank after the step change in  $C_i(t)$ . The change occurs at  $t = t_0$ , therefore, let  $t_0 = 0$ . Since  $C_i(t)$  is constant after the step change, we let  $C_i(t) = A$  for  $t \geq 0$ . The initial condition of the tank,  $x(0)$ , is the amount of  $x$  in the tank at  $t = t_0 = 0$ . The solution is

$$x(t) = V A + (x(0) - V A)e^{-\frac{F}{V}t} \quad (7)$$

If we assume that initially the tank had none of component  $x$ , that is,  $x(0) = 0$ , then equation (7) becomes

$$x(t) = V A (1 - e^{-\frac{F}{V}t}). \quad (8)$$

Figure 5.55 illustrates the effect of a step change in the input to a mixed tank. The values of  $t$  on the abscissa are  $t_1 - t_0 = V/F$ ,  $t_2 - t_0 = 2V/F$  and  $t_3 - t_0 = 3V/F$ , that is, they represent the number of residence times of the mixed tank after the input step change which occurs at  $t = t_0$ . Using equation (8) the values of  $x(t)$  for the figure at the different residence times are:

$$\begin{aligned} x(t_0) &= 0, \\ x(t_1) &= 0.63 V A, \\ x(t_2) &= 0.86 V A, \text{ and} \\ x(t_3) &= .95 V A. \end{aligned}$$

The important point to stress at this time is the effect of mixing in the tank on the output response after a step change in the input condition occurs. When measuring the reaction of a CELSS to a change in conditions,

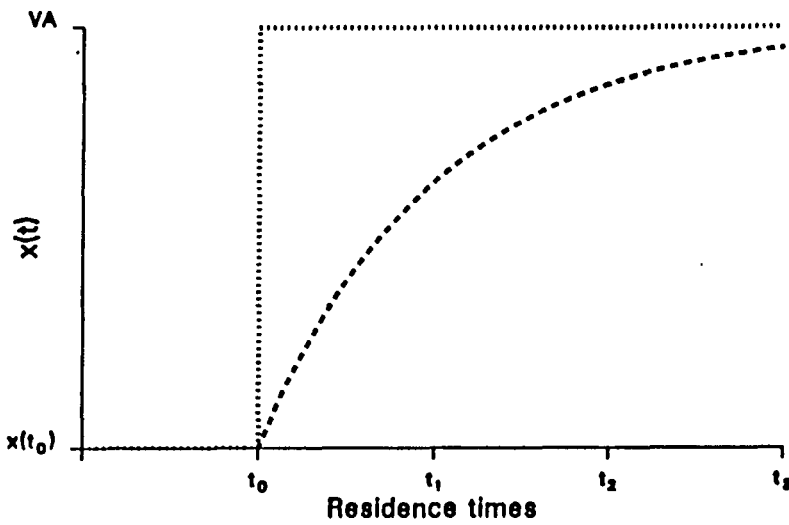


Figure 5.55. A step change in the input to the reactor results in an exponential change in the content of  $x$  in the mixed tank. The new equilibrium value for  $x$  in the tank is the dotted line, the theoretical value of  $x$  in the tank is the dashed line. The values of  $t_0$ ,  $t_1$ ,  $t_2$  and  $t_3$  are  $0$ ,  $V/F$ ,  $2V/F$  and  $3V/F$  respectively, that is,  $0$ ,  $1$ ,  $2$ , and  $3$  residence times after the step change.

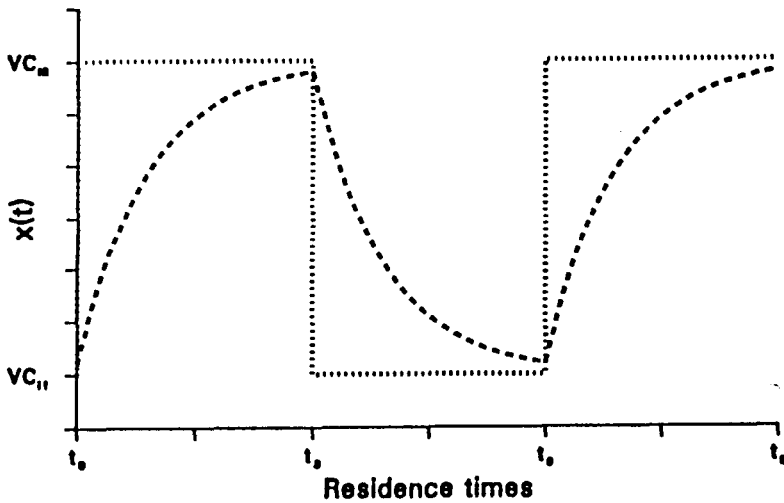


Figure 5.56. The effect on  $x(t)$  with a square wave input which changes every 3 residence times. The new equilibrium value for  $x$  in the tank for each step change in the input is the dotted line, the theoretical value of  $x$  in the tank is the dashed line. The input concentration varies between  $C_{i1}$  and  $C_{i2}$ .

one must be careful to separate out the effect of mixing in the volume and not mistake the exponential reaction of the tank itself to be the reaction of the biological components in the vessel to a change in conditions.

### Square Wave Input

We can extend the idea of the step function input to a series of step changes, that is, a square wave. The same principles apply in regard to the reaction of the tank to changes in the input. Figure 5.56 shows the effect of a square wave which changes values every 3 residence times. The input concentration varies between  $C_{i1}$  and  $C_{i2}$ . The system is allowed to reach most of the way to its new equilibrium condition before each step change occurs.

Figure 5.57 shows the reaction of the tank to a square wave input when the frequency of the waveform is increased. In this case, the changes occur every 1 residence time. The important thing to notice is that the mean of  $x(t)$  is the same

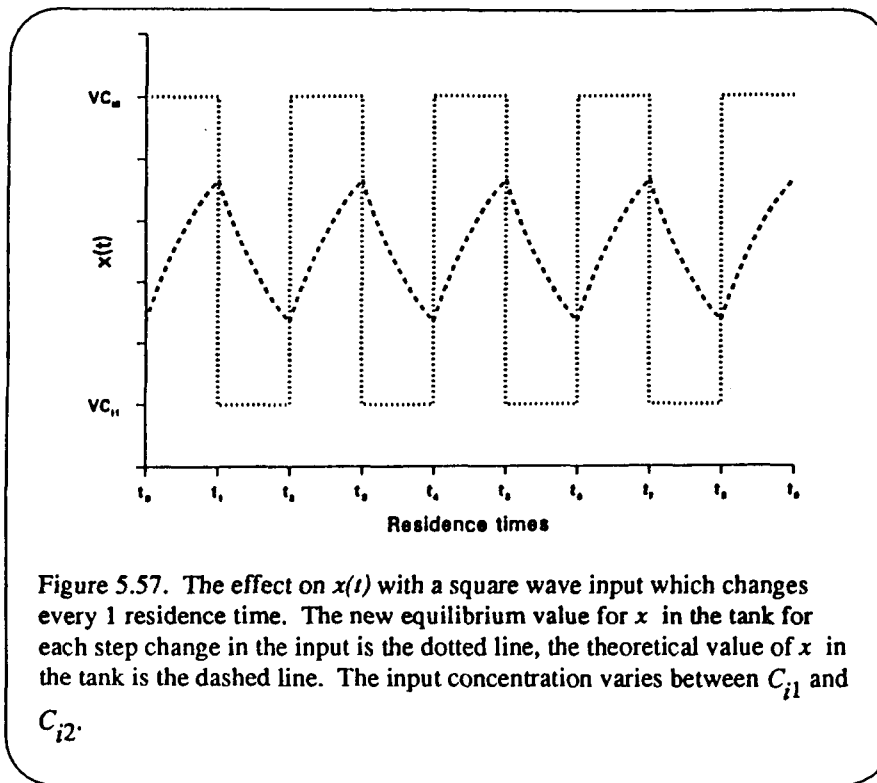


Figure 5.57. The effect on  $x(t)$  with a square wave input which changes every 1 residence time. The new equilibrium value for  $x$  in the tank for each step change in the input is the dotted line, the theoretical value of  $x$  in the tank is the dashed line. The input concentration varies between  $C_{i1}$  and  $C_{i2}$ .

as in the case shown in Figure 5.56, but the output variance is smaller. The system is not given much time to recover toward the new equilibrium position before the input is changed again. This illustrates a very important principle for unsteady-state measurements of a mixed tank reactor. The output response of a mixed tank is sensitive to the frequency of the input.

## Frequency Analysis of a Mixed Tank

The attenuation of frequencies passing through the system because of mixing is of concern when trying to measure unsteady-state conditions. Information about how the system is behaving is important to the maintenance and planning in a CELSS. Data associated with high frequency signals may be lost or so attenuated that they are difficult to observe. We can use a sine wave input to the mixed tank model to determine an upper limit on observable frequencies.

$$\text{Input} = F(A + B \sin \omega t) \quad (9)$$

$$\frac{dx}{dt} = F(A + B \sin \omega t) - \frac{F}{V}x(t) \quad (10)$$

$A$  is a constant,  $B$  is the amplitude of the sine wave and  $\omega$  is the frequency in radians per second. The solution is a combination of a constant term, an exponential term (or transient response) and a sinusoidal term (or forced response).

$$A + \left( x(0) - AV + \frac{V B \omega}{\frac{F}{V} + \omega^2 \frac{V}{F}} \right) e^{-\frac{F}{V}t} + \left( \frac{B}{\frac{F}{V} + \omega^2 \frac{V}{F}} \right) (F \sin \omega t - V \omega \cos \omega t) \quad (11)$$

If we let  $\omega = 0$ , that is there is no sinusoidal input, then we get the same result as the step function, equation (7).

$$x(t) = V A + (x(0) - AV) e^{-\frac{F}{V}t} \quad (12)$$

If we let  $t \rightarrow \infty$ , that is, we allow the transient response to be eliminated, then we get just the forced response of the system.

$$x(t) = V A + \left( \frac{B}{\frac{F}{V} + \omega^2 \frac{V}{F}} \right) (F \sin \omega t - V \omega \cos \omega t) \quad (13)$$

Equation (13) is of particular interest to us. We can use it to investigate the effects of frequency on the magnitude of the local maximum or minimum we take the derivative of equation (13) and then solve for  $t$  when

$$\frac{dx(t)}{dt} = 0.$$

$$\frac{dx(t)}{dt} = \left( \frac{B \omega}{\frac{F}{V} + \omega^2 \frac{V}{F}} \right) (F \cos \omega t + V \omega \sin \omega t) \quad (14)$$

$$0 = F \cos \omega t + V \omega \sin \omega t \quad (15)$$

$$\frac{\sin \omega t}{\cos \omega t} = -\frac{F}{V \omega} \quad (16)$$

$$t = -\left( \frac{1}{\omega} \right) \tan^{-1} \left( \frac{F}{V \omega} \right) \quad (17)$$

Figure 5.58 shows a logarithmic plot of these results. The abscissa is frequency (radians per second) and is labeled in decimal units of  $F/V$ . The ordinate,

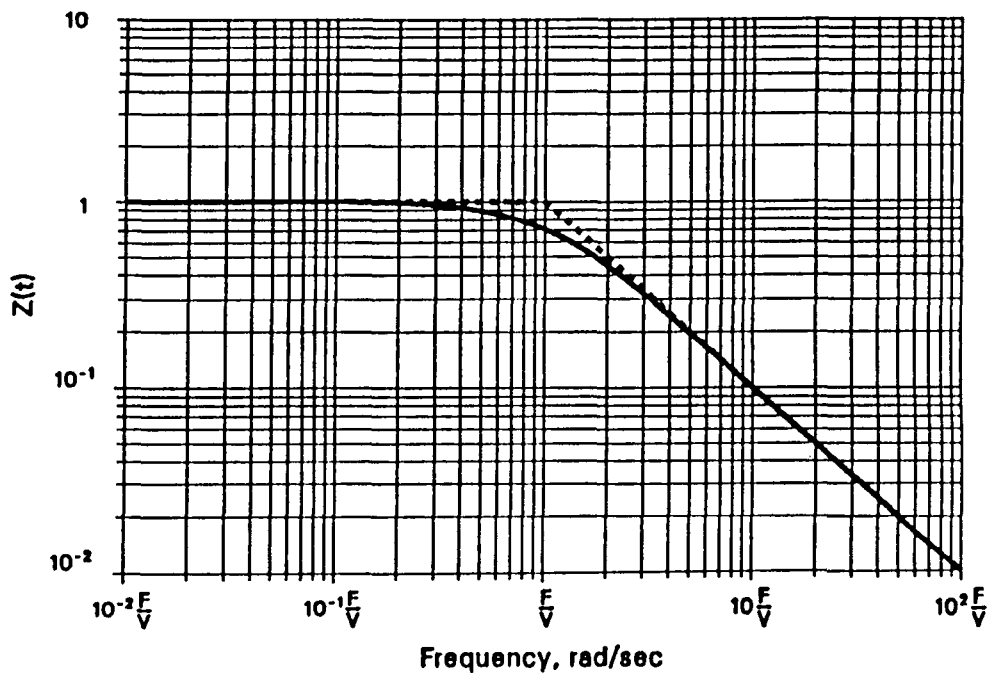


Figure 5.58. Logarithmic plot of the magnitude of the output response of a mixed tank as a function of the frequency of the input signal. The abscissa,  $\omega$ , has units of radians per second and is labeled in decimal units of  $F/V$ . The ordinate,  $Z(t) = (x(t) - AV)/BV$ , is calculated to remove the constant component of the input and is normalized to the sinusoidal component of the input. This figure is general for all mixed tanks.

$$Z(t) = \frac{x(t) - AV}{BV} \quad (18)$$

is calculated to remove the constant component of the input signal and is normalized with respect to the sinusoidal component. Figure 5.58 is general for any mixed tank. The dashed lines are imaginary extensions which converge to the *cutoff frequency* of the mixed tank,  $\omega_c$ , where,

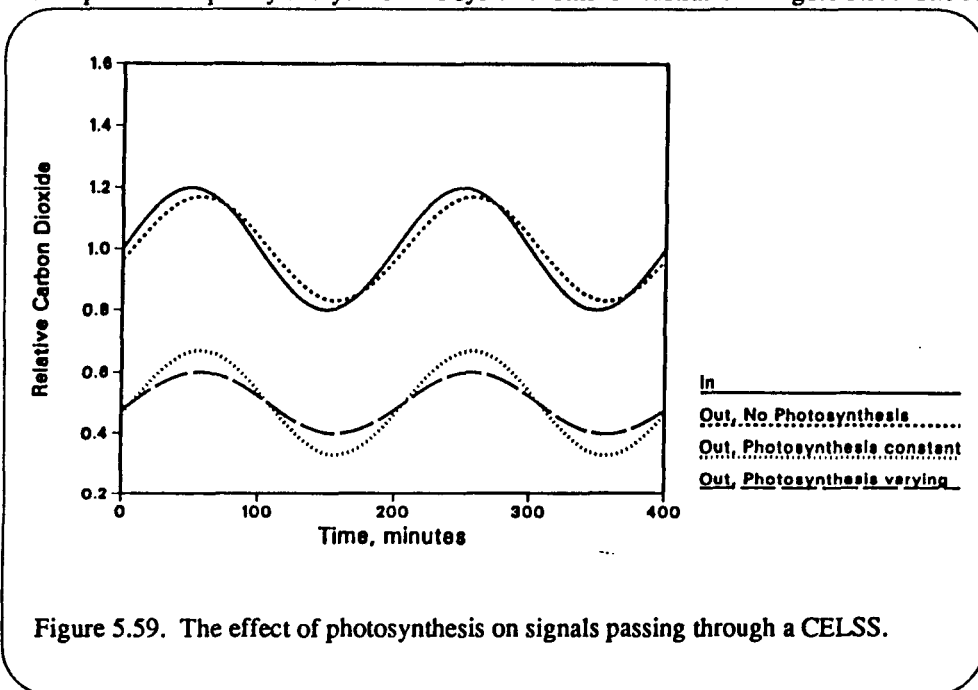
$$\omega_c = \frac{F}{V}. \quad (19)$$

Frequencies greater than  $\omega_c$  are filtered out of the system, that is, they are greatly attenuated. Frequencies less than  $\omega_c$  are passed through the system. Thus, the mixed tank reactor acts as a low pass filter with the characteristics described by Figure 5.58.

The implication for CELSS is that when trying to collect data about transient processes in the environment some information will be lost depending upon the volume of the system and the flow rate through it. If certain high frequency signals are expected to exist, it is possible to predict how attenuated they will be and, therefore, to determine how sensitive the monitoring equipment must be. Another method of measurement of a signal may be needed in order to detect it with any accuracy. The frequency response will also be important in evaluating the response of the plants to dynamic changes in  $\text{CO}_2$  concentration.

### Effect of Plants on the System

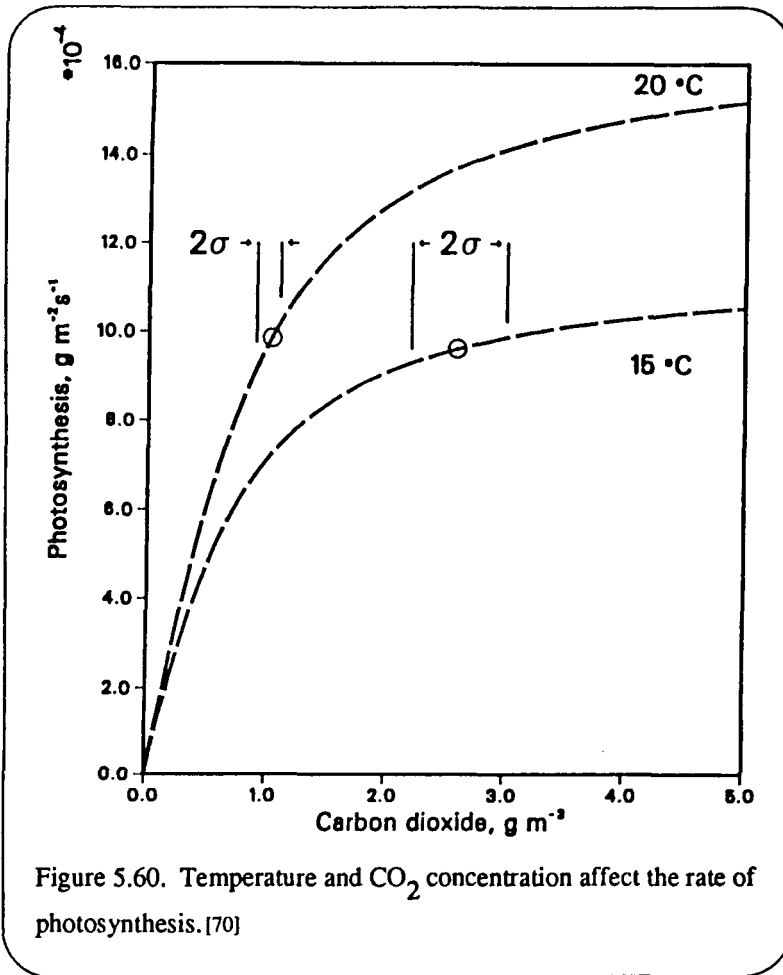
The intent of this research is to investigate the possibility of using plants as a proportional control system for  $\text{CO}_2$ . If they do exhibit some proportional control on the  $\text{CO}_2$  concentration, then we can expect this to show up in the frequency analysis of this system. This is illustrated in Figure 5.59. The solid line represents the



input of  $\text{CO}_2$  passing through the system at some frequency. If there were no plants in the system, then we can expect, as shown in the previous section, that there will be some signal attenuation and also a phase lag in the output. This is shown as the dashed line.

Suppose that plants are added to the system, but their photosynthetic rate is constant. The signal will be identical to the output with no plants except that it will be offset to a lower value of  $\text{CO}_2$  concentration. If the photosynthetic rate is proportional to  $\text{CO}_2$  concentration then there will be even more signal attenuation. This is shown by the line with the long dashes.

Photosynthesis is affected by temperature and  $\text{CO}_2$  concentration. This is illustrated in Figure 5.60. Two operating points are shown. Where the operating point is shown on the curve for  $15^\circ\text{C}$ , the curve is relatively



flat. Photosynthesis would show very little response to changes in CO<sub>2</sub> concentration. We could expect to see the standard deviation of the output signal to be large. If the operating point is located where the response to CO<sub>2</sub> concentration changes is strong, as illustrated by the point located on the curve for 20°C, then we could expect the standard deviation of the output signal to be reduced.

This points to a method to verify if plants can exhibit control of CO<sub>2</sub>. We can put a signal into a plant growth chamber and compare the measured output to a theoretical output which represents the effect of constant or no photosynthesis. Therefore, a mathematical filter is needed which can be used to produce a theoretical output from a given

input. This will allow us to account for the physical effects of the chamber and separate out the effects caused by photosynthesis.

### Output Filter Design

The input data will be collected as a discrete time series. This indicates that we need to use a discrete method for generating a theoretical output. We will use Equation (5) for the mixed tank reactor and replace the differential with a discrete approximation developed from the Taylor Series.

Given two points at  $t_1$  and  $t_2$  where  $t_2 > t_1$  then,

$$x(t_1) = x(t_2) - \frac{dx(t_2)}{dt} (t_2 - t_1) + \frac{d^2x(t_2)}{dt^2} \frac{(t_2 - t_1)^2}{2!} - \frac{d^3x(t_2)}{dt^3} \frac{(t_2 - t_1)^3}{3!} + \dots \quad (20)$$

If we let  $h = t_2 - t_1$ , the amount of time which occurs between the two points  $t_1$  and  $t_2$ , and let  $x(t_2) = x(t)$  and  $x(t_1) = x(t-1)$ , then,

$$x(t-1) = x(t) - \frac{dx(t)}{dt} h + \frac{d^2 x(t)}{dt^2} \frac{(t_2 - t_1)^2}{2!} \frac{h^2}{2!} - \frac{d^3 x(t)}{dt^3} \frac{h^3}{3!} + \dots \quad (21)$$

Finally, solving for  $dx(t)/dt$ ,

$$\frac{dx(t)}{dt} = \frac{x(t) - x(t-1)}{h} + \epsilon_r(t) \quad (22)$$

The term  $\epsilon_r(t)$  represents the error caused by the remainder of the terms in the series. Assuming this error to be small, then,

$$\frac{dx(t)}{dt} \approx \frac{x(t) - x(t-1)}{h} \quad (23)$$

Substituting Equation (23) for the differential in Equation (5),

$$\frac{x(t) - x(t-1)}{h} \approx FC_i(t) - \frac{F}{V} x(t), \quad (24)$$

$$x(t) \approx \frac{1}{1 + \frac{hF}{V}} (hFC_i(t) - x(t-1)) \quad (25)$$

This filter can be used to approximate the output of a mixed-tank reactor given discrete values for the input.

### Photosynthesis with the Step Function

The easiest signal to produce experimentally is the step function. In order to determine the effect of photosynthesis on the output, we will make the simplifying assumptions that:

1. respiration rate is independent of  $\text{CO}_2$  concentration, and
2. over a small operating range the response of photosynthesis to  $\text{CO}_2$  concentration changes is linear.

Therefore, from Equation (1),

Production = Respiration =  $R$ , and

Consumption = Photosynthesis =  $P_a = P_b x(t)$

Substitution into Equation (1) yields

$$\frac{dx(t)}{dt} = FC_i - \frac{F}{V}x(t) + R - (P_a + P_b)x(t) \quad (26)$$

and the solution is

$$x(t) = \frac{FC_i + R - P_a}{\frac{F}{V} + P_b} + \left( x(0) - \frac{FC_i + R - P_a}{\frac{F}{V} + P_b} \right) e^{-\left(\frac{F}{V} + P_b\right)t} \quad (27)$$

The slope of the photosynthetic response will change the time constant and decrease the amplitude of the equilibrium value of the output. This is the reaction we are attempting to detect in our initial experiments.

## Results of Preliminary Research

Experiments are being conducted using plant growth facilities provided by the Soil and Crop Sciences Department at Texas A&M University. A sealed plant growth chamber with a measured volume of 1.7 m<sup>3</sup> is being used to grow wheat (*Triticum aestivum* var. *Yacoro Rojo*). The chamber contains 22 pots with 3 plants in each pot. Three times a week (Monday, Wednesday and Friday) the oldest pot is removed and replaced with a newly planted pot. This provides a continuous age distribution of plants from seedlings to mature headed plants. The air for the growth chamber is obtained from outside the building. This means that the input signal is not constant. There is always a small variation due to traffic and wind. The flow rate of the air is approximately 120 liters per minute. A square wave of CO<sub>2</sub> is added to the incoming air. A large amplitude (≈100 ppm) is used to increase the signal/noise ratio. Additionally, an offset of CO<sub>2</sub> concentration can be added to increase the mean concentration to any desired level. An infrared gas analyzer is used to alternately measure the input and output air of the plant growth chamber. The temperature can be varied to study the effect of temperature change on the photosynthetic response.

Figure 5.61 shows the results when the lights are off in the chamber. The mean has been removed from each data set to allow comparison of the amplitudes and wave forms. The dotted line is the square wave input to the chamber. The dashed line shows the theoretical output using the filter described earlier. The solid line is the actual chamber output. There is little difference between the theoretical and actual output. The dashed line has been offset to left slightly to make it more visible.

Figure 5.62 shows the response when the plant growth chamber lights are on. The theoretical response is the response expected for the chamber when there is no photosynthesis. The actual response with photosynthesis shows the result predicted in the previous section. The amplitude and time constant are changed by photosynthesis.

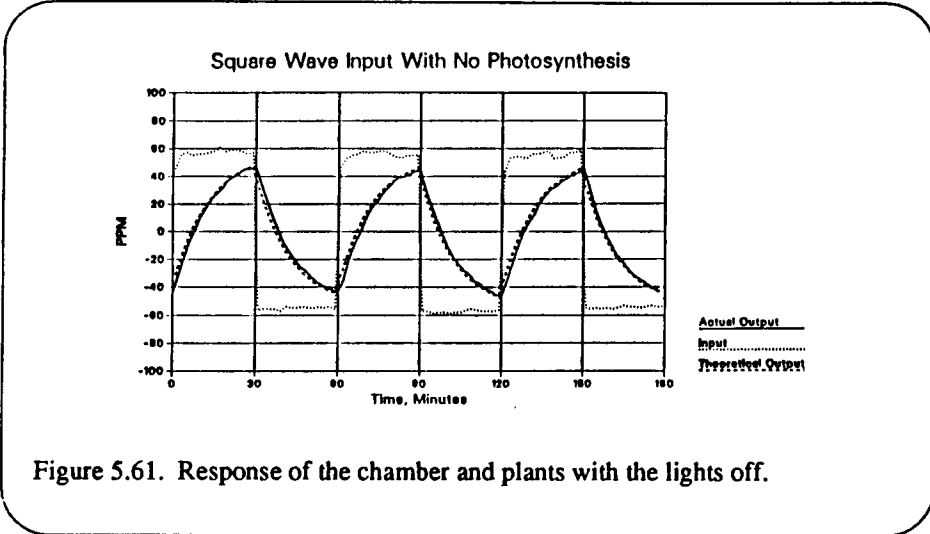


Figure 5.61. Response of the chamber and plants with the lights off.

These preliminary results indicate that plants may be used as a proportional control system. The magnitude of the response will depend upon the amount of plant material in the system, as well as environmental conditions in which the plants are grown. This research is

continuing to look at the change in response which temperature and CO<sub>2</sub> concentration produce. Further, we are developing statistical tests to measure the proportional response to be used when the input signal is white noise (random). This will reflect a situation more like the conditions which can be expected when a crew is producing the CO<sub>2</sub>.

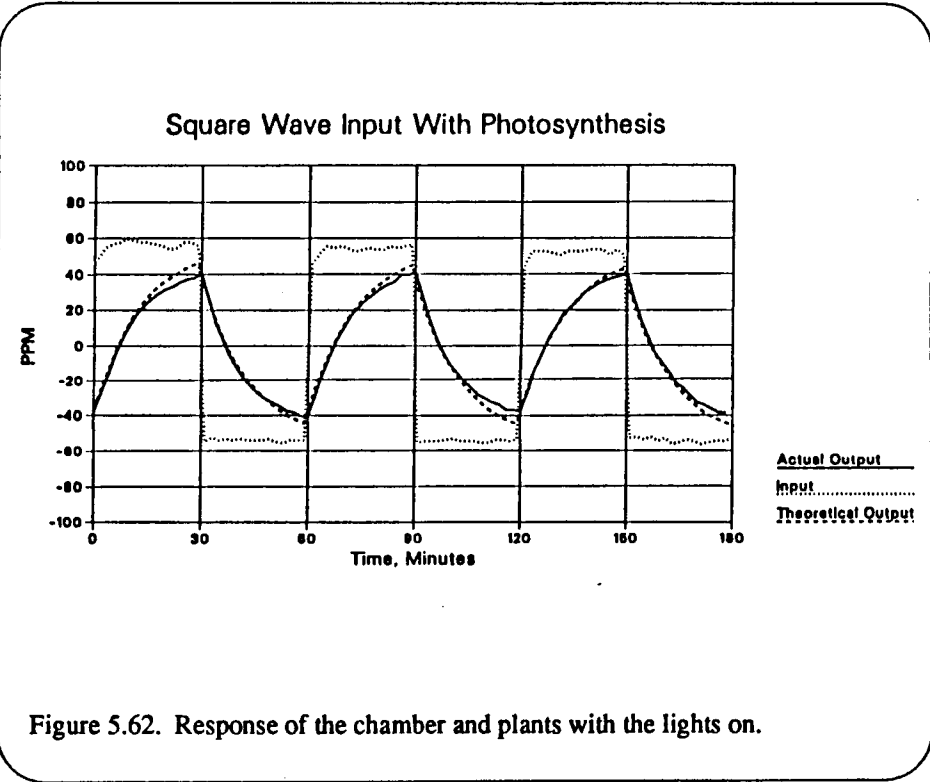


Figure 5.62. Response of the chamber and plants with the lights on.

- [1] Bockris, J.O'M., B.J. Piersma and E. Gileadi, *Electrochimica Acta* **9** (1967) 1329.
- [2] Sanderson, J.E., D.L. Wise and D.C. Augusten, *Biotechnol. Bioeng. Symp* **8** (1978) 131.
- [3] Levy, P.G., J.E. Sanderson, R.G. Kispert and D.L. Wise, *Enz. Microb. Technol.* **3** (1981) 207.
- [4] Sharifian, H. and D.W. Kirk, *J. Electrochem Soc.* **133** (1986) 921.
- [5] Tischer, R.G., B.P. Tischer, L. R. Brown, and J.C. Mickelson, *Dev. Ind. Microbiol.* **4** (1963) 253.
- [6] Tischer, R.G., B.P. Tischer and D. Cook, *Dev. Ind. Microbiol.* **3** (1962) 72.
- [7] Tischer, R.G., L. R. Brown and M.V. Kennedy, *Dev. Ind. Microbiol.* **6** (1965) 238.
- [8] Murphy, O.J., J.O'M. Bockris and D.W. Later, *Int. J. Hydrogen Energy*, **10** (1985) 453.
- [9] Okada G., V. Guruswamy and J.O.'M. Bockris, *J. Electrochem. Soc.* **128** (1981) 2097.
- [10] Coughlin, R.W. and M. Farooque, *Nature*, **279** (1979) 301.
- [11] Coughlin, R.W., M. Farooque, *J. Appl. Electrochem.* **10** (1980) 729.
- [12] Baldwin, R.P., K.F. Jones, J.T. Joseph, T.L. Wong, *Fuel* **60** (1981) 739.
- [13] Dhooge, P.M., D.E. Stilwell and S.M. Park, *J. Electrochem. Soc.* **129** (1982) 1719.
- [14] Dhooge, P.M. and S-M. Park, *J. Electrochem. Soc.* **130** (1983) 1029.
- [15] Taylor, N., C. Gibson, K.D. Bartle, D.G. Mills, and G. Richards, *Fuel* **64** (1985) 415.
- [16] Yao, S.J., S.K. Wolfenson, M.A. Krupper and K.J. Wu, in: *Charge and Field Effects in Biosystems*, edited by M.J. Allen and P.N. R. Usherwood (1984) 410, Abacus Press, Tunbridge Wells, UK.
- [17] Keller, R.W. J.M. Brown, S. K. Wolfson, K.V. Thrivinkraman and M.A. Krupper, *IEEE Frontiers in Engineering Health Care* **4** (1982) 24.
- [18] Yao, S.J., J.M. Brown, S. K. Wolfson, K.V. Thrivikraman and M.A. Krupper, *IEEE Frontiers in Engineering Health Care* **4** (1982) 24.
- [19] Wydeven, T. NASA Technical Memorandum 84368 (1983) Composition and Analysis of a Model Waste for a CELSS.
- [20] C.E. Verostko, D.F. Price, R. Garcia, D. Pierson, R.L. Sauer and R.P. Reysa, SAE Paper No. 871512, 17th Intersociety Conference on Environmental Systems, Seattle Washington, July 1987.
- [21] C.E. Verostko, R. Garcia, D.L. Pierson, R.P. Reysa, R. Irbe, SAE Paper No. 860983, 16th Intersociety Conference on Environmental Systems, San Diego, California, July 1986.
- [22] W. Larch (ed.) "Handbook of Water Purification," 2nd edition, 1987, Ellis Harwood, Chichester, U.K.
- [23] R.W. Keller, J.M. Brown, S.K. Wolfson and S.J. Yao, *IEEE Frontiers in Engineering Health Care* **2**, 1980 178.
- [24] S.H. Timberlake, G.T. Hong, M. Simson and M. Modell, SAE Paper No. 820872, 12th Intersociety Conference on Environmental Systems, San Diego, California, July, 1982.
- [25] J.D. Zeff, R. Schuman, E.F. Alhedeff, J. Wark, F.C. Farrell, D.R. Boyland and A. Forsythe, "UV Ozone Water Oxidation/Sterilization Process," AD-A038609, November 1969, U.S. Department of Commerce NTIS.
- [26] R.W. Keller, S.J. Yao, J.M. Brown, S.K. Wolfenson and M.V. Zerller, *Bioelectrochem. Bioenerg.* **7**, 1980, 469.
- [27] NASA Contract NAS 1-11662, Lockheed Missiles & Space Co., 1978.
- [28] H.P. Bennetto, *Life. Chem. Rep.* **2**, 1984, 363.
- [29] L.B. Wingard, C.H. Shaw and J.F. Castner, *Enz. Microb. Tech.* **4**, 1982, 137.

- [30] G. Del Duca and J.M. Fuscoe, *Intern. Sci. Technol.* 39, 1965, 56
- [31] G.G. Guilbault and M. Mascini (eds.) *Analytical Uses of Immobilized Biological Compounds for Detection, Medical and Industrial Uses*, 1988, Reidel Publishing Company, Boston.
- [32] P.W. Carr and L.D. Bowers, *Immobilized Enzymes in Analytical and Clinical Chemistry*, 1980, Wiley, New York.
- [33] A.L. Chaney and B.P. Marbach, *Clin. Chem.* 8, 1962, 130.
- [34] M-F. Cocquempot and D. Thomas, *Enzyme. Microb. Technol.* 6, 1984, 321.
- [35] M-F. Cocquempot, D. Thomas, M.L. Champigny and A. Moyse, *European J. Appl. Microbiol. Biotechnol.* 8, 1979, 37.
- [36] Amano and Taylor, *J. Am. Chem. Soc.* 76, 1954, 4201.
- [37] S.R. Logan and R.L. Moss, *Trans. Faraday. Soc.* 54, 1958, 922.
- [38] J.P. McGeer and H.S. Taylor, *J. Am. Chem. Soc.* 73, 1951, 2743.
- [39] Janert, H. 1922. Beitrag zur Beurteilung der klimatischen Wachstumsfaktoren Kohlensaure, Sauerstoff und Luftdruck. *Botanisches Archiv* 1:155-176, 201-210.
- [40] Andre, M. and C. Richaud. 1986. Can plants grow in quasi-vacuum? In: *Controlled Ecological Life Support Systems: CELSS '85 Workshop.* Eds. (MacElroy, Martello, and Smernoff), NASA TM 88215. pp. 395-404.
- [41] Musgrave, M.E., W.A. Gerth, W. Scheld, and B. R. Strain. 1988. Growth and mitochondrial respiration of mungbeans (*phaseolus aureus Roxb.*) germinated at low pressure. *Plant Physiology* 86:19-22.
- [42] Lehninger, A.L., *Biochemistry*. 2nd ed., New York: Worth Publishers, 1975.
- [43] Edwards, G. and D. Walker, *C<sub>3</sub>, C<sub>4</sub>: Mechanisms, and Cellular and Environmental Regulation of Photosynthesis*. Berkeley, CA: University of California Press, 1983.
- [44] Wong, C-H., *Journal of the American Chemical Society*, vol. 103, p. 6227, 1981.
- [45] Mitchell, P., *Biol. Rev.*, 41, p. 445, 1966.
- [46] Jagendorf, A.T. and E. Uribe, *Proc. Natl. Acad. Sci. USA*, 55, p. 170, 1966.
- [47] Witt, H.T., E. Schlodder, and P. Graber, *FEBS Letters*, 69 (1), p. 272, 1976.
- [48] Hamamoto, T., K. Ohno, and Y. Kagawa, *J. Biochem.*, 91 (5), p. 1759, 1982.
- [49] Knox, B.E. and T.Y. Tsong, *J. Biol. Chem.*, 259 (8), p. 4757, 1984.
- [50] Wagner, N., K. Dose, H. Koch, and H. Ringsdorf, *FEBS Letters*, 132 (2), p. 313, 1981.
- [51] Hub, H.H., B. Hupfer, H. Koch, H. Ringsdorf, *Angew. Chem. Int. Ed. Engl.*, 19 (11), p. 938, 1980.
- [52] Pabst, R., H. Ringsdorf, H. Koch, and K. Dose, *FEBS Letters*, 154 (1), p. 5, 1983.
- [53] Tien, H. Ti, *Bilayer Lipid Membranes (BLM) Theory and Practice*. New York: Marcel Dekker, Inc., 1974.
- [54] Takagi, Azuma, and Kishimoto, *Ann. Rept. Biol.*, 13, p. 107, 1965.
- [55] Montal, M., "Functional reconstitution of membrane proteins in planar lipid bilayer membranes," in *Techniques for the Analysis of Membrane Proteins*. C.I. Ragan and R.J. Cherry, eds. London: Chapman and Hall, 1986, chap 5, p. 99.
- [56] Castellan, G.W., *Physical Chemistry*. 2nd ed., Reading, MA: Addison-Wesley Publishing Company, 1971.
- [57] Bockris, J. O'M. and A.K.N. Reddy, *Modern Electrochemistry*. New York: Plenum Publishing, 1970.
- [58] Nguyen, T., Texas A&M University, private communication.
- [59] Tieke, B., G. Wegner, D. Naegle, and H. Ringsdorf, *Angew. Chem. Ent. Ed. Engl.*, 15 (12), p.

- 764, 1976.
- [60] Sone, N., M. Yoshida, H. Hirata, and Y. Kagawa, *J. Biol. Chem.*, 250, p. 7917, 1975.
- [61] Kagawa, Y., "Reconstitution of H<sup>+</sup> -ATpase," in *Membrane Bioenergetics*. C.P. Lee, G. Schatz and L. Ernster, eds. Massachusetts: Addison-Wesley, 1979, p. 177.
- [62] Drachev, L.A., A.A. Jasaitis, A.D. Kaulen, A.A. Kodrashin, E.A. Liberman, I.B. Nemeck, S.A. Ostroumov, A. Yu Semenov, and V.P. Skulachev, *Nature*, 249, p. 321, 1974.
- [63] Blok, M.C., K.J. Hellingwere and K. Vandam, *FEBS Letters*, 76, p. 45, 1977.
- [64] Jakobsson, S.P. 1972. Chemistry and distribution of recent basaltic rocks in Iceland. *Lithos* 5:365-386.
- [65] Oskarrson, N., G.E. Sigvaldasson and S. Steinthorsson. 1982. A dynamic model of rift zone pedogenesis and the regional petrology of Iceland. *J. Petrology* 23:28-74.
- [66] Williams, R.J. and J.J. Jadwick, 1980. Handbook of Lunar materials. NASA Reference Publication 1057. NASA Scientific and Technical Information Office. Washington, D.C.
- [67] Lofgren, G.E. and E.M. Lofgren. 1981. Catalog of lunar maria basalts greater than 40 grams. Part 1. Major and trace chemistry with megascopic descriptions and rock and thin section photographs. Lunar and Planetary Contribution 438. NASA, Johnson Space Center, Houston, TX.
- [68] Nobel, P.S. 1983. *Biophysical Plant Physiology and Ecology*. W.H. Freeman and Co., New York.
- [69] von Cammerer, S. and G.D. Farquhar. 1981. Some relationships between the biochemistry of photosynthesis and the gas exchange of leaves. *Planta* 153:376-387.
- [70] Campbell, G.S. 1977. *An Introduction to Environmental Biophysics*. Springer-Verlag, New York. pp. 116-119.

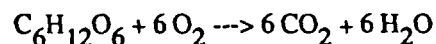
## 6. CONCEPTUAL DESIGN STUDIES

Human exploration of space requires development of numerous technologies which will permit crews to live and work in the space environment for months or even years. The development and maintenance of an enclosed ecological system (biosphere) is essential for manned space exploration. The National Commission on Space recommended that "NASA institute a major new effort to develop a space-qualified synthetic biosphere" as a key element for long-term manned activities.[1] Both the Ride Commission Report[2] and the Robbins Report[3] stressed the importance of developing and testing a fully operational bioregenerative life support system for use in space exploration within the next 20 years. The Committee on Advanced Space Technology[4] assessed the requirements for life support systems, noted the lack of technological progress in development of subsystems for processing solid wastes, and pointed out the necessity to advance this technology to further close the carbon loop. Waste processing and recycling is the next logical area requiring technology advancement to further close the materials loop in a regenerative, synthetic biosphere such as a spacecraft or spacebase.

During the past three years, an interdisciplinary team of engineers and scientists at Texas A&M University have been conducting research on various aspects of spaceflight life support systems.[5; 6] Particular interest has focused on potable water recovery, waste processing and recycling, development of computer simulation models to assess materials and process dynamics, plant growth characteristics under reduced pressure, and new approaches to food production and processing. Experience and insight into the function of component subsystems and the inter-relationship of candidate processes have led us to investigate the potential for several new processes (i.e., electrochemical waste decomposition, artificial chloroplast) as well as having the opportunity to reassess a hardware system and a process for waste recycling and potable water production developed by General Electric some 20 years ago.

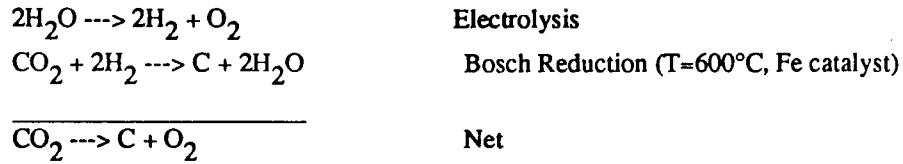
### 6.1 Air Revitalization

Astronauts convert food (such as glucose) into carbon dioxide and water

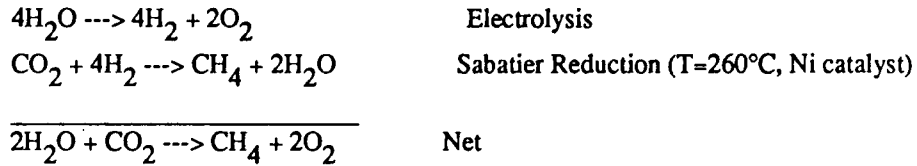


The water goes primarily into the urine (some is lost in breathing) and the carbon dioxide goes into the air. In order to revitalize the air, it is necessary to reduce the carbon dioxide and produce oxygen. The two technologies commonly considered for carbon dioxide reduction are the Bosch and Sabatier reactions. Although they are generally considered interchangeable, in fact, they are not. The Bosch reaction will always allow complete regeneration of oxygen while the Sabatier allows closure only if the food and trash are highly oxidized. This is explained further.

Both the Bosch and Sabatier systems require that water be split electrochemically to produce hydrogen and oxygen. The hydrogen is used to reduce carbon dioxide. In the Bosch reactor, the products are carbon and water.

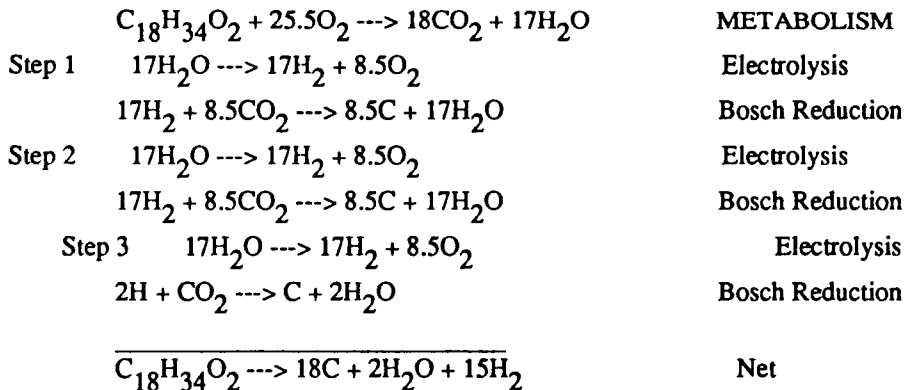


In the Sabatier reactor, the products are methane and water

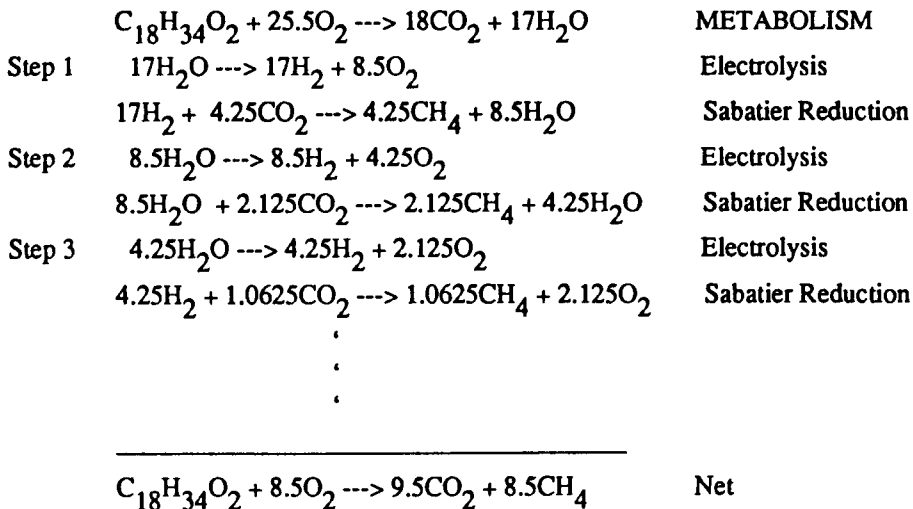


The Sabatier reactor has the advantage that the catalyst is not contaminated with the carbon deposits which occur in the Bosch reactor and a much higher single pass conversion rate. Unfortunately, the Sabatier reactor will not close the oxygen supply if there is metabolism of reduced foods or combustion of reduced trash.

To illustrate the lack of closure with the Sabatier reactor, consider a diet of pure fat (the most highly reduced food). The sequence of reaction steps for the Bosch reaction system is



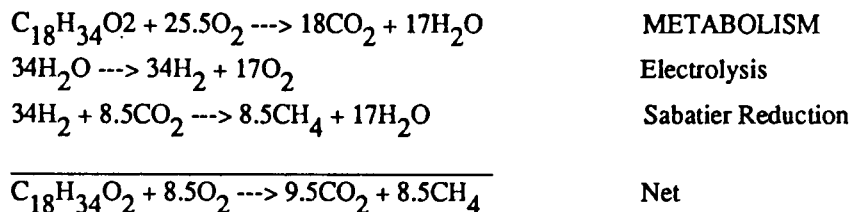
Notice that the net reaction requires no additional input of oxygen. The reaction sequence for the Sabatier reaction system is



The water coefficients (X) of the electrolysis/Sabatier reduction steps form the series

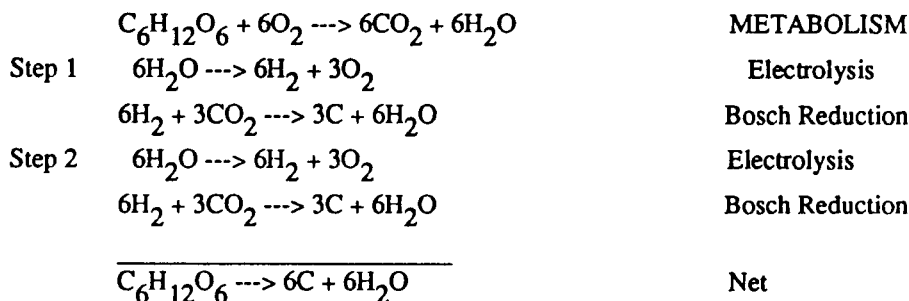
$$X + \frac{1}{2}X + \frac{1}{2} \frac{1}{2}X + \dots = \sum_{n=1}^{\infty} \frac{1}{2^{n-1}} X = 2X$$

where n is the step number. This infinite series converges to 2X so the Sabatier reaction sequence may be summarized as

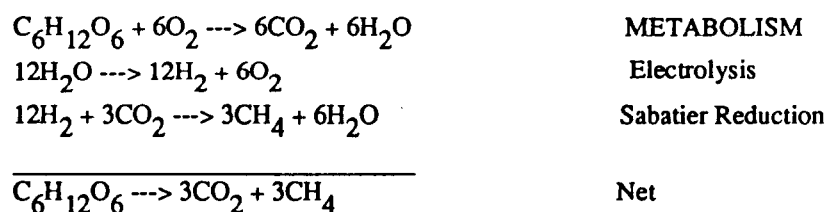


Again, notice that the net reaction requires additional oxygen output.

If the diet were solely composed of glucose, the Bosch reaction sequence is

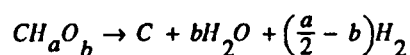


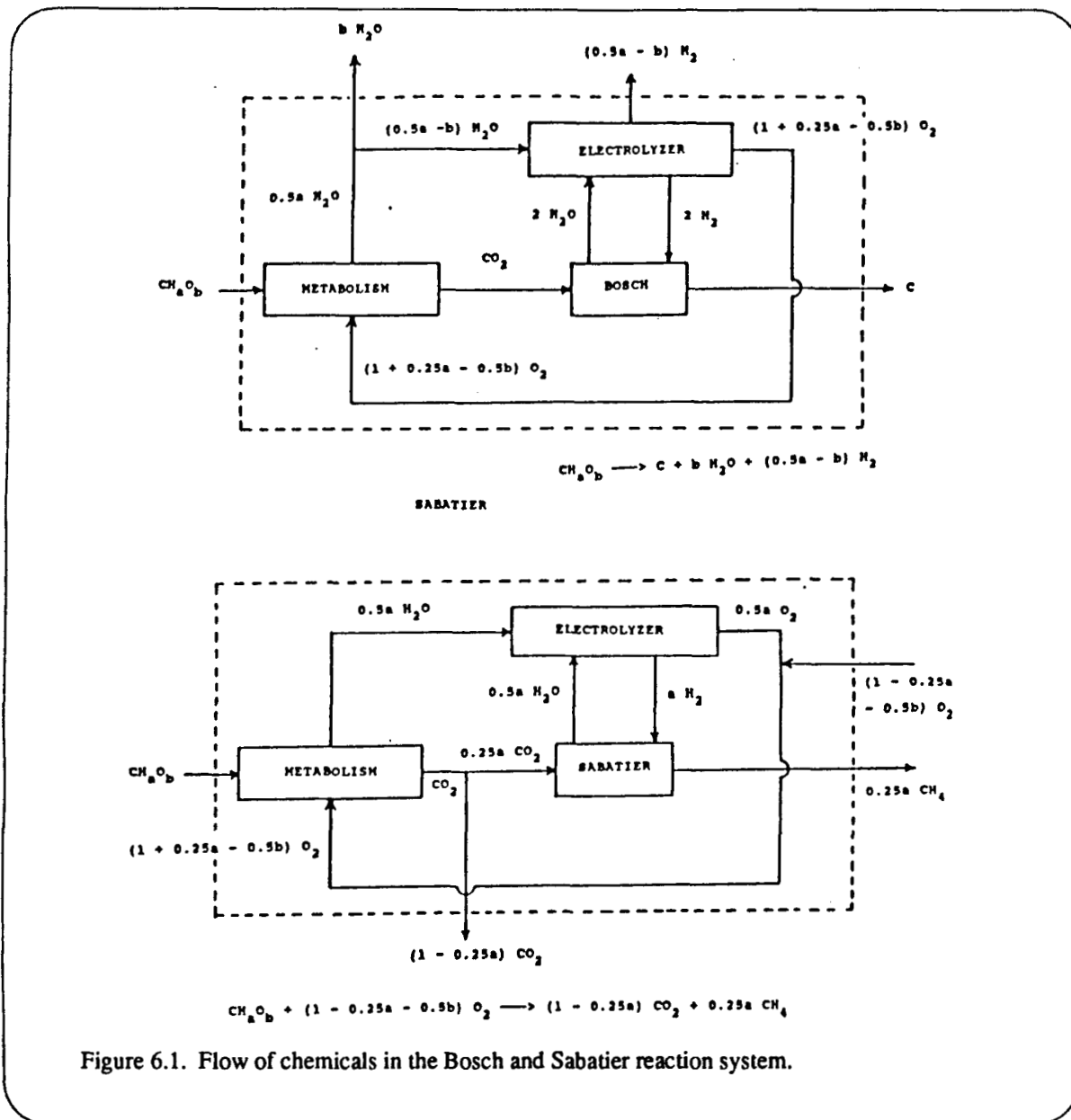
Using the summarized reaction sequence of the Sabatier reactor, the net reaction for a glucose diet is



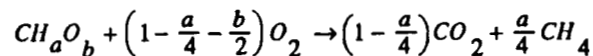
With the pure glucose diet, both the Bosch and Sabatier reactors do not require a net input of oxygen. However, since a pure glucose diet is impractical, the chemistry of the Bosch reactor is required.

The critical feature of the food which determines whether oxygen closure is possible is the C:H:O ratio. Consider the formula for generalized food;  $CH_aO_b$ . Figure 6.1 shows that the generalized net equation for a Bosch reactor is



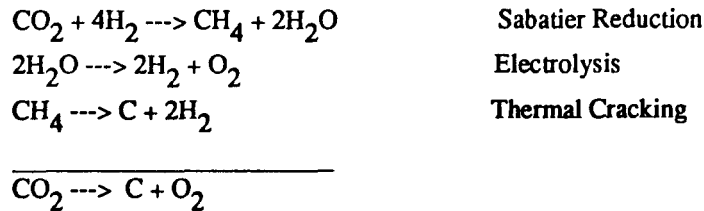


A net input of oxygen would never be required for the Bosch reactor. For the Sabatier reactor, the generalized net equation is



A net input of oxygen is not required only when  $1 - a/4 - b/2 \leq 0$  which is the case only for monomer sugars (e.g., glucose). This condition does not hold for other foods such as starch, sucrose, fats, or proteins, so if these foods are incorporated into the diet, net oxygen input will be required.

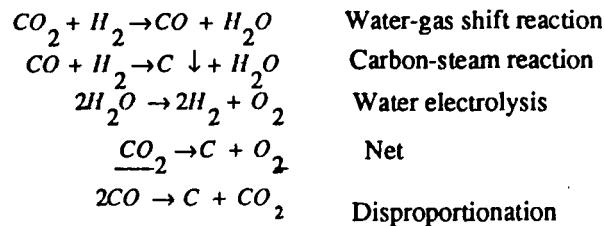
A "pseudo-Bosch" reactor can be created by thermally cracking the methane product of the Sabatier reactor.[7] The net reaction of this system is



which is identical to the Bosch chemistry. The decision to use a Bosch or "pseudo-Bosch" scheme would be based on system weight, reliability, controllability, energy usage, absence of side reactions, etc.

The thermal cracking of methane in the "pseudo-Bosch" scheme is a catalytic process. A limited number of carbon formation reactions can be performed by the catalyst, so there is a weight penalty associated with the need to replace the catalyst. It would be highly desirable to develop a non-catalytic approach to the formation of carbon.

One possible approach to development of "pseudo-Bosch" chemistry is the following:



This chemistry might be better than the thermal cracking of methane if it can be performed without a catalyst. This may be possible by running the carbon-steam reaction at a very high pressure. Le Chatelier's Principle indicates since there are fewer moles of gas on the right side of the carbon-steam reaction equation, the reaction can be favored by increasing the pressure.

## 6.2. Water Recovery

### Process Background

In the early 1950's, the Air Force and Navy were both anticipating manned spaceflight and were supporting studies to investigate environmental parameters necessary for life support. By the mid 1950's, work was in progress to develop a waste management system (WMS) for manned spaceflight which included methodologies for collection, transport, storing and disposal of wastes for missions up to 120 days.[8] Just as NASA was being formed in 1958, two major courses of technology development for waste management in space were beginning to take shape. The "operational" technology was designed to meet the basic requirements of the actual mission and was predicated on providing functional accommodation for collection, processing and storage of waste by the simplest means possible. During the early space programs (i.e., Mercury, Gemini and Apollo) this was accomplished by use of individual fecal collection bags, addition of a germicide to reduce or prevent gas production by bacteria and storing the waste. Urine was first collected via an in-suit assembly with subsequent overboard dumping of fluid waste.

The large volume of Skylab permitted use of a commode-type apparatus with on-board storage of all waste. The present Shuttle Waste Collection System (WCS) has evolved from this technology and all wastes are returned in an open-loop method. Space Station will use this same type of system and all waste will be returned, with exception of urine which is scheduled for process reclamation for crew hygiene purposes.

The "regenerative" waste management pathway also had its beginning at this time and included the more comprehensive technology concepts with prototype hardware systems being developed and tested during various simulation. This pathway however, has been characterized by a much more uneven background of development and during the era of the mid 1970's to the mid 1980's, little or no programmatic support for research in solid waste reclamation and recycling was funded within NASA. The primary reason was that short-term Shuttle missions could best be accommodated by open-loop life support system methods for supplying all air, water and food and collecting and returning all waste.

Before the decision was made to undertake the Shuttle program in the early 1970's, some of the life support system research was focused on waste processing and the potential for food production (i.e., algae), or reclaiming useful dietary supplement materials. The Air Force supported a major study to investigate possible methods of recovering usable materials from fecal waste in the space environment for the dietary supplement[9; [10] while other investigations were directed toward growth of algae as a dietary supplement and for atmosphere regeneration.[11]

At the same time, at least 20 aerospace companies and research institutions were involved in one or more aspects of life support system technology development. Langley Research Center awarded a contract to General Dynamics/Convair in 1963 to design, develop and fabricate an Integrated Life Support System. The objective of this project was to develop a preliminary definition of an advanced flight system capable of supporting a crew of four for one year in low-earth orbit with resupply intervals of 90 days[12]. Major emphasis was directed at advancing state-of-the-art technology for atmosphere control subsystems and for water management using

regenerative methods.

## Early System/Process Development

While size and weight constraints were forcing the "operational" waste management technology to utilize the simplest methods feasible (i.e., collect, stabilize and store), more comprehensive approaches were being investigated by aerospace industry contractors in anticipation of the longer-term manned missions of several months or up to one year. Whirlpool Corporation was investigating a wet oxidation process for combusting waste with air at high pressure.[13] General Electric had undertaken an in-house engineering development program for the Integrated Waste Management-Water System (WMWS)[14] and the Research Division of General American Transportation Corp. (GARD) was developing a prototype fecal waste management unit for Ames Research Center that was based upon automatic dehydration, pyrolysis and incineration of wastes.[15]

In 1968, a 60-day manned test of an advanced regenerative life support system was conducted in the McDonnell-Douglas Space Cabin Simulator using a 4-man test crew. Functional performance of subsystems for potable water recovery from urine and humidity condensate, recovery of oxygen from CO<sub>2</sub>, thermal control, two-gas atmosphere control, trace contamination removal and a fecal waste collector utilizing vacuum dehydration were tested.[16] Improved subsystems were used in the same simulator for a 90-day test in 1970, however it was not continuously manned during this simulation.[17] It was anticipated that the next step would be to conduct a manned simulation of 6 months which would include addition of even more comprehensive waste management/recycling capabilities (e.g. one of the above subsystems).

Process diagrams for each of the subsystems are shown in Figure 6.2. Table 6.1 shows the model waste which each developer was using as their respective input material.

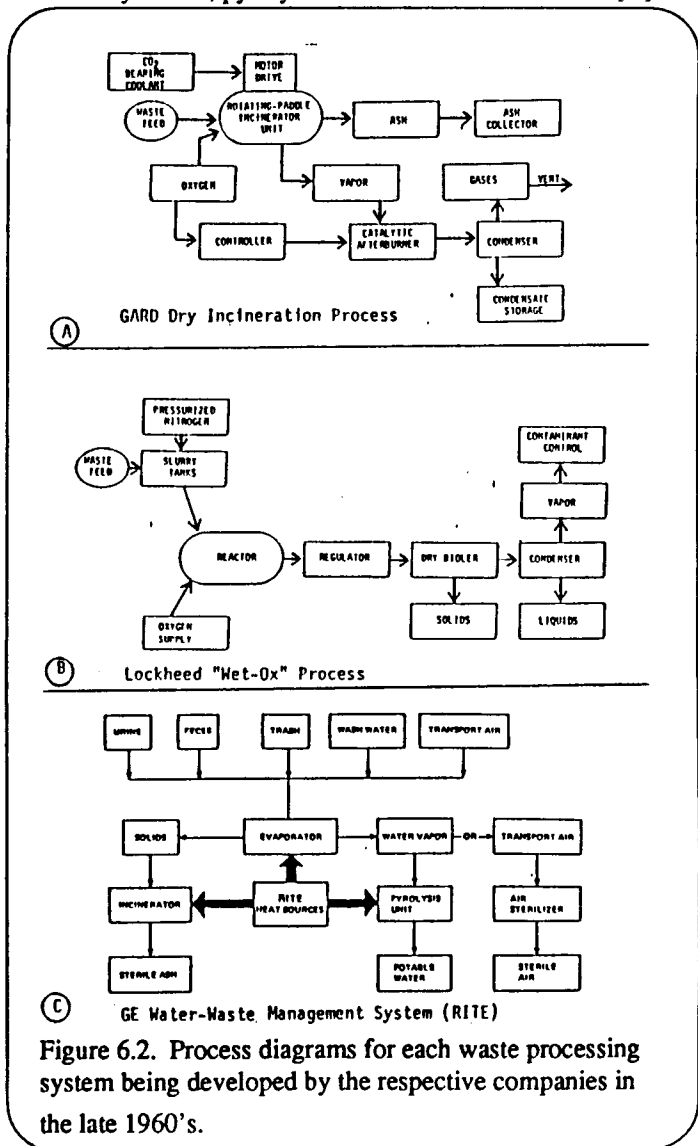


Figure 6.2. Process diagrams for each waste processing system being developed by the respective companies in the late 1960's.

Table 6.1. System characteristics.

<u>Subsystem</u>	<u>Waste Model Input Description</u>	<u>Subsystem</u>	<u>Waste Model Input Description</u>
GARD	600 gm fecal material 600 gm urine distillate containing 50% solids (toilet tissue, food scraps, plastic bags, photo film and fingernail clippings).	Lockheed	1.75 lbs feces 16 lbs urine
		GE	1.2 lbs feces, 14.0 lbs urine, 1.2 lbs trash, 24 lbs wash water, 20 lbs ECS concentrate

## Comparison and Evaluation of Water/Waste Processing Subsystems for Spacecraft

In 1973, NASA tasked the SAE Bioenvironmental Systems Study Group (BSSG) to analyze the technology status of spacecraft waste management systems by evaluating and comparing the alternative designs. The general considerations being used for development of systems at that time were that certain manned missions would require waste management capabilities for feces, urine, trash and waste-water concentrates, and that process(es) be able to convert these wastes to potable water, storable dry ash and produce vapor-phase products which would not impact the atmosphere control system. The GARD, GE and Lockheed processes were the topics of this comparison.

After careful review of background literature and reports, including meeting with each contractor to view the hardware, discuss technical approaches and review pertinent data, the BSSG concluded that a "common pathway" flowsheet could not be developed without further work because too many differences existed in the feed-streams. Furthermore, none of the contractors had organized the research and development of their respective systems to focus on a complete characterization of the input and output streams using material balances. As a result, definitive tradeoff studies could not be conducted unless assumptions and scaling could be employed to develop a common basis for a "paper comparison".

The BSSG identified four subtasks on which their evaluations would be made:

1. Establish a data base and current status for each system.
2. Develop a standardized input and output model.
3. Develop scaled-up flowsheets relative to input/output.
4. Tradeoff evaluation of scaled-up process.

Subtask 1 was completed by conducting discussions with each contractor and reviewing data which had been collected during performance of various tests as the respective systems were being developed. The significant variation of waste input models used by each contractor necessitated development of a standardized waste model to accommodate the BSSG's comparative calculations which would be used for comparisons. The standardized input model developed by the BSSG is shown in Table 6.2.

Subtask 3 was completed by scaling up each process to accommodate a 6-man input and each process was further optimized by adding additional subsystems where necessary to bring the three processes to a more

Table 6.2. Summary of Elemental Composition of Waste Solids "Standardized Model"

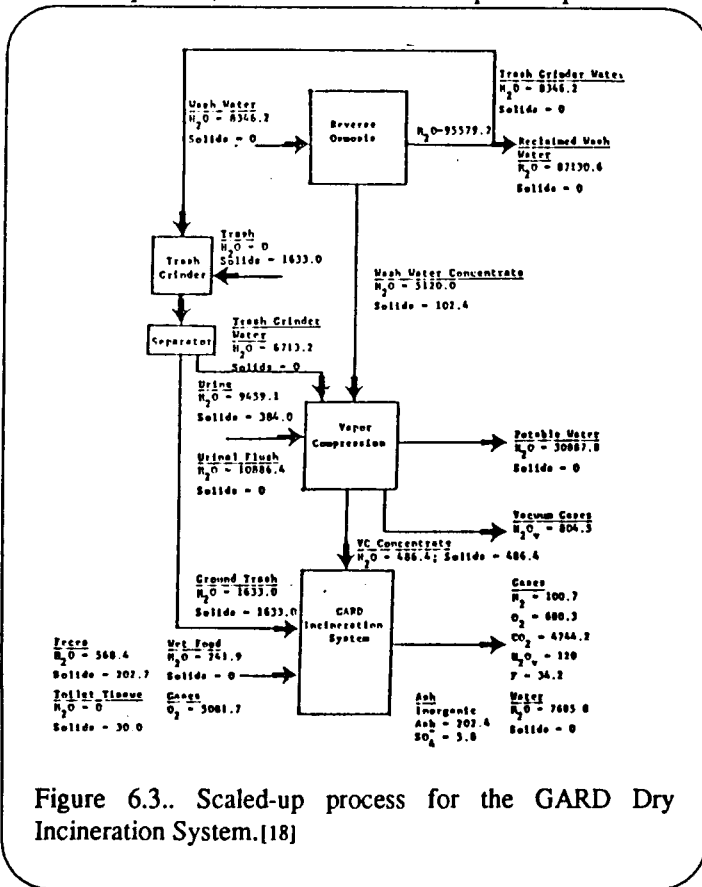
	grams per day - six-man crew							
	<u>Total Solids</u>	<u>C</u>	<u>N</u>	<u>O</u>	<u>H</u>	<u>S</u>	<u>F</u>	<u>Inorganic</u>
<u>Ash</u>								
Urine	384.0	70.22	84.12	66.08	15.59	1.38	-0-	146.61
Feces	202.7	137.29	8.11	23.78	23.78	0.56	-0-	9.18
Wash Water	102.04	40.55	3.48	24.78	5.94	-0-	-0-	27.65
Food	121.0	54.1	5.0	36.1	6.8	-0-	-0-	19.0
Trash	1633.0	978.4	-0-	475.8	144.6	-0-	34.2	-0-
Toilet Tissue	<u>30.0</u>	<u>13.22</u>	<u>-0-</u>	<u>14.82</u>	<u>1.86</u>	<u>-0-</u>	<u>-0-</u>	<u>-0-</u>
TOTAL:	2473.1	1293.88	100.71	641.36	198.57	1.94	34.2	202.44

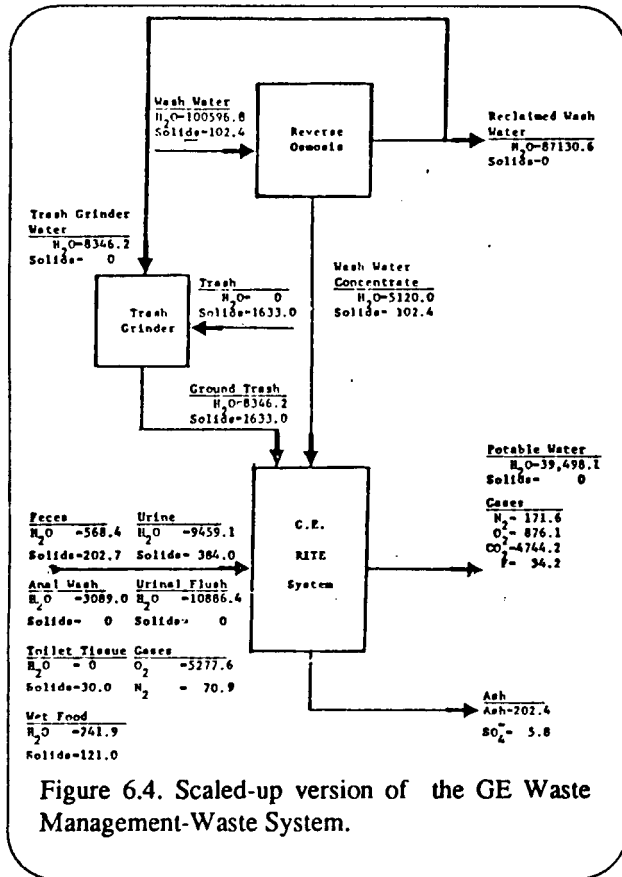
comparative level. A reverse osmosis unit was added to the GE system to preprocess water. For the Wet-Ox process, reverse osmosis, vapor compression distillation (to remove potable water from the effluent), and a dryer to recover water from the vapor compression concentrate effluent and produce a dry ash were added. For the GARD process, reverse osmosis and vapor compression were added. There was also a liquid-solid separator

added to the trash grinder to concentrate trash grinder water prior to entry into the vapor compression unit and solids into the incinerator. The scaled-up processes and accompanying calculations are shown in Figures 6.3, 6.4, and 6.5.

Trade-off evaluation of the scaled up processes was conducted using the following procedure:

- Establishment of a trade-off model
- Assessment of weight, volume, power and thermal penalties for each of the alternative processes
- Development of an evaluation scoring form applicable to the trade-off models
- Rating the alternative processes using point-selection criteria
- Analysis of scoring-evaluation results





The form of the evaluation model was:

$$S_{TOTAL} = (M_{CS})(M_{CP}) \sum_{i=1}^6 s_i, \text{ where}$$

$S_{TOTAL}$  = the total rating score for a given

candidate process;

$M_{CS}$  = Critical Safety Coefficient for the

candidate process;

$M_{CP}$  = Critical Performance Coefficient for the

candidate process;

$s_i$  = six comparison-category terms, scored

separately for the candidate process and then summed.

The terms for  $s$  in the above model were:

- \* General safety characteristics
- \* Operating complexity of the system
- \* Simplicity of interfacing
- \* Adaptability to flight conditions
- \* Versatility
- \* Penalties (weight, volume, power, thermal)

In the BSSG's Final Report to NASA,[18] the major conclusions and recommendations were:

1. All three processes offered feasible and viable approaches for water and waste processing.
2. Current test data for all three processes was inadequate, especially in terms of material balances.
3. From the estimates of design requirements, the GE system was the closest to satisfying the standardized input and output requirements and was the most advanced in terms of readiness.
4. Even if Safety and Performance factors of the GARD and Wet-Ox designs could be improved, the GE process still showed the most promise to meet future requirements for standardized input and output requirements.

The BSSG also recommended that future considerations for research should focus on:

1. Complete material and energy balances.
2. Catalytic oxidation of product streams as required to purify gas streams prior to interfacing with spacecraft atmosphere control systems.
3. A standardized input waste model as extremely useful for all future studies.

It should be noted that while this study was in progress, NASA was making major changes in program directions and by the time this report was issued in 1975, NASA had already suspended most or all funding for

this type of research. GE suspended further development and stored their system. The disposition of the hardware for the other two systems is not known. There are however, more recent studies on use of wet oxidation as a technology for processing of spacecraft derived wastes, but not using the hardware developed by Lockheed. Discussion of several of these investigations are found in subsequent sections.

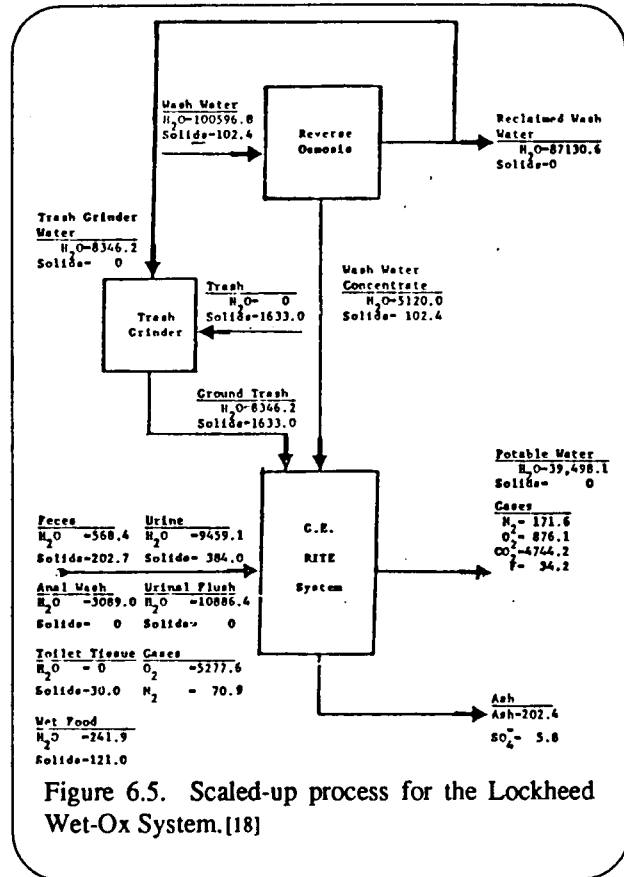
### Wet Air Oxidation

Wet Air Oxidation is a liquid phase process where organic material can be oxidized in an aqueous environment at temperatures of 180-372°C under pressures of 700-2200 psi.[19] Combustion is supported by addition of oxygen or air by compressed injection. Oxidation proceeds until an equilibrium is reached with a residence time of 30 minutes to several hours. Oxidation efficiency increases with time and temperature. Ammonia and acetic acid are prevalent in effluent water. A generalized schematic of the process is shown in Figure 6.6. [20]

Many common organic materials are easily oxidized in this process and reduction in COD for organics follows a general pattern shown in Figure 6.7. Acetic acid and other low molecular weight organics are routinely found in effluents, however in industrial applications these are easily degraded through biological oxidation.

Onisko and Wydeven[21] used this process to oxidize urine, feces, urine and feces, and lettuce solids to study nitrogen balance. After 2 hours at 275°C, ammonia accounted for 64-75% of the recovered nitrogen and N<sub>2</sub> gas was 23-34% within the combined range of 89-113%. Nitrous oxide was not detected by GC analysis and organic material was absent in the filtered precipitate which contained calcium, silicon, magnesium and phosphorous.

Using the wet oxidation process, Johnson and Wydeven[22] oxidized samples of a spacecraft model waste using different pressures, temperatures and process times to follow carbon and nitrogen material balances. Waste oxidation was also performed using different catalysts. At 498K (225°C), 1500 psig and a 1-hour oxidation time, the primary oxidation products were 65.3% CO<sub>2</sub>, 61.7% NH<sub>3</sub> and 5.5% N<sub>2</sub>. At 573 K (300°C), 1500 psig and 1-hour oxidation time, CO<sub>2</sub> increased to 78.6%, NH<sub>3</sub> decreased to 56.6% and N<sub>2</sub> increased to



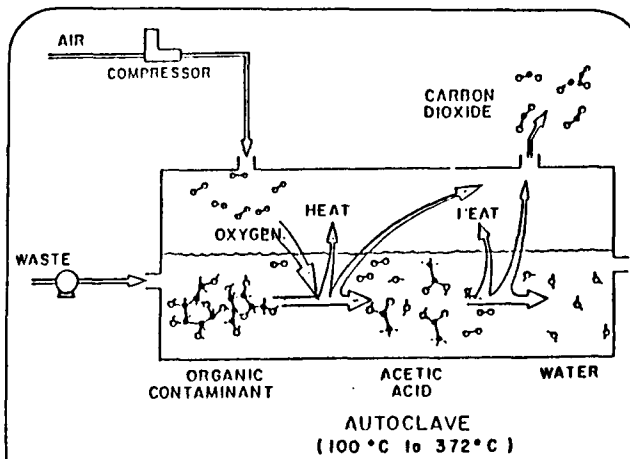


Figure 6.6. Generalized diagram of the wet oxidation process.[20]

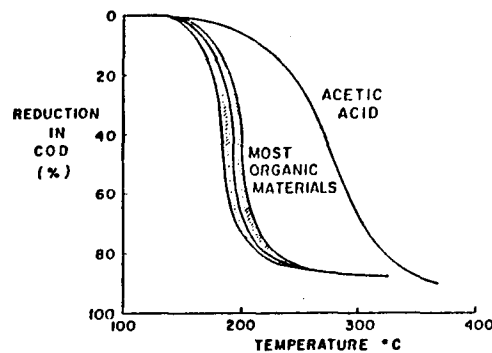


Figure 6.7. Wet oxidation profile for most organic materials except acetic acid which requires a higher temperature.

24.4%. An increase of both temperature and oxidation time appeared to have its greatest effect on conversion of ammonia to  $N_2$ . This was comparable with the finding of Timberlake, *et. al.* using supercritical water oxidation.[23]

The highest rate of conversion of the carbon feed to  $CO_2$  (89.9%) and organic nitrogen to  $N_2$  (78%) was obtained using ruthenium on alumina. It was also found that 4.8% methane was produced whereas methane production was undetected in the uncatalyzed process or when other catalysts were used. Nitrous oxide ( $N_2O$ ) was also detected as a nitrogenous product when ruthenium was used. Platinum on alumina was less effective than ruthenium, however no carbon monoxide and only a trace of methane was formed. Production of nitrogen gas was appreciably decreased while no nitrous oxide was detected.

Copper nitrate and cupric oxide were also used as catalysts. Both were more effective in converting organic carbon to  $CO_2$ , however both catalysts were reactive in the process and therefore cannot be considered as true catalysts. Copper nitrate was effective in converting ammonia to nitrogen gas, while cupric oxide was virtually ineffective and appeared to have suppressed ammonia conversion.

### Super Critical Water Oxidation

Water becomes supercritical when heated above  $374^\circ C$  at pressures greater than 217.6 atm. Below  $350^\circ C$ , as in the wet oxidation process, low molecular weight organics (i.e., acetic acid, methanol) are consistently found in effluents even with reactor retention times of 2-3 hours. Wet Oxidation conversion of organics is only 75-95% effective and a char is frequently present. At supercritical conditions, the feed organics are converted with greater than 99% effectiveness with residence times of 1 minute or less. Organics are reformed mostly to  $CO_2$  and nitrogen, but include gases such as  $CO$ ,  $H_2$ ,  $CH_4$  and small amounts of alcohols, aldehydes and furans. Inorganic salts however, are less soluble and are readily precipitated out of the aqueous phase. A flow

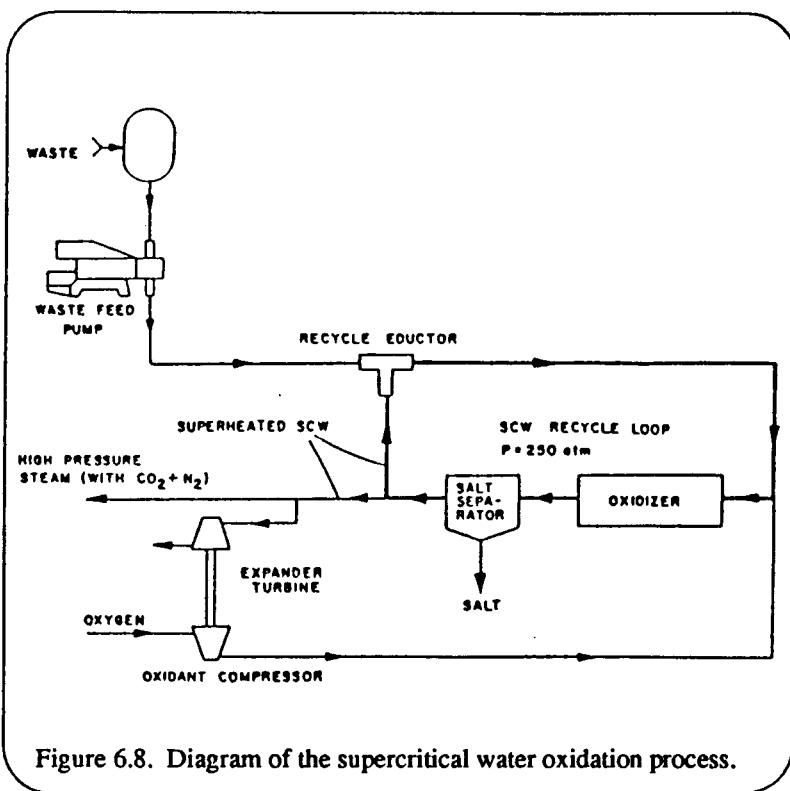


Figure 6.8. Diagram of the supercritical water oxidation process.

diagram of the supercritical water oxidation process is shown in Figure 6.8.

Modell commercialized the supercritical water oxidation process in the early 1980's through Modar, Inc. Earlier research has indicated applicability of the process to oxidizing organics[24] and it was immediately suggested that SWCO held promise as an appropriate waste management process subsystem for closed environment life support systems. Since ammonia must be removed and processed from waste water containing urine and that ammonia has been a primary problem of water recycling process technology for spaceflight recycling schemes, Timberlake, *et. al.*[23] investigated the effect of SCWO on urea destruction. Their findings indicated SCWO was capable of complete breakdown of urea to nitrogen, carbon dioxide and water without use of a specific catalyst. Nitrous oxide was present at 560°C, peaked in concentration at 632°C and disappeared at 670°C. No NOx gases were detected and a white precipitate found in the cooled reactor liquid corresponded to ammonium bicarbonate on the basis

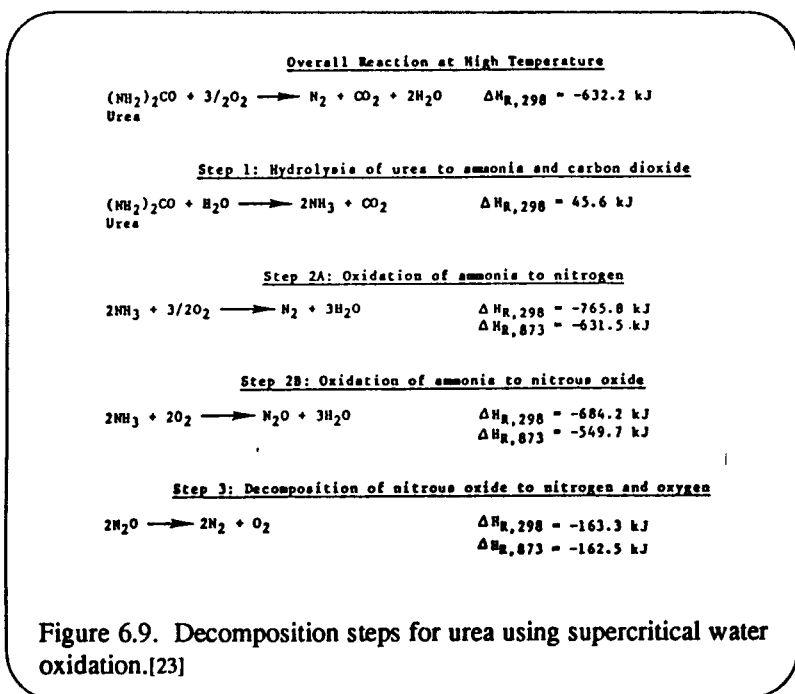


Figure 6.9. Decomposition steps for urea using supercritical water oxidation.[23]

of elemental analysis. Nitrogen balances however, were poor. Urea decomposition was described by the reactions shown in Figure 6.9.

Hong, *et.al*[25] processed different feeds of urine and feces solids (2.5-4%) at a rate of 19-31 g/min using

SCWO. There was essentially complete conversion of organic carbon to CO<sub>2</sub> or char, and organic nitrogen to N<sub>2</sub> and N<sub>2</sub>O. Process stream ash analysis revealed S, P, Cl, Na, K, Ca and Mg. Tradeoff studies were also conducted using more than 20 configurations of the SCWO subsystem. Using a 10-year launch weight analysis, the major conclusions were: all waste water could be processed with little penalty provided a heat exchanger was used; using cabin air as the oxidant carried little penalty but supplying air at the rate necessary for viable air trace contaminant control carried a significant penalty, and trash processing carried a large penalty unless carbon-containing gases could be vented to space.

Webly and Tester[26] studied the kinetics of oxidation for carbon monoxide, methane and ethanol, however efforts to develop reaction models to predict oxidation rates and hydrogen production have met with difficulty. Killilea, *et. al.*[27] have recently focused on development of impingement/filtration mechanisms for removal of solids from the SCWO effluent waste stream. The stickiness of precipitated salts appears to be a major obstacle in developing a functional cyclone-type separator.

Sedej[28] used SCWO as a basis for modeling ECLSS subsystems and suggested ways this process could be substituted for one or more components of waste processing and recycling. The modeling however, was focused on overview capabilities of SCWO to convert waste to gases and water and did not consider any biological aspects within the modeling concept (i.e., food production at any level).

Hall and Brewer[29] evaluated three concept design cases in conjunction with six ECLSS options to assess feasibility of using SCWO in the Space Station Reference Configuration. They found the technology was not sufficiently mature to meet the Space Station Initial Operation Configuration (IOC) of 1993, however the Evolutionary Space Station predicted for 2010 could benefit from the process. They also projected the technology combined with current capabilities for onboard food production was not a viable option to replace the stored food supply method (open loop), but with improvements in the food production technology, the outlook would be more favorable.

The advantages of SCWO are: aqueous waste streams containing both organics and inorganics of up to 25-30% (wt) can be processed; no catalysts are required; inorganics are readily precipitated from the aqueous phase; reactor residence times of less than one minute are practical; and the exotherm reaction provides preheat for feed streams to near the critical temperature. The disadvantages include: there is a major concern that the process must demonstrate that it can be safely operated at temperatures of 550-650°C and pressures of 250 atmospheres; the process is corrosive and a reliable mechanism for removal of inorganic precipitates must be developed and adapted; and post-treatment of the effluent stream must be integrated to handle gas effluents such as carbon monoxide and methane.

In the past several years, some NASA researchers have been looking ahead to long-duration manned missions and the topic of closed or controlled environment life support systems (CELSS) is taking on new meaning in terms of technology development. Waste processing to recycle materials is a distinct technology gap just as food production is. Because SCWO has been aggressively promoted by Modar, Inc., not only from a commercial standpoint, but for its potential application to spacecraft systems, it has assumed a leading position

as a candidate process. When researchers conduct modeling for CELSS evaluations, it appears that many select SCWO as the primary process for solid waste processing. This position may be well-justified because a review of the literature fails to reveal substantive studies focusing on other processes (with exception of a few studies on wet oxidation) with potential application to processing space environment wastes expected in a CELSS environment.

It should be noted however, that Slavin, *et al.*[30] compared parametric data for six waste management subsystems having potential application for Space Station: dry incineration, wet oxidation, supercritical water oxidation, vapor compression distillation, thermoelectric integrated membrane evaporation system and vapor phase catalytic ammonia removal. The incineration (GARD process), wet oxidation (Lockheed) and SCWO were evaluated because they were developed to process solid waste.

One conclusion of the study was that no one process emerged as the "best" subsystem. Ranking would depend upon which parameter was considered most important. Based on weight, volume, and logistics, the vapor compression distillation received the most favorable score with incineration placing fifth. If launch costs over a projected 10-year equipment life, or logistics were the most important factor, the incineration process scored best while the TIMES was the least acceptable.

Furthermore, it is noteworthy that little mention has been made of the SAE BSSG's findings in their extensive comparison made in 1975 and that even fewer references have included the GE WMWS as a viable technology approach to either solid waste processing or potable water recovery.

### **Alternative Waste Processing and Reclamation Technologies**

Life support aspects of a CELSS ultimately focus on four essential components which must be produced/recycled with as high a degree of closure as possible. These components are: air, water, food and waste. Reasonable physical-chemical subsystems exist for air revitalization and water reclamation and are currently being evaluated at Marshall Space Flight Center as potential Space Station life support subsystems. Even though one or more of these subsystems will find application in Space Station, work continues to improve a variety to technical aspects for these technologies.

It is important to note that several of the current competing technologies for both air revitalization and water reclamation had their beginning in the early 1960's and have been continuously investigated, improved and tested for over 25 years to reach their current state of development. In contrast, as described earlier in this report, there is an extensive technology gap for waste recycling subsystems and an even larger gap in our understanding of how food production could be integrated into the spacecraft or spacebase life support system.

It is also important to recognize the steps through which any technology must proceed to reach maturity as an operational subsystem and that these developmental steps provide vital information through which meaningful trade studies are conducted. These technology development steps are revisited in Table 6.3.

It is now time to reassess and/or reconsider technical aspects of the GE WMWS, which we have in our laboratory and are currently refurbishing. This is a prime example of a candidate subsystem which was

Table 6.3. Development steps through which a candidate subsystem must progress to achieve operational status.[30]

<b>TECHNOLOGY MATURITY DEVELOPMENT SCALE</b>	
<u>Descriptor Level</u>	<u>Scale</u>
Space operational	8
Engineering model tested in space	7
Prototype tested in relevant environment	6
Breadboard tested in relevant environment	5
Critical function demonstrated	4
Conceptual design tested	3
Conceptual design formulated	2
Basic principle observed/reported	1

reasonably well developed in the 1960's and early 1970's and even successfully tested in several simulations, one of which was for more than 200 days.[14] It is also a prime example of a candidate subsystem which has sat idle for 15 years without the benefit of incorporating technology advances which can be applied to upgrading this subsystem and providing test data which is vitally needed for trade studies.

The conceptual design studies performed by our team[5; 6] point out the importance of reclaiming and recycling materials within a CELSS, and waste processing/reclamation has been one of our primary interests. For our investigations to proceed after refurbishment of the GE hardware subsystem, one of

the first investigative priorities is to conduct materials balance studies on model wastes to obtain the necessary critical information. This research was one of the key recommendations of the SAE BSSG[18] in their comparative evaluation of waste processing technologies made in 1975. The incineration-pyrolysis characteristics require further investigation, not that this approach would be applied to oxidation and recycling of all solids, but only as a last-step process for 10-15% of the solids which could not be effectively processed by another means (i.e., wet oxidation, supercritical water oxidation, electrochemical decomposition, etc).

To date, most waste processing attention has focused on crew wastes (feces, urine, wash water), trash (paper and plastic) and food scraps. Additional liquid and solid wastes will be generated through facilities such as the Health Maintenance Facility (HMF) and with the addition of the United States Laboratory (USL) Module, waste-water and solid waste derived from nonhuman research (i.e., animal, biological and physical-chemical experiments) will be significantly increased. The potable and ultrapure water requirements for support of projected experiments being planned by USL researchers is conservatively estimated at 1,800 liters every 90 days.[31] These wastes will contain chemical species which may be corrosive or detrimental to water reclamation process subsystems (i.e., reverse osmosis, multifiltration, etc.). Other questions arise pertaining to brine concentrates derived from these water reclamation processes. The waste management-water system hardware we are refurbishing and testing appears to be well-suited to processing these wastes (i.e., water reclamation process brines and the life sciences/USL wastes). It is our intent to process these types of wastes and evaluate the process products.

On an even larger scale, when food production is integrated into the CELSS overview, considerable amounts of waste will be generated within this subsystem (i.e., spent growth media solutions, inedible biomass and byproducts of food processing). When looking at the potential food energy/carbon associated with inedible

ORIGINAL PAGE IS  
OF POOR QUALITY

biomass, it is reasonable to project that it would be more efficient to convert cellulose of the inedible biomass to a usable nutritional compound such as glucose, sorbitol or other hexose sugars via an enzymatic process and supplement this into the crew diet. Through such a conversion, both time and energy are conserved because waste (cellulose) does not have to be oxidized to CO<sub>2</sub> and water and then rebuilt through the biological processes to produce nutrient energy. A diagrammatic overview of several potential pathways is illustrated in Figure 6.10.

The WMWS subsystem offers a viable potential for water reclamation, especially in light of the fact that sterile, potable water can be produced for crew use without the necessity of adding a disinfectant such as iodine. The absence of disinfectant in ultrapure water for laboratory experiment purposes is also an important consideration and availability on demand relieves logistic penalties. A more extensive discussion of the water reclamation attributes of this subsystem are found elsewhere in this report.

Finally, we believe this approach merits study and serious consideration because of detracting features associated with wet oxidation and SCWO: 1) the high pressure (excess of 217 atm) poses potential safety considerations and 2) the process is highly corrosive when operated at these pressures and temperatures. Even if these processes find application as life support subsystems, it is important that alternative processes be investigated to expand our knowledge base about waste processing technologies. Furthermore, it is highly likely that more than one waste processing subsystem will be required to efficiently and effectively manage the broad range of waste which will be derived from future long-term space activities. Such data is essential for maximizing the overall CELSS technology development.

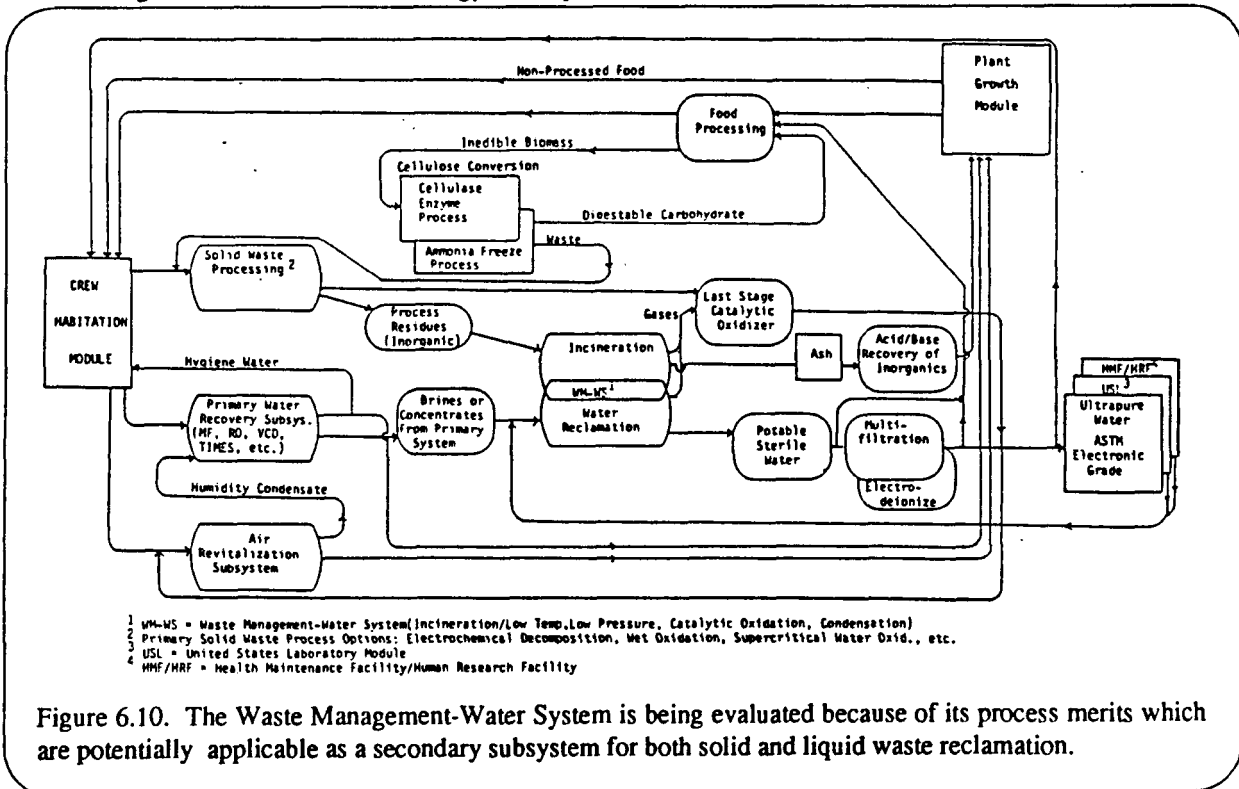


Figure 6.10. The Waste Management-Water System is being evaluated because of its process merits which are potentially applicable as a secondary subsystem for both solid and liquid waste reclamation.

### 6.3 Trash Management

Trash management (paper towels, food/drink containers, food scraps, etc.) is an important aspect of the total waste management requirements of spaceflight. Any wet trash is a potential source for microorganism proliferation, subsequently leading to contamination if not adequately controlled. Two topics, control of biodegradation and packaging, are discussed in the following sections and new approaches are explored as possible means for further controlling undesirable features associated with trash buildup in a spacecraft environment.

#### Disruption of Undesirable Biodegradation

The problem of odor production from stored wastes has attracted increasing attention as plans are developed for long-duration missions in closed environments. In order to deal effectively with this problem, it must be realized that odor production is almost entirely due to action of bacteria and other micro-organisms which are inoculated into the wastes due to human contact. This is true not only for food scraps, which "spoil" and become odorous only as a result of attack by bacteria and other micro-organisms, but also for wastes such as feces. Over half the bulk of human feces is usually made up of bacterial cells. The distinctive, unpleasant odor of human feces is largely due to the presence of indole, a common bacterial product resulting from bacterial nitrogen metabolism.

Although a few humans have been maintained in completely bacteria-free conditions, it is impossible in practice to sterilize active adults and keep them free of microbial contamination. The exact number and species of bacterial symbionts vary from individual to individual and even from day to day on a single individual, but it is generally true that an average human carries between 20 and 40 species of prokaryotic micro-organisms, plus another 5-15 species of eukaryotic micro-organisms. Commonly encountered prokaryotic organisms are listed in Table 6.4.

Table 6.4. Prokaryotic organisms.

<i>Staphylococcus</i> sp., especially <i>S. aureus</i> , <i>S. epidermidis</i>	<i>Lactobacillus</i> sp.
<i>Streptococcus</i> sp., especially <i>S. pyogenes</i> , <i>S. anginosus</i>	<i>Fusobacterium</i> sp.
<i>Peptococcus</i> sp.	<i>Bacteroides</i> sp.
<i>Peptostreptococcus</i> sp.	<i>Actinomyces</i> sp.
<i>Corynebacterium</i> sp.	<i>Bifidobacterium</i> sp.
<i>Eubacterium</i> sp.	<i>Mycobacterium</i> sp.
<i>Propionibacterium</i> sp.	<i>Veillonella</i> sp., especially <i>V. parvula</i> , <i>V. alcalescens</i>
<i>Escherichia coli</i>	<i>Acidaminococcus fermentans</i>
<i>Citrobacter</i> sp.	<i>Pseudomonas</i> sp.
<i>Enterobacter</i> sp.	<i>Haemophilus</i> sp., especially <i>H. influenzae</i> , <i>H. haemolyti</i>
<i>Acinetobacter</i> sp.	<i>cus</i> , etc.

Other genera, such as *Neisseria*, *Clostridium*, *Shigella*, *Treponema*, etc., are commonly associated with humans, but since these genera are usually encountered in pathological conditions, it is assumed that they will not be common among astronauts.

Some information about growth of human-associated bacteria will be useful to our discussion. (Also see Buchanan & Gibbons[32] and MacFaddin.[33])

*Staphylococcus* - aerobic or facultatively anaerobic, uses wide range of carbohydrates as carbon and energy sources, produces acetic acid, may produce small amounts of ammonia, hydrogen sulfide when degrading amino acids.

*Streptococcus* -- facultatively anaerobic, nutritional requirements complex, may produce ammonia when degrading amino acids, may produce lactic or acetic acids.

*Peptococcus* -- anaerobic, degrades a wide range of carbohydrates and proteins, with production of acetic, propionic, butyric, formic, lactic, and succinic acids. Produces ammonia when degrading proteins; H<sub>2</sub>S may also be detectable. Indole is sometimes produced.

*Peptostreptococcus* -- anaerobic, complex nutritional requirements, with production of acetic, formic, propionic, butyric, isobutyric, caproic, isocaproic, valeric and other acids. H<sub>2</sub>S and other "fetid odors" have been reported as products.

*Corynebacterium* -- aerobic and facultatively anaerobic, nutritional requirements often complex. May produce small quantities of short-chain organic acids. Not a major odor producer.

*Eubacterium* -- anaerobic, grows on a wide range of sugars, producing butyric and caproic acids; indole may be produced.

*Propionibacterium*-- anaerobic to aerotolerant, growth on carbohydrates and peptone. Produce propionic, acetic, and isovaleric acids. When degrading proteins, most strains produce ammonia, many produce indole.

*Escherichia coli* -- aerobic or facultatively anaerobic, grow readily on simple media, produces lactic, acetic, and formic acids.

*Citrobacter* -- aerobic or facultatively anaerobic, grow readily on simple media; some strains produce indole.

*Enterobacter* -- Facultatively anaerobic, metabolize carbohydrates; some strains produce indole.

*Acinetobacter*-- aerobic, grow well on simple media. Do not produce indole or H<sub>2</sub>S, but some strains reported to produce "a special, disagreeable odor" of unspecified chemical origin.

*Lactobacillus* -- anaerobic or facultatively anaerobic, often shows complex nutritional requirements. Produces lactic, formic, acetic, and succinic acids.

*Fusobacterium*-- Strict anaerobes, metabolize wide range of carbohydrates, peptone. Produce butyric (usually in large amounts), acetic, propionic, formic acids; many strains produce indole.

*Bacteroides*-- obligate anaerobes, metabolizing carbohydrates and peptone. Produce acetic, butyric, isobutyric, isovaleric, formic, and other acids. Some strains may produce H<sub>2</sub>S.

*Actinomyces* -- facultatively anaerobic, wide range of carbohydrates are fermented with production of acetic, formic, lactic, and succinic acids.

*Bifidobacterium* -- strict or facultative anaerobes, fermenting a wide range of carbohydrates with production of acetic, lactic, formic, and succinic acids.

*Mycobacterium* -- aerobic; nutritional requirements usually simple; little production of odorous compounds.

*Veillonella*-- anaerobic; complex nutritional requirements. Produce acetic and propionic acids; copious production of  $H_2S$  if substrate is rich in sulfur-containing organic compounds.

*Acidaminococcus*-- anaerobic; multiple nutritional requirements. May produce acetic and butyric acids, usually produce ammonia.

*Pseudomonas* -- aerobic; capable of growth on a wide range of carbohydrates, proteins, and other organic compounds. Some strains produce distinctive putrid odors which are not due to familiar organic acids or other common odorants.

*Haemophilus*-- aerobic or facultatively anaerobic, complex nutritional requirements, some strains produce indole.

As can be seen from the lists above, many of the bacterial genera normally associated with humans are capable of either aerobic or anaerobic growth; though some prefer or require anaerobic conditions. Most of the genera listed above are capable of growth at a wide range of temperatures. It must therefore be assumed that all of them will be present within a few hours in all parts of a spacecraft occupied by humans. This will also include waste lockers. As the lists indicate, most of the genera produce a wide range of odorous metabolic by-products, such as ammonia, hydrogen sulfide, acetic acid, butyric acid, indole, etc. It is thus inevitable that wastes such as food scraps, food containers, moist paper items, etc. will support a vigorous (and probably odorous) bacterial population. There are several strategies for dealing with this situation.

1. Ignore the odors or learn to tolerate them.
2. Prevent the growth of the odor-producing bacteria.
3. Manage the growth of the bacteria so as to minimize odor production.

Each of these approaches deserves comment.

1. Ignore the odors. This approach is now in use. For short missions, it is very unlikely that any bacterial by-products will reach concentrations detrimental to human physical well-being. Psychological stress may be increased by the presence of odorants.

2. Several strategies might be used to slow or halt growth of odor-producing bacteria. These strategies may be divided into physical methods and chemical methods. Physical methods include chilling or freezing, dessication, heat sterilization, irradiation with ultraviolet wavelengths, and incineration of wastes. Chemical methods would include addition of strong oxidants, phenolics, halogens, sterilants such as ethylene oxide, or growth inhibitors such as antibiotics.

Of the physical methods, UV irradiation is probably the least effective unless the wastes are finely ground and exposed to radiation while being stirred. Shading of cells by waste particles would make it difficult to ensure high efficiencies of sterilization. Heat sterilization is more efficient, but must be repeated for each addition of wastes. Heating to 121°C. for 20 minutes will be required to ensure elimination of bacteria. Chilling, freezing, and dessication are probably the simplest of the physical techniques for treatment of wastes for mission durations of a few days. It must be realized, however, that these techniques are not bactericidal, but only bacteriostatic. If the stored wastes are allowed to warm and/or rehumidify, bacterial growth will resume almost immediately. Incineration of the wastes precludes bacterial growth, since the reduced organic components are converted to oxidized forms that will not nourish the cells.

For chemical treatment methods, antibiotics are probably the least satisfactory. A mixture of broad-spectrum antibiotics would be required; and the wide diversity of bacterial genera would prove a challenge to the effective use of this method of control. Phenolics and halogens are more generally effective, but present the disadvantage that they are usually volatile at room temperature, and are likely to be far more toxic to human crew members than the bacterial by-products which they seek to eliminate. Strong oxidants such as ozone, sulfuric acid and commercially available cleaning solutions ("Nochromix", etc.) are less volatile and highly effective in destroying bacteria. In addition, these strong oxidants degrade the waste materials to non-nutritive forms. But the strong oxidants present dangers in use, since they are extremely caustic and corrosive. In summary, all physical and chemical methods of halting bacterial growth present certain drawbacks. Choice of such a method merely depends on identifying the least unacceptable.

3. For mission durations longer than a few days, the most satisfactory approach will probably involve cooperating with the bacteria, managing their growth so as to minimize odor production, or to produce the least objectionable odors. In general, this will require more or less constant gentle mixing and aeration of the slurry of wastes and bacterial cells. The most copious output of the most foul odors results from anaerobic growth of the cells. Reduced forms of nitrogen and sulfur are both volatile and highly offensive to humans. Likewise, many partially-reduced forms of carbon are offensive to humans. In contrast, oxidized forms of these elements seem less offensive. In the absence of oxygen, many bacteria release reduced metabolic by-products, while given adequate supplies of O<sub>2</sub>, oxidized products are released. This situation has long been recognized by civil engineers involved in operating public health facilities such as municipal sewage treatment plants. To carry out this sort of bacteria-mediated digestion of waste materials, a bioreactor-type module will be required. No such bioreactor, capable of continuous operation under microgravity conditions, is presently available. Although it may be quicker and less expensive in the short run to manage wastes by some method other than controlled bacterial digestion, it is not apparent that savings will necessarily be realized in the long run. Decisions must be taken as to whether a strategy of eliminating biological components or managing the biological components will be adopted

## Food Packaging

Food packaging is a major component of the waste stream. Typically, it consists of laminated plastic and metallic films. These materials cannot be broken down in the waste electrolyzer, which was shown to be an extremely efficient method of waste recycling (see Section 4). Although pyrolysis/combustion may be used to break down the plastic portion of the food packaging, the metallic film may form a slag and adversely affect the combustor.

An alternate concept in food packaging is to use biodegradable materials. An excellent candidate is pullulan, a polymer of maltotriose (i.e., three  $\alpha$ -1,4-linked glucose units) joined by  $\alpha$ -1,6 linkages.[34] It is produced by the microorganism *Pullularia pullulans* and is available from Hayashibara Biochemical Laboratories, Okayama, Japan.[34]

Pullulan may be formed into films as thin as 0.01 mm.[34] The films are colorless, transparent, tasteless, odorless, oil-resistant, and heat-sealable.[34] Importantly, it has an oxygen permeability about 1/4 to 1/2 that of cellophane and 500 to 1000 times less than polypropylene, so it prevents oxidation of fats and vitamins.[34] Pullulan may be eaten, but supplies no calories.[34] However, if the pullulan is treated with pullulanase, it is converted to glucose which will supply calories to the astronauts.

## 6.4 Contaminant Management

A systems level strategy is required for contaminant management because contaminants are generated by all the systems in the habitable environment, including the crew. Additionally, the contaminants can affect the performance of the crew as well as the operation of other life support systems.

### Airborne Contaminants

A sealed environment captures charged particles, microbial and chemical contaminants generated by the enclosed crew and equipment. In addition, some external radiation may produce contaminants within the enclosure. NASA has a stringent materials and process control regimen and still has identified hundreds of trace contaminants generated during the short Shuttle flights. As the degree of environmental closure increases, the problem of controlling airborne contaminants increases significantly. It is further exacerbated by increased scientific experimental pollution.

Our present state-of-the-art for contamination control relies on vehicle leakage, sorbents and low and high temperature catalytic oxidizers. Activated charcoal impregnated with phosphoric acid (low temperature-catalytic oxidizer) is used for the short duration Shuttle missions. A high temperature catalytic oxidizer with pre- and post-treatment by sorbents is a major candidate for Space Station.

The other life support systems also control trace airborne contaminants. For example, the condensing heat exchanger used for temperature and humidity control scrubs water soluble contaminants from the air flow. Also the carbon dioxide removal technique may remove trace gases. The result is a mixed blessing, in that it reduces the types of contaminants to be removed by the trace gas control system, while transferring the problem to the water and oxygen recovery systems. Specifically, the humidity condensate may contain trace chemicals which cannot be removed by the water recovery system, thus contaminating the user or the trace chemicals may degrade water recovery membranes, sorbents, and/or catalysts. The same potential for problems exists in the oxygen recovery system.

### Recommendations

- Identify potential contaminants from projected space industrialization, lunar and Mars missions.
- Develop a system level strategy for control of airborne contaminants consisting of several scenarios for different types of life support systems.
- Use the above scenarios in the selection process for life support equipment.
- Develop test plans to assure that contamination management is rigorously addressed in manned closed chamber tests.
- Identify newly developing materials and processes which could significantly lessen outgassing and/or types of gases generated.
- Implement a system level trace contaminant mass modeling.

## RITE System

When GE was conducting engineering design, component development and system simulation in the early 1970's on the Integrated Waste Management-Water System Using Radioisotopes for Thermal Energy (RITE system),[14] contaminant management was only partially controlled. An air sterilizer, nested in the heat block along with three catalytic oxidizers and the solids incinerator, processed approximately 20 CMF of air for up to 10 minutes. Transport air derived from the cabin atmosphere was used to entrain wastes (urine, feces or trash) into the collection devices and subsequently directed to the evaporator (reservoir). An in-line suction blower forced air through the air sterilizer where exit air temperature was approximately 400°F.

Although conventional microbial sampling techniques for post-air sterilizer sampling were not applicable because of high temperatures, secondary methods were unable to detect any viable micro-organisms in the air stream. GC-MS analyses of air sterilizer samples were not performed even though this air stream was designed to be returned to the cabin supply. During air sterilizer operation, while wastes were being entrained/transported to the evaporator, the low pressure side between the evaporator and the catalytic oxidizers and the solids incinerator was isolated by automatic valving. Following the temporary use of the air stream to transport incoming wastes, the air sterilizer process could also be isolated by valving and shut off.

The design of the RITE system solids incinerator and the catalytic oxidizers for the vapor stream were predicated on using the vacuum of space (achieved through use of mechanical vacuum pumps) to provide the reduced pressure (1.2 psi) for water evaporation in the reservoir at approximately 110°F. Therefore, exit gases from waste decomposition would be dumped overboard and not returned to the cabin air supply. Although the catalytic oxidation and pyrolysis features of the heat block components operating at 1400°F were theoretically designed to oxidize organics to H<sub>2</sub>, N<sub>2</sub>, CO<sub>2</sub> and water, other chemical species were detected in this vent gas stream. Table 6.5 shows a representative composition of gases detected by GC-MS analysis from one of the GE simulation tests.

Table 6.5. Percent composition gases based on most abundant species.

SAMPLE	H <sub>2</sub>	CH <sub>2</sub>	CH <sub>4</sub>	NH <sub>3</sub>	H <sub>2</sub> O	CO	N <sub>2</sub> /C <sub>2</sub> H <sub>4</sub>	NO	CO <sub>2</sub>	NO <sub>2</sub>	OTHER
Decomposition	16.4	16.2	10.4	1.4	5.7	1.4	43.3	0.3	5.0	--	Aromatic NC's; Sulfide, SO <sub>2</sub> ; HCl
Incineration	22.2	15.2	9.6	0.9	6.6	0.6	35.9	0.5	8.4	--	'

Materials balances were not a design objective of the GE studies, and as later pointed out by the SAE BSSG report,[18] this aspect was one of the major deficits of the GE simulation studies. It was suggested by the BSSG that a down-stream catalytic oxidizer component would further reduce air contaminants and any residual contaminants could be removed by passing the air stream through a charcoal bed.

This is a viable concept and Lockheed has designed a Trace Contaminant Control System (TCCS) for this purpose as part of the Space Station Air Revitalization Subsystem currently being evaluated at MSFC.[35; 36] Although there are no competing technologies for the TCCS, the basis for design and application of a spiral catalytic reactor is discussed in the following section.

As our studies progress on the GE hardware situated in the RECON Lab, we plan to obtain detailed analyses of post-catalytic and post-incinerator gases. These results will permit us to take a more direct approach to design and integration of an appropriate contaminant processing subsystem such as the TCCS, the Spiral Reactor or directing these gases into a biomass production unit.

### Novel Spiral Reactor

Contaminants build up in the cabin from outgassing of electronic equipment, human emissions, food, etc. The concentration of these contaminants must be maintained at low levels so that they do not affect crew performance. Figure 6.11 shows a schematic of a proposed contaminant removal system which uses a spiral reactor.

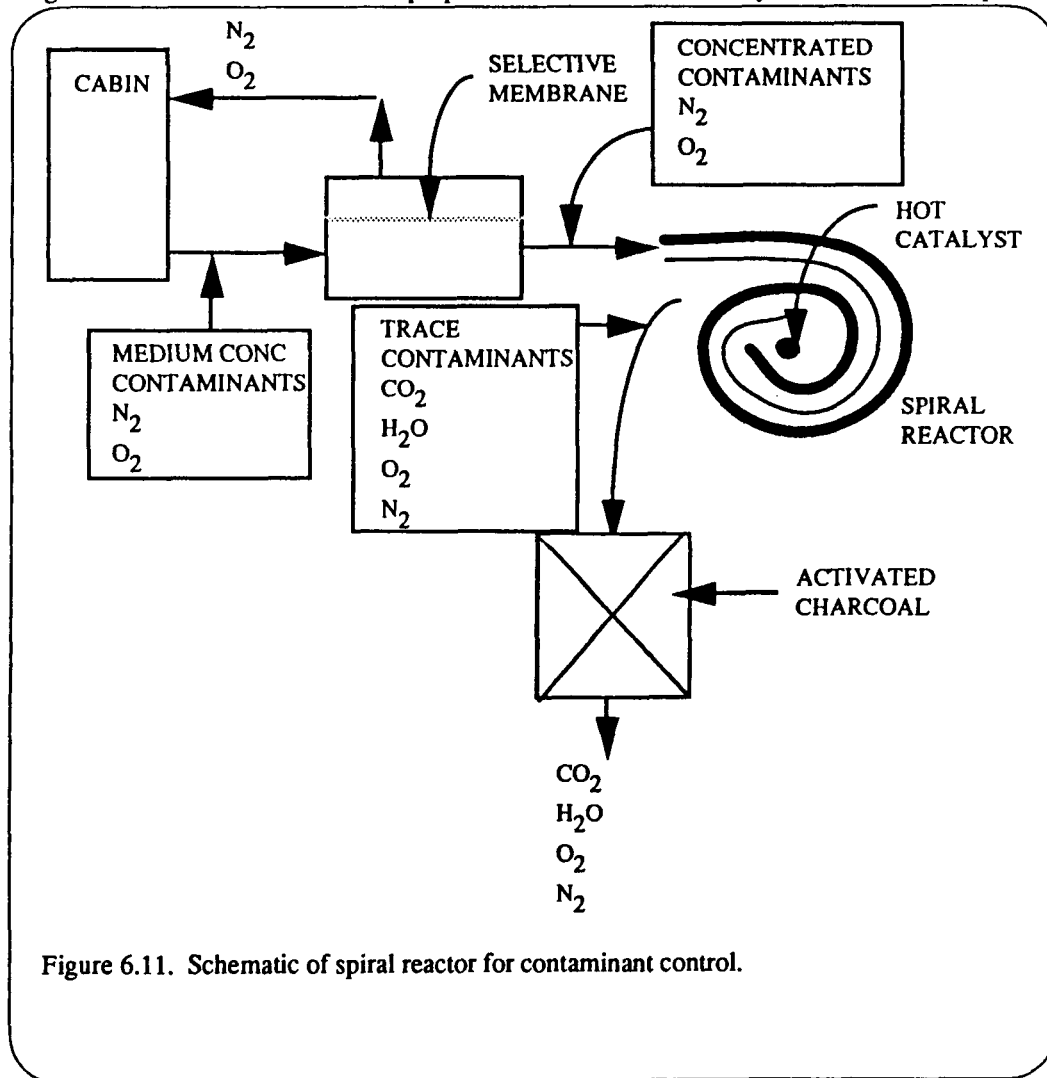


Figure 6.11. Schematic of spiral reactor for contaminant control.

A selective membrane removes oxygen and nitrogen from cabin air thus concentrating the contaminants. The concentrated contaminant stream flows through a spiral reactor.

The core of the spiral reactor is electrically heated to an elevated temperature. A high-surface-area platinum catalyst is located at the center of the spiral. Reactive contaminants are therefore combusted on this surface, producing CO<sub>2</sub> and H<sub>2</sub>O. The spiral acts as a counter-current heat exchanger so the amount of heat required to maintain the core temperature is minimal. This system has already been demonstrated to be effective at destroying cigarette smoke.[37] Since combustion reactions are rarely complete and there may be some toxic substances produced, it will be necessary to pass the exhaust gases through an activated charcoal filter to remove the final traces of contaminants. Since most of the original contaminants were combusted, the loading on the activated charcoal should be relatively low, so frequent replacement will not be necessary.

## **Rapid Detection of Microbial Contaminants in the Space Station Water System**

Water is an essential component for life support. The Space Station Water Management System will provide recycled water to meet both human and nonhuman needs. In terms of life support resources, water accounts for the single largest mass in a manned space vehicle.[38] As the scope of manned space activities diversifies, water requirements for nonhuman use (i.e., animal experiments) and a wide range of laboratory applications in the United States Laboratory (USL) Module will be significantly increased. Not only will the reclamation processes supply hygiene and potable water for crew use, but additional potable and ultra-pure water must be available for the variety of projected experiments being planned by USL researchers. The current projection is that 1,800 liters of additional water (both potable and ultrapure) will be required every 90 days.[31] With launch-to-orbit costs assumed at \$10,000 per pound, the monetary benefits of water reclamation subsystems are not only desirable, but essential.

Phase change processes (i.e., Air Evaporation System-AES; Thermoelectric Integrated Membrane Evaporation System-TIMES; Vapor Compression Distillation-VCD) use evaporation (distillation) to recover water from a waste stream and concentrate the contaminants into a brine. Non-phase change processes (i.e., Reverse Osmosis-RO; Multifiltration-MF) reclaim water by physical/chemical means using a phase interface of filters, membranes or adsorbents. Post-process treatment using carbon beds and deionization will further increase the water quality. With the additional demand for ultrapure water in the USL, second and third stage purifiers will be required to remove remaining contaminants from process water. Technologies currently being evaluated for these processes include conventional resin beds and electrodeionization for ion removal, membrane and ultrafiltration for particulate and bacterial removal, and UV oxidation, carbon adsorption and organic scavengers for organic removal.[31]

The Space Station water reclamation process, treatment and distribution systems must continuously be assessed in terms of mechanisms for limiting or preventing unwanted contaminants (i.e., chemical, microbial). Microbial contaminants in process water are a primary concern because of their ubiquitous presence and poten-

tial to proliferate once they gain entry into the water system. It is highly probable that water systems aboard the Space Station will become contaminated regardless of the design option chosen.[39]

A key factor for ensuring successful operation of the water reclamation and management subsystem is microbial contamination control and monitoring. Three levels of microbial assessment have been identified as necessary to safeguard the crew's health through daily use of reclaimed and recycled on-board water supply: (a) monitoring, (b) isolation, and (c) identification.[40] There is no single capability available to provide comprehensive water monitoring for the Space Station water system at this time.

Water contaminating bacteria can be difficult to identify. Traditionally, identification is accomplished through standard microbiology laboratory procedures, some of which utilize enrichment culturing followed by plating on selective and differential media. When these techniques are used, several days are required to complete the identification process and considerable time and supplies are expended. In the Space Station environment, these techniques will be impractical and must be supplemented by new methods which will be more efficient in terms of labor and logistics as well as reliability for identification.

There are other techniques for microbiological identification, some of which are reasonably well developed for special purposes, but which have not found widespread use because of technical aspects and cost of supporting instrumentation. There are also emerging technology approaches which have been demonstrated through proof of concept but have not been sufficiently refined to determine the scope of application. In the following, brief descriptions (including merits or deficits) of other techniques applicable to detecting and identifying water micro-organisms are provided.

It is our opinion that the emerging technology surrounding use of redox dyes (Section 6.4) has the greatest potential for becoming an adaptable technology to meet Space Station and space environment requirements for monitoring of bacterial contaminants in water or other fluid systems.

#### **Adenosine Triphosphate**

Adenosine triphosphate (ATP) is found in all living cells where its hydrolysis to adenosine diphosphate (ADP) and inorganic phosphate provides free energy for growth. A bioluminescent assay has been developed for ATP and can be used for the enumeration of bacteria in water and culture media.[41]

ATP is detected using a system based on the enzyme luciferase and luciferin. As ATP is hydrolyzed, light is emitted and is quantified using a photometer. The technique may be cumbersome in that it requires some sample preparation. Furthermore, the turnover rate of the ATP pool in growing bacteria is extremely high such that rapid quenching of the cells is required to avoid ATP hydrolysis.

#### **Impedance Measurements**

Sinusoidal voltages applied between electrodes can be used to detect the presence of suspended bacteria. Impedance is a complex entity made up of a resistive and a reactive component. These techniques provide an automated system for real-time determination of microbial populations in liquid phases and several such systems have been commercialized. The most well-known of these approaches is the Coulter Counter™ Method.[42] Its operation is based on the electrical conductivity (at certain frequencies of oscillating voltages)

of bacterial suspensions being lower than that of the fluid in which they are suspended; thus, the presence of suspended matter is detected directly by its effect on the oscillating field. In the Coulter Counter method, bacteria are detected in a flow system. The Bugmeter™ has been developed for suspended micro-organisms, specifically for monitoring biomass concentrations during fermentations.[43] These devices are portable, and user-friendly, do not require cumbersome procedures, and can provide continuous monitoring capabilities. Presently they do not have the required sensitivity for bacterial monitoring of sparse populations, though research and development are underway to address this shortcoming.

#### **Fatty Acid Analysis**

Biolipids are components of bacterial membranes and can be monitored using capillary gas-liquid chromatography (cGLC) with very good resolution.[44] Additional sensitivity can be achieved utilizing detection systems such as electron capture detectors (ECD) or mass spectrometry techniques.[45] This approach offers the capability of detecting 1 cell/ml, as well as providing capabilities for the analysis of biofilms. However, chemical derivitization is required to form, for example, methyl esters of the fatty acids.

#### **Direct Counting**

This may be achieved using Scanning Electron Microscopy or Epifluorescence Microscopy. These techniques are likely to be labor intensive though epifluorescence is technically simple to perform. Epifluorescence employs stains that fluoresce when excited by a given wavelength of light emitting light of a different wavelength.

#### **Flow Cytometry/Light Scattering**

During the past decade, highly sophisticated flow cytometry instrumentation (i.e., Ortho, Coulter, Becton-Dickenson, etc.) has found numerous analytical applications for eukaryotic cell studies. Light scatter and fluorescent dye characteristics of single cells in homogeneous or heterogeneous populations can be rapidly detected by specialized light detectors with simultaneous data collection and storage. Thousands of cells can be processed in seconds and cell parameters such as size, nucleic acid and protein content, immunofluorescence characteristics, etc. can be analyzed. Since most eukaryotic cells range in size (diameter) from 8 nm (red blood cell) to 40-60 nm (epithelial and tissue culture), instruments have been optimized in design to accommodate analytical requirements for cells in this size range.

To date, these instruments and procedures have not found practical application to bacterial studies because of technical aspects; primarily because bacteria are approximately 1/1,000 the size of eukaryotic cells. Instruments have been modified for bacterial applications; however, these studies generally used cell concentrations of at least 10/ml.[46] Reports on detection of minimal numbers of bacteria (i.e., in a water sample or biological fluid sample) are scarce, although Mansour, *et al.*[47] applied this technology to detecting 10-100 bacteria/ml in blood after lysing all blood cells. Less sample preparation time would be encountered using water or urine; however, cell debris and bacteria-size inorganic particles create significant detection problems at the present time.

Flow cytometry instrumentation has been proposed as a component of the cytometry subsystem for Space

Station. However, the practicality of application for bacteria detection and monitoring in water samples remains largely unexplored.

### **Viable Counts**

This approach involves growing bacteria using culture media. Potential problems include the selectivity introduced by the media and the time delay associated with bacterial growth.

Rapid identification of bacteria from clinical specimens (i.e., urine, nasal and throat) is routinely accomplished using automated systems such as the Auto-Microbic System (Vitek Systems, Inc.). Differential and selective media contained within a single multiple-well cassette permits identification of most clinical pathogens within 4-6 hours. Sample inoculation, incubation, periodic photometric color-indicator analysis and identification are automatically performed. These techniques, however, are not well developed for bioburden monitoring of environmental samples (water) and when used, generally result in non-identification. Even if significant advances are made in identification of water micro-organisms using this type of analyses, logistics in support of the system would likely impose prohibitive penalties.

### **Microbial Fuel Cells**

Micro-organisms can donate electrons to redox dyes which can be used to transfer electrons to an electrode. The magnitude of the electrical current generated in this way can be used to accurately quantify the concentration of viable bacterial cells.[48; 49] This approach has been commercialized. The main uses for these devices have been in the monitoring of polluted waters. They have the advantage of being low-cost, portable units with a high potential for continuous monitoring and automation. The limitation of this approach for space applications is the limited range,  $10^4$ - $10^7$  cells/ml. Nevertheless, there are many sensitive electroanalytic techniques available that have not yet been applied to the detection of low levels of redox dyes in biofuel cell devices. This could greatly enhance the sensitivity of this approach towards sparse populations of bacteria.

## **Microbial Sensor Development**

The approach outlined in this section describes the features of a portable electronic device for the rapid detection and enumeration of bacteria. The proposed device will be suitable for inflight use by virtue of its compact design and functional simplicity while being highly sensitive to detecting microbial metabolic activity. The device utilizes an electrode for the direct determination of microbial metabolic activity based on the principle that bacteria can generate small electrical currents in the presence of redox dyes.[49; 50; 51] The proposed device requires minimal sample pretreatment and the electronics can be miniaturized thus enabling the construction of a low-cost portable detecting unit. Furthermore, it is envisaged that the presence of low levels of disinfectants (e.g. iodine) that are routinely used to maintain water quality will not interfere significantly with the monitoring device. This prototype has several features which satisfy key criteria for water monitoring requirements in the spaceflight environment:

- \* detects only viable bacteria
- \* applicable to both Gram positive and negative species

- \* applicable to filamentous forms, including yeast and protozoa
- \* can be used at multiple sites
- \* user friendly
- \* functionally simple yet highly sensitive
- \* can be battery powered or adapted to onboard power supply
- \* high potential for automation

In addition, this technology will have widespread applications to the management of food and water supplies on earth as well as in space.

### Technical Background

Color changes due to the reduction of dyes have been used extensively for the detection of microbial activity in milk and other foods.[52] This action is usually ascribed either to the direct action of microbial growth lowering the redox potential of the dye or by the direct reduction of the dye by dehydrogenase enzymes (e.g., NADH dehydrogenases) that are found inside the cell. [50]

The reduction of redox dyes by bacteria has been utilized extensively in microbial fuel cells.[50; 51] Microbial fuel cells (biofuel cells) are presently undergoing a rapid phase of development as a means of electrical energy generation from renewable resources or factory waste products.[53; 54] The principle by which microbial fuel cells operate is shown in Figure 6.12. micro-organisms have powerful oxidizing capabilities and, during the degradation of organic material, generate metabolic intermediates inside the cells that are

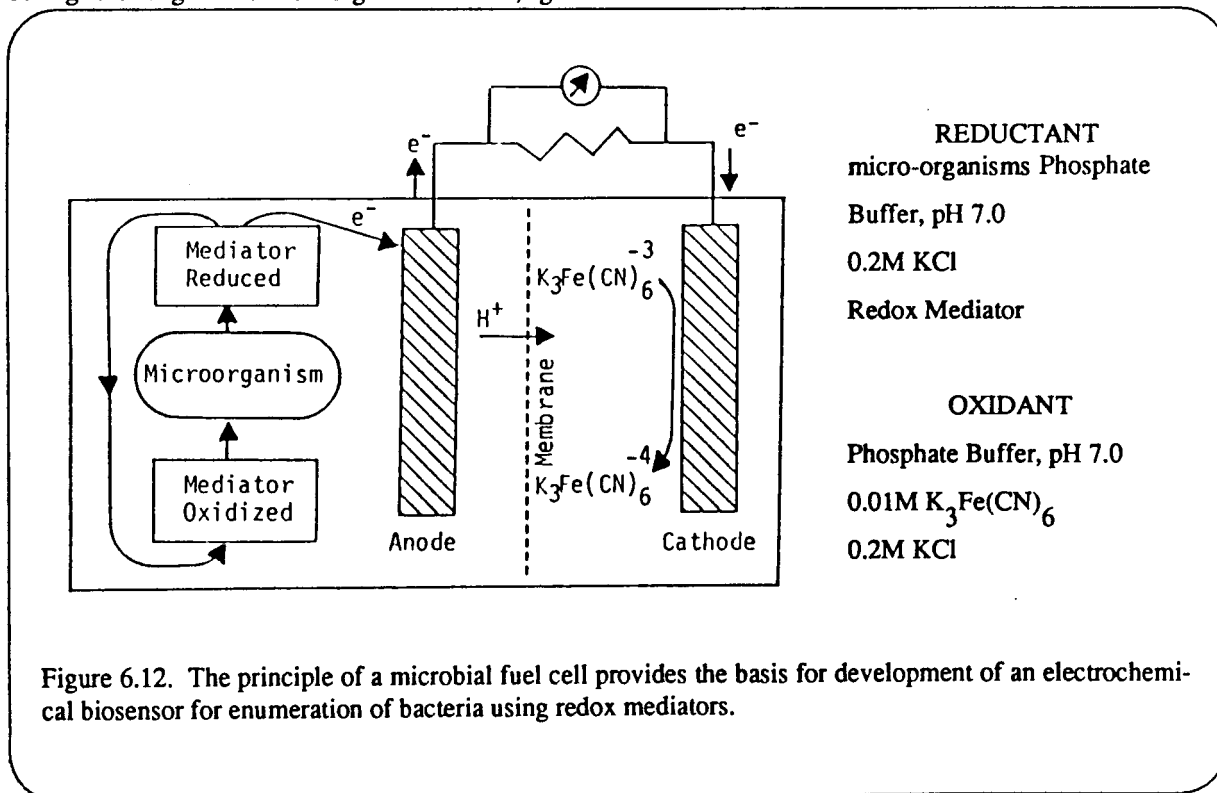


Figure 6.12. The principle of a microbial fuel cell provides the basis for development of an electrochemical biosensor for enumeration of bacteria using redox mediators.

during the degradation of organic material, generate metabolic intermediates inside the cells that are electron-rich. In the fuel cell, these electron-rich intermediates are turned into a flow of electrons through the use of redox dyes or redox mediators (i.e., low molecular weight electron acceptors) which are permeable to the bacterial cell membrane.[50; 55] The mediators, thus become reduced inside the cell and diffuse through the cell membrane where upon contact with a suitable electrode produce an electrical current; the electrical circuit is completed by the reduction of oxygen or a suitable electron acceptor (e.g., ferricyanide or oxygen) at the cathode (see Figure 6-12).

In addition to being able to penetrate the cell membrane, suitable mediators should possess the following characteristics:[55] (a) be non-toxic, (b) electrochemically active at the electrode surface, (c) have a standard redox potential near that of the redox couple providing the reducing action, which in many cases is  $\text{NAD}^+/\text{NADH}$ , (d) be chemically stable over a long period of time, and (e) reasonably soluble in a buffer solution at pH 7.0.

Several studies have shown that electrical currents generated by bacteria in the presence of redox mediators can be used as an accurate and convenient means of determining microbial cell concentrations in solutions. Nishikawa, *et al.*[56] utilized this concept for the direct determination the number of micro-organisms in polluted water. The device made use of a platinum anode and DPIC (2, 4-dichlorophenolindophenol) which was used as an electron transfer relay between the bacteria and the electrode at a potential suitable to ensure the oxidation of the DPIC with the subsequent determination of the steady state current change after the addition of the sample; the response time of the electrode system was 10 to 20 minutes. With known concentrations of *Bacillus subtilis* *Flavobacterium arbrescens* and *Pseudomonas aeruginosa* the measured current versus cell concentration was linear over the range  $10^4$  to  $10^6$  bacteria per ml. Experiments were performed on industrially polluted water and a preconcentration step involving membrane filtration was used. Results agreed well with the conventional colony count method.<sup>1</sup>

A similar technique involving a poised potential electrochemical cell was used by Turner *et al.*[49] with PES (phenazine ethosulphate) as the electron transfer relay. In this case, a number of bacterial species could be determined reproducibly between  $10^6$  and  $10^8$  bacteria per ml with a response time of 2 minutes. It was also recognized that bacteria utilizing endogenous substrates may limit the rate at which the redox mediator becomes reduced. Consequently, the cells were suspended in a buffered solution containing glucose. A recent study by Patchett *et al.* [58] focused on the use of this technique for the direct determination of bacterial contaminants in the dairy industry. Sensitivity down to  $10^5$  cells per ml was achieved using the redox mediator thionine, without a preconcentration step.

### Feasibility Studies

The objectives of this work are: (1) construct a portable electronic device for detection of electronic currents generated by bacteria in the presence of membrane-permeable redox dyes, and (2) identify the optimal

---

1. Caution should be exercised when making comparisons with existing methods such as colony counting which itself may have inherent errors such as clumping.[57]

conditions for direct detection and enumeration of water-borne bacteria over a wide range of concentrations (i.e.,  $10^2$  -  $10^6$ /ml). The development work will be performed on selected genera of bacteria that are typical contaminants previously found in the spacecraft potable water system (i.e., *Pseudomonas*, *Flavobacterium*, *Acinetobacter*, *Bacillus* and *Micrococcus*). The work will involve the following tasks:

1. Identification of the most effective redox dyes for transferring electrons between bacteria and the electrode and their optimum concentration.
2. Determination of the relationship of steady-state current against microbial cell concentration.
3. Develop techniques that will extend the concentration range over which micro-organisms can accurately be enumerated.
4. Perform experiments to assess if "cocktails" of redox mediators improve the accuracy of the technique when used on to water samples containing a variety of microbial species.
5. A major goal of the development of the sensor will be to improve the sensitivity to low levels of microbial contaminants. As yet, none of the analytical procedures available for the detection of low levels of electroactive components have been applied to this technology. Techniques such as the use of pulse voltammetry in combination with high-resolution microelectrodes can be applied to the detection of low levels of redox dyes and allow the enumeration of sparse populations of bacteria.
6. Hardware development and flight experiment.

## 6.5 Food Production

### Design of the Low Pressure Plant Growth Chamber

The ability to grow food plants at low atmospheric pressure has important implications for the design, deployment, and operation of space-based plant growth facilities. The use of higher plants in long-term Moon, Mars, or orbital-based missions requires that relatively large areas be dedicated to their growth. If plants are grown at Earth's atmospheric composition and pressure, then the plant growth facility must be capable of containing 100 kPa. If plants could be grown at reduced atmospheric pressure, however, several advantages could be achieved.

- \* A reduced pressure differential between the plant growth facility and its external environment might permit less massive materials to be used in its construction.
- \* Reducing the mass of the plant growth facility would reduce the total lift-off payload required to deploy the facility.
- \* The material used in the construction of an extraterrestrial (e.g., subterranean lunar) plant growth facility with a reduced pressure differential with respect to its environment could be a flexible polymer instead of rigid materials, which would reduce the payload volume required for deployment.
- \* A lower pressure differential between the plant growth facility and its environment would logarithmically reduce atmospheric leakage from the facility to its environment.
- \* The lower total pressure of the plant growth facility would require less  $N_2$  gas to be transported to supplement the physiologically active gases ( $CO_2$  and  $O_2$ ).

Our primary objective was to grow plants at the same concentration (moles/volume), or partial pressures, of  $CO_2$  and  $O_2$  in the presence or absence of  $N_2$  and determine if plant growth rate is affected by the pressure of the growth environment. Thus, the system must be able to establish and maintain a particular pressure and environmental regime; this regime must remain uninterrupted during a plant's entire growth with minimal monitoring. In addition, it must be possible to add and remove individual plant growth chambers from the system without disrupting the environment established in the other chambers.

Scale-up to food production scale can be estimated from experiments conducted in the semi-automated plant growth system which we developed. The system consists of four plant growth chambers enclosed within a large environmental chamber to maintain a constant light and temperature regime. Gas of defined composition (known  $N_2$ ,  $O_2$ , and  $CO_2$  partial pressures) flows at a controllable rate through each of the four plant growth chambers. The composition of this gas can be monitored entering and exiting the plant growth chambers by a separate instrumentation rack. The instrumentation rack contains all the control, monitoring, and data acquisition equipment.

Separate plant growth chambers were placed in a single environmental chamber<sup>2</sup> (Figure 6.13) to minimize environmental variability. At plant height, the normal light<sup>3</sup> flux is  $750 \text{ umole-m}^{-2}\text{-s}^{-1}$  and temperatures

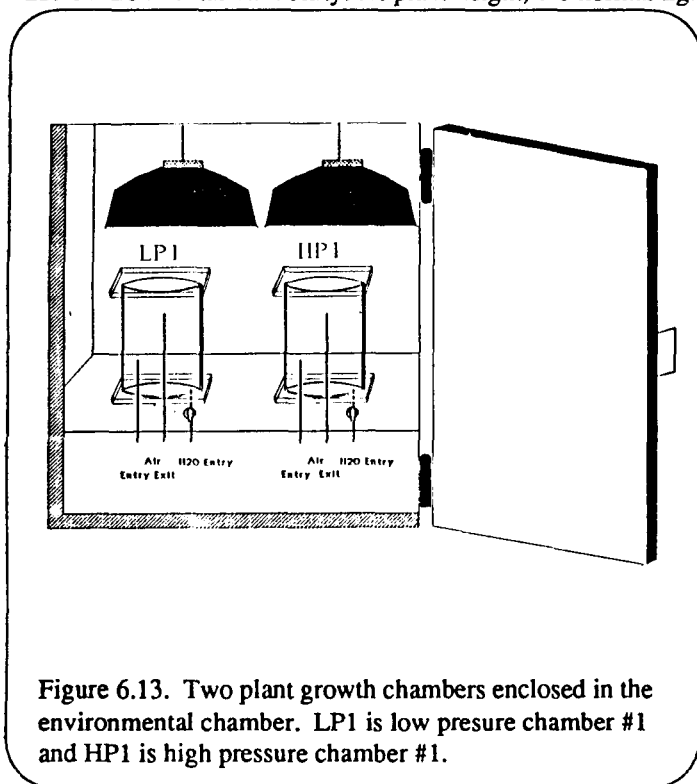


Figure 6.13. Two plant growth chambers enclosed in the environmental chamber. LP1 is low pressure chamber #1 and HP1 is high pressure chamber #1.

can be maintained within  $1^{\circ}\text{C}$  of the set point. Water can be added to the chamber by opening a valve connected to a water reservoir exposed to atmospheric pressure.

Gas for the low pressure system is mixed in standard 50 liter volume commercial cylinders using industrial grade<sup>4</sup> gas, and standard pressure tubing and regulators as required. The gas for the high pressure system comes predominantly from an air line piped into the lab from compressed air. This air stream can be modified by addition of other gases. Currently, only pure  $\text{CO}_2$  is added to the compressed air.

The flow rate of gas through the low pressure system is controlled by a standard mass flow controller<sup>5</sup>. This gas stream is

equally subdivided to each connected chamber by manually adjusting each chamber's rotometer<sup>6</sup> to the same level (see left side of Figure 6.14). As gas exits each chamber, it is routed to the central flow selector (center right in Figure 6.14). The gas flow from a chamber can be diverted either directly to the exit vacuum sink, or it can be diverted first to the instrument loop for gas analysis.

The pressure of the low pressure system is stabilized to its set point by a programmed feedback loop between a transducer pressure gauge<sup>7</sup> and the exit mass flow controller. If pressure increases or decreases in the low pressure system, then the mass flow controller opens or closes proportionally to compensate and eliminate such pressure differentials. In this manner, the pressure of the low pressure system can be maintained to within 0.1 kPa.

2. Our use and citation of various commercial products does not constitute an endorsement of these products. Growth chamber (model CEL 36-10 from Warren Sherer, Marshall, MI) has interior dimensions of 2.5 ft. width, 5 ft. height, and 4 ft. length; there is no humidity control.
3. The light system is composed of eight fluorescent lights mixed with two sodium vapor lamps.
4. Gas supplies obtained from Bailey Oxygen and Tool Company, Inc. Bryan, TX.
5. Mass flow controllers are of the 280 series from Tylan, Carson, CA.
6. Rotometers from Dwyer Instruments, Inc., Michigan City, IN.
7. Pressure gauge is an absolute pressure transducer, Model 122A, from MKS Instruments, Inc., Andover, MA.

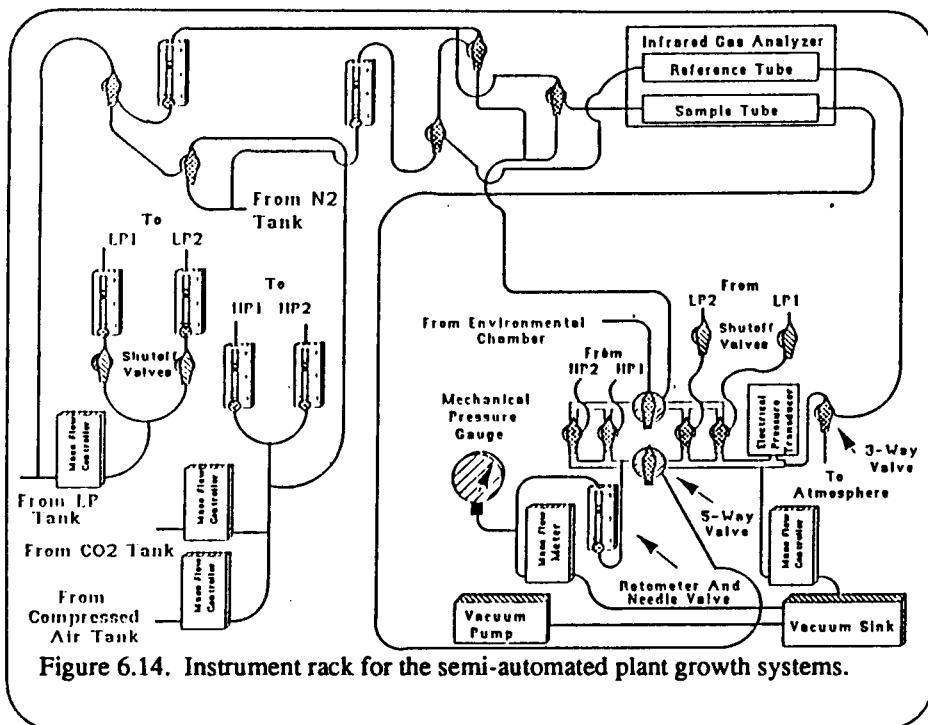


Figure 6.14. Instrument rack for the semi-automated plant growth systems.

The mass flow and gas composition through the high pressure system are controlled by two mass flow controllers (Figure 6.14). One controller regulates normal atmospheric air. Its rate of mass flow is a multiple of the entry mass flow rate of the low pressure system. The multiple is the fraction: (HP system pressure)/(LP system

pressure). This dictates that the volume flow is equal in both pressure regimes. The mass flow of the second entry mass flow controller on the high pressure system modifies the gas composition of the incoming atmospheric air to experimental composition. Thus the rate at which the second mass flow controller operates depends upon the rate of the first.

The high pressure system is set by adjusting the back pressure using a needle valve on the exit rotometer. The stability of this control is within 2 kPa, which is sufficient at high pressure, but tends to be unacceptable at lower pressures where it becomes a significant percent of the total pressure.

Using multi-port valves on the instrument rack, gas from any source (tank, chamber, or atmosphere) can be diverted to either the instrument loop, the reference loop, or both at the same time, and the pressure in either loop can be independently linked to either the low or high pressure system.

The data acquisition and process control of the semi-automated plant growth system is conducted by an IBM AT compatible computer via an ACRO-900<sup>8</sup> data acquisition control system. Our system contains three different modules. Two are used for gas flow and composition analysis and control. The third module is used for temperature sensing.

A commercial software program<sup>9</sup> receives, processes, generates, and stores the digital signals associated

8. The ACRO-900 system is configured with modules ACRO-916, ACRO-921, and ACRO-931, from Acrosystems Corp., Beverly, MA.

9. The data acquisition and process control program is called Labtech Notebook from Laboratory Technologies Corp., Wilmington, MA.

with the data acquisition and process control of the semi-automated plant growth system. The program maintains constant mass flow and pressure in the low pressure system, and generates a file for each data channel (mass flows, compositions and temperatures).

A gas chromatograph<sup>10</sup> with a standard thermal conductivity detector<sup>11</sup> operated at 70°C and 200 mA. Helium carrier gas at 60 kPa and a flow of 20 ml/min with a column<sup>12</sup> temperature of 25°C was used to test gas composition.

## Novel Lighting Source for Plant Growth

3M has recently developed a thin film which can pipe light. This Scotch Optical Lighting Film is 0.020 inches thick and has tiny ridges which cause the light to disperse evenly along the surface. The film is formed from either acrylic or polycarbonate.[59] This film has obvious applications to the growth of higher plants on algae in space.

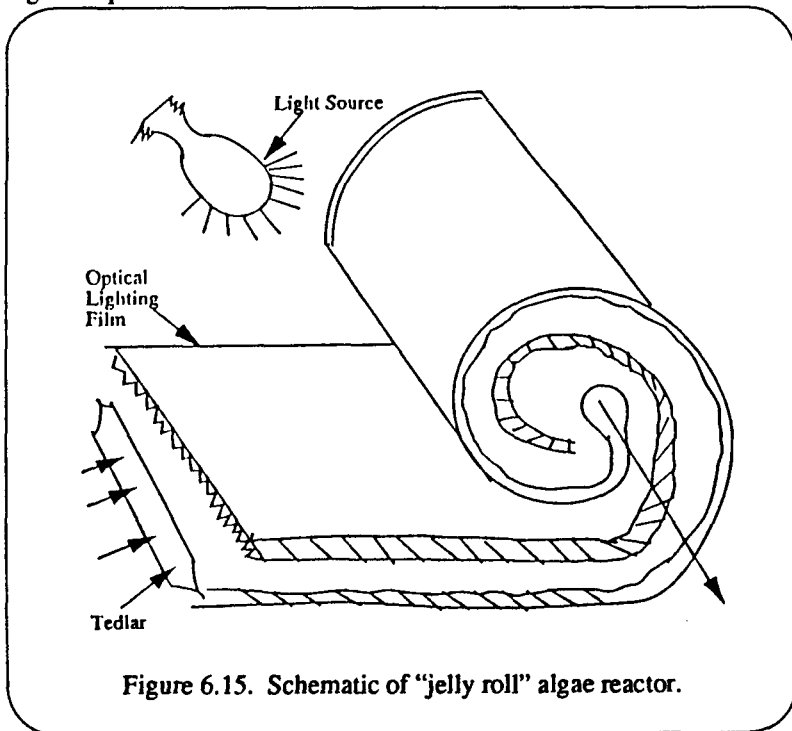


Figure 6.15. Schematic of "jelly roll" algae reactor.

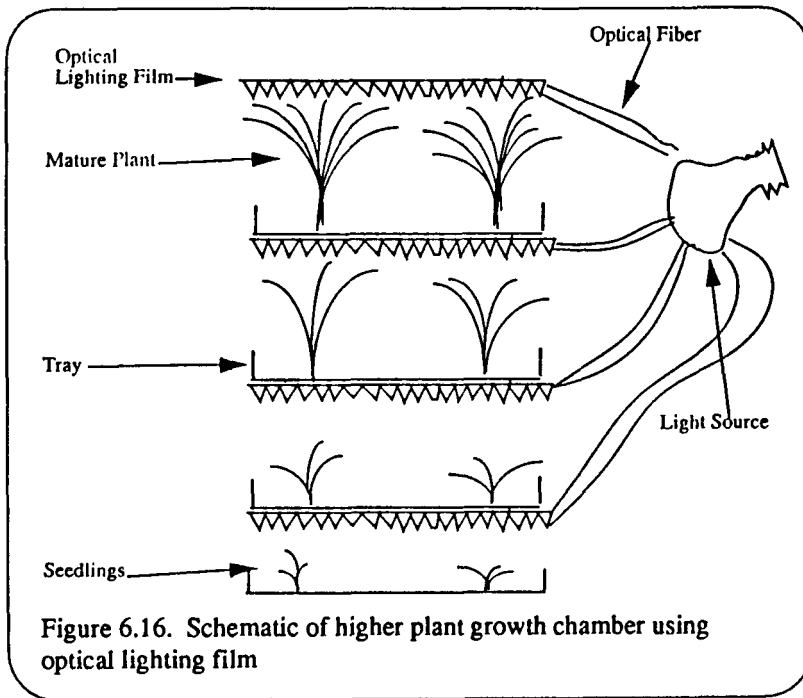
## Higher Plant Growth

Figure 6.15 shows a higher plant growth chamber which uses the optical film. Plants grow in trays using hydroponics or soil, whichever is more appropriate to the species. The trays are stacked on top of each other. The spacing between the trays is variable so valuable space is not wasted by seedlings. The underside of each tray (except for the bottom one) has the optical lighting film attached. An optical fiber connects the optical lighting film to the light source which can be artificial or solar.

10. Gas chromatograph was a Varion Aerograph, Series 1700. Varian Inst. Co., Sunnyvale, CA.

11. Thermal Conductivity Detector was a Model 10-952-wf from Gow-Mac, Inc., Bound Brook, NJ.

12. CTR-1 column. This column actually consists of 2 columns: one is contained within another. The inner column is a molecular sieve, which separates O<sub>2</sub> and N<sub>2</sub>. The outer column is a porous polymer which can separate CO<sub>2</sub> from air. Catalog # 8700 from Alltech Associates, Inc., Deerfield, IL.



## Algae Growth Chamber

The optical lighting film may be used to culture algae as well as higher plants. Figure 6.16 shows a schematic of a "jelly roll" algae reactor. Tedlar (a Teflon film) would be heat sealed or clamped at the edges forming a rectangular channel. Tedlar is a superior choice because it has a high transparency. Since it is extremely inert, it may be sterilized with chemical sterilants. Alternatively, it could be sterilized using heat. Because Tedlar is so slippery, it will be difficult for algal films to coat the interior.

Optical lighting film will be placed adjacent to the Tedlar rectangular channel. The entire assembly will be rolled around a central tube much like a jelly roll. The liquid flowing into the Tedlar channel flows out through the central tube. The entire system is illuminated from the side.

The "jelly roll" algae reactor should have extremely high illumination efficiency since the illumination path should be very short. Harvesting and cooling will be performed in other pieces of equipment.

## 6.6 Food Processing

### Higher Plant Processing

#### The Importance of Food Processing in Space

The permanent presence of humans in space requires efficient life support systems that include satisfying basic human dietary needs for food. NASA has identified eight plants (wheat, rice, white or Irish potato, sweet potato, soybean, peanut, lettuce, sugar beet) for intensive study, growth, harvesting and processing in a space environment.[60] Several combinations of these plants can meet most if not all human dietary needs for calories, carbohydrates, proteins, fats and fiber.

Most of the research effort on plant growth thus far, however, has concentrated on the design of space-based plant growth facilities,[61] and on intensive cultivation techniques to maximize food production while minimizing space requirements.[62] Toward that end, studies have presently achieved chamber designs and plant growth techniques by which the caloric requirements of one man can be met by only 25 m<sup>2</sup> of cultivated surface area using either wheat[63] or potatoes.[64]

Nevertheless, a key component of this food production process which has been relatively neglected is the processing of the raw, harvested food material into a form edible by humans. Procedures and equipment are needed by which these crops can be processed easily into edible, nutritious foods without requiring excessive lift-off weight, energy and power reserves of the space facilities, and the astronauts' time.

The processing of foods in a space environment is not likely to be an easy task. Wheat, rice and soybean contain outer protective husks or hulls that protect the inner nutritive portions from the environment. An oil-bearing seed such as soybean typically requires cleaning, thermal preconditioning, cracking, hull separation and thermal conditioning prior to conventional extraction methods to obtain high yields of edible oil. While rice and soybean contain anti-nutritional factors that can be deactivated by cooking or by other thermal methods, conventional cleaning, cracking and hull separation procedures, as they exist now, require a gravitational field and thus would not be applicable in space. The adaptation of food processing technology to space environments (orbiting space station, Lunar base, Mars missions) therefore becomes a critical component to the successful conquest of space.

#### Considerations

There are several important points to be considered in planning, developing and processing procedures for long-duration space environments. These include designs to:

1. Develop novel methods and procedures for separating proteins, simple and complex carbohydrates, fats or triglycerides, fiber and gums from the selected plants.
2. Reconstitute the constituents in an optimum manner from nutritional, taste, flavor, and texture viewpoints.
3. Institute a sensor development and evaluation program required for continuous monitoring of changing food properties during processing and storage for nutritional and safety reasons.

## **Background**

Many types of plants have evolved various defense mechanisms to discourage herbivory, even by humans. These range from outer protective hulls or shells, which must be removed, to inedible or toxic chemicals, which must be denatured or eliminated.

The milling of wheat, which is a very carefully controlled process, illustrates the often tedious procedures involved in preparing a crop for human consumption. The first step is the thorough cleaning of the grain to remove any foreign substance. During this process the brush of the grain is removed. The cleaned grain is then moistened slightly in order to soften the outer layers so that they may be more easily removed subsequently. The moistened grain is then passed between iron rollers. The first of these rollers is corrugated and breaks up the grains. Each successive pair of rollers grinds the grain into finer and finer particles. Early in this grinding, the coarse flakes of bran and the germ are removed. These are disposed of or ground up separately. The ground grain is passed through fine bolting silks which insure a very even grade of fineness of the flour particles. Every precaution must be taken in flour mills to prevent the accumulation of dust particles in the atmosphere, since they may form very dangerous explosive mixtures.

## **Preliminary Evaluation**

We instituted a preliminary evaluation toward identifying problems in food processing likely to be specific to space applications. The objectives of our analysis were to:

1. Evaluate current food processing technologies with respect to their suitability or adaptability for food processing in a space environment.
2. Identify special food processing needs and limitations for a long-term space crew with respect to nutritional requirements, plant growth and harvesting facilities, space-related environmental complications (e.g., no or low gravity) and mass, power and time constraints.
3. Review processing equipment with emphasis on miniaturization and single-step equipment integration.

## **Processing Requirements**

The primary emphasis of our preliminary evaluation was on the four selected plants that contain hulls or husks: wheat, rice, soybeans and peanuts. We conclude that soybean hulls can be eaten if properly cooked to constitute a high-fiber, low-protein meal, but the long-term effects on the human digestive system are uncertain. Hull or husk removal for wheat, rice and peanuts is, however, considered necessary. Processing efforts will be more difficult for these plantings than for white and sweet potatoes, sugar beets and lettuce. We propose conventional microwave heating for white and sweet potatoes, sugar beets and brown rice (i.e., de-husked rice), dry roasting of de-hulled peanuts, no processing at all for lettuce, and extrusion cooking of blends of soybeans and wheat. The long-term emphasis must be on extrusion cooking of selected blends of ingredients in order to minimize time constraints in food preparation.

## Extrusion Processing

Conventional processes for extraction of vegetable oils from the two oilseeds of interest to NASA, peanut and soybean, are based on solvent extraction techniques. A comparison of direct solvent extraction with prepress/solvent extraction and screw pressing operations is given in Figure 6.17. (Because of the high oil content of peanuts, screw pressing is required prior to direct solvent extraction.) Solvent extraction operations lead

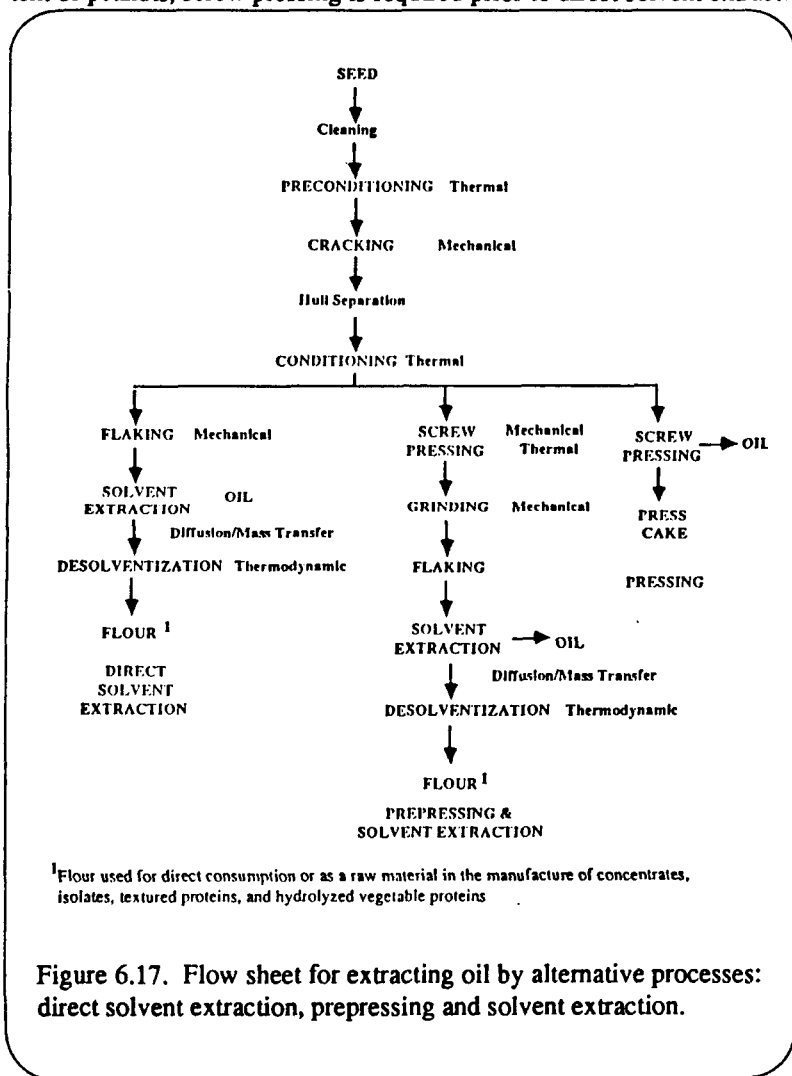


Figure 6.17. Flow sheet for extracting oil by alternative processes: direct solvent extraction, prepressing and solvent extraction.

to the evolution of combustible vapors which could pose serious safety threats to the crew of a space-based station. The combustible vapors of interest in oilseeds processing are limited primarily to commercial grade hexane and, to a lesser extent, to the lower molecular weight alcohols (ethyl and isopropyl), the petroleum ethers and acetone.[65] Only ethyl alcohol has any potential as an extractant for deep space missions or colonies on Mars or the Moon, because it can be obtained easily by fermentation reactions involving potatoes, sugar beets, rice and wheat.

Today's extractors are based on modifications and improvements on immersion and percolation bed extractors introduced by the Germans prior to World War II. The immersion extractor employs a U-tube system and conveys the oilseed

by a screw through a solvent stream introduced in the opposite part of the U-tube system. This type of extractor was marketed some thirty or more years ago, but it is rarely used today. In the percolation extractor the solvents and miscella (oil in solvent solution) flow by gravity through a bed of solids. Because of the need for a gravitational field, this extraction principle is not applicable to the space environment. A comprehensive discussion of the details of solvent extraction is clearly outside of the scope of this report, since several reviews the size of textbooks are needed to treat handling and cleaning of materials, size reductions, preconditioning, hull separation, thermal conditioning, mechanical conditioning, extraction, evaporation, stripping, filtration, and desolventizing.

In the initial phases of extended space habitation, screw pressing operations could readily be used to extract oils from the oilseeds, although at reduced efficiencies compared to current procedures on Earth. For example, continuous screw presses are used commercially to reduce the residual oil down to different levels, generally 5-9% (i.e., a hard press) and 10-15% (i.e., pre-press operation for solvent extraction), in comparison to a typical 1% for solvent extraction operations. The recent use of enzymes to destroy oil pocket membranes present in canola[66] and earlier in soybean, rice bran and peanuts, affords the potential for improvements in residual oil reductions for screw pressing and for the minimization or elimination of complex, high-cost mechanical and/or thermal pretreatment operations for soybean and possibly for wheat.

Research at the Food Protein R&D Center has shown that extrusion of soybean and rice bran can be used to inactivate anti-nutritional factors associated with these plantings. Additional studies have shown that low-cost edible and palatable products can be made from combinations of whole (de-hulled) soybean, ground wheat flour with combinations of whole and ground degermed white corn and sugar by heating in a single step in a short residence time extruder.[67] Elevated product temperatures during extrusion deactivate trypsin and urease activities. These temperatures typically range from 190 to 240°F (88 to 115°C).

A critical issue pertaining to both extrusion and screw press operations is that the equipment used therein is characterized by heavy and bulky sizes with throughputs ranging from the hundred-pound-per-hour level to the thousand-pound range, even for pilot-scale sized equipment. Scaling down of equipment to much smaller sizes and weights requires not only that geometrical similarity must be preserved, but that similar shear and thermal stresses must also be produced during extrusion and screw pressing in order to anticipate similar behavior. This necessitates that a modeling effort be undertaken in conjunction with experimental studies on smaller diameter extruders to attempt to duplicate the performance demonstrated by Farnsworth and Wagner[67] in earlier studies.

Similar issues pertain to the removal of hulls or husks from rice, soybean, wheat and peanuts. Furthermore, different equipment is used for each planting because of differences in overall size, hull thickness and hardness, and also due to characteristic differences in the edible inner portions of these foods. The Food Protein R&D Center has various hullers applicable to soybean and peanuts, and routinely processes these oilseeds as part of its mission to the Natural Fibers and Food Protein Commission of Texas. In addition, a Forsberg attrition mill which is applicable to dehulling barley might function on wheat and rice. While these methods are available, they are considered to pose too high a price on weight considerations for lift-off into space. The development of enzymes for hull removal offers an attractive alternative which should be fully explored before devoting much effort to conventional dehulling approaches.

Rapid analysis instrumentation is needed for continuous monitoring of changing food properties during processing and storage for nutritional and safety reasons. Such instrumentation must be fully automated and relatively easy to use by astronauts who will have other duties and limited time, while being sufficiently rugged to function in-line or on-line whenever required. It must nevertheless be sufficiently sophisticated with capabilities to monitor at least protein, starch, sugars, oils, water, lipase, urease, trypsin inhibitor, and aflatoxin. Earlier

efforts in the rapid analysis area[65] need to be updated and applied to a broader base of foods of interest to NASA.

### AFEX Processing of Plant Waste

The Ammonia Freeze Explosion (AFEX) process may be used to convert cellulosic plant residues to sugar. The sugar may be consumed directly by the astronauts or fed to other animals or microbes.

The AFEX process contacts the plant residue with liquid ammonia at room temperature and 120 psig for about 15 minutes. This decrystallizes the cellulose. Then, the pressure is instantaneously released to 1 atm. The liquid ammonia violently flashes causing the cellulose fibers to be disrupted, thus greatly increasing the accessible surface area of the cellulose. The temperature drops to  $-30^{\circ}\text{F}$  during the flash. The combined chemical/physical effects of the AFEX process significantly enhances the reactivity of the cellulose to attack by cellulase enzymes. Figure 6.18 shows that AFEX-treated wheat straw produces twice as much sugar with only an eighth the enzyme compared to untreated wheat straw.

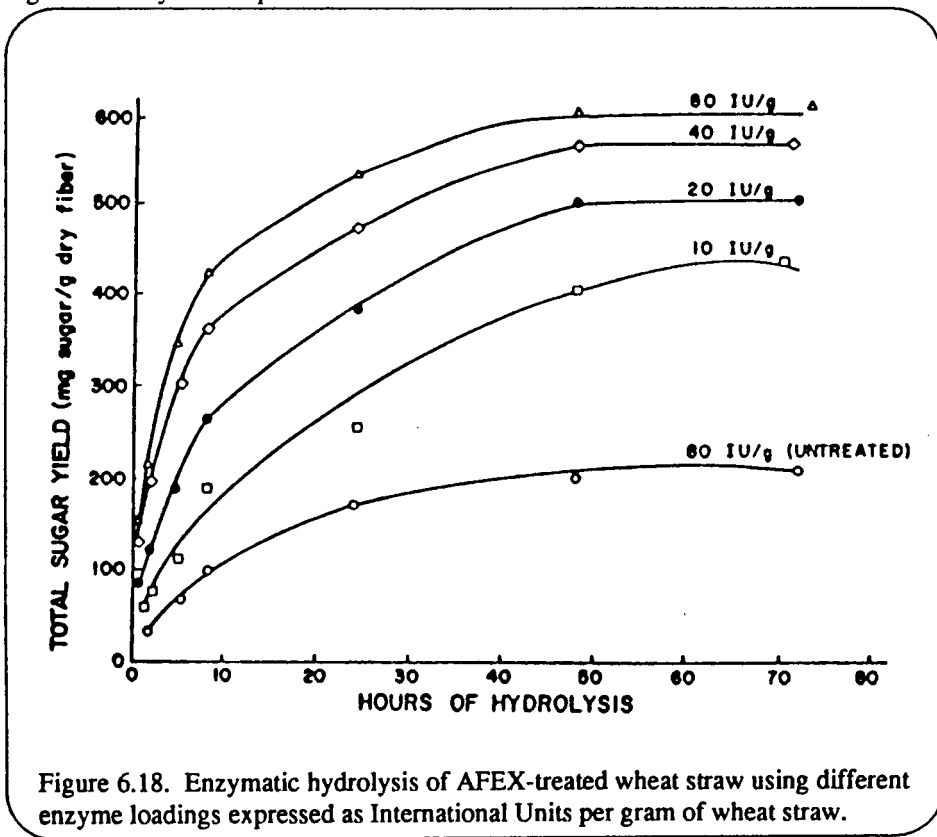


Figure 6.18. Enzymatic hydrolysis of AFEX-treated wheat straw using different enzyme loadings expressed as International Units per gram of wheat straw.

A schematic of an AFEX unit suitable for space applications is shown in Figure 6.19. The plant residue is loaded into the reactor. Then liquid ammonia is added by opening Valve C. After waiting 15 minutes, Valve A is quickly opened, which allows the ammonia to flash into the flexible bag. Then Valve B is opened, allowing the compressor to remove the ammonia from the flexible bag. The high-

pressure ammonia vapors are condensed and collected in the ammonia tank for reuse. Any ammonia which remains in the plant residue will be removed by heating the reactor to room temperature, which drives off the ammonia. The ammonia vapors are compressed, condensed, and collected for recycling.

The AFEX process is very similar to steam explosion. However, it has many benefits compared to steam explosion. Because the AFEX process occurs at room temperature and below, the valuable protein components of the plant residue are not damaged. Steam explosion subjects the biomass to high temperatures which destroy

the protein. Also, the high temperature of steam explosion degrades the biomass forming potentially toxic organic acids. Lastly, AFEX-treated plant residues are much more reactive to cellulose because of the strong decrystallizing effects of ammonia.

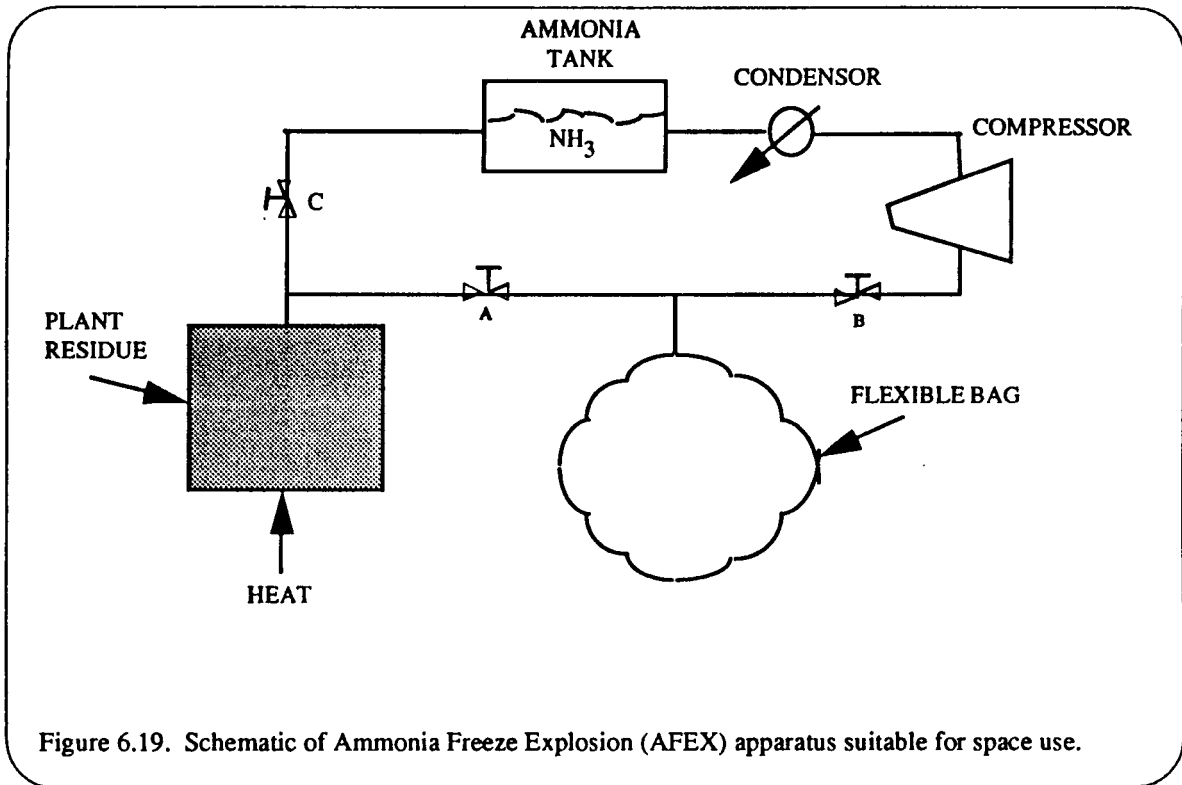


Figure 6.19. Schematic of Ammonia Freeze Explosion (AFEX) apparatus suitable for space use.

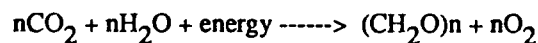
## Algae Processing

If humans are to survive in space, they must be supplied with breathable air, edible and nutritious food, and drinkable water. In addition, wastes must be disposed of. Although it is possible for missions of short duration and small crew sizes to load on board all the required supplies and gradually use them up over the course of the mission, this is impractical for long missions or large crew sizes. An alternative approach is to recycle wastes and regenerate air, water, and food via on-board systems. Recycling of air and water can be accomplished using physico-chemical technologies (distillation, filtration, electrolysis, catalytic reduction, etc) but no such techniques are available for food production. A chemical technique for direct food synthesis, the so-called formose reaction, has been explored, but has been unsuccessful. The formose reaction synthesizes sugars by a catalyzed reaction between  $CO$  and  $H_2$ . But since the reaction produces equi-molar amounts of the D and L isomers, and since organisms such as humans can utilize only the D isomers, a maximum of 50% of the product would be usable as food. Because a wide variety of sugars is formed, including some which are indigestible by humans, even less is available. Furthermore, certain toxic compounds including formaldehyde are formed in side-reactions. Feeding studies with rats have shown that when as much as 40% of the diet is

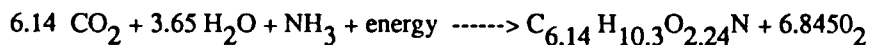
biological one is presently available to synthesize food. Food can be produced only by growing organisms. This being the case, we must select the best organisms and learn how best to grow and process them.

A wide range of organisms for food production have been proposed for use in space. Clearly, the best organisms for space food production are photosynthetic ones, because they contribute not only to food production but to air regeneration as well (replenishment of O<sub>2</sub>, removal of CO<sub>2</sub>). Although other organisms (yeast, hydrogen-utilizing bacteria, methanol-utilizing bacteria, and even fish and shrimp) have been proposed, all of these increase the load on other life-support systems. Photosynthetic organisms (algae and higher plants) are clearly more suitable.

All photosynthetic food-production systems depend on the same fundamental process, namely oxygenic photosynthesis. Although photosynthesis actually consists of several dozen partial reactions occurring in sequence, it can be summarized as



where (CH<sub>2</sub>O)<sub>n</sub> represents carbohydrate such as might be used for food. Energy is supplied as visible light. In fact, the above equation is an oversimplification, because the final product of photosynthesis by any organism is more of that organism. For example, the product of photosynthesis by algae is more algal cells. Because algal cells are not 100 percent carbohydrate, but contain other reduced organic molecules as well, there is not a 1:1 stoichiometry between CO<sub>2</sub> uptake and O<sub>2</sub> production. Therefore, a more accurate equation should be used to describe the overall process of the bioreactor:



The C<sub>6.14</sub> H<sub>10.3</sub> O<sub>2.24</sub> N product in this equation reflects the overall composition of a typical *Spirulina* cell. But even this equation is incomplete, because growing algal cells also incorporate sulfur, phosphorus, potassium, iron, magnesium, and about 10-15 other elements. But carbon, hydrogen, oxygen, and nitrogen account for 96-98 percent of the mass of the algal cells, and therefore the above equation accounts for virtually all the algal biomass accumulation.

Algal bioreactors originally appeared attractive as components of CELSS because of their gas exchange capacities, i.e. removal of CO<sub>2</sub> from cabin atmosphere and replenishment of O<sub>2</sub>. It is obvious that such gas exchange is accomplished only as a by-product of biomass production. That is, CO<sub>2</sub> removal and O<sub>2</sub> release are stoichiometrically coupled to accumulation of algal cells. Unless these algal cells are consumed by the astronauts, they represent an ever-increasing mass of waste product that must be stored. In such a case, food stores would gradually be exchanged for stored algal biomass.

The same analysis applies to any photosynthetic organism that is not completely consumed in astronaut diets. Higher plants such as wheat, soybeans, etc. typically produce about 50-60 percent of their mass as edible portions. The remaining 40-50 percent of the biomass is inedible by humans and must be stored, dumped, or decomposed. Only that fraction of biomass production that can be eaten by the crew represents a net

contribution toward closure of the system with regard to O<sub>2</sub>. In order to approach complete closure of a regenerative system, it is necessary that the photosynthetic organism form at least part of the astronaut diet.

Higher plants have the advantages of familiarity, palatability, and reasonably well-defined growth requirements. In addition, processing techniques in earth gravity are reasonably well understood, although detailed procedures for harvesting, cleaning, milling, storage, cooking, and other preparation in low-gravity situations have barely been considered and are certainly not now ready for use. Unfortunately, higher plants take up a great deal of volume and usually produce a significant fraction (40-60%) of their total biomass as inedible material (stems, husks, etc.). Because of the species-specific architecture of higher plants, it is often difficult to deliver necessary light levels to them efficiently, so if electric lamps supply the light, power requirements are high. In addition, higher plants tend to be deficient in certain essential amino acids, so that long-term human consumption of a diet based solely on higher plants would probably require amino acid supplements from some other source.

Algae have the advantages of extreme compactness, ease of handling, and high production efficiency. Micro-algae such as *Spirulina*, *Scenedesmus*, and others are routinely grown in bio-reactors which lend themselves to automated or computerized management including growth and harvesting. In general, requirements for algal growth are well-defined. Like higher plants, algae must be processed before human consumption. Neither algae nor higher plants are suitable in their raw state for a large fraction of the human diet.

Nutritional properties of algae have been examined; available information has been exhaustively reviewed by Becker.[71] Microalgae such as *Spirulina* have been shown to be rich in essential amino acids, especially those typically missing from higher plants. Algae such as *Spirulina* in almost their raw, unprocessed state have been included in the diets of various peoples for thousands of years. Likewise, complex polysaccharides such as alginates and carageenans are extracted from kelps and other marine macro-algae and included in virtually all commercially produced ice creams and puddings sold in the U.S. today. There have therefore been reasons to believe that raw algae might be suitable for astronaut diets. But lab feeding experiments with chickens, rats, and human volunteers have not borne out this optimism. It is now evident that certain difficulties arise when raw algae make up a major portion of the human diet. These difficulties are as follows:

1. Many species, such as *Chlorella* and other green algae, possess tough cellulosic cell walls which are largely indigestible by humans.
2. Some species are unpalatable to North Americans due to taste, odor, and color. It appears that these problems are associated with the high pigment content of the cells, and can be minimized or eliminated by removal of the pigments (chlorophyll, carotenoids, etc.).
3. Algal cells, like all micro-organisms, possess a higher nucleic acid content per cell than do higher organisms. Since nucleic acids contain purines, ingestion of raw micro-organisms produces a high-purine diet. The end-product of purine catabolism in humans is uric acid. Uric acid is only slightly soluble at the pH of

human body fluids; thus there is some risk that urates may be deposited in the renal tract (kidney stones) or in the skeletal joints (gout), if the diet contains excessive purines.

4. Some species, especially among the blue-green algae (cyanobacteria) produce toxic compounds under certain growth conditions.

The features mentioned above clearly require two kinds of management strategies to make algal biomass suitable for human nutrition. First, we must choose the appropriate species and strain(s), those which are known to have a thin, easily broken outer wall and which produce no toxic materials, Second, we must develop appropriate processing techniques to remove pigments and nucleic acids. Both steps are necessary to obtain biomass which is palatable, easily digestible, and nutritious for humans.

Fortunately, progress has already been made on the first requirement. Species of algae have already been identified which possess thin walls and produce no toxins. The blue-green alga, *Spirulina*, has an outer wall so thin and fragile that it is disrupted merely by drying cells. Furthermore, *Spirulina* has been consumed by primitive peoples in Central America and Africa for hundreds of years and today is consumed by hundreds of thousands of people in North America as a health aid or diet supplement. No problems with toxicity have been reported. *Spirulina* has received FDA approval as a food additive and dietary supplement. This is not to say that *Spirulina* will necessarily prove to be the optimal organism for human diets, but merely that our experience with this particular species demonstrates that it is possible to find an alga which meets our requirements. Some strains of the green alga, *Scenedesmus*, also appear to have easily rupturable walls and to show an absence of toxin production. Other suitable species can probably be isolated with little difficulty.

Less work has been done on the second strategy, namely the processing techniques for removal of undesirable compounds. Perhaps the most serious problems here are the pigments and the purines. In addition to the taste, odor, and color problems associated with high pigment contents, there is also danger of photosensitized skin irritations in human subjects who receive excessive pigments in the diet. According to reports from Japan, chlorophyll degradation products such as pheophorbide-A caused photosensitized skin irritation in humans who consumed *Chlorella*. The Japanese Ministry of Health established the standard in 1981 that pheophorbide concentration in *Chlorella* products sold commercially should not exceed 100 mg/100 gram of material. Chlorophyll concentrations in algal cells vary with growth conditions (especially light intensity) but are usually about 1.5-4.5% of the dry weight. Likewise, conversion rates from chlorophyll to pheophorbides vary with processing and storage conditions. It is therefore most difficult to predict pheophorbide levels in a given batch of cells, but in general it is obvious that processing techniques which remove as much of the cell pigments as possible will be desirable.

All micro-organisms contain relatively high amounts of nucleic acids (DNA and RNA) in their cells. However, the value for algae (3-6% of dry weight) is lower than that for yeast (8-12% of dry weight) and for bacteria (up to 20% of dry weight). Nevertheless even for algae it will be necessary to lower the nucleic acid fraction by processing if algae are to contribute a major fraction of the human diet. The Protein-Calorie Advisory Group of the United Nations has recommended[72] that nucleic acid consumption by adult humans

should not exceed 4.0 gm/day from all sources. Some authorities now recommend a maximum nucleic acid intake of 2 gm/day for adult humans.[73] It has been estimated that if a human's entire diet were supplied by algae, the human would consume about 500-600 grams of algal material per day. To stay within PAG recommendations, the algal material should contain no more than about 0.66% nucleic acids (dry weight), that is about a ten-fold decrease in nucleic acid content after processing.

Several techniques have been suggested for removal of nucleic acids from micro-organisms. Maul *et al.*[74] showed that in yeast, the nucleic acid content could be decreased from 7% (initial) to about 1% (after treatment) by a heat-shock treatment. Yeast cells were heated to 65°- 70°C for 15-20 seconds, then held for about one hour at 50-60°C. During the post-heat holding period, nucleic acids leaked out of the cells. More recently, Karel and co-workers have used enzymatic degradation techniques to decrease nucleic acid content of *Scenedesmus* cell material by 92%.[75]

Removal of pigments must also be accomplished if an algae-derived diet is to be palatable. Nakhost *et al.*[76] have described extraction techniques for pigment removal. They carried out a 2-step process, using supercritical CO<sub>2</sub> followed by CO<sub>2</sub> plus anhydrous ethanol. The final product was a gray flour-like protein isolate which contained virtually no pigments, but retained about 43% of the protein content of the original cells. In addition to heat-shock and solvent extraction techniques, there are other methods for removal of unwanted components from foodstuffs. Three techniques deserve mention, namely use of ultrafiltration/reverse osmosis, use of zeolites and bleaching clay-zeolite blends, and use of electrostatic separation systems.

Commercial applications of electric field separations have been in practical use for over forty years in the petroleum and petrochemical industries. In these operations, coalescence of a polar dispersed phase in non-conductive hydrocarbons or removal of particulates from water-free hydrocarbons is accomplished. Well-known examples include crude oil desalting, caustic refining, and removal of catalyst fines from cat cracker bottoms. These advanced separation methods are discussed in the technical literature under electrofining (i.e. D.C. induced dipole coalescence in a uniform field), dielectrophoresis (i.e. motion of a neutral particle due to a non-uniform field acting on its permanent or induced dipole) and electrofiltration (i.e. removal of particulates in a packed bed under imposed D.C. fields).[77;78;79]

Application of electrical fields to polar alternative solvents for extraction of algal cell suspensions and slurries appears promising since it has been known for some time that electric fields can be used to enhance rate processes, in particular to increase rates of mass transfer in extraction columns by 3 to 10 fold.[80]

Adsorption processes are used widely in the chemical, biochemical, and petroleum industries, both for purification (removal of trace impurities) and for bulk separations. While adsorption purification systems have been in operation for many years for air and water treatment, sugar decolorization, etc., the advent of large-scale adsorption processes for bulk separation is a more recent development which became practically feasible only after improved absorbents with sufficient selectivity to differentiate chemically similar species had been developed.

Zeolites are highly crystalline, hydrated aluminosilicates of ideal crystalline and uniform pore structures. They have been of considerable interest as catalysts for over twenty years because of high activity and selectivity in various acid catalyzed reactions. Minimum channel diameters (openings) range from around 0.3-1.0 nm. This fine pore structure permits only certain molecules to penetrate into the interior while only certain products can escape. In addition to their well known use as catalysts, zeolites have been used in adsorption separations on the basis of molecular size or so-called "molecular sieving" as in the separation of n-paraffins from isoparaffins.

About 40 different zeolite framework structures have been discovered although only a few of these have found commercial application. Access to the pores of zeolite A is restricted by 8-membered oxygen rings of free aperture 4.3 Å in the unobstructed  $\text{Ca}^{++}$  (5A) form. This is reduced to about 3.8 Å in the  $\text{Na}^+$  (4A) form and to 3.0 Å in the  $\text{K}^+$  (3A) form. These adsorbents are therefore useful for applications involving size-selective adsorption of relatively small molecules.

The pores of the X and Y zeolites, which are restricted by 12-membered oxygen rings, are larger, having a free aperture of about 8.1 Å and these zeolites are therefore useful as adsorbents for relatively large molecules. The frameworks of the X and Y zeolites are identical; the difference lies in the Si/Al ratio which controls the cation density and therefore significantly affects the adsorptive properties.

The third commonly-used zeolite adsorbent is the intermediate pore (10-membered oxygen ring) zeolite which has a free aperture of about 6.0 Å. This zeolite was first prepared by Mobil in the early 1970's and named ZSM-5. At about the same time the pure silica analog, with the same framework structure, was prepared by Union Carbide and named silicalite. In many adsorbent applications these materials are interchangeable.[81]

As a result of the uniformity of the micropores, which are of molecular dimensions, zeolite adsorbents show a rather sharp sorption cut-off with increasing molecular size, thus raising the possibility of size-selective molecular sieve separations.

Recent developments in the construction of cylindrical ceramic membranes of defined pore sizes have opened new possibilities for filtration, separation, and purification of specific molecular structures. With pore diameters of a few nanometers, it becomes feasible to use ceramic membranes for fractionating foodstuff components so as to remove unwanted constituents.

- [1] "Pioneering the Space Frontier." The Report of the National Commission on Space. Bantam Books, Inc. NY, NY. 1985.
- [2] "Leadership and America's Future in Space. A Report to the Administration." Sally K. Ride, NASA. 1987.
- [3] "Exploring the Living Universe. A Strategy for Space Life Sciences." A Report of the NASA Life Sciences Strategic Planning Study Commission. F.C. Robbins (Chairperson). NASA. 1988.
- [4] "Space Technology To Meet Future Needs." Commission on Advanced Space Technology; Commission on Engineering and Technology Systems; National Research Council and National Academy Press. Washington, DC. 1987.
- [5] "Conceptual Design for a Food Production, Water and Waste Processing, and Gas Regeneration Module." O.W. Nicks (Team Leader), NASA Grant No NAG 9-161. July, 1987.
- [6] "Progress Report: Regenerative Life Support System Research During the Period September 1987-March 1988." O.W. Nicks (Team Leader). NASA Grant No. NAG 9-253.
- [7] G.P. Noyes and R.J. Crusick, "An advanced Carbon Reactor System for Carbon Dioxide Reduction," 16th Intersociety Conference on Environmental Systems, San Diego, CA, pp 761-768 (1986)
- [8] Ingram, W.T. "The Engineering Biotechnology of Handling Wastes Resulting From a Closed Ecology System." AFOSR Report No. TR 58-148, ASTIA Doc. No AD 162277. Feb. 1958.
- [9] Goldblith, S.A. and E.L. Wick. "Analysis of Human Fecal Components and Study of Methods for Their Recovery in Space Systems." ASD Tech. Rept. 61-419. 1961.
- [10] Pipes, W.O. and J.E. Quon. "Growth of Chlorella on Products From the Incineration of Human Wastes." Tech. Doc. Rept. AMARL-62-116. 1962.
- [11] Miller, R.L. and C.H. Ward. "Algal Bioregenerative Systems." In: Atmosphere in Space Cabins and Environments. Appleton-Century-Crofts. K. Kammermeyer (Ed). 1966.
- [12] Pecoraro, J.N., A.O. Pearson, G.L. Drake and J.R. Burnett. "Contributions of a Developmental Integrated Life Support System to Aerospace Technology." AIAA Tech. Report No. 67-924. Oct. 1967.
- [13] Wheaton, R.B., J.R.C. Brown, R.V. Ramirez and N.G. Roth. "Investigation of the Feasibility of Wet Oxidation For Spacecraft Waste Treatment." NASA CR 66450. 1966.
- [14] Schelkopf, J.D., F.J. Witt and R.W. Murray. "Integrated Waste Management-Water System Using Radioisotopes For Thermal Energy." U.S. Atomic Energy Commission, Contract No. AT (11.1)-3036. GE Doc. No 74SD4201, May, 1974.
- [15] Fields, S.F. et. al. "Development of an Integrated Zero-G Pneumatic Transporter/Rotating Paddle Incineration/Catalytic Afterburner Subsystem For Processing Human Waste Onboard Spacecraft." NASA CR 114764. 1974.
- [16] Jackson, J.K., M.S. Bonura and D.F. Putnam. "Evaluation of a Closed-Cycle Life-Support System

- During a 60-Day Manned Test." SAE Tech. Paper #680741. 1967.
- [17] "Preliminary Results From An Operational 90-Day Manned Test of a Regenerative Life Support System. NASA SP-261. 1971.
- [18] Spurlock, J.M., M. Modell, J. Pecoraro, D.F. Putnam and L.W. Ross. "Evaluation and Comparison of Alternative Designs for Water/Solid-Waste Processing Systems for Spacecraft." NASA Contract No NASw-2439. 1975.
- [19] Zimmerman, F.J. "Wet Air Combustion." *Ind. Water and Waste*, 6: 102-106. 1961.
- [20] Cadotte, A.P. and R.G.W. Laughlin. "The Wet-Ox Process for Industrial Waste Treatment." In: *Waste Treatment and Utilization*, M. Moo-Young and G.J. Farquhar (Eds). Pergamon Press, New York, 1979. pp 157-172.
- [21] Onisko, B.L. and T. Wydeven. "Wet Oxidation as a Waste Treatment in Closed Systems." SAE Tech. Paper #81-ENAs-22. Intersociety Conf. on Environmental Systems. San Francisco, CA 1981.
- [22] Johnson, C.C. and T. Wydeven. "Wet Oxidation of a Spacecraft Model Waste." SAE Tech. Paper #851372. 15th Intersociety Conf. On Environmental Sys. San Francisco, CA. 1985.
- [23] Timberlake, S.H., G.T. Hong, M. Simson and M. Modell. "Supercritical Water Oxidation for Wastewater Treatment: Preliminary Study of Urea Destruction." SAE Tech. Paper #820872. 12th Intersociety Conf. on Environmental Sys. San Diego, CA 1982.
- [24] Amin, S., R.C. Reid and M. Modell. "Reforming and Decomposition of Glucose in an Aqueous Phase." SAE Technical Paper # 75-ENAs-21. 1975.
- [25] Hong, G.T., P.K. Fowler, W.R. Killilea and K.C. Swallow. "Supercritical Water Oxidation: Treatment of Human Waste and System Configuration Tradeoff Study." SAT Tech. Paper # 871444. 17th Intersociety Conf. on Environmental Sys. Seattle, WA. 1987.
- [26] Webley, P.A. and J.W. Tester, 1988. "Fundamental Kinetics and Mechanistic Pathways for Oxidation Reactions in Supercritical Water." SAE Tech. Paper # 881039. 18th Intersociety Conf. on Environmental Sys., San Francisco, CA 1988.
- [27] Killilea, W.R., G.T. Hong, K.C. Swallow and T.B. Thomason. "Supercritical Water Oxidation: Microgravity Solids Separation." SAE Tech. Paper # 881038. 18th Intersociety Conf. on Environmental Systems. San Francisco, CA. 1988.
- [28] Sedej, M.M. "A Physicochemical Environmental Control/Life Support System for the Mars Transit Vehicle." In: *Manned Mars Mission. Working Group Papers. NASA TM-89321, Vol. 2*, pp 787-796. 1986.
- [29] Hall, J.B. and D.A. Brewer. "Supercritical Water Oxidation: Concept Analysis for Evolutionary Space Station Application." SAE Tech. Paper #860993. 16th Intersociety Conf. on Environmental Systems. 1986.
- [30] Slavin, T.J., F.A. Liening, M.W. Oleson. "CELSS Waste Management Systems Evaluation." SAE Tech. Paper #860997. 16th Intersociety Conf. on Environmental Systems. 1986.
- [31] Hitt, A.J., III, R.H. Renfro, D.F. Schien and E. Streams. "Criteria Definition and Performance

- Testing of a Space Station Experiment Water Management System." SAE Tech. Paper #881019. 18th Intersociety Conference on Environmental Systems, San Francisco, CA. July, 1988.
- [32] Buchanan, R.E. and N.E. Gibbons, eds. *Bergey's Manual of Determinative Bacteriology, Eighth Edition*, Williams & Wilkins Co., Baltimore, *passim*, 1974.
- [33] MacFaddin, J.F. *Biochemical Tests for Identification of Medical Bacteria*, Williams & Wilkins Co., Baltimore, 1976.
- [34] Shokichi Yuen, Pullulan and Its New Applications, Hayashibara Biochemical Laboratories, Inc., Okayama, Japan (February 1974).
- [35] Jackson, J.K., E.A. Worden, R.B. Boyda and R.L. Johnson. "Initial Results of Integrated Testing of a Regenerative ECLSS at MSFC." SAE Tech. Paper #871454. 17th Intersociety Conf. on Environmental Systems. July, 1987.
- [36] Ray, C.D., K.Y. Ogle, R.W. Tippos, R.L. Carrasquillo and P. Wieland. "The Space Station Air Revitalization Subsystem Design Concept." SAE Tech. Paper #871448. 17th Intersociety Conf. on Environmental Systems. July, 1987.
- [37] Stuart W. Churchill, Professor of Chemical Engineering, University of Pennsylvania, Philadelphia, PA, personal communication.
- [38] Janik, D.S., R.L. Sauer, D.L. Pierson and Y.R. Thorstenson. Quality Requirements for Reclaimed/Recycled Water. NASA Tech. Memorandum 58279. March, 1987.
- [39] Space Station Water Quality. JSC Doc. #32024. March, 1987.
- [40] Pierson, D.L. and H.D. Brown. Inflight Microbial Analysis Technology. SAE Tech. Paper #8714493. 17th Intersociety Conference on Environmental Systems, July, 1987.
- [41] Stannard, C.J., and J.M. Wood, *J. Appl. Bacteriol.* 55 (1983) 71-74.
- [42] Kubitschek, H.E., *Methods in Microbiology* 1 (1969) 593-610.
- [43] Harris, C.M., R.W. Todd, S.J. Bungard, R.W. Lovitt, J.G. Morris and D.B. Kell, *Enzyme Microb. Technol.*, 9 (1987) 181-186.
- [44] Stratford, B.C., In: *Atlas of Medical Microbiology: Common Human Pathogens* (1977) Blackwell Scientific Publications, Edinburgh.
- [45] Odham G., A. Tunlid, G. Westerdahl, L. Larsson, J.B. Guckert and D.C. White, *J. Microbiological Methods* 3 (1985) 331-334.
- [46] Shapiro, H.M. *Practical Flow Cytometry*. Alan R. Liss, Inc. New York, 1988.
- [47] Mansour, J.D., J.A. Robson, C.W. Arndt and T.H. Schulte. Detection of *Escherichia coli* in blood using flow cytometry. *Cytometry* 6:186. 1985.
- [48] Nishikawa, S., S. Saki, I. Karube, T. Matsunaga and S. Suzuki, *Appl. Environmental Microbiol.*, 43 (1982) 814-818.
- [49] Turner, A.P.F., G. Ramsey and I.J. Higgins, *Biochem. Soc. Trans* 11 (1983) 445-448.
- [50] Bennetto, H.P. *Life Chemistry Report* 2 (1984) 363-451.
- [51] Roller, S.D., H.P. Bennetto, G.M. Delaney, J.R. Mason, J.L. Stirling and C.F. Thurston. *Chem. Tech. Biotechnol.* 34B (1984)3-12.
- [52] Luck, H., *Kieler Milchforsch. Furschung.* 34 (1982) 108-116.
- [53] Bennetto, M.P., G.M. Delaney, J.R. Mason, S.D. Roller, J.L. Stirling and C.F. Thurston. *Proc. 1st World Conference Biotechnology* (Biotech 1983). Online Publications, Ltd. London, 655.
- [54] Roller, S.D., H.P. Bennetto, G.M. Delaney, J.R. Mason, J.L. Stirling and C.F. Thurston. *Proc. 1st World Conference Biotechnology* (Biotech 1983). Online Publications, Ltd., London, 655.
- [55] Tanaka, K., C.A. Vega and R. Tamamushi. *Bioelectrochem. Bioenerg.* 11 (1983) 135-143.
- [56] Nishikawa, S., S. Sakai, I. Karube, T. Matsunaga and S. Suzuki. *Appl. Environmental Micro.* 43 (1982) 814-818.
- [57] Sharpe, A.N., *Food Technology.* (March 1979) 71-74.

- [58] Patchett, R.A., A.F. Kelly, and R.G. Knoll. *Applied Microbiol. Biotechnol.* 28 (1988) 26-31.
- [59] Gilmore, V.E., *Popular Science*, p. 76 (May 1988).
- [60] Tibbitts, T.W. and D.K. Alford (1982) Controlled ecological life support system: Use of higher plants. NASA Conference Publication 2231. Ames Research Center, Moffett Field, California.
- [61] Oleson, M.W., and R.L. Olson (1986). Controlled Ecological Life Support System (CELSS) Conceptual Design Option Study, NASA Contractor Report 177421
- [62] Oleson, M.W., T.J. Slavin and R.L. Olson (1987). Lighting considerations in a controlled environmental life support system. SAE Technical Paper Series #8711435; 17th Intersociety Conference on Environmental Systems, Seattle, Washington.
- [63] Bugbee, G.G. and F.D. Salisbury (1985). Wheat production in the controlled environments of space. *Utah Science* 46:145-152.
- [64] Wheeler, R.M. and T.W. Tibbitts (1987). Utilization of potatoes for life support systems in space: III. Productivity at successful harvest dates under 12-hr and 24-hr photoperiods. *American Potato Journal* 64:311-320.
- [65] Wagner, J.P., J.T. Farnsworth and E.W. Lusas (1986). Rapid analysis instruments for oilseeds and oil mill products. Food Protein Research Development Center Publication, August 1986. Texas Engineering Experiment Station.
- [66] Sosulski, K., F.W. Sosulski, and E. Coxworth (1988). Carbohydrase hydrolysis of canola to enhance oil extraction with hexane. *Journal of the American Oil Chemical Society* 65:357-361.
- [67] Farnsworth, J.T. and J.P. Wagner (1986). The preparation of low cost foods by extrusion. U.S. Department of Agriculture Document, Office of International Cooperation and Development.
- [68] Akerlof, G.C. Feasibility of regeneration of carbohydrates in a closed-circuit respiratory system. *J. Spacecraft I* (3), pp. 303-310, 1964.
- [69] Shapira, J. Space feeding: approaches to the chemical synthesis of food. *Cereal Science Today* 13 (2), pp. 58-63, 1968.
- [70] Berman, G.A., Synthetic carbohydrate: an aid to nutrition in the future. Final Report, NASA-CR-136152, NTIS-N-74-11904, 1973.
- [71] Becker, E.W., Nutritional properties of microalgae: potentials and constraints. In *Handbook of Microalgal Mass Culture*, A. Richmond, ed., CRC Press, pp. 339-420, 1986.
- [72] Protein Advisory Group. PAG ad hoc working group meeting on clinical evaluation and acceptable nucleic acid levels of single-cell protein for human consumption. *PAG Bulletin* 5 (3), p. 17, 1975.
- [73] Scrimshaw, N.S. *Single Cell Protein, Vol. II*, S.R. Tannenbaum and D.E.I. Wang, eds. MIT Press, Cambridge, Mass, 1975.
- [74] Maul, S.B., A.J. Sienskey, and S.R. Tannenbaum, *Nature*, 228, p. 181, 1970.
- [75] Kamarei, A.R., Z. Nakhost, and M. Karel, SAE Technical Paper Series 851388. Society of Automotive Engineers, Inc., Warrendale, Pa., 1985.
- [76] Nakhost, A., M. Karel, and V.J. Krukonis. Non-conventional approaches to food processing in CELSS. I - Algal proteins; characterization and process optimization. *Adv. Space Res.* 7 (4), pp. (4)29-(4)38, 1987.
- [77] Waterman, L.C. Electrical Coalescers, *Chem. Eng. Progress* 61 (10), pp. 51-17, 1975.
- [78] Bailes, P.J. Solvent extraction in an electric field, *Ind. Eng. Chem Process Dev* 20, pp. 564-570, 1981.
- [79] Bailes, P.J. and S.K.L. Larkai, An experimental investigation into the use of high voltage d.c. fields for liquid phase separations, *Trans. Chem. Eng.* 59, pp. 229-236, 1981.
- [80] Wagner, J.D. Charge generation and transport during flow of low conductivity fluids. In *Handbook of Fluids in Motion*, N.P. Cheresinoff and R. Gupta, eds., Ann Arbor Science, Ann

Arbor, Michigan. Chapter 41, pp. 1138-1141, 1983; Also Wagner, J.D., Coalescence Apparatus for Electrostatically Resolving Emulsions. U.S. Patent No. 4, 3981-698 (5 July 1983).

- [81] Ruthven, D.M. Zeolites as selective adsorbents. *Chemical Engineering Progress*, February 1988, 42-50.